Modeling Nitrogen and Energy Metabolism in the Bovine

Meng Meng Li

Thesis submitted to the faculty of the Virginia Polytechnic Institute and State University in partial fulfillment of the requirements for the degree of

Doctor of Philosophy

in

Dairy Science

Mark D. Hanigan

Leluo Guan

Robin R. White

Rebecca R. Cockrum

December 7, 2018

Blacksburg, VA

Keywords: cattle, microbes, nutrient digestion, rumen metabolism

Modeling Nitrogen and Energy Metabolism in the Bovine

Meng Meng Li

Academic Abstract

The objectives of this research were to: 1) evaluate the accuracy of the Molly cow model predictions of ruminal metabolism and nutrient digestion when simulating dairy and beef cattle diets, 2) advance representations of N recycling between blood and the gut and urinary N excretion in the model, 3) improve the representation of pH and to refit parameters related to ruminal metabolism and nutrient digestion in the model, 4) investigate how ruminal pH affects the microbial community, expression of carbohydrate-active enzyme transcripts (CAZymes), fiber degradation, and short chain fatty acid (SCFA) concentrations. To achieve the first objective, a total of 229 studies (n = 938 treatments) including dairy and beef cattle data, published from 1972 through 2016, were collected from the literature and used to assess the model accuracy and precision based on root mean squared errors (RMSE) and concordance correlation coefficients (CCC). Only slight mean and slope bias were exhibited for ruminal outflow of NDF, starch, lipid, total N, and non-ammonia N, and for fecal output of protein, NDF, lipid, and starch. However, ruminal pH was poorly simulated and contributed to problems in ruminal nutrient degradation and VFA production predictions. To achieve the second objective, representations including ruminal ammonia outflow, intestinal urea entry, microbial protein synthesis in the hindgut, and fecal urea N excretion, were added in the model. Total urea entry, gut urea entry, and urinary urea elimination rates collected from 15 published urea kinetics studies were used to derive related parameters. Significant improvements in predictions of variables describing ruminal N metabolism, blood urea metabolism and urinary N secretion were exhibited after the modifications. To achieve the third objective, a dataset assembled from the

literature containing 284 peer reviewed studies with 1223 treatment means was used to derive parameter estimates for ruminal metabolism and nutrient digestions. After refitting the parameters, the model is even more robust in representing ruminal nutrient degradation compared to the initial model. Adding ammonia concentration as a driver to the pH equation increased the precision of predicted ruminal pH, and thereby, the precision of predicted VFA concentrations due to an improved representation of pH regulation of VFA production rates. To achieve the fourth objective, six cannulated Holstein heifers with an initial BW of 362 ± 22 kg (mean ± SD) were subjected to 2 treatments in a cross-over design. The treatments were 10 days of intraruminal infusions of both 1) distilled water (Control), and 2) a dilute blend of hydrochloric and phosphoric acids to achieve a pH reduction of 0.5 units (LpH). Statistical analyses indicated 19 bacterial genera and 4 protozoal genera were affected by low ruminal pH. We observed significant correlations between 54 microbes (43 bacterial and 11 protozoal genera) and 25 enzymes, of which 8 key enzymes participated in reactions leading to SCFA production, suggesting that the ruminal microbial community alters fiber catalysis and fermentation in response to altered pH through a shift in carbohydrate-active enzyme transcripts (CAZymes) expression. Overall, after the modifications and reparameterizations, 19.7 to 37.5% of RMSE with essentially no slope bias and minor mean bias were exhibited for of ruminal and fecal outflow of ADF, NDF, fat, and protein, suggesting the model is properly to represent nutrient degradation and digestion in the bovine. Considering ruminal microbes and CAZymes in predicting ruminal volatile fatty acid concentrations could explain more variance of observations.

General Audience Abstract

The purpose of this research was to improve ruminal nutrient metabolism and nutrient digestion representations in the Molly cow model. First, the model accuracy and precision were assessed using a dataset including 229 studies (n = 938 treatments) conducted with dairy and beef cattle. The model evaluation results indicated the mechanisms encoded in the model relative to ruminal and total tract nutrient digestion are properly represented. However, ruminal pH was very poorly represented in the model with a RMSE of 4.6% and a concordance correlation coefficient (CCC) of 0.0. Although VFA concentrations had negligible mean (2.5% of MSE) and slope (6.8% of MSE) bias, the CCC was 0.28 implying that further modifications with respect to VFA production and absorption are required to improve model precision. As identified by the residual analyses, the representations of N recycling between blood and the gut were improved by considering ruminal ammonia outflow, intestinal urea entry, microbial protein synthesis in the hindgut, and fecal urea N excretion in the model. Observations of total urea entry, gut urea entry, and urinary urea elimination rates were collected from 15 published urea kinetics studies were used to derive related parameters. After the modifications, prediction errors for ruminal outflows of total N, microbial N, and non-ammonia non-microbial N were 39.5, 27.8 and 35.9% of the respective observed mean values. Prediction errors of each were approximately 10% units less than the corresponding values before model modifications and fitting due primarily to decreased slope bias. The revised model predicted ruminal ammonia and blood urea concentrations with substantially decreased overall error and reductions in slope and mean bias. After that, ammonia concentration as a driver was added to the pH equation, and a dataset assembled from the literature containing 284 peer reviewed studies with 1223 treatment means was used to derive parameter estimates for ruminal metabolism and nutrient digestions. Refitting the parameters significantly improved the accuracy and precision of the model predictions for ruminal nutrient

outflow (ADF, NDF, total N, microbial N, non-ammonia N, and non-ammonia, non-microbial N), ammonia concentrations, and fecal nutrient outflow (protein, ADF, and NDF). Therefore, the improved model can be used to simulate nutrient degradation and digestion in the bovine. Although minor mean and slope bias were observed for ruminal pH and VFA concentrations, the small values for concordance correlations indicated much of the observed variation in these variables remains unexplained. To further explain variance in ruminal metabolism and understand how ruminal pH affects the microbial community, expression of carbohydrate-active enzyme transcripts (CAZymes), fiber degradation, and short chain fatty acid (SCFA) concentrations, six cannulated Holstein heifers with an initial BW of 362 ± 22 kg (mean ± SD) were subjected to 2 treatments in a cross-over design. We observed 19 bacterial genera and 4 protozoal genera were affected by low ruminal pH, and significant correlations between 54 microbes (43 bacterial and 11 protozoal genera) and 25 enzymes, of which 8 key enzymes participated in reactions leading to SCFA production. In summary, after the modifications and reparameterizations, the model is even more robust to represent nutrient degradation and digestion in bovine compared to the initial model. More variance of observations of ruminal volatile fatty acid concentrations could be explained by considering ruminal microbes and CAZymes expressions in further study.

Dedication

This thesis is dedicated to my beloved family!

Sincerely appreciate all your encouragement and support!

Acknowledgements

First and foremost, I would like to express my earnest appreciation to my advisor Dr. Hanigan for all your patient guidance and support. You not only gave me an incredible opportunity to pursuit my dream for scientific research, but also always offer me helpful and useful suggestions on both research and life. You are always there to encourage and support me. Without your help, I am not able to develop critical and independent thinking and to overcome all the obstacles in the completion this research work. It's my greatest honor to be your student and to complete my PhD program under your supervision.

I would like to express my sincere acknowledgements to the members of my supervisory committee Dr. Guan, Dr. White, and Dr. Cockrum. Thank you for your time, suggestions and valuable input over the years. Special thanks to Dr. White for teaching me how to code in R and helping me during my animal trial.

I would like to thank our lab technician, Tara, and all the past and present PhD, master and undergraduate students in the lab for helping me during my animal trial and class. I would like to thank all the faculty, staff, and students in the Department of Dairy Science for their kindness and help. I also would like to thank the farm crew at Kentland Farms for their help and support during the animal trial.

I would also like to thank the financial support from the Virginia Agricultural Experiment Station, the Hatch Program of the National Institute of Food and Agriculture, U.S. Department of Agriculture; the College of Agriculture and Life Sciences Pratt Endowment at Virginia Tech, and the Alberta Livestock and Meat Agency Ltd.

Finally, I must thank my parents for giving birth to me and supporting me spiritually throughout my life. To my wife Meiting, thank you for your love, encouragement, and support. To my son Ethan, you are my pride and joy of my life.

Table of Contents

List of Tables

List of Figures

Chapter 1: General Introduction

Still-growing global population figures and per-capita meat and milk consumption imply increased pressure on the global food supply system (Wirsenius et al., 2010). In contrast to monogastric animals, ruminants have a relatively low efficiency of nutrient utilization. Approximate 15 to 26% of energy efficiency and 18 to 30% nitrogen efficiency were reported for dairy cows (Arndt et al., 2015), and around 3 to 8% nitrogen efficiency and 4 to 12% energy efficiency were reported for beef cattle (Wilkinson, 2011). Hence, it is essential to advance animal production through a continuously improved understanding of nutrient digestion and metabolism (Baldwin, 1995).

A mathematical model is a description of a system using mathematical concepts and equations. As described by Bjork (1973), there are some advantages of mathematical models compared with verbal models which are word equations to represent the real situations, such as the mathematical models are more readily falsifiable; they force theoretical precision and promote data analysis; and their assumptions can be more easily studied. Therefore, mathematical models have multiple practical applications which can be used to 1) predict the response of a system to changes of input; 2) aid in the evaluation of hypothesis; 3) provide quantitative description and understanding of mechanisms within a system; 4) identify gaps in current knowledge (Dijkstra, 1993).

Mathematical models, such as the NRC (2001) and Cornell Net Carbohydrate and Protein System (Fox et al., 1992; Russell et al., 1992; Sniffen et al., 1992; O'Connor et al., 1993), have been widely used in animal nutrition for estimating animal requirement and nutrients derived from feeds (Dumas et al., 2008). Significant improvements have been achieved in terms of improving production performance, reducing feed cost, and decreasing nutrient excretion

(Tedeschi et al., 2005). However, the level of aggregation of such empirical models does not capture critical components of some metabolic reactions, and thus do not completely reflect the potential range of nutritional efficiency. Given the static nature of these models, it is also difficult to simulate management strategies that are time dependent (Hanigan et al., 2006). Molly is a dynamic and mechanistic cow model (Baldwin et al., 1987a; 1987b; 1987c). It is a moderately complicated system representing current knowledge of nutrient digestion and metabolism (Li et al., 2018a). Therefore it allows assessment of energy and nitrogen efficiency by comparing various biological measurements (Hanigan et al., 2006).

The main objective of the current study was to model nitrogen and energy metabolism in the bovine based on the Molly cow model with the long-term of improving feed efficiency through assessing different nutritional strategies before implementing changes on a farm. In chapter 2, we evaluated the accuracy of the Molly cow model predictions of ruminal metabolism and nutrient digestion and identified deficiencies in the model using simple linear regression of residuals. Residual analyses identified ruminal ammonia concentrations as a factor contributing to ruminal pH prediction errors. Therefore, the representations of ruminal urea N recycling need to be improved to increase the accuracy of ruminal ammonia concentrations. In chapter 3, representations of N recycling between blood and the gut and urinary N excretion were modified which yielded unbiased predictions of ammonia concentration. In chapter 4, ammonia concentration as a driver was added to the pH equation, and a large dataset was used to derive parameter estimates for ruminal metabolism and nutrient digestions. Although the accuracy and precision of predicted ruminal pH and VFA concentrations were increased after the modification and refitting the parameters, much of the observed variation remains unexplained. To further explain variance in ruminal metabolism, the pH shift effects on the microbial community,

expression of carbohydrate-active enzyme transcripts (CAZymes), fiber degradation, and short chain fatty acid (SCFA) concentrations were investigated in chapter 5. The results indicated considering ruminal microbes and CAZymes in predicting ruminal volatile fatty acid concentrations could explain more variance of observations.

Reference

Arndt, C., J. Powell, M. Aguerre, P. Crump, and M. Wattiaux. 2015. Feed conversion efficiency in dairy cows: Repeatability, variation in digestion and metabolism of energy and nitrogen, and ruminal methanogens. J Dairy Sci 98(6):3938-3950.

Baldwin, R. 1995. Modeling ruminant digestion and metabolism. Springer Science & Business Media.

Baldwin, R. L., J. France, D. E. Beever, M. Gill, and J. H. Thornley. 1987a. Metabolism of the lactating cow: III. Properties of mechanistic models suitable for evaluation of energetic relationships and factors involved in the partition of nutrients. Journal of Dairy Research 54(01):133-145.

Baldwin, R. L., J. France, and M. Gill. 1987b. Metabolism of the lactating cow: I. Animal elements of a mechanistic model. Journal of Dairy Research 54(01):77-105.

Baldwin, R. L., J. H. Thornley, and D. E. Beever. 1987c. Metabolism of the lactating cow: II. Digestive elements of a mechanistic model. Journal of Dairy Research 54(01):107-131.

Bjork, R. A. 1973. Why mathematical models? American Psychologist 28(5):426.

Dijkstra, J. 1993. Mathematical modelling and integration of rumen fermentation processes. Dijkstra.

Dumas, A., J. Dijkstra, and J. France. 2008. Mathematical modelling in animal nutrition: a centenary review. The Journal of Agricultural Science 146(2):123-142.

Fox, D., C. Sniffen, J. O'connor, J. Russell, and P. Van Soest. 1992. A net carbohydrate and protein system for evaluating cattle diets: III. Cattle requirements and diet adequacy. Journal of animal science 70(11):3578-3596.

Hanigan, M., H. Bateman, J. Fadel, and J. McNamara. 2006. Metabolic models of ruminant metabolism: recent improvements and current status. J Dairy Sci 89:E52-E64.

Li, M. M., R. R. White, and M. D. Hanigan. 2018. An evaluation of Molly cow model predictions of ruminal metabolism and nutrient digestion for dairy and beef diets. J Dairy Sci 101(11):9747-9767.

NRC. 2001. Nutrient requirements of dairy cattle. 7th ed. National Academy Press, Washington, D.C. National Research Council.

O'Connor, J., C. Sniffen, D. Fox, and W. Chalupa. 1993. A net carbohydrate and protein system for evaluating cattle diets: IV. Predicting amino acid adequacy. Journal of animal science 71(5):1298-1311.

Russell, J. B., J. O'connor, D. Fox, P. Van Soest, and C. Sniffen. 1992. A net carbohydrate and protein system for evaluating cattle diets: I. Ruminal fermentation. Journal of animal science 70(11):3551-3561.

Sniffen, C., J. O'connor, P. Van Soest, D. Fox, and J. Russell. 1992. A net carbohydrate and protein system for evaluating cattle diets: II. Carbohydrate and protein availability. Journal of animal science 70(11):3562-3577.

Tedeschi, L. O., D. G. Fox, R. D. Sainz, L. G. Barioni, S. R. d. Medeiros, and C. Boin. 2005. Mathematical models in ruminant nutrition. Scientia Agricola 62(1):76-91.

Wilkinson, J. 2011. Re-defining efficiency of feed use by livestock. Animal 5(7):1014-1022.

Wirsenius, S., C. Azar, and G. Berndes. 2010. How much land is needed for global food production under scenarios of dietary changes and livestock productivity increases in 2030? Agricultural Systems 103(9):621-638.

Chapter 2: Quantitative literature review: An evaluation of Molly cow model predictions of ruminal metabolism and nutrient digestion for dairy and beef diets

Abstract

Model evaluation, as a critical process of model advancement, is necessary to identify adequacy and consistency of model predictions. The objectives of this study were 1) to evaluate the accuracy of Molly cow model predictions of ruminal metabolism and nutrient digestion when simulating dairy and beef cattle diets; and 2) to identify deficiencies in representations of the biology that could be used to direct further model improvements. A total of 229 studies (n = 938 treatments) including dairy and beef cattle data, published from 1972 through 2016, were collected from the literature. Root mean squared errors (RMSE) and concordance correlation coefficients (CCC) were calculated to assess model accuracy and precision. Ruminal pH was very poorly represented in the model with a RMSE of 4.6% and a CCC of 0.0. Although VFA concentrations had negligible mean (2.5% of MSE) and slope (6.8% of MSE) bias, the CCC was 0.28 implying that further modifications with respect to VFA production and absorption are required to improve model precision. The RMSE was greater than 50% for ruminal ammonia and blood urea-N concentrations with high proportions of error as slope bias indicating that mechanisms driving ruminal urea N recycling are not properly simulated in the model. Only slight mean and slope bias were exhibited for ruminal outflow of NDF, starch, lipid, total N, and non-ammonia N, and for fecal output of protein, NDF, lipid, and starch, indicating the mechanisms encoded in the model relative to ruminal and total tract nutrient digestion are properly represented. All variables related to ruminal metabolism and nutrient digestion were more precisely predicted for dairy cattle than for beef cattle. This difference in precision was mostly related to the model's inability to simulate low forage diets included in the beef studies. Overall, ruminal pH was poorly simulated and contributed to problems in ruminal nutrient

degradation and VFA production predictions. Residual analyses suggested ruminal ammonia concentrations need to be considered in the ruminal pH equation, and therefore the inaccuracies in predicting ruminal urea N recycling must also be addressed. These modifications to model structure will likely improve model performance across a wider array of dietary inputs and cattle type.

Key words: digestion, model evaluation, ruminal metabolism

Introduction

A basic goal of ruminant nutritionists is to advance animal production through a continuously improved understanding of nutrient digestion and metabolism (Baldwin, 1995). Baldwin and his colleagues constructed a dynamic and mechanistic model (named Molly) by combining key biological elements of digestion and metabolism (Baldwin et al., 1987a; 1987b; 1987c). It is a moderately complicated system of equations describing flows of chemical entities through a series of digestive and metabolic processes. Several evaluations of digestive and metabolic elements of Molly have been undertaken, which have guided structural changes and reparameterization of the model (Hanigan, 2005; Johnson and Baldwin, 2008). Additional modifications with respect to digestive parameter estimates (Hanigan et al., 2013) and ruminal digesta outflow (Gregorini et al., 2015) have been undertaken and integrated in the Molly cow model which have yielded increased accuracy of model predictions. Essentially all of this work has been conducted using data derived from dairy cattle which have included very few observations with high forage (forage percentage > 70 %) and essentially no observations with very low forage feeding levels (forage percentage < 30 %) as commonly fed to beef cattle. A key aim of a mechanistic model such as Molly is, however, to capture mechanisms that allow simulations across the full range in diets and cattle categories.

It was hypothesized that the Molly model properly represents nutrient digestion and ruminal metabolism for high and low forage diets. The objectives of the current work were 1) to evaluate the accuracy of the Molly cow model predictions of ruminal metabolism and nutrient digestion when simulating high and low forage diets; and 2) if deficiencies are identified in the model, to identify representations of the underlying biology that could be used to direct further model improvements.

Materials and Methods

Model Description

The current work was conducted using a modified version of Molly containing updated digestion and metabolism parameters (Hanigan et al., 2013) and an improved representation of ruminal digesta outflow (Gregorini et al., 2015). Model simulations were conducted using ACSLX (3.1.4.2, Aegis Technologies Group Inc., Huntsville, AL). The model was set to simulate 14 d to ensure it had reached steady state, and only predictions from the last day of the run were compared with observed values.

Model input values were either derived from literature observations or were assumed as described previously (Hanigan et al., 2013; Ghimire et al., 2014). Briefly, the model was set to use observed dietary ingredient intakes, ingredient nutrient composition, DMI, and BW as inputs, and it was assumed dietary intake was constant throughout the day. Because 32, 21, 54, 2, and 78% of studies did not report each of ADF, NDF, starch, CP, and fat either as dietary concentrations or intakes, tabular values from NRC (2001) were used to replace the missing values. Starch solubility and degradation were predicted from Tamminga et al. (1990) or Miller-Webster and Hoover (1998), and ADF degradability was predicted from the equation of Huhtanen et al. (2010). Reference bypass values for protein were calculated from the B and C fractions of CP using the NRC reported Kd and a fixed ruminal residence time for each feed as

described by Hanigan et al. (2013). This allowed summation of the nonlinear elements among feeds to determine a dietary value which was then used to back calculate to a rate of degradation by rearrangement of the initial equation. This reference rate constant was used in the model with previously derived slope and intercept adjustments to represent the base rate of degradation. Additional adjustments of the rate of degradation occur during each run based on prevailing ruminal conditions predicted by the model, e.g. the size of the microbial protein pool. The same approach was used for starch and ADF using estimated undegradability as a reference input.

To minimize mis-specification, predicted dietary nutrients were compared to reported values and any bias within study was used to adjust ingredient nutrients for that study to align observed and predicted data as described by Hanigan et al. (2013) and as follows. Bias for each nutrient (*n*) within each study (*s*) was derived by summation of the difference between the reported (*Obs*) dietary nutrient intake and that predicted (*Pred*) from summation of tabular ingredient (*i*) values for each diet (*d*), and used to adjust ingredient nutrient concentrations to match reported nutrient values among treatments (*j*):

$$Bias_{s,n} = \sum_{d=1}^{N_d} \left(Obs_{s,d,n} - Pred_{s,d,n} \right)$$

Bias was converted to a proportional adjustment ($Adj_{s,n}$) using the nutrient sum for all diets in the study:

$$Adj_{s,n} = Bias_{s,n} \Big/ \sum_{d=1}^{N} Pred_{s,d,n}$$

Adj was subsequently used to adjust the nutrient content of each ingredient (*Rev*) among diets within each study:

$$Rev_{s,i,n} = Obs_{s,i,n} \times \left(1 + Adj_{s,n} \right)$$

This approach utilizes the diet formulas and adjusted nutrient composition of ingredients to determine nutrient differences among diets within a study, and ensures that the mean nutrient content of those diets equals the observed mean values where such values have been reported. This avoids the introduction of mean input bias to the analyses and balances formulation information and reported nutrient data to better predict nutrients for each diet. Additionally, because it is applied at the ingredient level, secondary nutrients are comparably adjusted with the primary nutrient, e.g. calculated RUP will change proportional to the change in CP for each ingredient. This approach also avoids the dichotomy of effectively adjusting the nutrient content of a single ingredient to more than 1 value within a study, which would be the case if nutrients for each diet were assumed to be reported without error and used to exactly match nutrient inputs to the reported value for each diet.

Rumen fluid osmolarity is calculated by dividing the sum of the moles of soluble substrates (soluble carbohydrate, ammonia, VFA, lactate, amino acids, and soluble ash) by rumen liquid volume. Osmolarity of soluble ash was calculated by dividing soluble ash weight by the molecular weight of sodium bicarbonate and multiplying by an osmolarity factor of 1.7 (Argyle and Baldwin, 1988). Soluble ash intake is the product of DMI and the fractional content of soluble ash, where the soluble ash fraction is calculated by subtracting a fixed insoluble ash fraction of 1.2% from total dietary ash (Argyle and Baldwin, 1988).

In Molly, particle size distribution is one of the determinants of rates of particulate degradation and outflow from the rumen (Gregorini et al., 2015). Briefly, large particles are subject to size reduction through rumination and mastication; medium particles are subject to passage at a slow rate and to degradation through rumination and mastication and by microbial activity; small particles are subject to degradation by microbial activity and passage at a high

rate. The particle distribution in the diet is used to determine inputs to each particle pool and the size of those pools in the rumen are predicted by integration of inputs and outputs as for other pools in the rumen. However, very few experimental studies reported dietary particle size distributions. We therefore derived three empirical equations to estimate accumulated percentages of particles above each of the 3 sieves in a Penn State Particle separator based on dietary forage percentages (*ForP*, % of diet DM). A dataset of particle distributions and dietary forage content was collected from the literature (Turgeon et al., 1983; Kononoff and Heinrichs, 2003; Kononoff et al., 2003; Rustomo et al., 2006; Maulfair et al., 2011; Maulfair and Heinrichs, 2013; Ramirez et al., 2016), and used to derive the following prediction equations:

$$LargeP = 0.0023 \times ForP^2 + 0.0035 \times ForP + 0.2 \ (R^2 = 0.95, n = 8)$$

$$MediumP = -0.008 \times ForP^2 + 1.48 \times ForP + 1.2 \ (R^2 = 0.95, \mathrm{n} = 8)$$

$$SmallP = -0.003 \times ForP^2 + 0.72 \times ForP + 56.6 \ (R^2 = 0.58, \mathrm{n} = 8)$$

where *LargeP* (% of DM retained) is the cumulative percentage of particles retained above the 19.05 mm sieve; *MediumP* (% of DM retained) is the cumulative percentage of particles retained above the 7.87 mm sieve; and *SmallP* (% of DM retained) represents the cumulative percentage of particles retained above the 1.78 mm sieve.

Data Collection

Data used for model evaluation were collected from 153 publications with 574 treatments conducted with dairy cattle and 76 publications with 364 treatments conducted with beef cattle. The dairy data included observations from both lactating and nonlactating animals, and consisted of the 62 experiments used by the 2001 Dairy NRC Committee (NRC, 2001) which were used for a prior evaluation and reparameterization by Hanigan et al. (2013) plus an additional 91 studies published from 2000 to 2016. A complete list of the dairy studies is included in White et al. (2017), and a copy of the data can be downloaded from the National Animal Nutrition

Program website (awaiting upload). The beef data set contained observations from growing and finishing cattle. A listing of beef studies is presented in Supplement I.

Studies selected for inclusion in the data set contained DMI, diet formula information, and measurements of nutrient digestibility or ruminal metabolism. All reported data were treatment means. Body weight is a required model input. Reported initial BW was used to initialize the model for dairy cows, and the average of the initial and final BW was used for beef cattle. The average BW for dairy cattle in the data set was 595 kg with a SD of 64 kg (n = 522). Body weight was not reported for 52 treatments in the dairy data set. In these cases, initial BW was set to 600 kg. The average BW for beef cattle in the data set was 457 kg with a SD of 140 kg (n = 322). Body weight was not reported for 32 treatments in the beef data set. In those cases BW was estimated from reported EBW, shrunk BW or carcass weight based on the equations of Lofgreen et al. (1962).

Variables used to evaluate model predictions included ruminal outflow of DM, ADF, NDF, starch, lipid, total N, microbial N, non-ammonia N, and non-ammonia, non-microbial N (**NANMN**); and fecal excretion of DM, protein, ADF, NDF, lipid, and starch. Ruminal pH, ammonia concentrations, VFA concentrations, and blood urea-N concentrations were also used to evaluate ruminal fermentation parameters. A statistical summary of the observations is presented in Table 2-1. Observed data were assessed for variance and normality. Given the relatively discrete diet types, the input and observed data were not normally distributed for many measurements. Exceptions were starch intake, ruminal digestibility of OM and ADF, total tract digestibility of ADF and NDF, and blood urea concentrations. This does not imply that the population of all diets cannot be normally distributed, only that the sampling of diets within the population was not homogenous, and likely cannot be homogenous given the nature of diet

design. This does not impact model performance, and most measures of model performance will be unaffected as the model will account for differences in diets resulting in normally distributed residual errors. Individual data points with absolute values greater than 3 standard deviations from the mean were considered outliers and, around 1% of the observations were removed from the dataset.

High forage and low forage diets were identified based on the forage percentage and used to categorize the data. If the forage percentage was equal to or greater than 70%, the diet was categorized as a high forage diet; if the forage percentage was equal or less than 30%, the diet was categorized as a low forage diet. The remainder were categorized as moderate forage. Using these criteria, the data set contained 10% high forage diets, 33% low forage diets, and 57% moderate forage diets. Both dairy and beef data were included in the low, moderate, and high forage diets. A summary of nutrient composition for the 3 categories is described in Table 2-2.

Model Evaluation

Mean squared error (**MSE**) which is the sum of the squared residual errors divided by the number of observations (Boardman, 1979) was used to calculate the root MSE (**RMSE**) and to partition the MSE into slope and mean bias (Bibby and Toutenburg, 1977). Concordance correlation coefficients (**CCC**) were also calculated from the residuals. This value represents the correlation between observed and predicted variables (Lawrence and Lin, 1989).

Multivariate regression of residuals for predictions of ruminal nutrient outflow and ruminal metabolites on animal, dietary and ruminal fermentation parameters were conducted to identify model elements for improvement. The presence of a significant relationship suggests the model might not properly represent the effects or fate of that nutrient. These residual analyses were conducted by regressing residuals on observed BW, DMI, dietary nutrient composition (ADF, rumen undegraded ADF, NDF, forage NDF, starch, soluble starch, rumen undegraded

starch, CP, soluble CP, RUP, NPN, urea, lipid, lignin, ash, roughage), predicted ruminal pH, and predicted ammonia concentrations. When examining residual errors of prediction for ruminal pH or ammonia, that variable was not included as an independent variable in the regression model. Study effect was included as a random variable and regressions were conducted using a backward elimination approach with a significance level of 0.1. Multicollinearity was assessed by calculation of variance inflation factors (**VIF**) with variables having VIF greater than 10 removed from the regression model (Craney and Surles, 2002). In these analyses, positive coefficients indicated the model underpredicted responses to the independent variable while negative coefficients implied overprediction of responses. As illustrated in Figure 2-1, there was a negative correlation between ruminal pH and residuals of ruminal ADF outflow. Residuals of ruminal ADF outflow decrease with increased predicted ruminal pH being slightly underpredicted at low pH and becoming overpredicted at high pH.

Simple linear regression analyses of residuals for fecal nutrient excretions (DM, protein, ADF, NDF, starch and lipid) were conducted by regressing residuals on predicted ruminal outflow of a nutrient. Significant regression coefficients indicated digestion coefficients were improperly specified. Positive coefficients indicated fecal nutrient outputs were underpredicted with increased ruminal nutrient outflow, while negative coefficients implied fecal nutrient outputs were overpredicted. Data handling and residual analyses were conducted using R software (ver. 3.3.0).

Results and Discussion

Bias Adjustment for Nutrient Compositions

A summary of bias adjustments for dietary nutrients is shown in Table 2-3. Without bias adjustments, RMSE (% of mean) for dietary CP, NDF and ADF concentrations was 11.2, 13.8 and 18.5%, respectively. Bias corrections reduced the RMSE for CP, NDF, and ADF to 8.9,

10.8, and 14.1%, respectively. The decreased RMSE were primarily due to decreased mean and slope bias.

Nutrient Outflow from the Rumen

The initial evaluation of RMSE for nutrient digestion and ruminal metabolism was conducted across diet types (Table 2-4). Root mean squared errors of ruminal outflow of DM, ADF, NDF, lipid and total N were 17.9, 25.8, 26.3, 14.1 and 19.4%, respectively, and CCC were 0.8, 0.8, 0.7, 0.9, and 0.8 indicating that the model simulated ruminal outflow of these nutrients with reasonable accuracy and precision. Gregorini et al (2015) developed an improved representation of ruminal digesta outflow in the model. Although the modifications did not substantially improve the accuracy of digestive functions in their analyses, the model did reproduce more realistic trends in rumen particle outflow, fermentation patterns, digestion and methane yields. Previous studies assumed all diets had the same particle size distribution, with no consideration of particle size on ruminal outflow and residence time. In the current work, we used an empirical equation to predict particle distribution based on dietary forage percentages. It would have been better to use observed data, but in the absence of such information, LargeP, MediumP and SmallP were predicted with a RMSE of 19.2, 9.5 and 11.8%, and a CCC of 0.98, 0.98 and 0.74 (Figure 2-2), suggesting that forage content captures much of the variation in particle size distribution. Because particle size, in practice, varies with degree of mixing or length of time that the ration spends in a mixer wagon, those equations may not be an appropriate representation of all diets and thus may have contributed to performance issues for the disparate beef diets. However, in most cases, the direction of change in the particle size of the diets should have been correct as forage will always have longer mean particle size than concentrates provided the forage is not ground or highly processed.

Ruminal ADF and NDF Outflow. Both ruminal ADF and NDF outflow were underpredicted with an average mean bias of 19% and 0.1% slope bias (Table 2-4), indicating that degradation rates of cellulose and hemicellulose were over specified. Residual errors for ruminal ADF outflow were positively correlated with dietary concentrations of rumen undegraded starch, ash and NPN (excluding urea); and negatively correlated with BW, dietary concentrations of forage NDF, urea, ruminal pH, and ruminal ammonia concentrations (Table 2-7). There was a positive correlation between residual errors for NDF outflow and dietary concentrations of ADF, forage NDF, rumen undegraded starch and lipid; and a negative correlation with BW, dietary concentrations of NDF, CP, ruminal pH and ruminal ammonia concentrations. The correlations with ADF, NDF, starch, forage, and pH are likely all related to the common mechanism of ruminal pH. Indeed, residual errors for both ADF and NDF outflow were negatively correlated with predicted ruminal pH, indicating that as pH increases, residuals for outflow become less, i.e. the change in outflow with respect to the change in pH is too great. This indicates the inhibition of fiber degradation by low pH encoded in the model is too responsive causing large changes in fiber degradation across the range in pH (Figure 2-1). The model uses a constant of 0.1875 kg/kg reduction in degradation per 0.1 unit drop in ruminal pH below 6.2 (Baldwin, 1995). Based on the residuals, it would appear there is no break point at 6.2, and the inhibition slope should be less. From pH 5.5 to 6.0, the change in residual error for predicted digestibility is approximately 10% units. Dividing by 5 increments of 0.1 pH change yields a slope bias of 0.2 which is almost the same as the inhibition constant suggesting that inhibition is near 0 within this pH range. Assuming predictions of pH are related to reality, which is open for question, further work is required to address this mechanism in the model.

The negative correlations of residual errors for predictions of ruminal ADF and NDF outflow with dietary CP and ruminal ammonia indicate changes in degradation rates were overly responsive to those driving variables. Considering that predicted ammonia concentrations have a substantial RMSE (Table 2-4) which might have created an artificial relationship, residuals of ruminal ADF and NDF outflow were also regressed on observed concentrations, and found to also be negatively correlated with observed concentrations ($P < 0.05$). This indicated that the initial regression was not entirely driven by model bias. However, the model does not contain a direct link between fiber degradation rates and nitrogen inputs or factors. Those rates are only a function of fiber pool size, pH, and microbial mass. Therefore the over responsiveness must be driven through inappropriate changes in microbial activity due to one of those factors within the model. The lack of a correlation between microbial flow and ruminal ammonia suggests the problem lies with pH.

Predictions of microbial growth in the model are driven primarily by energy supply with the yield per unit of ATP affected by ruminal ammonia concentrations and amino acid and peptide concentrations in a saturation dependent manner with a half maximal response at 0.2 mM for ammonia and 0.1 mM for amino acids and peptides (Baldwin, 1995; Hanigan et al., 2009a; Hanigan et al., 2013). Thus under almost all normal feeding conditions, the modeled ammonia response is saturated. If true, the fiber problem seems more likely to be the related to inappropriate microbial responsiveness to CP and soluble CP, although the data are not entirely consistent. The microbial responses will be discussed further below.

Ruminal Starch Outflow. Ruminal starch outflow was predicted with a RMSE of 60.5% (19.8% mean bias and 1.8% slope bias) and CCC of 0.4. High errors in observed ruminal starch outflow with a mean of 2.21 kg/d and a standard deviation of 1.48 kg/d (Table 2-1) contribute to

the substantial RMSE. A portion of this error is likely due to varied sample collection and measurement methods. There was a negative correlation between residual errors for starch outflow and BW, dietary concentrations of rumen undegraded ADF, lignin and ruminal pH, and a positive correlation with DMI, dietary concentrations of NDF, forage NDF, soluble starch, and dietary CP (Table 2-7). These correlations implied that ruminal starch degradability varied depending on forage source, starch fermentability, and CP level. Variations in grain type and the processing method likely contributed to much of the variance in starch degradability, since these sources of variation could not be completely represented in the model inputs due to limited reporting of ingredient characteristics. The positive correlation between residuals of ruminal starch outflow and DMI, dietary concentrations of NDF and forage NDF indicates that increasing dietary concentrations of NDF and forage NDF resulted in too large of changes in starch degradation rates. Forages impact feeding behavior and rumen particle dynamics generally resulting in reduced particle passage rates. However, the proportion of amylolytic microbes also decreases with decreased fiber content (Thoetkiattikul et al., 2013), contributing to decreased starch degradation capacity. The Molly model simulates pools of amylolytic and cellulolytic microbes from a common microbial pool based on the relative proportions of amylose and cellulose in the diet. The overall rate of microbial growth is driven by the rate of soluble sugar formation from each of the substrate pools (Baldwin, 1995) which is affected by the particulate surface area (Gregorini et al., 2015). Passage of each pool of microbes is determined by the proportion of each microbial pool attached to particles, and the liquid and particulate passage rates (Gregorini et al., 2015). Because the amylolytic microbes are not directly affected by fiber supply, any correlation in residuals would reflect the correlations among dietary NDF and dietary starch and the potential effect of dietary fiber on starch passage rates. As substrate degradation is

partially driven by the microbes, there is an inherent feed forward loop within the system, but growth is ultimately limited by the overall supply of substrate. The residual errors suggest that the shift in predicted amylolytic pool size in response to changing NDF intake is too large resulting in overly large changes in starch degradation rates. This could possibly be related to under-responsiveness in ruminal passage to ruminal load (discussed below). More dietary forage generally results in greater ruminal load. If this causes increased rates of passage and reduced residence time, changes not currently represented in the model, this could explain the interaction among dietary fiber and starch degradation.

The negative correlation between residuals of ruminal starch outflow and dietary lignin indicates ruminal starch outflow is overpredicted and starch degradation rate is underpredicted when high lignin diets are simulated. Lignin is crosslinked to polysaccharides and protein in plant cells and is largely undegradable in the rumen (Van Soest et al., 1991a), which is resistant to digestive enzymes leading to underestimated starch degradation rate. Our result is consistent with finding reported by White et al. (2017), suggesting that the inhibitory effect of lignin on nutrient degradation needs to be considered in the model.

Ruminal Total N, NAN and NANMN Outflow. Ruminal outflow of total N and non-ammonia N had a RMSE of 19% with an average of 2.5% mean and slope bias and a CCC of 0.8, suggesting that both total N and non-ammonia N outflow from the rumen were accurately and relatively precisely predicted by the model. However non-ammonia, non-microbial N outflow was underpredicted with a RMSE of 40.3% (24.4% mean bias and 0.2% slope bias) and a CCC of 0.4. The moderate mean bias indicates that ruminal protein degradation was overestimated which could be addressed by a reduction in the scalar used to reference in situ determined RUP to the model rate constant for protein degradation. Non-ammonia, non-

microbial N residuals were negatively correlated with dietary concentrations of rumen undegraded ADF, forage NDF, urea, and lipid; and ruminal pH and ammonia concentrations (Table 2-7), and positively correlated with dietary NPN concentrations (excluding urea). The negative correlation between residual errors of ruminal NANMN outflow and dietary concentrations of rumen undegraded ADF indicates that with increased ruminally degraded ADF, ruminal NANMN outflow was increasingly over predicted. Kohn and Allen (1995) reported that plant proteins are trapped in a fiber matrix, implying that increased fiber content might contribute to decreased protein degradability. The model considers ruminal protein degradation as a mass action function of the insoluble protein pool size and the microbial pool size with the rate constant set by the in situ predicted RUP as described above. As fiber degrades more slowly, on average, than protein, assuming that all of the protein degrades at a constant rate may contribute to the over prediction when more of the protein is tied up in fiber. The differential rates should be captured by the *in-situ* data, yet the relationship exists. It is also possible the relationship is driven by the effects on increasing ruminal fiber load on ruminal passage rates. If protein turnover is reduced as more fiber is provided in the diet, the extent of degradation in the rumen would increase. Such an effect is represented in the model, however, the change in turnover associated with increasing fiber may not be fully captured.

The negative relationship between dietary NDF and residuals for predictions of ruminal NANMN outflow seems to contradict the negative relationship with ruminal pH, as pH is generally increasing as fiber increases. Thus, there may be different mechanisms. The latter suggests that protein degradation may be inhibited as ruminal pH declines. Endres and Stern (1993) observed a reduction in protein degradation when pH decreased from 6.3 to 5.9. Bach et al. (2005) demonstrated that ruminal pH can influence protein degradation by changing either

predominant microbial species or enzyme activities, and ruminal proteolytic activity decreased as pH decreased. Therefore, it can be hypothesized that a reduction in proteolytic activity as a consequence of low pH would lead to proportionally greater ruminal NANMN outflow. As the model does not contain such a mechanism, the observed error patterns suggest that such an effect should be added to the model

Residuals of ruminal NANMN outflow were negatively correlated with dietary lipid, suggesting that as dietary lipid increased, feed protein degradation was underpredicted. Baldwin (1995) included a representation of the inhibitory effect of fat on fiber and protein degradation in the model. Those effects were found to be overstated and modified to reflect lesser influence by Hanigan et al. (2013). The negative correlation herein using more data suggest the prior work was not correct or necessary. It is possible, that the changes in representing particle passage undertaken by Gregorini et al. (2015) may have altered the apparent responses to fat, or the addition of test data herein included a wider range of dietary fat content which has more clearly demonstrated the mechanism. In either case, a more thorough examination of the problem is warranted.

Residual errors for ruminal NANMN outflow were also negatively correlated with dietary urea concentrations, and positively correlated with dietary NPN concentrations. Plant nucleic acids are contained within the NPN fraction as defined by the model, which account for 30-70% of NPN (Holt and Sosulski, 1981) and have a low solubility. This material has low susceptibility to microbial proteases and, thus, low degradability (Cecava et al., 1991). Yet it is assumed to be quantitatively converted to soluble AA and ammonia in the model which might explain the under predicted responses in NANMN outflow as dietary NPN input increases. It is more difficult to envision a mechanism that would explain the urea results. The results indicated

that urea somehow stimulates protein degradation in the rumen. Given that proteases derive from the microbes, it is possible that it has a stimulatory effect on microbial growth rates above the N concentrations normally considered to be sufficient. This may be more likely to occur on a number of the high grain, feedlot diets (Huntington and Archibeque, 2000; Griswold et al., 2003). However, there is no evidence for bias in predictions of microbial flow with respect to dietary urea, and thus little support for such a hypothesis.

Microbial N Outflow. Microbial N outflow was predicted with an RMSE of 30.5%, which partitioned as 18.4% mean bias and 0.01% slope bias. Compared to total N and non-ammonia N outflow which had RMSE of less than 19%, it seems microbial growth is not well represented. Residual errors of microbial N outflow were positively correlated with DMI, dietary concentrations of CP, lignin, roughage and ruminal pH, and negatively correlated with BW, dietary concentrations of ADF, soluble CP, RUP and ash (Table 2-7). The positive correlation between microbial N outflow residuals and dietary lignin indicates microbial N outflow is underpredicted when high lignin diets are fed, which is consistent with the inhibitory effect of lignin on nutrient degradation as discussed above. The negative correlation with soluble CP suggests that increasing dietary soluble N (ammonia, AA and peptide) results in too large of changes in predicted ruminal microbial N outflow. Russell et al. (1992) found that nonstructural carbohydrate-degrading bacteria are the primary users of AA and peptides, and structural carbohydrate-degrading bacteria prefer to use ammonia. As noted above, microbial growth predictions in the model are driven by ruminally available ATP, amino acid and peptide concentrations, and ammonia concentrations (Baldwin, 1995). The current results suggest that the stimulatory effect of soluble N is too large leading to erroneous predictions of microbial growth. However, the negative correlation with RUP does not support such a point unless it is

capturing some components of urea recycling to the rumen. If the over responsiveness of microbial growth to soluble N is valid, it suggests the over responsiveness of fiber degradation noted above may be at least partially due to challenges in the representation of N effects on microbial growth. However predictions of ammonia and pH predictions must be corrected, and the model retested to verify that relationship. The positive relationship of residuals with DMI, roughage, and ruminal pH may all be reflective of too small of passage rate changes as intake and forage load increases, and passage plus high substrate supply associated with low pH conditions. Because the regressions only examined linear effects, any quadratic relationships would be reflected through a combination of multiple linear elements. A quadratic response in the residuals for microbial N outflow relative to dietary concentrations of CP, soluble protein and RUP was examined based on the fitted linear regression model. Both dietary CP and soluble protein had a quadratic relationship with microbial N outflow residuals (P = 0.08 and 0.01), which might explain why all three variables were in the model with seemingly opposing slopes.

Body Weight Effect on Ruminal Nutrient Outflow. The negative correlations of residual errors for predictions of ruminal ADF, NDF, starch, NAN, and microbial N outflow from the rumen with BW indicate that flows are overpredicted at high BW and the reverse at low BW. The particle passage model (Gregorini et al., 2015) is driven solely by the proportion of insoluble matter in liquid and the liquid outflow rate with no regulation. Liquid volume is a function of ruminal osmolarity as determined from the solute load in the rumen. This representation has no maximal value, but given that solute load is a function of DMI which is a biological input, there is in essence an upper limit to the volume. However, this upper limit is solely a function of DMI and dietary characteristics dictating the soluble matter. Obviously the rumen cannot hold an unlimited volume of material. The negative relationship of residual errors for all of these entities

with BW seems to suggest that rumen volume may be increasing disproportionately at high BW leading to increased residence time and extent of digestion, i.e. the rate constant for passage increases as ruminal volume gets large relative to a given animal size. As the larger animals were all dairy animals, it seems quite likely they would have larger rumen volumes on average than the beef animals given the selection pressure for milk yield and DMI, and they may have higher passage rate constants to mitigate the large increases in DMI. Regulation of particle and fluid passage was not considered by Gregorini et al. (2015) due to the very limited quantity of data available for characterization of the particle passage equations, and this pattern of errors was not previously observed, perhaps due to the restriction of evaluations to data derived solely from dairy animals. This problem could be addressed through the addition of the concept of a maximal rumen volume driven by BW and perhaps breed. Passage rate could be modified to include the relative rumen fill as an affecter of the rate of passage.

Ruminal Metabolism

Ruminal pH. Ruminal pH was predicted with a RMSE of 4.6% with 0.4% mean and 4.1% slope bias (Figure 2-3) which was consistent with the previous report after reparameterization of a modified pH prediction equation (Hanigan et al., 2013; Gregorini et al., 2015). However, the CCC was -0.004 (Figure 2-3), indicating that the model explains none of the variance in observed ruminal pH. The predicted ruminal pH ranged from 5.99 to 6.32, while the observed ranged from 5.50 to 6.81, which is four times greater than predicted. Residual analyses indicated that errors were negatively correlated with dietary concentrations of soluble starch and ash and ruminal ammonia concentrations, and positively correlated with dietary ADF and NPN (Table 2-8), implying that the empirical representation of pH in the rumen is not fully representative. According to the Henderson-Hasselbalch equation, ruminal pH should be affected by acid-base relevant factors including H^+ production rates; VFA, lactic acid, bicarbonate, and

ammonia concentrations; partial pressure of CO_2; and the buffering capacity of feed and microbial matter (Dijkstra et al., 2012). The model predicts ruminal pH using only total ruminal VFA and lactate concentrations as described by Argyle and Baldwin (1988). Those equations were subsequently re-parameterized by fitting to a dairy data set by Hanigan et al. (2013), which improved the RMSE. However, the negative correlation between pH residuals and dietary soluble starch implies that the effect of VFA production may be overpredicted when high soluble starch diets are fed.

The positive correlation between pH residuals and dietary ADF suggests ruminal pH was underpredicted with high forage diets, indicating that pH was affected by fiber buffering capacity which is not reflected in the model. Bicarbonate is the most important ruminal buffer, which can enter the rumen through saliva secretion or in the bicarbonate dependent absorption of VFA (Dijkstra et al., 2012). Long forage particles in the diet can affect digesta stratification and promote ruminating and salivary secretion, which helps neutralize the accumulated acids in the rumen (Yang et al., 2001). Considering fiber buffering effects may improve representations of ruminal acid-base balance leading to accurate predictions of ruminal pH.

Ammonia has a high pKa (9.21), and thus is primarily present in the rumen as NH_4^+ (Dijkstra et al., 2012). Abdoun et al. (2007) indicated that at pH of 6.5 or lower, NH_3 is predominately absorbed as NH_4^+ by a putative K channel, which can neutralize acidity through the disposal of NH_4^+. Argyle and Baldwin (1988) adapted the ruminal pH equation from Briggs et al. (1957) where the original equation used total ruminal VFA, lactate, and ammonia concentrations as driving variables. The residuals regression analyses suggested that ammonia concentrations need to be reinstated as a variable to reflect H^+ removal during absorption, and such a change could yield a better representation of ruminal pH predictions. However,

predictions of ruminal ammonia and VFA should be unbiased if such a scheme is to be introduced.

Ruminal VFA Concentrations. Root mean squared errors for total VFA, acetate, propionate and butyrate concentrations were 19.6, 19.7, 35.2, 28.6%, respectively, with an average of 2.1% of MSE as mean bias and 6.8% as slope bias. Although low proportions of error as mean and slope bias were observed, CCC ranged from 0.18 to 0.36 indicating there was a large amount of unexplained variation. All of the VFA concentrations were underpredicted even though ruminal degradation of ADF, NDF and starch were overestimated. The discrepancy in mean biases in VFA and ruminal nutrient degradation predictions suggests that either rates of production or absorption are improperly represented in the model. Although a portion of the residual variation is likely due to sampling variability (Lane et al., 1968), regression analyses indicated that residual errors for each of the VFA concentrations were negatively correlated with ruminal pH (Table 2-8). The model predicts individual VFA from fermentable soluble carbohydrate, hemicellulose and cellulose, dietary amino acids and lactic acid from silage as originally described by Murphy et al. (1982). Production rates of each are influenced by ruminal pH where the yield of propionate is increased, and the yields of acetate and butyrate are reduced with low pH (Argyle and Baldwin, 1988). Thus, the lack of precision in predicting pH seems to be contributing to reduced precision in predicting VFA concentrations. Dijkstra et al. (1993) demonstrated that low ruminal pH supplied more protons for the conversion of the dissociated VFA to the acid form to facilitate diffusion across the rumen epithelium, leading to increased fractional absorption rates. Currently, this mechanism is not encoded in the model and its absence is consistent with the observed residual errors given the negative correlation between ruminal pH and residual VFA concentrations.

All VFA residual errors were also negatively correlated with dietary soluble CP, indicating VFA production errors were also driven by protein fermentation and possibly microbial activity in response to RDP and ammonia. Parker et al. (1995) indicated that the exchange of protons between ammonia and VFA might potentially stimulate their absorption rates, implying that directly adding the effect of ammonia on VFA absorption rates or indirectly in the ruminal pH equation might reduce model errors for VFA concentrations.

Residual errors for all of the VFA were also positively correlated with BW and dietary ash concentrations, suggesting that at high dietary ash concentrations ruminal VFA concentrations were underpredicted. Collectively these indicate that the effects of rumen liquid volume and rumen water dynamics on VFA kinetics might be inappropriately predicted. Dietary ash can be elevated due to soil contamination of forages. Mayland and Sneva (1983) found that the sodium concentration of soil was 1630 μg/g, while that of forages was 93 μg/g, thus dietary sodium and soluble ash content can be influenced by soil contamination. Meyer et al. (2004) indicated dietary sodium intake is positively correlated with water intake, which is consistent with our results, as the increased dietary ash concentrations might stimulate water intake leading to greater liquid outflow and under predicted VFA concentrations. Water consumption was set at 4.7 L/kg DMI. Although the osmotic effects of ash on rumen water dynamics are incorporated in the model, regression results indicated that this relationship is not well represented, which might reflect lack of knowledge regarding ash solubility and the relationship between osmolarity and fluid movement. The latter was based on the effects of sodium bicarbonate, assuming there were two ions per mole of ash, and osmolality from ash was calculated as moles of ash multiplied by an osmolarity of 1.7, which might lead to prediction errors as the composition of ash in rumen fluid varies due to entry of other ions including potassium, calcium, magnesium, and chloride.

Because the soluble ash molecular weight was assumed to be that of sodium bicarbonate, calculated molarity also can be biased. Finally, as only the soluble fraction of ash affects osmolality and water balance, variation in ash solubility would have contributed to variation in predictions of fluid osmolality given our assumed fixed insolubility proportion (Argyle and Baldwin, 1988). Sorting out these potential effects will require a concerted effort to collect such information across a range of diets.

Ruminal Ammonia Concentrations. Ruminal ammonia concentrations exhibited a RMSE of 49.9% with 0.1% of mean bias and 43.7% of MSE segregating with a negative slope bias (Figure 2-4 and Table 2-4). The substantial slope bias implies that mechanisms related to ruminal N metabolism are improperly represented. Residual errors for ruminal ammonia were negatively related with DMI, dietary concentrations of rumen undegraded NDF, forage NDF, rumen undegraded starch, CP, NPN, and ruminal pH, and positively related with dietary concentrations of rumen undegraded ADF, RUP and ash (Table 2-8). The positive correlations with dietary RUP and negative correlations with DMI and dietary concentrations of CP indicates that increased dietary N intake was associated with over predicted ruminal ammonia concentrations; or alternatively, increased dietary RUP was associated with underpredicted ammonia concentrations. These errors might suggest that protein degradation rates saturate with protein availability. Alternatively, the correlations might imply that protein sources affect incorporation rates of ammonia N into microbial N. It seems logical that microbes would obtain a greater proportion of N from ammonia when high RUP diets were fed due to decreased availability of proteolytic end products, however, that is contrary to the observed correlation and thus does not appear to explain the prediction errors.

The negative correlations between residual errors for ruminal ammonia concentrations and rumen undegraded NDF and rumen undegraded starch, imply that ruminal ammonia residual errors are positively correlated with ruminally fermentable CHO, and ammonia concentrations are under predicted when cattle are fed highly fermentable CHO diets and over predicted with high forage diets. Cameron et al. (1991); Reynolds and Kristensen (2008) indicated that the amount and degradability of dietary CHO can affect ammonia absorption, given that incorporation of ammonia N into microbial protein is energy-dependent. Cameron et al. (1991) demonstrated that infusions of readily fermentable CHO decreased ammonia concentrations because of increased N uptake by ruminal microbes. Microbial growth predictions appear to contribute to the problem by being over responsive to fermentable CHO supply as evidenced by negative correlations between residuals for predictions of ruminal microbial N outflow and starch intake. Thus high starch diets would lead to excessive sequestration of ruminal ammonia which contributes to the problem. However, this does not appear to be the sole contributor.

Blood urea-N Concentrations. Predictions of blood urea-N concentrations had a RMSE of 51.8% with 28.8% mean bias and 33.5% negative slope bias (Figure 2-5 and Table 2-4). Residuals of blood urea-N concentrations were negatively correlated with DMI, dietary NDF concentrations, and ruminal ammonia concentrations, and positively correlated with dietary soluble protein concentrations (Table 2-8). The negative correlation between residual blood urea-N concentrations and DMI indicates that blood urea-N concentrations are overpredicted with high DMI, possibly related to high BW (Clauss et al., 2007). Urinary urea excretion is calculated in the model as the product of blood urea concentrations (mole/L) and a fixed excretion constant of 2134 L/d (Baldwin, 1995), implying that the excretion rate constant of a small animal is the same as a large animal at equal blood urea concentrations. This appears to be an oversight in

model construction as kidney clearance will be a function of concentration and body mass reflecting the greater blood flow and kidney mass in a larger animal. Most functions in the model that must scale with BW are defined using the pool size, which will scale with BW, rather than with a concentration, hence our assumption that this was an oversight by whomever added the representation. Modifying the existing urinary urea secretion equation to use blood urea pool size which scales with BW would increase the accuracy of model predictions of blood urea-N and might help address the rumen ammonia problem given the correlation among these two variables.

The negative correlation between blood urea-N residuals and ruminal ammonia concentrations suggests that increased ammonia concentrations are correlated with over predictions of blood urea-N. Reynolds and Kristensen (2008) demonstrated substantial N cycling between the blood urea and gut lumen ammonia pools. High rates of cycling confer greater response flexibility within the system. For example, if the rate of cycling between 2 pools is 100%/d, a 50% change in the first pool and no change in the size of the 2nd pool will result in a 40% change in the net difference between the fluxes. However, if all else is held constant and the cycling rate is increased to 200%/d, the net cycling difference caused by the change in size of the first pool will increase to 80%. Thus accumulation of N in either the ruminal ammonia or the blood urea pools with insufficient responses in the other pool is an indication that the rate of cycling is too low. With too low of cycling rates, increased intake of soluble N would lead to greater than expected changes in ruminal ammonia as the net difference in the rates of transfer between the ruminal and blood pools would not be great enough to buffer the increase in ruminal ammonia. In this case, blood urea concentrations would be under predicted. Increased rates of cycling between ruminal ammonia and blood urea would dampen ruminal ammonia

concentration changes and enhance blood urea changes in response to ruminal N load. Based on concentration changes only, one would be able to derive minimal cycling rates, but not maximal as further increases above the minimum would result in identical concentrations. An exact solution would require fitting to ammonia absorption and urea transfer data derived from isotope experiments such as those using the double-labelled urea approach (Reynolds and Kristensen, 2008; Wickersham et al., 2008a; 2008b; 2009; Bailey et al., 2012a; Batista et al., 2016).

Fecal Output

Fecal DM, ADF, NDF, and Lipid Excretion. Residual errors of predicted fecal DM and ADF excretion were 24.9% and 21.5% with on average 37% mean bias and 8% slope bias. Predicted fecal output of NDF and lipid had RMSE of 22.8 and 31.8% with on average 14% mean bias and 1% slope bias (Table 2-4). Fecal DM and ADF excretion were positively correlated with their predicted ruminal outflow (Table 2-9). Thus as ruminal outflow increased, fecal DM and ADF output were underpredicted, suggesting an ADF digestion coefficient of 0.118 is an overestimate (Hanigan et al., 2013). Residual errors of fecal NDF and lipid outflow were not significantly correlated with their ruminal outflow, indicating prediction errors for fecal NDF and lipid outflow are not driven by encoded digestion coefficients. Further analyses indicated residual errors for fecal output of DM, ADF, and NDF were all negatively correlated with BW, with overpredictions at high BW, and underpredictions at low BW. In the current work, BW ranged from 240 to 807 kg, which is wider than the range of 480 to 731 kg in the data used by Hanigan et al. (2013). Digestive efficiency can be modelled as the result of an interplay of gut capacity, feed intake and digesta passage (Clauss et al., 2007). Of these, capacity is at least partially dictated by BW. Because intestinal digestibility is represented solely as mass action functions of ruminal outflow in the model, correlations between BW and fecal nutrient residual errors likely reflect the lack of a representation of maximal capacity (Ellis et al., 2014), and

indicate that adding BW as an effector of intestinal digestibility would improve model performance with respect to lower gut nutrient digestion.

Fecal Starch Excretion. Predicted fecal starch excretion had a RMSE of 73.4% (2.8% mean bias and 1% slope bias) and a CCC of 0.35 suggesting relatively poor prediction quality (Table 2-4). However, starch digestion occurs predominantly in the rumen and is nearly complete in the total tract. Thus predicting fecal starch excretion is subject to considerable relative error as the mass is relatively small. Residual errors of fecal starch excretion tended to be negatively correlated with predicted ruminal starch outflow ($P = 0.09$) (Table 2-9), suggesting fecal starch excretion is overpredicted with increased ruminal starch outflow. Because there is no slope bias in the predictions, this suggests the cause of a portion of the fecal starch error are errors in predicting ruminal starch outflow. Because the model uses a fixed digestion coefficient of 0.81 to simulate lower gut digestion (Hanigan et al., 2013), optimizing the digestion coefficient will not address the prediction errors. Additional progress in predicting intestinal digestibility may require alternative representations such as the more complicated mechanistic model of Mills et al. (2017).

Fecal Protein Excretion. Residual errors for fecal protein excretion exhibited a RMSE of 18% (0.1% mean bias and 19% slope bias) and a CCC of 0.89 (Table 2-4). Ruminal N outflow had a slight mean bias and slope bias which contributed to fecal error. Residual fecal output errors were positively correlated with predicted ruminal protein outflow (Table 2-9), indicating that fecal protein output is under predicted when ruminal protein outflow is high. This implies that intestinal protein digestion is less efficient at high protein flow than predicted with the current static digestion coefficient. The model does not consider endogenous protein secretion

into the lower gut, but this should result in the opposite problem as the apparent digestion coefficient should increase with greater protein flow.

Evaluations by Cattle Category and Diet Type

Cattle Category. Dairy and beef data were evaluated separately to assess differences between animal type with respect to predictive capacity of the model. Residual analyses indicated that all variables related to ruminal metabolism and nutrient digestion were predicted with lesser RMSE for dairy cattle than for beef cattle (Table 2-5). The model was originally designed to represent biological elements of the dairy cow (Baldwin et al., 1987a; 1987b; 1987c). It has been modified and advanced using primarily dairy data, thus it is to be expected that the model performed better when simulating moderate forage diets typical of those fed to dairy cattle. Root mean squared errors for predictions of ruminal nutrient outflow (total N, microbial N and NAN), fecal nutrient excretion (protein, NDF and lipid), ruminal pH, and ammonia, acetate, propionate, butyrate and blood urea-N concentrations were much greater for beef data than for dairy data (Table 2-5), primarily due to mean biases, suggesting that prediction accuracy could be improved through optimization of model parameters. Substantial slope biases for ruminal outflow of ADF, NDF, starch, total N, and microbial N were observed when beef data were simulated. Regression analyses of residuals indicated that BW was negatively correlated with errors of prediction for ruminal outflow of ADF, NDF, starch, and microbial N, while DMI was positively correlated with residuals for ruminal outflow of DM, starch and microbial N (Table 2-7). These suggest that the combinations of BW and DMI might have contributed to accuracy and precision problems for these variables. When DMI was expressed per kg of BW, the mean was 0.03 kg/kg of BW for dairy cattle and 0.02 kg/kg of BW for beef cattle. One would thus expect greater digestive efficiency for the beef cattle than for dairy cattle due to digestibility depression as DMI increases (Clauss et al., 2007). The current model

represents greater ruminal outflow as DMI increases, but it does not represent reduced ruminal residence time which would alter the extent of digestion. The regressions suggest that the relative DMI should be used to regulate ruminal passage rates so that greater DMI relative to BW causes a reduction in ruminal digestibility.

Diet Type. The nutrient composition of beef cattle diets vary more than dairy cattle diets, due primarily to different feeding scenarios (Ellis et al., 2007). Descriptive statistics show that the mean forage percentage for dairy diets was 51.8% with a standard deviation of 13.4%, whereas it was 29.3% with a standard deviation of 32.1% for beef cattle diets. High forage and low forage diets are more commonly used for beef animals, and limited evaluations of the model have been conducted with such diets. When simulating nutrient digestion and ruminal metabolism for high and low forage diets (Table 2-6), the average RMSE was approximately 5% units greater than for the combined data or when compared to the dairy data which was composed almost completely of moderate forage diets (Table 2-4). Based on the results of RMSE and CCC, the model tended to more accurately predict ruminal metabolism and nutrient flows for high forage diets than low forage diets, except for ruminal outflow of ADF, NDF and microbial N (Table 2-6). However, there was greater slope bias for ammonia and blood urea-N concentrations; and ruminal outflow of ADF, NDF, starch and microbial N when simulating high forage diets. In the model, empirical equations were used to represent the relationship between forage percentage and particle size, and the model simulates three particle size pools with homogenous nutrient content to simulate ruminal digesta outflow. This latter simplification might introduce some error as the large particle pool likely includes more fiber and less starch than the small particle pool. As the pools have different rates of passage, the residence time of starch might be overpredicted and that of fiber underpredicted which could lead to the observed

errors of prediction. In the current study, the model underpredicted ruminal starch outflow and overpredicted ADF and NDF outflow when it was evaluated using high forage diets. The opposite was observed when the model was assessed with low forage diets. These biases equate to an overprediction of ruminal starch digestion and an underprediction ruminal fiber digestion on high forage diets which is consistent with the potential bias in representation of residence time. However, these problems could also reflect the challenges with predicting pH and ruminal ammonia concentrations and the impact on microbial activity. Additional basic metabolic data characterizing the underlying biology is needed to discriminate among these hypotheses and correct the prediction problems.

Conclusions

In summary, the Molly model performed relatively well on diets with moderate levels of forage except for predictions of ruminal pH, ruminal ammonia concentrations which exhibited significant slope bias, and ruminal outflow of starch and NANMN which had poor precision. However, it performed poorer on diets with extreme concentrations of forage, although the number of diets represented in those categories was more limited, and thus subject to less certainty. Model weakness requiring improvements appeared to be related to predictions of ruminal pH and N cycling across the ruminal wall, and digestibility depressions associated with high intakes relative to BW. Residual analyses identified ruminal ammonia concentrations as a factor contributing to ruminal pH prediction errors. Incorporation of the concept of a maximal digestive capacity in the rumen and intestine also merits consideration to improve predictions of ruminal outflow, ruminal fermentation, and fecal output. Adoption of these changes should yield a model that provides unbiased predictions of nutrient digestion across the full range of cattle diets used in North America.

Acknowledgements

This work was funded, in part, by the Virginia Agricultural Experiment Station and the Hatch Program of the National Institute of Food and Agriculture, U.S. Department of Agriculture; the College of Agriculture and Life Sciences Pratt Endowment at Virginia Tech, and the Alberta Livestock and Meat Agency Ltd. (grant 2015F055R).

References

Abdoun, K., F. Stumpff, and H. Martens. 2006. Ammonia and urea transport across the rumen epithelium: a review. Anim. Health Res. Rev. 7(1-2):43-59.

Argyle, J. and R. Baldwin. 1988. Modeling of rumen water kinetics and effects of rumen pH changes. J. Dairy Sci. 71(5):1178-1188.

Bach, A., S. Calsamiglia, and M. Stern. 2005. Nitrogen metabolism in the rumen. J. Dairy Sci. 88:E9-E21.

Bailey, E., E. Titgemeyer, K. Olson, D. Brake, M. Jones, and D. Anderson. 2012. Effects of ruminal casein and glucose on forage digestion and urea kinetics in beef cattle. J. Anim. Sci. 90(10):3505-3514.

Baldwin, R. 1995. Modeling ruminant digestion and metabolism. Springer Science & Business Media.

Baldwin, R. L., J. France, D. E. Beever, M. Gill, and J. H. Thornley. 1987a. Metabolism of the lactating cow: III. Properties of mechanistic models suitable for evaluation of energetic relationships and factors involved in the partition of nutrients. J. Dairy Res. 54(01):133-145.

Baldwin, R. L., J. France, and M. Gill. 1987b. Metabolism of the lactating cow: I. Animal elements of a mechanistic model. J. Dairy Res. 54(01):77-105.

Baldwin, R. L., J. H. Thornley, and D. E. Beever. 1987c. Metabolism of the lactating cow: II. Digestive elements of a mechanistic model. J. Dairy Res. 54(01):107-131.

Bibby, J. and H. Toutenburg. 1977. Prediction and improved estimation in linear models. Wiley.

Boardman, T. J. 1979. Prediction and improved estimation in linear models. Taylor & Francis.

Briggs, P., J. Hogan, and R. Reid. 1957. Effect of volatile fatty acids, lactic acid and ammonia on rumen pH in sheep. Crop and Pasture Sci. 8(6):674-690.

Cameron, M., T. Klusmeyer, G. Lynch, J. Clark, and D. Nelson. 1991. Effects of urea and starch on rumen fermentation, nutrient passage to the duodenum, and performance of cows1. J. Dairy Sci. 74(4):1321-1336.

Cecava, M., N. Merchen, L. Berger, R. Mackie, and G. Fahey. 1991. Effects of dietary energy level and protein source on nutrient digestion and ruminal nitrogen metabolism in steers. J. Anim. Sci. 69(5):2230-2243.

Clauss, M., A. Schwarm, S. Ortmann, W. J. Streich, and J. Hummel. 2007. A case of non-scaling in mammalian physiology? Body size, digestive capacity, food intake, and ingesta passage in mammalian herbivores. Comparative Biochemistry and Physiology Part A: Molecular & Integrative Physiology 148(2):249-265.

Craney, T. A. and J. G. Surles. 2002. Model-dependent variance inflation factor cutoff values. Quality Engineering 14(3):391-403.

Dijkstra, J., H. Boer, J. Van Bruchem, M. Bruining, and S. Tamminga. 1993. Absorption of volatile fatty acids from the rumen of lactating dairy cows as influenced by volatile fatty acid concentration, pH and rumen liquid volume. Br. J. Nutr. 69(2):385-396.

Dijkstra, J., J. Ellis, E. Kebreab, A. Strathe, S. López, J. France, and A. Bannink. 2012. Ruminal pH regulation and nutritional consequences of low pH. Anim. Feed Sci. Technol. 172(1-2):22-33.

Ellis, J., E. Kebreab, N. Odongo, B. McBride, E. Okine, and J. France. 2007. Prediction of methane production from dairy and beef cattle. J. Dairy Sci. 90(7):3456-3466.

Ellis, J., J. Dijkstra, A. Bannink, E. Kebreab, S. Archibeque, C. Benchaar, K. Beauchemin, J. Nkrumah, and J. France. 2014. Improving the prediction of methane production and

representation of rumen fermentation for finishing beef cattle within a mechanistic model. Can. J. Anim. Sci. 94(3):509-524.

Endres, M. and M. Stern. 1993. Effects of pH and diets containing various levels of lignosulfonate-treated soybean meal on microbial fermentation in continuous culture. J. Dairy Sci. 76(Suppl 1):177.

Ghimire, S., P. Gregorini, and M. D. Hanigan. 2014. Evaluation of predictions of volatile fatty acid production rates by the Molly cow model. J. Dairy Sci. 97(1):354-362.

Gregorini, P., P. Beukes, G. Waghorn, D. Pacheco, and M. Hanigan. 2015. Development of an improved representation of rumen digesta outflow in a mechanistic and dynamic model of a dairy cow, Molly. Ecological Modelling 313:293-306.

Griswold, K., G. Apgar, J. Bouton, and J. Firkins. 2003. Effects of urea infusion and ruminal degradable protein concentration on microbial growth, digestibility, and fermentation in continuous culture 1. J. Anim. Sci. 81(1):329-336.

Hanigan, M. 2005. Quantitative aspects of ruminant predicting animal performance. Anim. Sci. 80(01):23-32.

Hanigan, M. D., J. A. Appuhamy, and P. Gregorini. 2013. Revised digestive parameter estimates for the Molly cow model. J. Dairy Sci. 96(6):3867-3885.

Hanigan, M. D., C. C. Palliser, and P. Gregorini. 2009. Altering the representation of hormones and adding consideration of gestational metabolism in a metabolic cow model reduced prediction errors. J. Dairy Sci. 92(10):5043-5056.

Holt, N. and F. Sosulski. 1981. Nonprotein nitrogen contents of some grain legumes. Can. J. Plant Sci. 61(3):515-523.

Huhtanen, P., S. Ahvenjärvi, G. Broderick, S. Reynal, and K. Shingfield. 2010. Quantifying ruminal digestion of organic matter and neutral detergent fiber using the omasal sampling technique in cattle—A meta-analysis1. J. Dairy Sci. 93(7):3203-3215.

Huntington, G. and S. Archibeque. 2000. Practical aspects of urea and ammonia metabolism in ruminants. J. Anim. Sci. 77(E. Suppl.):1-11.

Johnson, H. A. and R. L. Baldwin. 2008. Evaluating model predictions of partitioning nitrogen excretion using the dairy cow model, Molly. Anim. Feed Sci. Technol. 143(1-4):104-126.

Kohn, R. and M. Allen. 1995. In vitro protein degradation of feeds using concentrated enzymes extracted from rumen contents. Anim. Feed Sci. Technol. 52(1-2):15-28.

Kononoff, P. and A. Heinrichs. 2003. The effect of corn silage particle size and cottonseed hulls on cows in early lactation. J. Dairy Sci. 86(7):2438-2451.

Kononoff, P., A. Heinrichs, and H. Lehman. 2003. The effect of corn silage particle size on eating behavior, chewing activities, and rumen fermentation in lactating dairy cows. J. Dairy Sci. 86(10):3343-3353.

Lane, G., C. Noller, V. Colenbrander, K. Cummings, and R. Harrington. 1968. Apparatus for Obtaining Ruminoreticular Samples and the Effect of Sampling Location on pH and Volatile Fatty Acids1. J. Dairy Sci. 51(1):114-116.

Lawrence, I. and K. Lin. 1989. A concordance correlation coefficient to evaluate reproducibility. Biometrics:255-268.

Lofgreen, G., J. Hull, and K. K. Otagaki. 1962. Estimation of empty body weight of beef cattle. J. Anim. Sci. 21(1):20-24.

Maulfair, D., M. Fustini, and A. Heinrichs. 2011. Effect of varying total mixed ration particle size on rumen digesta and fecal particle size and digestibility in lactating dairy cows. J. Dairy Sci. 94(7):3527-3536.

Maulfair, D. and A. Heinrichs. 2013. Effects of varying forage particle size and fermentable carbohydrates on feed sorting, ruminal fermentation, and milk and component yields of dairy cows. J. Dairy Sci. 96(5):3085-3097.

Mayland, H. and F. Sneva. 1983. Effect of soil contamination on the mineral composition of forage fertilized with nitrogen. Journal of range management: 286-288.

Meyer, U., M. Everinghoff, D. Gädeken, and G. Flachowsky. 2004. Investigations on the water intake of lactating dairy cows. Livest. Prod. Sci. 90(2):117-121.

Miller-Webster, T. and W. Hoover. 1998. Nutrient analysis of feedstuffs including carbohydrates. Anim. Sci. Report (1).

Mills, J., J. France, J. Ellis, L. Crompton, A. Bannink, M. Hanigan, and J. Dijkstra. 2017. A mechanistic model of small intestinal starch digestion and glucose uptake in the cow. J. Dairy Sci. 100(6), 4650-4670.

Murphy, M., R. Baldwin, and L. Koong. 1982. Estimation of stoichiometric parameters for rumen fermentation of roughage and concentrate diets. J. Anim. Sci. 55(2):411-421.

NRC. 2001. Nutrient requirements of dairy cattle. 7th ed. National Academy Press, Washington, D.C. National Research Council.

Parker, D., M. Lomax, C. Seal, and J. Wilton. 1995. Metabolic implications of ammonia production in the ruminant. Proc. Nutr. Soc. 54(2):549-563.

Ramirez, H. R., K. Harvatine, and P. Kononoff. 2016. Forage particle size and fat intake affect rumen passage, the fatty acid profile of milk, and milk fat production in dairy cows consuming dried distillers grains with solubles. J. Dairy Sci. 99(1):392-398.

Reynolds, C. and N. B. Kristensen. 2008. Nitrogen recycling through the gut and the nitrogen economy of ruminants: an asynchronous symbiosis. J. Anim. Sci. 86(E. suppl.):E293-E305.

Russell, J. B., J. O'connor, D. Fox, P. Van Soest, and C. Sniffen. 1992. A net carbohydrate and protein system for evaluating cattle diets: I. Ruminal fermentation. J. Anim. Sci. 70(11):3551-3561.

Rustomo, B., O. AlZahal, N. Odongo, T. Duffield, and B. McBride. 2006. Effects of rumen acid load from feed and forage particle size on ruminal pH and dry matter intake in the lactating dairy cow. J. Dairy Sci. 89(12):4758-4768.

Tamminga, S., A. Van Vuuren, C. Van der Koelen, R. Ketelaar, and P. van der Togt. 1990. Ruminal behaviour of structural carbohydrates, non-structural carbohydrates and crude protein from concentrate ingredients in dairy cows. Neth. J. Agri. Sci. 38(3B):513-526.

Thoetkiattikul, H., W. Mhuantong, T. Laothanachareon, S. Tangphatsornruang, V. Pattarajinda, L. Eurwilaichitr, and V. Champreda. 2013. Comparative analysis of microbial profiles in cow rumen fed with different dietary fiber by tagged 16S rRNA gene pyrosequencing. Curr. Microbiol. 67(2):130-137.

Turgeon, O., D. Brink, and R. Britton. 1983. Corn particle size mixtures, roughage level and starch utilization in finishing steers diets. J. Anim. Sci. 57(3):739-749.

Van Soest, P., J. Robertson, and B. Lewis. 1991. Symposium: carbohydrate methodology, metabolism, and nutritional implications in dairy cattle. J. Dairy Sci. 74(10):3583-3597.

White, R., Y. Roman-Garcia, J. Firkins, M. VandeHaar, L. Armentano, W. Weiss, T. McGill, R. Garnett, and M. Hanigan. 2017. Evaluation of the National Research Council (2001) dairy model and derivation of new prediction equations. 1. Digestibility of fiber, fat, protein, and nonfiber carbohydrate. J. Dairy Sci. 100(5):3591-3610.

Wickersham, T., E. Titgemeyer, and R. Cochran. 2009. Methodology for concurrent determination of urea kinetics and the capture of recycled urea nitrogen by ruminal microbes in cattle. Animal 3(3):372-379.

Wickersham, T., E. Titgemeyer, R. Cochran, E. Wickersham, and D. Gnad. 2008a. Effect of rumen-degradable intake protein supplementation on urea kinetics and microbial use of recycled urea in steers consuming low-quality forage. J. Anim. Sci. 86(11):3079-3088.

Wickersham, T., E. Titgemeyer, R. Cochran, E. Wickersham, and E. Moore. 2008b. Effect of frequency and amount of rumen-degradable intake protein supplementation on urea kinetics and microbial use of recycled urea in steers consuming low-quality forage. J. Anim. Sci. 86(11):3089-3099.

Yang, W., K. Beauchemin, and L. Rode. 2001. Effects of grain processing, forage to concentrate ratio, and forage particle size on rumen ph and digestion by dairy cows1. J. Dairy Sci. 84(10):2203-2216.

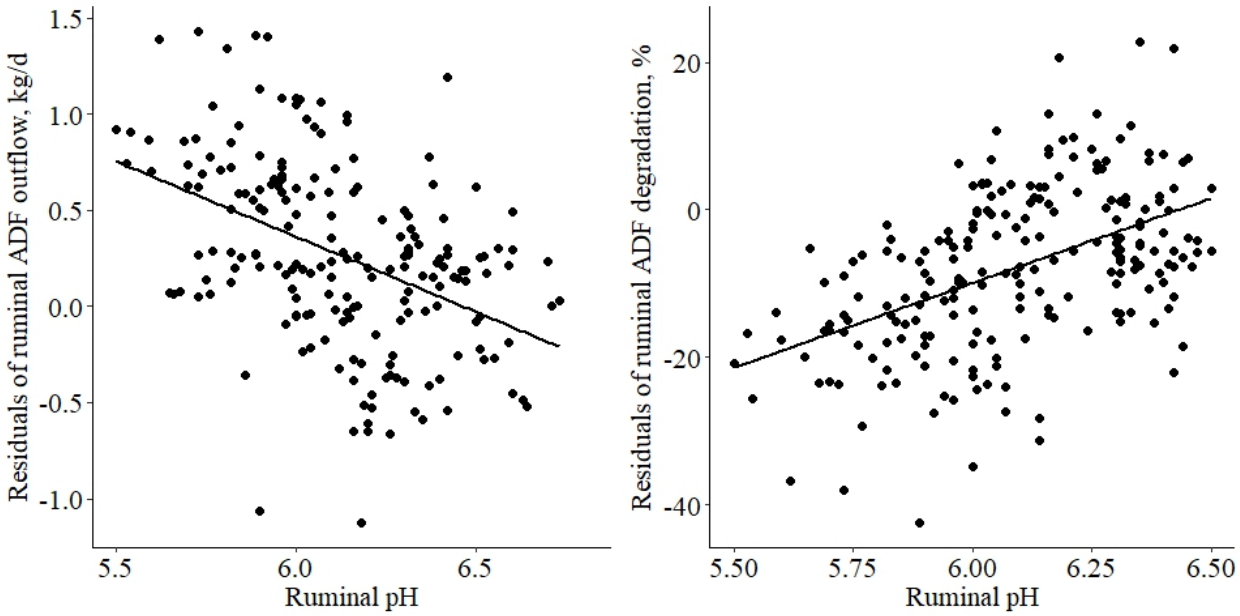

Figure 2-1. Residuals for ruminal ADF outflow (kg/d) or degradation (%) versus ruminal pH.

Residuals are calculated as observed minus predicted values.

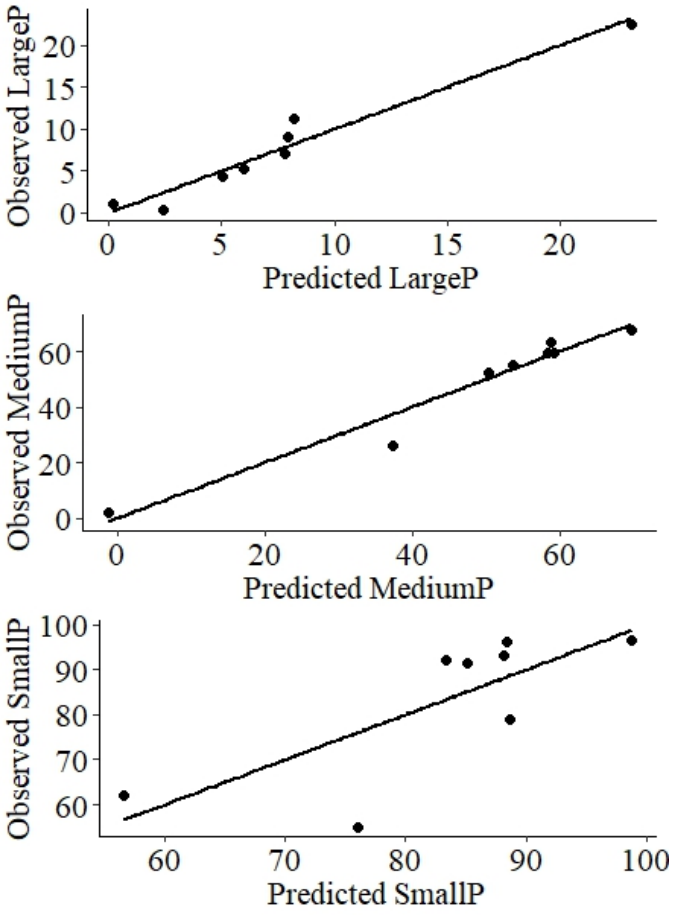

Figure 2-2. Observed versus predicted accumulated percentages of particles. LargeP (% of DM retained) is the cumulative percentage of particles retained above the 19.05 mm sieve; MediumP (% of DM retained) is the cumulative percentage of particles retained above the 7.87 mm sieve; and SmallP (% of DM retained) represents the cumulative percentage of particles retained above the 1.78 mm sieve. LargeP, MediumP and SmallP were predicted with a root mean squared error of 19.2, 9.5 and 11.8%, and a concordance correlation coefficient of 0.98, 0.98 and 0.74.

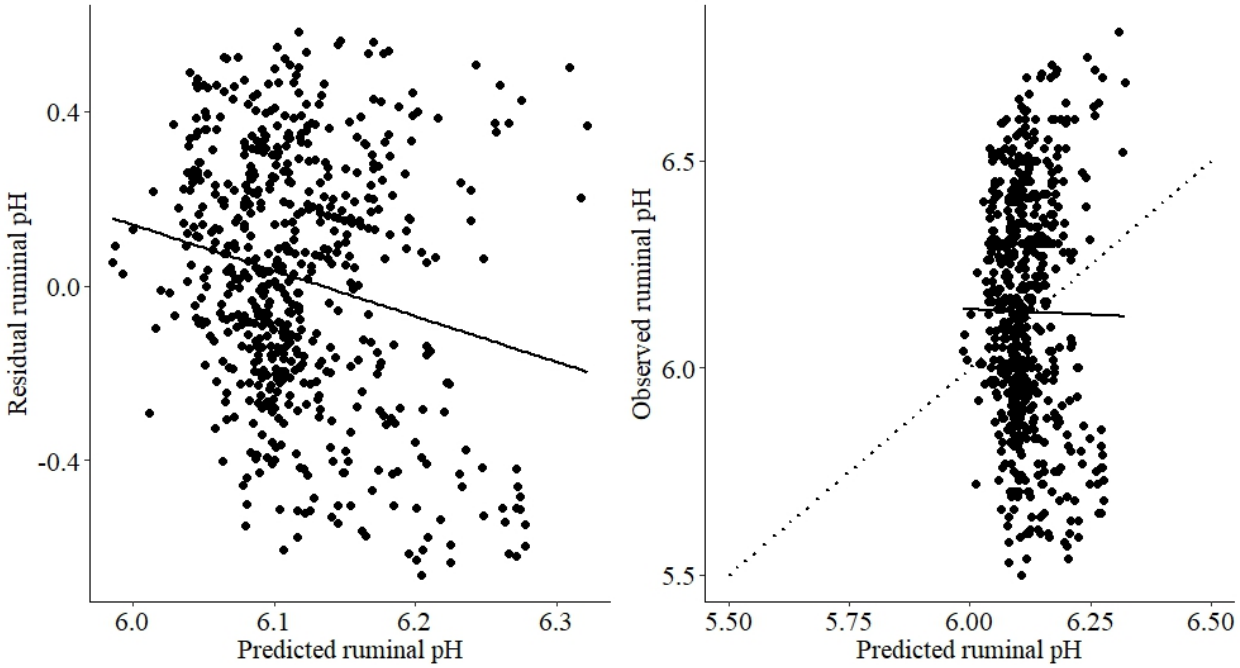

Figure 2-3. Observed or residual ruminal pH for predictions of ruminal pH (Concordance correlation coefficient = -0.004, root mean squared error = 4.6%, mean bias = 0.4% MSE, slope bias = 4.1% MSE, n = 611). MSE represents mean squared error; the solid line represents the regression line, and the dotted line represents the line of unity.

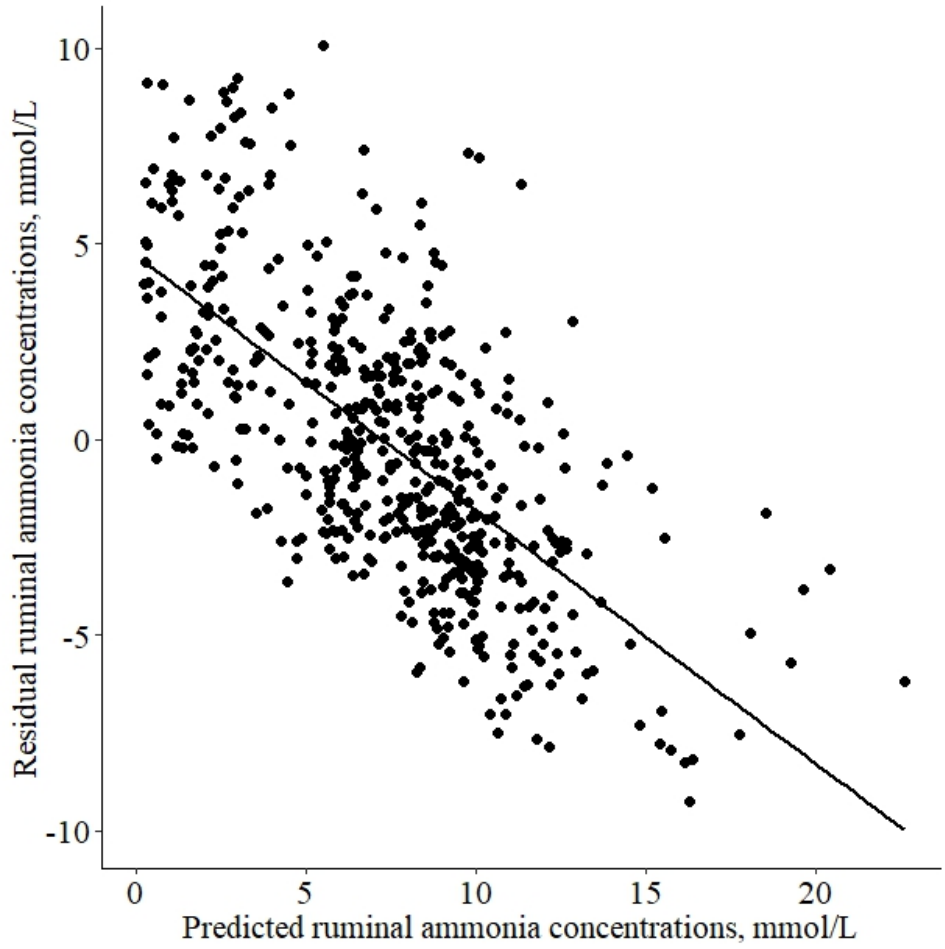

Figure 2-4. Residual errors for predicted ruminal ammonia concentrations (root mean squared error = 49.9%, mean bias = 0.1% MSE, slope bias = 43.7% MSE, n = 538). MSE represents mean squared error.

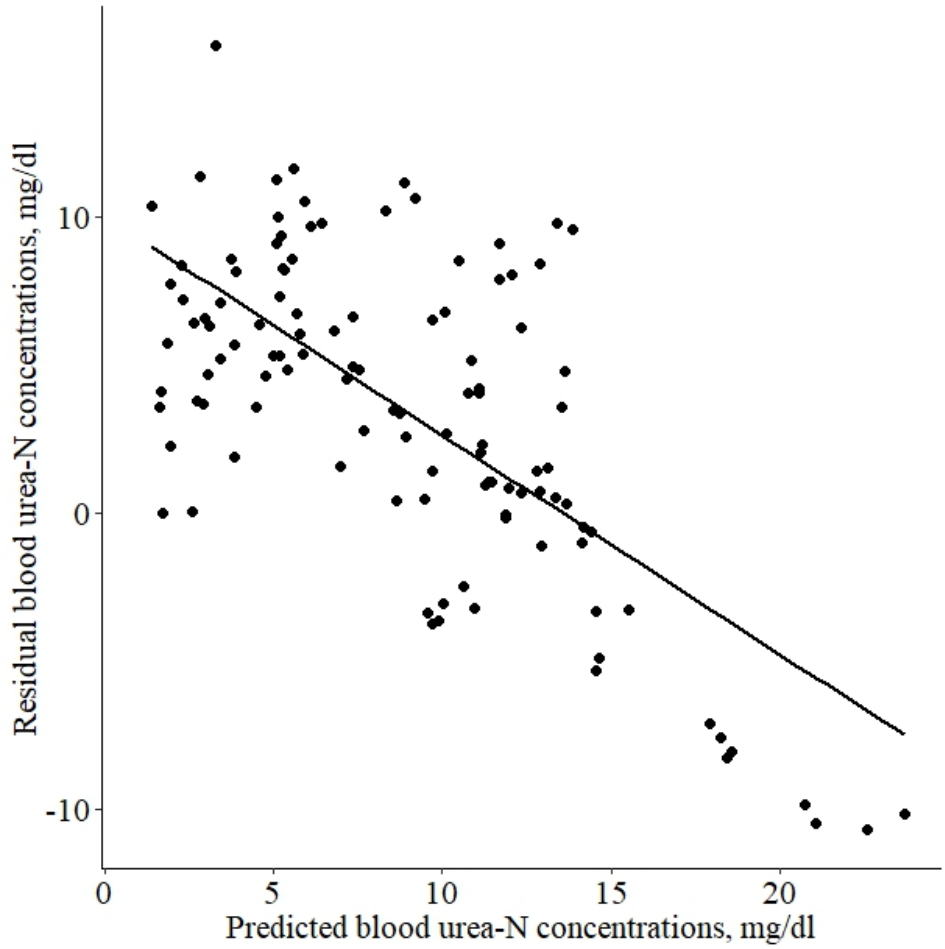

Figure 2-5. Residual errors for predicted blood urea-N concentrations (root mean squared errors = 51.8%, mean bias = 28.8% MSE, slope bias = 33.5% MSE, n=114). MSE represents mean squared error.

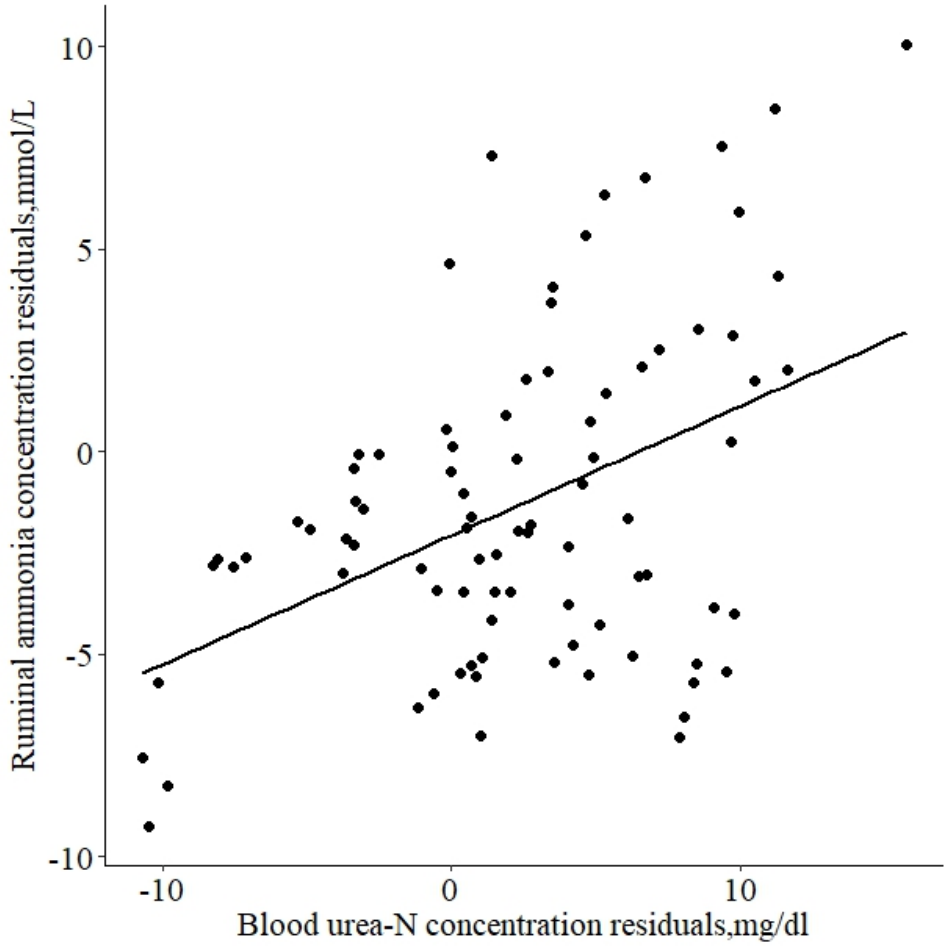

Figure 2-6. Ruminal ammonia concentration residuals versus blood urea-N concentration residuals.

Table 2-1. Observed nutrient intakes, ruminal digestibility, ruminal outflow and metabolism, and total tract digestibility.

Items	N	Mean	SD	Min	Max
Body weight, kg	886	548	117	240	807
Intake, kg/d					
DM	938	15.3	6.2	3.0	30.4
OM	632	15.9	5.3	2.8	29.5
ADF	353	3.5	1.4	0.3	6.7
NDF	538	5.9	2.2	1.0	12.4
Starch	346	5.2	2.0	0.2	11.0
Ruminal digestibility, %					
OM	473	57.2	10.7	19.6	84.2
Nitrogen	320	56.6	13.7	9.2	91.0
ADF	273	40.3	12.8	6.2	77.5
NDF	459	44.4	13.0	4.8	84.4
Starch	292	66.0	18.5	4.5	94.2
Lipid	39	9.0	9.9	-17	26.2
Ruminal outflow, kg/d					
DM	152	13.7	4.1	2.2	24.2
OM	430	10.2	4.1	1.7	20.6
ADF	225	2.2	0.9	0.2	4.2
NDF	342	3.4	1.3	0.7	6.5
Starch	225	2.2	1.5	0.03	5.8
Lipid	30	1.0	0.4	0.5	2.0
Total N	510	0.5	0.2	0.07	1.0
Microbial N	625	0.3	0.1	0.05	0.7
Non-ammonia N	566	0.5	0.2	0.07	1.1
Non-ammonia, non-microbial N	560	0.2	0.1	0.01	0.6
Rumen fermentation					
pH	611	6.1	0.3	5.5	6.8
Ammonia,mg/dl	538	12.4	5.1	0.1	30.3
Blood urea-N, mg/dl	114	12.3	4.2	1.7	23.4
Total VFA, mM	584	108.8	21.9	37.1	161
Acetate, % of VFA	629	60.9	6.6	36.4	77.3
Proionate, % of VFA	629	23.2	6.0	12.5	44.0
Butyrate, % of VFA	629	11.7	2.0	5.7	19.9
Total tract digestibility, %					
DM	396	68.9	6.5	48.2	85.7
OM	606	70.9	6.8	43.8	87.4
Nitrogen	560	67.88	5.2	51.5	82.0
ADF	326	45.2	11.6	11.9	77.2
NDF	546	51.0	11.5	13.2	84
Starch	312	92.6	6.7	68.4	99.7
Lipid	92	72.1	13.8	20.9	93.6

Table 2-2. Nutrient composition of low, moderate, and high forage diets[1].

Items	Low Forage		Moderate Forage		High Forage	
	Mean	SD	Mean	SD	Mean	SD
CP, %	15.1	3.2	16.8	2.4	15.7	4.5
Fat, %	4.7	1.8	3.9	1.7	2.7	0.7
Starch, %	47.5	11.3	30.6	7.7	19.7	9.9
NDF, %	21.2	8.6	33.4	6.4	50.9	13.5
ADF, %	10.6	5.2	20.1	4.6	32.7	10.3
Lignin, %	2.4	1.2	3.5	1.0	4.9	1.6

[1] Both dairy and beef data were included in the low, moderate, and high forage diets.

Table 2-3. Consequence of dietary nutrient bias adjustments on predicted dietary nutrient composition.

Items	CP, %		NDF, %		ADF, %	
	Initial	Final	Initial	Final	Initial	Final
Observed Mean	17.1	17.1	32.9	32.9	19.5	19.5
Predicted Mean	17.2	17.2	32.0	32.3	20.3	20.1
RMSE[1], % mean	11.2	8.9	13.8	10.8	18.5	14.1
Mean Bias, % MSE[2]	0.3	0.6	4.0	3.3	5.6	4.6
Slope Bias, % MSE	32.8	21.3	13.0	5.8	12.3	3.8
Residual Error, % MSE	66.9	78.2	83.1	90.9	82.1	91.6

[1] Root mean squared error
[2] Mean squared error

Table 2-4. Model evaluations using a combination of dairy and beef data.

Items	n	Observed mean	Predicted mean	RMSE[1], % mean	Mean Bias, % MSE[2]	Slope Bias, % MSE	CCC
Ruminal outflow, kg/d							
DM	152	13.7	12.3	17.9	34.3*	13.8*	0.77
ADF	225	2.2	1.9	25.8	25.0*	0.02	0.75
NDF	342	3.4	3.0	26.3	11.9*	0.2	0.73
Starch	225	2.2	1.6	60.5	19.8*	1.8*	0.41
Lipid	30	1.0	1.0	14.1	0.3	0.3	0.92
Total N	510	0.5	0.5	19.4	3.8*	2.5*	0.83
Microbial N	625	0.3	0.3	30.5	18.4*	0.01	0.66
Non-ammonia N	566	0.5	0.5	19.2	0.004	3.9*	0.78
NANMN[3]	560	0.2	0.2	40.3	24.4*	0.2	0.44
Ruminal fermentation parameters							
pH	611	6.1	6.1	4.6	0.4	4.1*	-0.004
Ammonia, mmol/L	538	7.3	7.4	49.9	0.1	43.7*	0.42
VFA, mmol/L	584	108.8	103.0	19.6	7.3*	5.0*	0.36
Acetate, mmol/L	598	66.3	65.4	19.7	0.4	2.9*	0.35
Propionate, mmol/L	592	24.8	24.6	35.2	0.1	8.6*	0.18
Butyrate, mmol/L	592	12.8	12.6	28.6	0.5	10.8*	0.23
Blood urea-N, mg/dl	114	12.3	8.9	51.8	28.8*	33.5*	0.24
Fecal outflow, kg/d							
DM	391	5.2	4.3	24.9	49.3*	13.7	0.84
OM	527	4.6	3.8	26.4	43.3	9.5	0.79
Protein	500	0.9	0.9	18.6	0.1	19.0	0.89
ADF	243	1.9	1.7	21.5	24.9*	1.5	0.88
NDF	445	2.8	2.6	22.8	7.2*	0.3	0.85
Lipid	78	0.2	0.3	31.8	19.8*	1.5	0.86
Starch	261	0.3	0.3	73.4	2.8*	1.0	0.35

[1] Root mean squared error
[2] Mean squared error
[3] Non-ammonia, non-microbial N
* denotes model bias is significantly different from 0 ($P < 0.05$).

Table 2-5. Model evaluations by cattle category[1].

Items	n		RMSE[2], % mean		Mean Bias, % MSE[3]		Slope Bias, % MSE		CCC	
	Dairy	Beef	Dairy	Beef	Dairy	Beef	Dairy	Beef	Dairy	Beef
Ruminal outflow, kg/d										
ADF	204	21	24.9	44.6	29.5*	5.0	1.1	22.1*	0.65	0.56
NDF	299	43	25.6	27.8	13.7*	0.5	1.7*	20.2*	0.6	0.66
Starch	180	45	56.7	82.8	29.4*	11.7*	0.1	54.0*	0.29	0.002
Total N	440	70	18.1	39.1	7.9*	20.1*	0.3	32.1*	0.74	0.29
Microbial N	557	68	29.1	57.0	18.4*	19.3*	0.5	34.0*	0.56	0.13
NAN	540	26	18.6	58.9	0.2	59.1*	1.9*	11.2*	0.75	0.09
NANMN[4]	536	24	39.9	40.7	25.7*	0.4	0.8*	1.0	0.38	0.57
Ruminal fermentation parameters										
pH	452	159	4.1	6.0	6.5*	9.6*	0.003	0.4	0.04	0.03
Ammonia, mmol/L	430	108	44.9	67.4	10.1*	55.9*	26.6*	11.2*	0.46	0.27
VFA, mmol/L	430	154	16.9	27.0	3.7*	18.5*	3.2*	1.5	0.23	0.25
Acetate, mmol/L	432	166	18.4	23.8	0.3	0.9	2.5*	8.4*	0.16	0.26
Propionate, mmol/L	432	160	28	48.7	7.8*	22.5*	2.6*	0.9	0.21	0.21
Butyrate, mmol/L	432	160	24.2	39.5	1.2*	16.0*	5.7*	1.9	0.17	0.17
Blood urea-N, mg/dl	74	40	44	65.3	5.6*	90.5*	37.8*	2.8*	0.25	0.16
Fecal outflow, kg										
DM	255	136	22.7	30.4	65.4*	19.3*	2.2*	15.3*	0.58	0.61
OM	389	138	24.8	29.9	56.9*	5.9*	0.8*	11.0*	0.59	0.71
Protein	372	128	15.7	39.3	3.5*	39.6*	10.6*	0.04	0.81	0.61
ADF	186	57	19.6	35.5	30.9*	6.3	0.2	3.6	0.75	0.72
NDF	333	112	19.7	44.7	6.2*	11.0*	1.0	3.7*	0.72	0.57
Lipid	53	25	23.5	84.9	12.9*	36.6*	1.6	10.1*	0.84	0.32
Starch	156	105	64.8	95.9	7.3*	0.5	4.9*	10.7*	0.17	0.18

[1] Ruminal DM outflow was not reported because of limited observations.
[2] Root mean squared error
[3] Mean squared error
[4] Non-ammonia, non-microbial N
* denotes the model bias is significantly different from 0 ($P < 0.05$).

Table 2-6. Model evaluations by diet type[1].

Items	n		RMSE[2], % mean		Mean Bias, % MSE[3]		Slope Bias, % MSE		CCC	
	High	Low	High	Low	High	Low	High	Low	High	Low
Ruminal outflow, kg/d										
DM	8	13	16.6	16.6	1.9	3.6	37.5*	38.5*	0.92	0.84
ADF	12	18	34.5	25.8	3.4	47.5*	58.4*	12.7*	0.42	0.91
NDF	23	29	37.4	21.8	8.3	5.5	40.9*	12.0*	0.73	0.93
Starch	2	37	10.0	74.1	32.9*	6.8	67.1*	18.7*	0.99	0.38
Total N	34	52	26.4	28.0	16.3*	0.8	12.8*	33.5*	0.80	0.88
Microbial N	45	60	43.4	42.3	0.004	36.3*	17.5*	0.7	0.52	0.74
Non-ammonia N	32	36	20.8	30.3	0.005	9.1	4.4	22.1*	0.72	0.85
NANMN[4]	35	31	32	36.2	21.3*	14.2*	0.02	14.7*	0.7	0.83
Ruminal fermentation parameters										
pH	58	92	4.9	6.7	59.4*	54.5*	4.6*	3.3*	0.14	-0.01
Ammonia, mmol/L	54	65	52.2	66.8	4.3	68.3*	40.1*	5.4*	0.75	0.20
VFA, mmol/L	62	85	22.0	28.1	2.4	41.9*	0.8	4.2*	0.60	0.10
Acetate, mmol/L	62	101	24.2	27.1	1.8	2.4	0.01	17.1*	0.45	0.01
Propionate, mmol/L	62	89	34.0	49.2	43.2*	39.9*	4.7*	1.7	0.57	0.03
Butyrate, mmol/L	62	89	35.0	38.8	8.0*	14.6*	1.6	14.3*	0.55	-0.04
Blood urea-N, mg/dl	24	19	67.8	61.5	8.9	88.8*	79.5*	0.1	0.34	0.11
Fecal output, kg										
DM	42	88	25.7	33.3	2.1	12.0*	6.5	48.1*	0.90	0.85
OM	36	100	29.8	31.1	23.0*	3.3	0.6	37.1*	0.78	0.88
Protein	30	98	19.3	36.2	2.1	25.1*	0.2	18.7*	0.94	0.8
ADF	15	38	27.4	32.4	61.9*	23.9*	22.9*	63.2*	0.74	0.93
NDF	39	73	41.0	33.6	0.004	9.4*	16.6*	0.03	0.66	0.89

[1]High forage diet: forage percentage > 70%; Low forage diet: forage percentage < 30%. Fecal lipid and starch output were not reported because of limited observations.

[2] Root mean squared error

[3] Mean squared error

[4] Non-ammonia, non-microbial N

* denotes the model bias is significantly different from 0 ($P < 0.05$).

Table 2-7. Multivariate regression analyses of residual errors for predicted ruminal outflow[1].

Independent variables	Predicted ruminal outflow							
	DM (kg/d)	ADF (kg/d)	NDF (kg/d)	Starch (kg/d)	Nitrogen (g/d)	Microbial N (g/d)	NAN[2] (g/d)	NANMN[3] (g/d)
Intercept	-4.23	6.71	7.95	0.41	366.66	-137.4	411.7	334.7
Animal parameters								
BW, kg	0.005 (1.4)[4]	-0.001 (1.1)	-0.001 (1.2)	-0.002 (1.6)		-0.21 (1.7)	-0.25 (1.3)	
DMI, kg	0.16 (1.9)			0.09 (2.2)		3.78 (2.0)	7.68 (1.6)	
Dietary parameters								
ADF	-0.11 (1.8)		0.03 (4.6)			-2.0 (2.7)		
Rumen undegraded ADF				-0.11 (5.0)				-2.40 (1.2)
NDF			-0.03 (5.1)	0.11 (3.1)			-6.46 (2.9)	
Forage NDF		-0.005 (1.2)	0.01 (1.1)	0.01 (1.7)	0.96 (1.5)		-1.40 (4.1)	-0.46 (1.3)
Starch								
Soluble starch				0.05 (2.1)	6.64 (1.5)			
Rumen undegraded starch	-0.21 (1.6)	0.04 (1.2)	0.06 (2.1)					
CP			-0.07 (2.2)	0.08 (2.0)		4.77 (3.3)		
Soluble CP	-0.29 (1.4)					-9.68 (3.0)		
RUP	0.35 (1.2)					-7.05 (1.9)	-4.74 (1.3)	
NPN		0.04 (1.2)					8.45 (1.6)	11.2 (1.4)
Urea		-0.32 (1.1)						-24.3 (1.1)
Lipid	0.27 (1.1)		0.14 (1.1)				-9.15 (1.1)	-3.97 (1.0)
Lignin				-0.42 (2.5)	10.54 (1.4)	9.38 (1.7)	10.77 (2.2)	
Ash		0.04 (1.1)				-6.69 (1.4)	-13.03 (1.3)	
Roughage	0.03 (1.7)					1.18 (2.5)	2.20 (5.0)	
Ruminal fermentation parameters								
Ruminal pH		-1.0 (1.1)	-1.1 (1.2)	-0.69 (1.4)	-60.39 (1.2)	30.0 (1.6)	-36.2 (1.4)	-38.6 (1.3)
Ruminal ammonia, mmol/L		-0.06 (1.2)	-0.04 (1.8)		-3.26 (1.2)		-6.11 (1.3)	-5.63 (1.2)
R^2	0.49	0.44	0.33	0.41	0.13	0.13	0.31	0.13
RMSE[4]	1.5	0.38	0.69	0.96	83.85	68.82	79.68	64.85
P value	< 0.0001	< 0.0001	< 0.0001	< 0.0001	< 0.0001	< 0.0001	< 0.0001	< 0.0001

[1]Study effect was included as a random variable.
[2]Non-ammonia, non-microbial N
[3]Independent variables listed were significant ($P < 0.1$). Variance inflation factors (VIF) are shown in parentheses.
[4]Root mean squared error

Table 2-8. Multivariate regression analyses of residual errors for predicted ruminal and blood metabolites[1].

Independent variables	Predicted ruminal metabolites						
	pH	Ammonia (mmol/L)	VFA (mmol/L)	Acetate (mmol/L)	Propionate (mmol/L)	Butyrate (mmol/L)	Blood urea-N (mg/dl)
Intercept	-0.02	20.32	200.47	63.5	99.12	34.45	19.62
Animal parameters							
BW, kg			0.03 (1.5)[2]	0.03 (1.1)	0.01 (1.4)	0.01 (1.3)	
DMI, kg		-0.23 (1.5)	-0.43 (2.1)		-0.40 (1.8)	-0.20 (1.8)	-0.51 (2.7)
Dietary parameters							
ADF					0.22 (5.2)		
Rumen undegraded ADF	0.02 (1.8)	0.15 (3.5)					
NDF		-0.08 (3.7)	-0.46 (2.1)	-0.23 (2.3)	-0.31 (4.8)	-0.07 (2.2)	-0.22 (1.4)
Forage NDF		-0.01 (1.8)		0.07 (1.9)	-0.03 (1.9)		
Starch				-0.14 (3.0)		-0.10 (2.9)	
Soluble starch	-0.01 (2.1)						
Rumen undegraded starch		-0.11 (2.0)	-0.71 (2.1)				
CP		-0.33 (2.5)	1.61 (2.9)	0.98 (3.4)	0.43 (3.0)		
Soluble CP			-3.22 (2.4)	-1.77 (3.3)	-1.45 (3.0)	-0.45 (1.8)	0.60 (4.8)
RUP		0.17 (1.5)	-2.00 (1.7)	-1.99 (1.8)	-0.63 (1.9)	-0.25 (1.3)	
NPN	0.04 (1.3)	-0.52 (2.7)					
Urea				-4.17 (1.2)			
Lipid					0.34 (1.1)		
Lignin			2.22 (1.7)		0.62 (1.8)	-0.41 (1.7)	
Ash	-0.01 (1.4)	0.20 (1.4)	1.39 (1.4)	0.59 (1.4)	0.48 (1.4)	0.20 (1.4)	
Roughage							
Ruminal fermentation parameters							
Ruminal pH		-1.61 (1.3)	-32.79 (1.5)	-11.70 (1.4)	-14.48 (1.4)	-4.3 (1.4)	
Ruminal ammonia, mmol/L	-0.02 (1.1)		0.72 (1.5)	0.90 (1.5)		0.12 (1.4)	-0.49 (6.8)
R^2	0.28	0.54	0.35	0.22	0.53	0.29	0.60
RMSE[3]	0.23	2.44	15.9	11.48	5.96	3.08	3.56
P value	< 0.0001	< 0.0001	< 0.0001	< 0.0001	< 0.0001	< 0.0001	< 0.0001

[1] Study effect was included as a random variable.
[2]Independent variables listed were significant ($P < 0.1$). Variance inflation factors (VIF) are shown in parentheses.
[3]Root mean squared error

Table 2-9. Simple linear regression analyses of residual errors for predicted fecal outputs.

Regression variable	Predicted fecal outputs (kg/d)					
	DM	Protein	ADF	NDF	Starch	Lipid
Intercept	-0.38 (< 0.001)[1]	-0.23 (< 0.001)	0.09 (0.11)	0.26 (<0.001)	0.09 (0.008)	-0.05 (0.004)
Predicted ruminal DM outflow, kg/d	0.13 (< 0.001)					
Predicted ruminal protein outflow, kg/d		0.08 (< 0.001)				
Predicted ruminal ADF outflow, kg/d			0.06 (0.03)			
Predicted ruminal NDF outflow, kg/d				-0.03 (0.21)		
Predicted ruminal starch outflow, kg/d					-0.03 (0.09)	
Predicted ruminal lipid outflow, kg/d						0.02 (0.22)
R^2	0.31	0.19	0.02	0.003	0.01	0.02
RMSE[2]	0.76	0.15	0.35	0.62	0.23	0.007
P value	< 0.0001	< 0.0001	0.03	0.21	0.09	0.23

[1]*p* value is shown in parentheses.
[2]Root mean squared error

Chapter 3: A revised representation of urea and ammonia nitrogen recycling and use in the Molly cow model

Abstract

Accurately predicting nitrogen (N) digestion, absorption and metabolism will allow formulation of diets that more closely match true animal needs from a broad range of feeds thereby allowing maximization of N utilization, N efficiency, and profit. The objectives of this study were to advance representations of N recycling between blood and the gut and urinary N excretion in the Molly cow model. The current work includes enhancements 1) representing ammonia passage to the small intestine; 2) deriving parameters defining urea synthesis and ruminal urea entry rates; 3) adding representations of intestinal urea entry, microbial protein synthesis in the hindgut, and fecal urea N excretion; and 4) altering existing urinary N excretion equations to scale with BW, and adding purine derivatives as a component of urinary N excretion. After the modifications, prediction errors for ruminal outflows of total N, microbial N, and non-ammonia non-microbial N were 39.5, 27.8 and 35.9% of the respective observed mean values. Prediction errors of each were approximately 10% units less than the corresponding values before model modifications and fitting due primarily to decreased slope bias. The revised model predicted ruminal ammonia and blood urea concentrations with substantially decreased overall error and reductions in slope and mean bias. Prediction errors for gut urea N entry were 36.3% with 4.9% mean bias and 1.2% slope bias which was also a substantial improvement. Adding purine derivatives to urinary N predictions significantly improved the accuracy of predictions of total urinary N output. However, urinary urea N secretion remains poorly predicted with 55.6% prediction errors due mostly to overestimated urea N entry rates. Adding representations of undigested microbial nucleic acids, microbial protein synthesized in the hindgut and urea N excretion in the feces decreased prediction errors for fecal N excretion from 48.9 to 30.2%. The revised model predicts that urea N entry into blood accounts

for approximately 64% of dietary N intake of which 55% is recycled to gut lumen. Between 48 and 67% of the urea recycled to the gut flows into the rumen largely depending on diets, which accounts for 23 to 63% of total ruminal ammonia production, and 64 to 71% of this ammonia N is captured in microbial protein. Model simulation results suggested that feeding a moderately low CP, high RUP diet could increase ruminal N efficiency by 20%.

Key words: efficiency; model; nitrogen;

Introduction

The ability to recycle urea N to the rumen represents an evolutionary advantage of ruminants allowing them to efficiently utilize N, especially during periods of dietary protein deficiency. Baldwin and coworkers included concepts and essential features of N metabolism in a mathematical model of the dairy cow named Molly (Baldwin et al., 1987a; 1987b; 1987c), allowing researchers to evaluate different management strategies and feeding practices before implementation. Hanigan et al. (2013) reported biased predictions of ruminal ammonia concentrations and microbial N outflow, and Li et al. (2018) observed high proportions of ruminal ammonia and blood urea prediction errors due to slope bias. The latter work identified improper representations of urinary urea N secretion and urea N cycling between blood and the rumen as the primary drivers of the ammonia and blood urea prediction errors.

To address existing model problems, measurements of gut urea entry and urinary urea secretion rates are necessary to uniquely define N recycling between the rumen and blood and to define urea balance. Lobley et al. (2000) described a double labelled urea approach to measure urea kinetics in ruminants, and developed a mass movement model to estimate flux rates. The application of this approach has resulted in the generation of a significant number of flux

observations in cattle in the last 20 years, which can be used to examine model assumptions and address potential errors in the model.

The objectives of this study were to update the representations of N cycling across the gut, fecal N excretion, and urinary N secretion in the model to more closely reflect the underlying biology, and to evaluate model prediction accuracy with respect to N and urea kinetics. The work included 1) representing ammonia passage to the small intestine; 2) deriving parameters defining urea synthesis and ruminal urea entry rates; 3) adding representations of intestinal urea entry rate, microbial protein synthesis in the hindgut, and fecal urea excretion; 4) altering the existing urinary N excretion equations to scale with BW, and adding purine derivatives as a component of urinary N excretion. We hypothesized that these updates would result in significant improvements in predictions of ruminal N cycling, microbial outflow from the rumen, and urinary N excretion.

Materials and Methods

Data Collection

Observations of total urea entry, gut urea entry, and urinary urea elimination rates were collected from 15 published papers (Archibeque et al., 2001; 2002; Ruiz et al., 2002; Marini and Van Amburgh, 2003; Wickersham et al., 2008a; Wickersham et al., 2008c; Wickersham et al., 2009; Brake et al., 2010; Brake et al., 2011; Bailey et al., 2012b; a; Titgemeyer et al., 2012; Davies et al., 2013; Holder et al., 2015; Batista et al., 2016) representing 69 treatment means. The only selection criteria was that the work was conducted in cattle. Three of the studies were conducted using dairy cattle, and 12 studies were conducted using beef cattle. The observed data are summarized in Table 3-1.

Model Description

The mechanistic and dynamic functions of the Molly model pertaining to ruminal urea N recycling and urinary urea elimination have been described by Baldwin (1995). A schematic of the key elements is presented in Figure 3-1. As an overview, dietary insoluble protein degradation in the rumen is defined as the balance between rates of degradation and passage. Microbes in the rumen utilize a portion of the soluble protein and AA and ammonia to support microbial growth, and they also catabolize an additional portion of the protein and AA resulting in release of ammonia. Urea entering the rumen is quantitatively converted to ammonia. Mass action functions are employed to simulate insoluble protein degradation, microbial metabolism of soluble N, ruminal ammonia absorption, intestinal protein digestion, AA absorption, hepatic urea synthesis, and urinary urea excretion. Microbial growth and urea recycled to the rumen through ruminal epithelium, and utilization for anabolic purposes are represented using Michaelis-Menten equations. Conversions among urea, ammonia, and AA are estimated stoichiometrically with adherence to mass balance principles. Concentrations of the key metabolites are predicted at any point in time as state variables in a system of ordinary differential equations, which are numerically integrated over time. State variables include ammonia, soluble protein and AA, insoluble protein and microbes in the rumen, as well as urea and AA in the blood. These mathematical equations are encoded in and solved using ACSL (ver. 3.1.4.2, Aegis Technologies Group Inc., Huntsville, AL).

Model inputs were prepared as previously described (Li et al., 2018a) with some modifications. Briefly, dietary nutrient composition (DM, protein, ADF, NDF, lignin, crude fat, starch, and ash) was generated for each treatment by summation of feed values according to the dietary formulas. If the nutrient composition of the constituent ingredients was reported, those values were used, otherwise tabular values from an integrated feed library were used in place of

the missing values. The feed library was generated from the NRC (2001) feed library, a library derived from commercial laboratory data (collected by the National Animal Nutrition Program; www.animalnutrition.org) (Tran et al., 2016), and the CNCPS feed library. Order of use to construct the integrated library gave preference to the commercial library, followed by the NRC 2001 library, and the CNCPS library. Mean nutrient bias was calculated for each nutrient (OM, protein, ADF, NDF, crude fat, and starch) across diets within each study as the difference between calculated dietary nutrient inputs and those reported in the publication when available (Hanigan et al. (2013). The relative bias for the study was used to adjust the nutrient content of each ingredient weighted for the contribution of that ingredient to the dietary nutrient sum for the study. This retained the ingredient level information while reducing dietary mis-specifications and avoiding the introduction of nutrient bias. Rumen protein and starch degradation were calculated following White et al. (2017a; 2017b). Rumen ADF degradation was generated using the same data set and statistical approach as White et al. (2017b):

$$f_{RdADF}(\%, DM) = 47.5 - 16.3 \times St + 0.02 \times St^2 + 0.91 \times DMI \quad (1)$$

where f_{RdADF} represented rumen ADF degradation, % of DM; *St* was dietary starch concentrations, % of DM; DMI was expressed as kg/d. The concordance correlation coefficient (CCC) for this equation was 0.91, and the root mean squared error (RMSE) was 11% of mean.

Model Modifications

Model modifications were made to the version of Molly described by Gregorini et al. (2015) following conservation of mass principles. For purposes of this description, state variables, generally nutrients, metabolites, or the volume of a pool such as rumen liquid (kg, L, or mole), were denoted as $Q_{A,Y}$ where *A* denoted the nutrient or metabolite in compartment *Y*; $C_{A,Y}$ represented the concentration of *A* in compartment *Y* (kg/L or mole/L; primarily in ruminal

fluid or blood); the flux of nutrients within the system was denoted as $F_{AB,YZ}$ (kg/d or mole/d) where *A* denoted a substrate, *B* a product, *X* the location of the conversion, and in the case of transfer from one compartment to another with or without interconversion, *Z* represented the receiving compartment; $f_{AB,YZ}$ represented a stoichiometric constant for conversion of substrate *A* to product *B*; $K_{AB,YZ}$ represented a rate constant (variable units) for conversion of *A* to *B*, and $X_{AB,YZ,}$ denoted a sensitivity exponent for conversion of *A* to *B* (variable units); J_A represented a rate constant of inhibitor A. Specification of a single entity (*A*) or pool location (*Y*) was used when no conversion or location change occurred.

Initial model evaluations indicated that residuals for ruminal microbial N outflow were positively correlated with ruminal ammonia concentrations, suggesting that microbial N flow from the rumen was underpredicted as ruminal ammonia concentrations increased. Therefore, an exponential factor (X_{EAm}) was added to the microbial growth equation to allow adjustment of sensitivity to ruminal ammonia concentrations if required ($F_{MiG,Rum}$, kg/d).

$$F_{MiG,Rum} = \left(F_{ATPF,Rum} - F_{ATPM,Rum}\right) \times \left(0.012 + \frac{K_{YATP,Rum}}{1 + K_{AaMi,Rum} / C_{Aa,Rum}}\right) \times \left(\frac{1}{1 + (K_{AmMi,Rum} / C_{Am,Rum})^{X_{EAm}}}\right) \times \left(1 + \frac{C_{Lipid,Fd}}{C_{Fat,Fd} \times K_{Fat,Fd}}\right) \quad (2)$$

where $F_{ATPF,Rum}$ represented ATP production generated from nutrient fermentation in the rumen (mole/d); $F_{ATPM,Rum}$ represented ATP used for microbial maintenance (mole/d); $K_{YATP,Rum}$ was an efficiency variable defining the yield of microbial DM per mole of ATP (kg/mole); $K_{AaMi,Rum}$ and $K_{AmMi,Rum}$ were rate constants for the effect of ruminal concentrations of amino acids and ammonia on microbial growth (L/mole); and $C_{Aa,Rum}$ and $C_{Am,Rum}$ represented ruminal concentrations of amino acids and ammonia (mole/L); $C_{Lipid,Fd}$ was the dietary concentration of endogenous lipid (%, intrinsic plant lipids excluding storage oils and fats); $C_{Fat,Fd}$ represented the

dietary concentration of added fat (%); and $K_{Fat,Fd}$ was the rate constant for the effect of added fat on microbial growth (%/%).

Ammonia passage to the small intestine ($F_{Am,RumInt}$, mole/d) was simulated as a mass action function of the ruminal ammonia pool size ($Q_{Am,Rum}$, mole) and rumen liquid outflow rate ($K_{Liq,RumInt}$, $^{-}$d):

$$F_{Am,RumInt} = Q_{Am,Rum} \times K_{Liq,RumInt} \quad (3)$$

The differential equations describing the change in $Q_{Am,Rum}$ with respect to time, ruminal total N outflow (kg/d), and ruminal NANMN outflow (kg/d) were altered to include consideration of $F_{Am,RumInt}$.

Ammonia flow from the rumen was assumed to be completely absorbed and converted to urea in the liver as was previously assumed for ammonia absorbed from the rumen:

$$F_{AmUr,Rum} = (F_{Am,RumBld} + F_{Am,RumInt}) \times f_{AmUr} \quad (4)$$

where $F_{AmUr,Rum}$ was ammonia conversion to urea (mole/d); $F_{Am,RumBld}$ represented ruminal ammonia absorption (mole/d); and f_{AmUr} was the stoichiometric coefficient for conversion of ammonia to urea (0.5 mole NH_3/mole urea).

Urea recycling to the rumen is represented as the sum of transfer across the ruminal epithelium ($F_{Ur,BldRum(Trans)}$, mole/d) and salivary delivery ($F_{Ur,BldRum(Sal)}$, mole/d) (Baldwin, 1995). Those 2 fluxes were summed to provide an overall ruminal urea entry rate ($F_{Ur,BldRum}$, mole/d) which could be compared to the measured urea entry rates:

$$F_{Ur,BldRum} = F_{Ur,BldRum(Trans)} + F_{Ur,BldRum(Sal)} \quad (5)$$

Lapierre and Lobley (2001) demonstrated that gut urea entry was composed of ruminal urea entry and intestinal urea entry. To estimate intestinal urea entry rate from a single measured gut entry rate ($F_{Ur,BldGut}$, mole/d) requires an assumption of the fractional transfer into the rumen

and the intestine. The true split is driven by tissue mass, the transport activity per unit of mass, and blood flow. The latter is proportional to tissue activity and fermentation rate in the lumen (Storm et al., 2011; Storm et al., 2012), and thus it was assumed that ruminal and post-ruminal entry was proportional to DM disappearance in each compartment ($f_{DMDis,Rum}$, kg/kg).

$$F_{DMDis,Rum} = F_{DM,FdRum} - F_{DM,RumInt} \quad (6)$$

$$F_{DMDis,Int} = F_{DM,RumInt} - F_{DM,IntFec} \quad (7)$$

$$f_{DMDis,Rum} = \frac{F_{DMDis,Rum}}{F_{DMDis,Int}} \quad (8)$$

$$F_{Ur,BldInt} = \frac{F_{Ur,BldRum(Trans)}}{f_{DMDis,Rum}} \quad (9)$$

$$F_{Ur,BldGut} = F_{Ur,BldRum} + F_{Ur,BldInt} \quad (10)$$

where rumen DM disappearance ($F_{DMDis,Rum}$, kg/d) was calculated by subtracting ruminal DM outflow ($F_{DM,RumInt}$, kg/d) from DMI ($F_{DM,FdRum}$, kg/d); post-rumen disappearance DM ($F_{DMDis,Int}$, kg/d) was equal to ruminal DM outflow minus fecal DM outflow ($F_{DM,IntFec}$, kg/d); $F_{Ur,BldInt}$ is the intestinal urea entry rate (mole/d). This may overestimate post-ruminal entry as much of the DM disappearance is not from fermentative action. Additional data is required to refine this estimate.

Urea recycled to the lower gut is assumed to be converted to ammonia, and then captured by microbes as microbial N in the hind gut ($F_{UrMi,Int}$, mole/d), excreted in the feces ($F_{Ur,IntFec}$, mole/d) or reabsorbed ($F_{UrAm,Int}$, mole/d). Lapierre and Lobley (2001) indicated the contribution of urea N to support microbial protein synthesis is minor in the lower gut compared to that in the rumen. It seems likely capture by microbes would be proportional to fermentation rate, and given that DM disappearance was used to define the entry, it was further assumed that 25% of that entering the intestine was captured in microbial N thus approximating proportionality with

fermentative activity. This fractional capture also partially offsets any overestimation of gut entry when proportioned by DM disappearance.

$$F_{UrMi,Int} = 0.25 \times F_{Ur,BldInt} \tag{11}$$

$$F_{Ur,IntFec} = K_{Ur,IntFec} + K_{SlpUr,IntFec} \times F_{Ur,BldInt} \tag{12}$$

$$F_{UrAm,Int} = \frac{F_{Ur,BldInt} - F_{UrMi,Int} - F_{Ur,IntFec}}{f_{AmUr}} \tag{13}$$

where $K_{SlpUr,IntFec}$ and $K_{Ur,IntFec}$ were parameters used to estimate fecal urea excretion.

The representation of urea synthesis ($F_{AmUr,Liv}$, mole/d) was modified to include the contribution from ammonia absorbed from the hind gut:

$$F_{AmUr,Liv} = F_{AaUr,Vis} + F_{AaUr,Gest} + F_{AmUr,Rum} + F_{UrAm,Int} \times f_{AmUr} \tag{14}$$

where $F_{AaUr,Vis}$ represented deamination of amino acids in the viscera. Viscera is assumed to be the primary site of amino acid degradation with the remainder occurring in the gravid uterus ($F_{AaUr,Gest}$, mole/d) as described by Hanigan et al. (2009b).

Urinary urea excretion ($F_{Ur,BldUrin}$, mole/d) was originally described as a mass action function of blood urea concentrations (Baldwin, 1995). However, as Li et al (2018) pointed out blood urea concentrations do not scale with body mass, and thus flux was biased with respect to body size. This is a deviation relative to all other equations of this type in the model, and thus was a mistake which was corrected by altering the equation to be driven by the blood urea pool size ($Q_{Ur,Bld}$, moles) which does scale with BW:

$$F_{Ur,BldUrin} = Q_{Ur,Bld} \times K_{Ur,BldUrin} \tag{15}$$

where $K_{Ur,BldUrin}$ represented the mass action constant for urea excretion by the kidney.

Digested microbial non-protein N was assumed to be composed entirely of purines and pyrimidines and entirely excreted in the urine after derivatization in the liver. This is a deviation

from the earlier model which did not represent absorption of nucleic acids from microbes. Thus, total urinary N ($F_{N,Urin}$, kg/d) consisted of urinary urea-N ($F_{UrN,BldUrin}$, kg/d) plus purine derivative-N ($F_{Nn,MiUrin}$, kg/d).

$$F_{Nn,MiUrin} = F_{Mi,RumInt} \times f_{MiNnNn} \times K_{Pi,MiFec} \times 0.16 \quad (16)$$

$$F_{UrN,BldUrin} = \frac{F_{Ur,BldUrin}}{f_{AmUr}} \times K_{MwtN} \quad (17)$$

$$F_{N,Urin} = F_{UrN,BldUrin} + F_{Nn,MiUrin} \quad (18)$$

where $F_{Mi,RumInt}$ was the ruminal microbial protein outflow (kg/d); f_{MiNnNn} represented the fraction of total microbial N that was non-protein N; $K_{Pi,MiFec}$ represented the intestinal digestion coefficient for microbial protein which was 0.75; K_{MwtN} was the N molecular mass of 0.014 kg/mole.

Fecal N excretion ($F_{N,IntFec}$, kg/d) was updated to reflect absorption of non-protein microbial N and urea recycled in to the hind gut:

$$F_{N,IntFec} = (F_{Pi,MiFec} + F_{Nn,MiFec} + F_{Pi,IntFec} + \frac{F_{UrMi,Int}}{f_{AmUr}} + \frac{F_{Ur,IntFec}}{f_{AmUr}}) \times K_{MwtN} \quad (19)$$

where $F_{Pi,MiFec}$ was undigested microbial protein N (mole/d); $F_{Nn,MiFec}$ was undigested non-protein microbial N (mole/d); $F_{Pi,IntFec}$ represented undigested insoluble feed protein N (mole/d); $F_{UrMi,Int}$ referred to microbial N captured from recycled urea N in the hindgut (mole/d); $F_{Ur,IntFec}$ was N excreted in feces (mole/d) that was derived from blood urea; f_{AmUr} was a stoichiometric parameter (0.5 mol/mol) for conversion of substrate ammonia to product urea.

Infusion Variables

A number of studies were conducted that used infusions of casein, glucose or VFA (Wickersham et al., 2008a; Wickersham et al., 2008c; Bailey et al., 2012a; b; Titgemeyer et al., 2012; Batista et al., 2016). To represent their treatment effects, consideration of infused nutrients

was added to the model as follows. Ruminally infused VFA were added as additional fluxes to each of the VFA differential equations ($dQ_{Ac,Rum}/dt$, $dQ_{Pr,Rum}/dt$, $dQ_{Bu,Rum}/dt$, mole/d):

$$\frac{dQ_{Ac,Rum}}{dt} = F_{Ac,FdRum} + F_{CsAc,Rum} + F_{AaAc,Rum} + F_{LaAc,Rum} + F_{InfAc,Rum} - F_{Ac,RumBld} - F_{Ac,RumInt} \quad (20)$$

$$\frac{dQ_{Pr,Rum}}{dt} = F_{Cs\,\mathrm{Pr},Rum} + F_{Aa\,\mathrm{Pr},Rum} + F_{La\,\mathrm{Pr},Rum} + F_{Inf\,\mathrm{Pr},Rum} - F_{\mathrm{Pr},RumBld} - F_{\mathrm{Pr},RumInt} \quad (21)$$

$$dQ_{Bu,Rum} / dt = F_{Bu,FdRum} + F_{CsBu,Rum} + F_{AaBu,Rum} + F_{InfBu,Rum} - F_{Bu,RumBld} - F_{Bu,RumInt} \quad (22)$$

where $F_{Ac,FdRum}$ and $F_{Bu,FdRum}$ represented fluxes of dietary acetate and butyrate from silage (mole/d); $F_{CsAc,Rum}$, $F_{CsPr,Rum}$ and $F_{CsBu,Rum}$ referred to acetate, propionate, and butyrate derived from carbohydrate fermentation in the rumen (mole/d); $F_{AaAc,Rum}$, $F_{AaPr,Rum}$ and $F_{AaBu,Rum}$ were conversions of amino acid to each of the VFA (mole/d); $F_{LaAc,Rum}$ and $F_{LaPr,Rum}$ represented conversions of lactate to acetate and propionate (mole/d); $F_{InfAc,Rum}$, $F_{InfPr,Rum}$ and $F_{InfBu,Rum}$ represented ruminal VFA infusion rates (mole/d) of each; $F_{Ac,RumBld}$, $F_{Pr,RumBld}$ and $F_{Bu,RumBld}$ represented absorptions of each of the VFA (mole/d); and $F_{Ac,RumInt}$, $F_{Pr,RumInt}$ and $F_{Bu,RumInt}$ referred to VFA passage from the rumen (mole/d).

Ruminally infused glucose was added as a flux to the soluble carbohydrate differential equation (mole/d):

$$\frac{dQ_{Cs,Rum}}{d_t} = F_{ScTCs,Rum} + F_{StCs,Rum} + F_{HaCs,Rum} + F_{HcCs,Rum} + F_{CeCs,Rum} + F_{InfGl,Rum} - F_{CsFv,Rum} - F_{CsMi,Rum} - F_{Cs,RumInt} \quad (23)$$

where $F_{ScTCs,Rum}$ and $F_{StCs,Rum}$ represented dietary intake of total soluble carbohydrate expressed in 6-carbon equivalents and soluble starch (mole/d); $F_{HaCs,Rum}$, $F_{HcCs,Rum}$ and $F_{CeCs,Rum}$ referred to ruminal degradations of starch, hemicellulos and cellulose to soluble carbohydrate (mole/d); $F_{InfGl,Rum}$ was ruminal glucose infusion (mole/d); $F_{CsFv,Rum}$, $F_{CsMi,Rum}$ and $F_{Cs,RumInt}$ represented

soluble carbohydrate degradation, utilization for microbial growth, and passage from the rumen (mole/d).

Abomasally infused glucose was assumed to be completely absorbed and thus added to the absorbed glucose flux ($F_{Gl,IntBld}$, mole/d):

$$F_{Gl,IntBld} = F_{HaGl,Int} + F_{Cs,RumInt} + F_{MiGl,Int} + F_{MiLGl,Int} + F_{InfGl,Int} \quad (24)$$

where $F_{HaGl,Int}$ was dietary starch digestion (mole/d); $F_{MiGl,Int}$ represented microbial starch digestion in the lower gut (mole/d); $F_{MiLGl,Int}$ referred to a flux which equals 2 units of glycerol from digested microbial lipid (mole/d); $F_{InfGl,Int}$ was post-ruminal glucose infusion.

Ruminally infused casein was incorporated as a component of the diet with the assumption it was 100% soluble. Post-ruminally infused casein was also considered as a dietary ingredient with 0 solubility and a 0 rate of ruminal degradation so that all of it passed from the rumen.

Model changes were verified for mathematical consistency using a reference observation from the dataset. Predictions of ruminal ammonia, microbes and blood urea pool size (mole) with respect to simulation time were assessed before and after model modifications to determine if the changes inappropriately altered overall model balance. The reference inputs were a 598 kg Holstein cow consuming 26.3 kg DM/d of a diet containing CP, fat, starch, NDF, and ADF of 16.6, 5.5, 33.7, 29.8, and 18.9% of DM.

Simulation settings, parameter estimation, and model evaluations

The model was solved using a 4th order, variable step Runge-Kutta integration algorithm with a maximum step size of 0.005 d. Model stability and time to steady state were assessed by simulating for 14 d using the reference inputs, followed by alteration of the rate constant for ruminal ammonia absorption ($K_{Am,RumBld}$) from 10.44 d^{-1} to 20 on day 14, continuation of the run

for another 14 d, and then returning the rate constant to 10.44, and continuation of the simulation for an additional 14 d (Figure 3-2A). This process was repeated after model modification and parameter estimation using a starting and ending value of 5.01 d^{-1} for $K_{Am,RumBld}$ (Figure 3-2B). Pool sizes of ruminal ammonia, microbes and blood urea were recorded by day and plotted with respect to time to verify model stability and code accuracy, and to assess model behavior and time to steady state.

Model parameters listed in Table 3-3 were estimated simultaneously by fitting to the observed data using the Direction Set optimization algorithm (Press, 2007) provided in ACSL to maximize the log-likelihood function (LLF). Predicted values were sampled at steady state on d 14 (Figure 3-2) for comparison to observed values.

Model accuracy and precision were assessed based on the LLF, root mean squared errors (RMSE); the proportions of MSE associated with mean bias, slope bias, and dispersion (Bibby and Toutenburg, 1977); and concordance correlation coefficients (CCC) (Lawrence and Lin, 1989). Residual errors were also visually appraised to identify any additional patterns that may have been resident in the data.

Following model modifications and parameter estimation, simulations were conducted to assess N efficiency using two different feeding scenarios. The simulated animal was initialized as a Holstein cow weighing 600 kg at day 70 of lactation and consuming 20 kg of DM per day. For feeding strategy 1, there were 11 dietary CP concentrations ranging from 10 to 20% of DM. The diets all contained fat, starch, soluble starch, NDF, ADF, and ash concentrations of 6, 30, 9, 30, 20, and 6 % of DM, respectively, and thus the CP was substituted for residual OM which is primarily pectins and organic acids. Dietary RUP concentration was set to 6% of DM for all diets with variation in RDP being the sole contributor to varying dietary CP. This resulted in dietary

RDP concentrations from 4 to 14% of DM. For feeding strategy 2, dietary CP was held constant at 16% of DM and 9 different concentrations of RUP ranging from 10% to 90% of CP were used. In this case, RUP was substituted for RDP given a constant CP content. The remaining nutrient concentrations were the same as for feeding strategy 1. Model predictions of total ruminal N outflow ($F_{N,RumInt}$, kg/d), microbial N outflow ($F_{MiN,RumInt}$, kg/d), NANMN outflow ($F_{NANMN,RumInt}$, kg/d), ammonia N converted to ruminal microbial N ($F_{AmMi,Rum}$, kg/d), ammonia generated in the rumen from recycled urea ($F_{UrAm,Rum}$, mole/d), total ammonia production ($F_{Am,Rum}$, mole/d), blood urea entry rate ($F_{AmUr,Liv}$, mole/d), gut urea entry rate ($F_{Ur,BldGut}$, mole/d), and urinary urea excretion ($F_{Ur,BldUrin}$, mole/d) were collected. The proportion of microbial N synthesized from ammonia N was calculated as $F_{AmMi,Rum}$ divided by $F_{MiN,RumInt}$. The proportion of total ammonia generated from recycled urea were calculated as $F_{UrAm,Rum}$ divided by $F_{Am,Rum}$.

Regression Analyses

Regressions were conducted using a mixed linear model with study as a random effect using the lmer function of the lme4 package (version 1.1-17; Bates et al., 2014) in R (version 3.3.0; R development Core Team, 2015) to quantify relationships between observed dietary N intake and observed ruminal N outflow, observed blood urea entry or predicted ruminal ammonia production rate, and relationships between observed blood urea entry and observed gut urea entry or urinary urea excretion. R^2_m and R^2_c were used to represent coefficients of determination. R^2_m is the marginal R^2, which represents the proportion of variance that can be explained by the fixed effect, and R^2_c is the conditional R^2, which indicates the proportion of variance that can be explained by the fixed effect plus the random effect.

Results and Discussion

Steady State and Model Verifications

Profiles of ruminal ammonia, microbes and blood urea pool size (mole) with respect to simulation time before and after the perturbations of the ruminal ammonia absorption constant are shown in Figure 3-2. After 10 days of model simulation, changes in pool sizes of these three variables were negligible, suggesting that all the variables associated with these N pools had reached steady state. When challenging the model by changing the rate constant for ruminal ammonia absorption ($K_{Am,RumBld}$, d^{-1}) on day 14 and day 28, the model returned to apparent steady state in 7 days, supporting selection of a simulation time of 14 days to represent steady state values. The model was found to be stable and returned to initial pool sizes after perturbation when the parameter values were returned to the initial values on day 28, suggesting the code was acting as expected.

Increasing $K_{Am,RumBld}$ on day 14 significantly decreased ruminal ammonia pool size in the modified model (Figure 3-2). As a consequence, microbial pool size was decreased, and blood urea pool size was increased (Figure 3-2B), which contrasts with the very small changes in microbial and blood urea pool sizes for the initial model (Figure 3-2A). Thus the altered model and parameters resulted in greater microbial growth sensitivity to ruminal ammonia concentrations which was consistent with our previous observations of model behavior (Li et al, 2018).

Ruminal Ammonia Metabolism

Ruminal ammonia, as a major end-product of ruminal fermentation, is a vital indicator of ruminal N metabolism. Ammonia is produced from microbial degradation of dietary amino acids, dietary non-protein nitrogen, and blood urea entering the rumen, and is utilized by microbes to synthesize protein, absorbed from the rumen or passes from the rumen in the liquid

fraction (Figure 3-1). After model improvements and refitting to literature data, the RMSE for ruminal ammonia concentrations decreased from 75.9 to 48.3% with a substantial decrease in mean bias from 55.1 to 0.5% and in slope bias from 5.8 to 0.4%. These results support our hypothesis regarding the form of representing these transactions, however precision was still relatively poor.

Nolan (1975) demonstrated that the ammonia pool can completely turnover in less than 2 h. Thus time of sampling relative to a meal is an important determinant of ruminal ammonia concentrations. In most cases, the animals were fed frequently to minimize this problem, but even with 2 h feeding intervals, there could be variation in ammonia concentrations if the diet is highly degradable. Ammonia concentrations could be affected by sampling locations and methods. Wohlt et al. (1976) reported that concentrations of ruminal ammonia were greatest in the dorsal region of the rumen, and ammonia concentrations were lower in samples obtained by stomach tube compared to samples taken via rumen cannula.

Substantial amounts of ammonia are generated from microbial degradation of dietary protein in the rumen. On average, ruminal NANMN outflow accounted for 46% of incremental dietary N intake (Figure 3-3C), and thus 54% of dietary protein was degraded in the rumen. Intercept and slope scalars ($K_{RUP,Rum,}$ and $K_{SlpRUP,Rum}$) were introduced by Hanigan et al. (2013) to scale in situ measures of ingredient CP degradation rates so the model predictions more closely aligned with observed extent of degradation. In theory, if the in situ measures and the model were perfect representations of reality, the intercept would be 0 and the slope would be 1. Given the needed adjustments of in situ assessments, one must conclude that either protein degradation rates determined in situ are biased or the model structure is biased. The observation that $K_{RUP,Rum,}$ and $K_{SlpRUP,Rum}$, moved towards 0 and 1 as compared to the earlier estimates and model structure

implies that model structure is at least part of the problem, although ingredient protein degradation rates were also updated (White et al., 2017a). The revised estimate of the in situ adjustment parameters slightly decreased RMSE of ruminal NANMN from 38.6 to 35.9% with a slope bias decrease from 29.8 to 12.8%. The slope bias was positive which suggests the model tended to underestimate ruminal NANMN outflow when high undegraded protein diets were fed (Figure 3-4A). However, this slope bias was obviously affected by 2 high leverage points as displayed in Figure 3-4A. Because of the lack of neighboring observations, it seems unlikely that this is contributing to the ammonia prediction error.

A portion of ammonia comes from microbial hydrolysis of recycled urea either directly transferred from blood across ruminal epithelium or via saliva. In the model, urea flowing into the rumen via saliva is calculated from blood urea concentrations multiplied by saliva volume, and urea passing across rumen epithelium is simulated using a Michaelis-Menten equation driven by blood urea concentrations and inhibited by ruminal ammonia concentrations (Baldwin, 1995). Refitting the maximal rate of blood urea conversion to ruminal ammonia ($Vm_{UrAm,Rum}$) and the inhibition constant for the effect of ammonia on blood urea conversion to ruminal ammonia (J_{Am}) resulted in an increase in the maximal rate ($Vm_{UrAm,Rum}$) from 56.7 to 69 ± 1.6 mmol/d (Table 3-3), and a slight decrease in the ruminal ammonia inhibition constant (J_{Am}) from 0.003 to 0.0026 ± 8.46×10^{-5} L/mole. The revised parameters resulted in decreased RMSE for predictions of gut urea N entry from 81.2 to 36.3%, primarily due to decreased mean bias from 58.4 to 4.9%. A larger $Vm_{UrAm,Rum}$ indicates greater maximal rates of transfer of blood urea into the rumen. At ruminal ammonia concentrations of 5, 10, and 15 mM, 44, 31, and 24% of the maximal urea transfer rate would be achieved with J_{Am} at 0.0026, supporting the inhibitory effect of ruminal ammonia on urea transfer.

Ammonia is an essential substrate for microbial protein synthesis. Microbial N outflow represents approximately 51% of incremental total dietary N intake (Figure 3-3B). Model simulation results indicated approximately 64 to 71% of microbial N was derived from ammonia depending on the diet (Figure 3-10C and Figure 3-11C), which were consistent with estimates of the contribution of total ammonia N to bacterial N ranging from 64% to 80% (Pilgrim et al., 1970; Nolan and Leng, 1972). Fitting the maximal rate of growth of microbes from amino acids ($K_{YATP,Rum}$) resulted in a value of 0.055 ± 0.001 kg/mole as compared to the prior value of 0.03. The affinity constant for microbial growth stimulation by ammonia ($K_{AmMi,Rum}$) was estimated at 7 ± 0.16 mM compared to the prior value of 0.2 (Hanigan et al., 2013), and the newly introduced ammonia sensitivity exponent (X_{EAm}) was estimated at 8.85 ± 0.58 mole/mole. $K_{AmMi,Rum}$ indicates the concentration of ruminal ammonia when microbial growth is half of the maximal rate. Although the work of Satter and Slyter (1974) demonstrated that microbial growth was maximized at an ammonia concentration of 1.5 mM, Reynal and Broderick (2005) indicated that ammonia concentrations above 8.4 mM might be needed to maximize microbial protein synthesis. Hanigan et al. (2013) previously solved for a half maximal concentration of 0.2 mM, but the ammonia concentrations predicted by the model were very biased leading to the current work. The derived value for X_{EAm} was much greater than expected indicating significant sensitivity of microbial growth to ammonia concentrations, and it was well defined by the data resulting in improved predictions of microbial growth. At ammonia concentrations of 8 and 10 mM, 50% and 89% of maximal growth would be achieved with $K_{AmMi,Rum}$ at 7 mM using the revised equation. Fitting the data herein decreased prediction errors of ruminal microbial N outflow from a RMSE of 56.6% to 27.8%, due to a reduced mean bias from 25.1 to 10.4% and a reduced slope bias from 55 to 10.6% (Table 3-2). However, the initial prediction error of ruminal

N outflow was much greater than observed by Hanigan et al. (2013), possibly due to the limited observations herein which had a narrow range in ruminal N outflow observations (25.3 to 110.6 g/d). Additional parametrization work should be undertaken using a larger data set.

The mass action rate constant ($K_{Am,RumBld}$) used to represent ammonia absorption (Baldwin, 1995) solved for a value of 5.94 d^{-1} as compared to the prior 10.44 d^{-1} which reduced the mean prediction bias. As displayed in Figure 3-5, predicted ruminal ammonia N absorption rates averaged 23% of incremental dietary N intake with a range from 10 to 40% which is consistent with the studies of Lapierre et al. (2005) and Firkins and Reynolds (2005) where net PDV ammonia N absorption represented between 30 and 42% of dietary N intake. The reduction in the rate constant was partially due to consideration of ammonia outflow from the rumen in the liquid fraction. In the absence of such consideration, all ammonia leaving the rumen was by absorption. Ammonia N passage averaged 0.3 mole/d which is 20% of the total ammonia N flux and 6% of total N outflow. This was consistent with observed proportions of 4 to 10% of total N flow from the rumen (Chan et al., 1997; Zhu et al., 1997). This change in representation had no effect on total ammonia absorption as it was assumed that ruminal ammonia outflow was completely absorbed (Smith, 1969).

The RMSE for total ruminal N outflow was reduced from 55 to 39.5% after model changes and parameterization, and CCC increased from 0.56 to 0.67 (Table 3-2). Mean and slope bias represented 22.4 and 22.3% of MSE, respectively. Several high-leverage points were observed by examination of the residuals' plots, which contributed to the moderate mean bias and slope bias (Figure 3-4).

Blood Urea Metabolism

The RMSE of blood urea concentrations was substantially decreased from 100 to 49 %, and CCC increased from 0.12 to 0.75, suggesting that both accuracy and precision of predicted

blood urea concentrations were enhanced. Mean bias and slope bias were decreased from 46 to 0.1%, and 12 to 2.1%, primarily due to improved representations of ruminal ammonia metabolism and blood urea metabolism.

Predictions of blood urea N entry exhibited a RMSE of 26.3% (2.8% mean bias and 3.2% slope bias) and a CCC of 0.84, indicating that the model represented the mechanisms of hepatic ureagenesis accurately. Blood urea N entry accounted for approximately 64% of incremental dietary N intake (Figure 3-6), suggesting that hepatic ureagenesis is a major cross-road in terms of whole body N exchange. It also suggests that anabolic use of dietary N is 36%. In the current work, we added representations of intestinal urea entry, which altered urea distribution and ammonia absorption from the digestive tract. Previous studies indicated that some blood urea is recycled to the lower gut, and captured in microbial protein (Nolan and Leng, 1972; Bailey et al., 2012a). Considering there is less fermentable energy for microbial growth in the hind gut than in the rumen and recognizing that proportioning the split between ruminal and intestinal urea entry may be biased, we assumed 25% of recycled urea to the intestine was utilized for microbial protein synthesis, part was excreted in feces as ammonia, and the remainder was reabsorbed from the hind gut. These modifications contribute to N cycling without necessitating entry of urea into the rumen as previously represented.

Amino acid catabolism is another source of hepatic ureagenesis. Approximately, 15 to 35% of absorbed amino acids are utilized as an energy source by the gut tissues on a daily basis (Lobley and Lapierre, 2003; Apelo et al., 2014). Daily use of essential amino acids by the liver can be as high as 35 to 50% of that absorbed when high protein diets are fed or animal production is low (Lapierre et al., 2005). The remaining amino acids are primarily used for milk protein synthesis. Of those cleared by the splanchnic tissues, the majority are catabolized and

converted to ammonia and carbon skeletons (Hanigan et al., 2004; Lapierre et al., 2005). To prevent hyperaminoacidaemia, ammonia is converted to urea in the liver. Although the mechanisms of amino acid catabolism are simulated in the model (Baldwin, 1995; Hanigan et al., 2009b), there are limited data to evaluate the accuracy of amino acid N contributions to urea synthesis. To estimate that contribution, we initially assumed all of the observed retained N was used for lean body tissue growth, and we compared that to lean body tissue deposition predicted by the model. Those predictions exhibited a RMSE of 172.4% with a mean bias of 85.6% and a slope bias of 1.7% in the initial model. The predicted retained N was -15 g/d, suggesting that animals lost body weight during the experimental periods, which was the inverse of the observed retention of 25 g/d. We addressed this problem simultaneously with urea recycling by fitting the maximal rate of the AA conversion to body protein ($Vm_{AaOth,Vis}$, mole/d) to the data. This resulted in an increase in the parameter from 223 to 539 g/d, resulting in a decreased prediction error of retained N to an RMSE of 59%, mean bias of 19.4%, and slope bias of 50.2%, which was an improvement; but the slope bias suggests that the representation of overall N balance systematically deviates from observed values. It is possible this error is due to the accumulation of errors in measured N balance. Unexplained N losses, such as gaseous forms of N or nitrate formation, might result in excessively high N balance (Firkins and Reynolds, 2005).

Reynolds and Kristensen (2008) concluded that increasing dietary N intake was associated with increased blood urea entry (Figure 3-6), but the effect of N intake on gut urea entry was small. However, that is not consistent with the data. As shown in Figure 3-7, gut urea entry linearly increased with dietary N intake (Figure 3-7A) and N intake relative to metabolic BW (Figure 3-7B). Approximately 55% of synthesized urea was recycled to the gut lumen (Figure 3-8A). Urea N recycled to the rumen account for 23 to 63% of total ruminal ammonia

production depending on dietary CP content and RUP proportions (Figure 3-10C and Figure 3-11C), thus representing a significant contribution to overall ruminal N balance.

Urinary urea excretion also increased linearly with increased dietary N intake (Figure 3-9A) and N intake relative to metabolic BW (Figure 3-9B). Approximately, 39% of synthesized urea was eliminated in urine (Figure 3-8B). Reynolds and Kristensen (2008) observed that fractional gut urea entry and urinary urea N secretion varied with dietary protein concentrations in a reciprocal manner. Similar results were found in the current work (Figure 3-7C and Figure 3-9C), although the relationship is not strong. However, the relations between the fraction of gut urea entry or urinary urea secretion with dietary protein concentration are easily misleading, because high dietary protein concentration does not necessarily equate to high protein intake. When the fractional rates were regressed on dietary N intake with respect to metabolic BW, gut entry quadratically decreased, whereas urinary excretion quadratically increased (Figure 3-7D and Figure 3-9D).

Urinary N Excretion

Urinary N is mainly derived from urea at 55 to 62% of total urinary N (Gonda and Lindberg, 1994) with lesser contributions from purine derivatives and ammonia. Altering the representation of urea excretion to be a function of the pool size rather than concentration and refitting to the data resulted in a fractional excretion rate of 2.5 d^{-1} and substantial reductions in RMSE from 133 to 56% and increased CCC from 0.45 to 0.79 suggesting a considerable improvement associated with the change in representation. However, the precision of predicted urinary urea was still poor. Several studies indicated that renal processes such as the glomerular filtration rate and urea recycling from the glomerular filtrate were affected by CP (Rabinowitz et al., 1973; Eriksson and Valtonen, 1982) and NaCl (Godwin and Williams, 1984). Residual analyses indicated urinary urea residuals were positively correlated with CP intake (P <0.05),

suggesting that urinary urea secretions were underestimated when high protein diets were fed. Spek et al. (2013) demonstrated the urinary urea secretion tended to be negatively related to the renal urea reabsorption ratio for high protein diets, whereas no significant effect was observed for low protein diets. This was partially consistent with our result, suggesting that the addition of inhibitory effects of protein on urea reabsorption might improve the representations of urinary urea secretion. There was no correlation between urinary urea residuals with ash intake, which was consistent with previous studies, as the effects of dietary NaCl on urinary urea secretion were not significant (Spek et al., 2012; 2013). However, the amount of explained variation in urinary urea secretion increased 8% when NaCl was included in the model (Spek et al., 2013). Sorting out these potential effects will require a concerted effort to collect such information to build a more complicated model to reflect the effects of CP and NaCl on rental mechanisms of urea absorption and secretion.

Adding representations of the excretion of purine derivatives in urine improved both accuracy and precision of urinary N predictions from a CCC of 0.76 to 0.84 and slightly decreased RMSE from 38 to 35%. The improvement was largely due to removal of slope bias which decreased from 11.2% to 1.2%.

Fecal N Excretion

Compared with the initial model, several nitrogenous components were considered in the feces, including undigested microbial nucleic acids, microbial protein synthesized in the hind gut, and ammonia generated from fecal urea hydrolysis. Considering there is no urea pool in the gut, fecal N generated from urea hydrolysis was simulated as a linear function of intestinal urea entry rate. An intercept scalar ($K_{Ur,IntFec}$) and a slope scalar ($K_{SlpUr,IntFec}$) were derived to predict fecal excretion of N derived from urea based on the observed values. The endogenous urea N lose in feces ($K_{Ur,IntFec}$) was 0.11, and the fractional transfer of urea N entering the gut to feces

($K_{SlpUr,IntFec}$) was 0.0001. The negligible slope estimate suggests that there was not a linear relationship between intestinal urea entry and fecal N from catabolized urea, which implies fecal urea N excretion was constant among diets as N intake varied. Because the model does not consider endogenous protein losses and we fitted these parameters against both fecal urea excretion and total fecal N output, $K_{Ur,IntFec}$ could be used to represent total endogenous N loss in feces which includes urea, sloughed cells and enzyme secretions into the gut. As a result, consideration of these additional N compounds in feces allowed the intestinal digestion coefficient ($K_{Protein,IntFec}$) to more closely reflect true protein digestion at 0.79 as compared to the prior 0.68. This digestion coefficient was consistent with studies from monogastric animals. The true ileal digestibility of N was 76.9 to 78.2% in growing rats (Donkoh and Moughan, 1994), 75 to 83% in growing pigs (Furuya and Kaji, 1989; Hess et al., 2000), and 75 to 86% in broiler chickens (Huang et al., 2005; Gabriel et al., 2008). The RMSE for fecal N excretion was slightly increased from 28 to 35%, but slope bias was substantially decreased from 28.1 to 0.4%, suggesting that the changes did improve the representation of total fecal N output although additional progress is likely possible.

Model Simulations

When RUP N intake is held constant at 192 g/d while RDP N intake is increased from 128 to 448 g/d, microbial N outflow increased from 129 to 349 g/d and, consequently, total N outflow increased from 358 to 573 g/d (Figure 3-10A). This led to an increase in blood urea N entry from 150 to 371 g/d and increased urinary urea N secretion from 59 to 255 g/d (Figure 3-10B). Although gut urea N entry rate was slightly increased as dietary RDP N intake increased from 128 to 320 g/d, and slightly decreased when fed higher than 320 g/d (Figure 3-10B), proportions of total ammonia that were generated from recycled urea in the rumen decreased continuously from 50.3 to 23% (Figure 3-10C), primarily due to increased ammonia production

rate and the inhibitory effect of ammonia on urea transfer from blood to rumen. With increased RDP intake, more amino acids and peptides are theoretically available for microbial protein synthesis in the rumen, which contributed to decreased proportions of microbial protein N that captured from ruminal ammonia N from 69 to 64% (Figure 3-10C). Under this feeding strategy, both proportion of ammonia degraded from recycled urea, and proportion of microbial N captured by ammonia N were decreased, resulting in a decrease of ruminal N efficiency from 112 to 89% (Figure 3-10D).

When N intake was constant (512 g/d), increased RUP proportions from 10 to 90% resulted in increased ruminal NANMN outflow from 135 to 377 g/d and decreased ruminal microbial N outflow from 348 to 184 g/d. However, the increased NANMN flow was greater than the reduction in microbial N flow leading to linear increases in total ruminal N outflow from 485 to 562 g/d (Figure 3-11A). As a result, blood urea N entry was slightly increased from 279 to 291 g/d (Figure 3-11B). When the proportion of RUP increased from 10 to 90%, ruminal ammonia was insufficient to support microbial protein synthesis as RDP declined despite increased flux of urea N into the rumen to maintain ruminal ammonia balance, and decreased urinary urea N secretion (Figure 3-11B). In this scenario, proportions of ammonia production incorporated from recycled urea increased from 23 to 63 %, as inhibition effect of ammonia on ruminal urea entry was alleviated, and proportions of rumen microbial N captured from ammonia N increased from 65 to 71% (Figure 3-11C). These changes contributed to increased ruminal N efficiency from 94 to 111% (Figure 3-11D).

Conclusions

Significant improvements in predictions of variables describing ruminal N metabolism, blood urea metabolism and urinary N secretion were achieved including removal of slope bias for predictions of ruminal microbial N outflow, blood urea concentrations and fecal N excretion,

and reductions in mean bias for predictions of ruminal ammonia concentrations and urinary N excretion. Predicted blood urea entry and gut urea N entry exhibited negligible mean bias and slope bias, implying the representation captured the main mechanisms of ruminal urea N recycling.

In ruminants, hepatic ureagenesis is a major cross-road of whole body N exchange. Urea N entry into blood accounts for approximately 64% of dietary N intake of which 55% is recycled to the gut lumen. Depending on the diet, urea recycled to the gut account for 23 to 63% of total ruminal ammonia production, and between 64 and 71% of this ammonia N is captured in microbial protein. Thus this is a significant component of the ruminal N system.

Our model simulation results suggested that although feeding a moderately low CP diets with high RUP proportions might decrease microbial protein synthesis in the rumen, this feeding strategy allows greater proportions of feed protein to escape the rumen, greater capture of recycled urea N by rumen microbes, and reduced urinary urea excretion. The combination of these resulted in increased total metabolizable protein supply. Thus from a N standpoint, and depending on dietary N costs, maximizing microbial N flows may not be the best strategy for optimizing animal performance and certainly is not the best solution for minimizing environmental impact.

Acknowledgements

This work was funded, in part, by the National Research Initiative Competitive from the USDA National Institute of Food and Agriculture (Grant No. 2007-35206-17848) and the Virginia Agricultural Experiment Station and the Hatch Program of the National Institute of Food and Agriculture, U.S. Department of Agriculture; the College of Agriculture and Life Sciences Pratt Endowment at Virginia Tech; and the Alberta Livestock and Meat Agency Ltd. (grant 2015F055R).

References

Apelo, S. A., J. Knapp, and M. Hanigan. 2014. Invited review: Current representation and future trends of predicting amino acid utilization in the lactating dairy cow. J. Dairy Sci. 97(7):4000-4017.

Archibeque, S., J. Burns, and G. Huntington. 2001. Urea flux in beef steers: effects of forage species and nitrogen fertilization. J. Anim. Sci. 79(7):1937-1943.

Archibeque, S., J. Burns, and G. Huntington. 2002. Nitrogen metabolism of beef steers fed endophyte-free tall fescue hay: effects of ruminally protected methionine supplementation. J. Anim. Sci. 80(5):1344-1351.

Bailey, E., E. Titgemeyer, K. Olson, D. Brake, M. Jones, and D. Anderson. 2012a. Effects of ruminal casein and glucose on forage digestion and urea kinetics in beef cattle. J. Anim. Sci. 90(10):3505-3514.

Bailey, E., E. Titgemeyer, K. Olson, D. Brake, M. Jones, and D. Anderson. 2012b. Effects of supplemental energy and protein on forage digestion and urea kinetics in growing beef cattle. J. Anim. Sci. 90(10):3492-3504.

Baldwin, R. 1995. Modeling ruminant digestion and metabolism. Springer Science & Business Media, Berlin, Germany.

Baldwin, R. L., J. France, D. E. Beever, M. Gill, and J. H. Thornley. 1987a. Metabolism of the lactating cow: III. Properties of mechanistic models suitable for evaluation of energetic relationships and factors involved in the partition of nutrients. J. Dairy Res. 54(01):133-145.

Baldwin, R. L., J. France, and M. Gill. 1987b. Metabolism of the lactating cow: I. Animal elements of a mechanistic model. J. Dairy Res. 54(01):77-105.

Baldwin, R. L., J. H. Thornley, and D. E. Beever. 1987c. Metabolism of the lactating cow: II. Digestive elements of a mechanistic model. J. Dairy Res. 54(01):107-131.

Bates, D., M. Mächler, B. Bolker, and S. Walker. 2014. Fitting linear mixed-effects models using lme4. arXiv preprint arXiv:1406.5823.

Batista, E., E. Detmann, E. C. Titgemeyer, S. Valadares Filho, R. Valadares, L. Prates, L. Rennó, and M. Paulino. 2016. Effects of varying ruminally undegradable protein supplementation on forage digestion, nitrogen metabolism, and urea kinetics in Nellore cattle fed low-quality tropical forage. J. Anim. Sci. 94(1):201-216.

Bibby, J. and H. Toutenburg. 1977. Prediction and improved estimation in linear models. Wiley.

Brake, D., E. Titgemeyer, and M. Jones. 2011. Effect of nitrogen supplementation and zilpaterol–HCl on urea kinetics in steers consuming corn‐based diets. J. Anim. Physiol. Anim. Nutr. 95(4):409-416.

Brake, D., E. Titgemeyer, M. Jones, and D. Anderson. 2010. Effect of nitrogen supplementation on urea kinetics and microbial use of recycled urea in steers consuming corn-based diets1. J. Anim. Sci. 88(8):2729-2740.

Chan, S., J. Huber, C. Theurer, Z. Wu, K. Chen, and J. Simas. 1997. Effects of supplemental fat and protein source on ruminal fermentation and nutrient flow to the duodenum in dairy cows. J. Dairy Sci. 80(1):152-159.

Davies, K., J. McKinnon, and T. Mutsvangwa. 2013. Effects of dietary ruminally degradable starch and ruminally degradable protein levels on urea recycling, microbial protein production, nitrogen balance, and duodenal nutrient flow in beef heifers fed low crude protein diets. Can. J. Anim. Sci. 93(1):123-136.

Donkoh, A. and P. Moughan. 1994. The effect of dietary crude protein content on apparent and true ileal nitrogen and amino acid digestibilities. Br. J. Nutr. 72(1):59-68.

Eriksson, L. and M. Valtonen. 1982. Renal urea handling in goats fed high and low protein diets. J. Dairy Sci. 65(3):385-389.

Firkins, J. and C. Reynolds. 2005. Whole animal nitrogen balance in cattle. Nitrogen and phosphorus nutrition of cattle: reducing the environmental impact of cattle operations.(Eds E Pfeffer, A Hristov) pp:167-186.

Furuya, S. and Y. Kaji. 1989. Estimation of the true ileal digestibility of amino acids and nitrogen from their apparent values for growing pigs. Anim. Feed Sci. Technol. 26(3-4):271-285.

Gabriel, I., M. Lessire, H. Juin, J. Burstin, G. Duc, L. Quillien, J. Thibault, M. Leconte, J. Hallouis, and P. Ganier. 2008. Variation in seed protein digestion of different pea (Pisum sativum L.) genotypes by cecectomized broiler chickens: 1. Endogenous amino acid losses, true digestibility and in vitro hydrolysis of proteins. Livest. Sci. 113(2-3):251-261.

Godwin, I. and V. Williams. 1984. Renal control of plasma urea level in sheep: The diuretic effect of urea, potassium and sodium chloride. Exp. Physiol. 69(1):49-59.

Gonda, H. L. and J. E. Lindberg. 1994. Evaluation of dietary nitrogen utilization in dairy cows based on urea concentrations in blood, urine and milk, and on urinary concentration of purine derivatives. Acta Agriculturae Scandinavica A-Animal Sciences 44(4):236-245.

Gregorini, P., P. Beukes, G. Waghorn, D. Pacheco, and M. Hanigan. 2015. Development of an improved representation of rumen digesta outflow in a mechanistic and dynamic model of a dairy cow, Molly. Ecol. Modell. 313:293-306.

Hanigan, M., L. Crompton, C. Reynolds, D. Wray-Cahen, M. Lomax, and J. France. 2004. An integrative model of amino acid metabolism in the liver of the lactating dairy cow. J. Theor. Bio. 228(2):271-289.

Hanigan, M. D., J. A. Appuhamy, and P. Gregorini. 2013. Revised digestive parameter estimates for the Molly cow model. J. Dairy Sci. 96(6):3867-3885.

Hanigan, M. D., C. C. Palliser, and P. Gregorini. 2009. Altering the representation of hormones and adding consideration of gestational metabolism in a metabolic cow model reduced prediction errors. J. Dairy Sci. 92(10):5043-5056.

Hess, V., P. Ganier, J.-N. Thibault, and B. Seve. 2000. Comparison of the isotope dilution method for determination of the ileal endogenous amino acid losses with labelled diet and labelled pigs. Br. J. Nutr. 83(2):123-130.

Holder, V., J. Tricarico, D. Kim, N. Kristensen, and D. Harmon. 2015. The effects of degradable nitrogen level and slow release urea on nitrogen balance and urea kinetics in Holstein steers. Anim. Feed Sci. Technol. 200:57-65.

Huang, K., V. Ravindran, X. Li, and W. Bryden. 2005. Influence of age on the apparent ileal amino acid digestibility of feed ingredients for broiler chickens. Bri. Poult. Sci. 46(2):236-245.

Lapierre, H., R. Berthiaume, G. Raggio, M. Thivierge, L. Doepel, D. Pacheco, P. Dubreuil, and G. Lobley. 2005. The route of absorbed nitrogen into milk protein. Animal Science 80(1):11-22.

Lapierre, H. and G. Lobley. 2001. Nitrogen recycling in the ruminant: A review. J. Dairy Sci. 84:E223-E236.

Lawrence, I. and K. Lin. 1989. A concordance correlation coefficient to evaluate reproducibility. Biometrics:255-268.

Li, M. M., R. R. White, and M. D. Hanigan. 2018. An evaluation of Molly cow model predictions of ruminal metabolism and nutrient digestion for dairy and beef diets. J. Dairy Sci. 101(11):9747-9767.

Lobley, G., D. Bremner, and G. Zuur. 2000. Effects of diet quality on urea fates in sheep as assessed by refined, non-invasive [15N15N] urea kinetics. Br. J. Nutr. 84(4):459-468.

Lobley, G. and H. Lapierre. 2003. Post-absorptive metabolism of amino acids. Publication-European Association for Animal Production 109:737-756.

Marini, J. and M. Van Amburgh. 2003. Nitrogen metabolism and recycling in Holstein heifers. J. Anim. Sci. 81(2):545-552.

Nolan, J. 1975. Quantitative models of nitrogen metabolism in sheep. Digenstion and Metabolism in the Ruminant.

Nolan, J. and R. Leng. 1972. Dynamic aspects of ammonia and urea metabolism in sheep. Br. J. Nutr. 27(1):177-194.

Pilgrim, A., F. Gray, R. Weller, and C. Belling. 1970. Synthesis of microbial protein from ammonia in the sheep's rumen and the proportion of dietary nitrogen converted into microbial nitrogen. Br. J. Nutr. 24(2):589-598.

Press, W. H. 2007. Numerical recipes : the art of scientific computing. 3rd ed. Cambridge University Press, Cambridge, UK ; New York.

R development Core Team. 2015. R: A language and environment for statistical computing. http://www.R-project.org.

Rabinowitz, L., R. A. Gunther, E. S. Shoji, R. A. Freedland, and E. H. Avery. 1973. Effects of high and low protein diets on sheep renal function and metabolism. Kidney international 4(3):188-207.

Reynal, S. and G. Broderick. 2005. Effect of dietary level of rumen-degraded protein on production and nitrogen metabolism in lactating dairy cows. J. Dairy Sci. 88(11):4045-4064.

Reynolds, C. and N. B. Kristensen. 2008. Nitrogen recycling through the gut and the nitrogen economy of ruminants: an asynchronous symbiosis. J. Anim. Sci. 86(14_suppl):E293-E305.

Ruiz, R., L. Tedeschi, J. Marini, D. Fox, A. Pell, G. Jarvis, and J. Russell. 2002. The effect of a ruminal nitrogen (N) deficiency in dairy cows: evaluation of the Cornell net carbohydrate and protein system ruminal N deficiency adjustment. J. Dairy Sci. 85(11):2986-2999.

Satter, L. D. and L. L. Slyter. 1974. Effect of ammonia concentration of rumen microbial protein production in vitro. Br. J. Nutr. 32(2):199-208.

Smith, R. 1969. Section G. General. Nitrogen metabolism and the rumen. J. Dairy Res. 36(2):313-331.

Spek, J., A. Bannink, G. Gort, W. Hendriks, and J. Dijkstra. 2012. Effect of sodium chloride intake on urine volume, urinary urea excretion, and milk urea concentration in lactating dairy cattle. J. Dairy Sci. 95(12):7288-7298.

Spek, J., A. Bannink, G. Gort, W. Hendriks, and J. Dijkstra. 2013. Interaction between dietary content of protein and sodium chloride on milk urea concentration, urinary urea excretion, renal recycling of urea, and urea transfer to the gastrointestinal tract in dairy cows. J. Dairy Sci. 96(9):5734-5745.

Storm, A. C., M. D. Hanigan, and N. B. Kristensen. 2011. Effects of ruminal ammonia and butyrate concentrations on reticuloruminal epithelial blood flow and volatile fatty acid absorption kinetics under washed reticulorumen conditions in lactating dairy cows. J. Dairy Sci. 94(8):3980-3994.

Storm, A. C., N. B. Kristensen, and M. D. Hanigan. 2012. A model of ruminal volatile fatty acid absorption kinetics and rumen epithelial blood flow in lactating Holstein cows. J. Dairy Sci. 95(6):2919-2934.

Titgemeyer, E., K. Spivey, S. Parr, D. Brake, and M. Jones. 2012. Relationship of whole body nitrogen utilization to urea kinetics in growing steers. J. Anim. Sci. 90(10):3515-3526.

Tran, H., A. Caprez, P. Kononoff, P. Miller, and W. Weiss. 2016. Automation of statistical procedures to screen raw data and construct feed composition databases. J. Anim. Sci. 94(suppl_5):681-682.

White, R., Y. Roman-Garcia, J. Firkins, P. Kononoff, M. VandeHaar, H. Tran, T. McGill, R. Garnett, and M. Hanigan. 2017a. Evaluation of the National Research Council (2001) dairy model and derivation of new prediction equations. 2. Rumen degradable and undegradable protein. J. Dairy Sci. 100(5):3611-3627.

White, R., Y. Roman-Garcia, J. Firkins, M. VandeHaar, L. Armentano, W. Weiss, T. McGill, R. Garnett, and M. Hanigan. 2017b. Evaluation of the National Research Council (2001) dairy model and derivation of new prediction equations. 1. Digestibility of fiber, fat, protein, and nonfiber carbohydrate. J. Dairy Sci.100(5), 3591-3610.

Wickersham, T., E. Titgemeyer, and R. Cochran. 2009. Methodology for concurrent determination of urea kinetics and the capture of recycled urea nitrogen by ruminal microbes in cattle. Animal : an international journal of animal bioscience 3(3):372-379.

Wickersham, T., E. Titgemeyer, R. Cochran, E. Wickersham, and D. Gnad. 2008a. Effect of rumen-degradable intake protein supplementation on urea kinetics and microbial use of recycled urea in steers consuming low-quality forage. J. Anim. Sci. 86(11):3079-3088.

Wickersham, T. A., E. C. Titgemeyer, R. C. Cochran, and E. E. Wickersham. 2008b. Effect of undegradable intake protein supplementation on urea kinetics and microbial use of recycled urea in steers consuming low-quality forage. Br. J. Nutr. 101(2):225-232.

Wohlt, J., J. Clark, and F. Blaisdell. 1976. Effect of Sampling Location, Time, and Method of Concentration of Ammonia Nitrogen in Rumen Fluid1. J. Dairy Sci. 59(3):459-464.

Zhu, J., S. Stokes, and M. Murphy. 1997. Substitution of neutral detergent fiber from forage with neutral detergent fiber from by-products in the diets of lactating cows. J. Dairy Sci. 80(11):2901-2906.

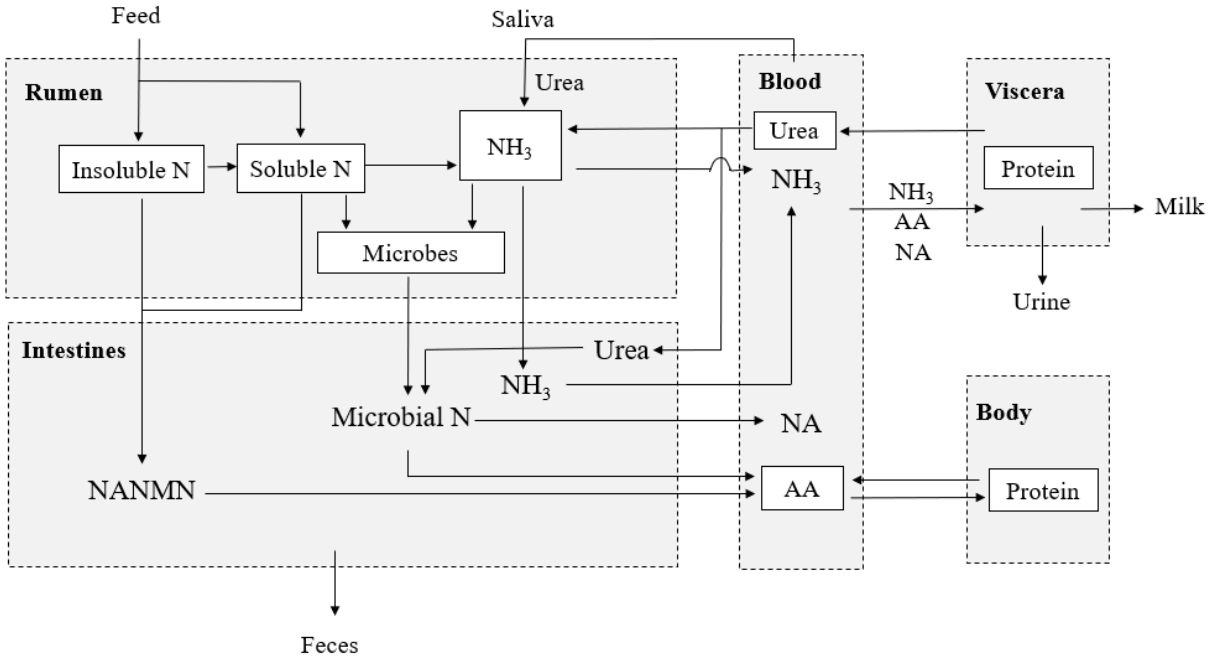

Figure 3-1. A schematic diagram of nitrogen metabolism in the Molly model. NANMN represents non-ammonia, non-microbial nitrogen; NA is nucleic acids. Boxes with dashed lines are compartments; boxes with solid lines represent pools; arrows indicate fluxes.

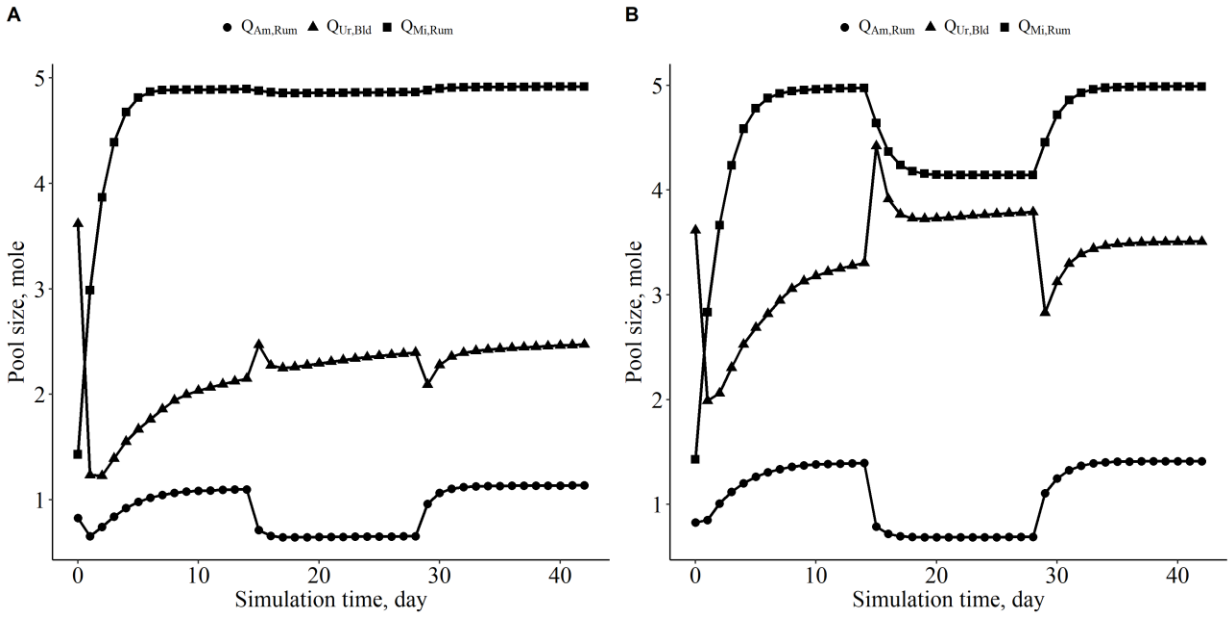

Figure 3-2. Ruminal ammonia ($Q_{Am,Rum}$), microbes ($Q_{Mi,Rum}$) and blood urea ($Q_{Ur,Bld}$) pools (mole) with respect to simulation time for the initial model (A) and the modified model (B). The rate constant for ruminal ammonia absorption ($K_{Am,RumBld}$, d^{-1}) was set to 10.44 at the start of the simulation for the initial model, changed to 20 on day 14, and returned to 10.44 on day 28. $K_{Am,RumBld}$ was set to 5.01 at the start of the simulation for the modified model, set to 20 on day 14; and returned to 5.01 on day 28.

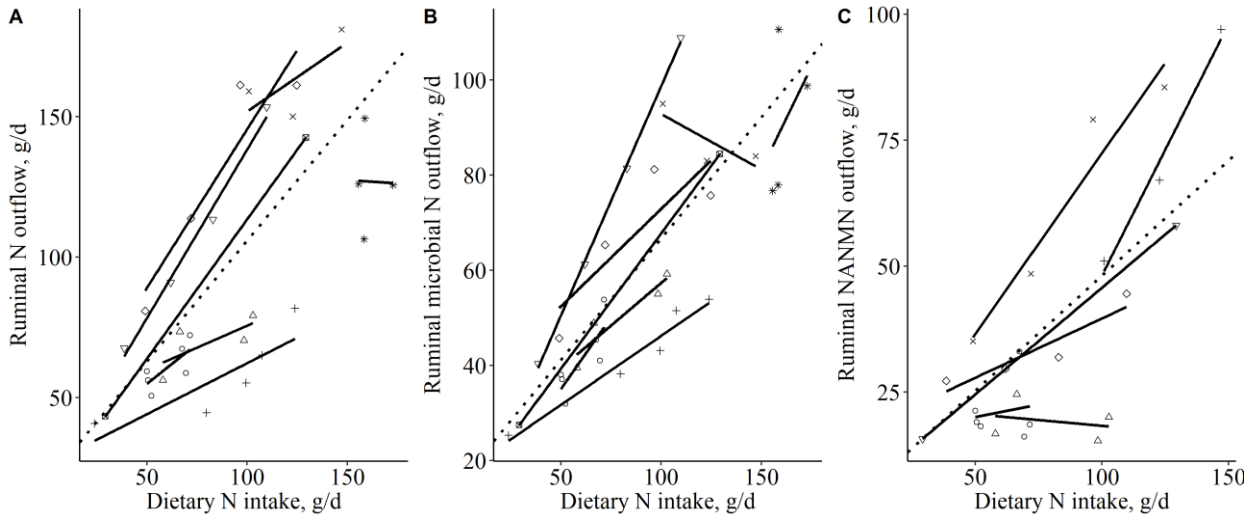

Figure 3-3. Relationships between observed dietary N intake and ruminal N, microbial N and non-ammonia, non-microbial N (NANM) outflow. The solid lines represent the results of linear regression for individual studies. The dotted line indicates the global regression for the full data set. Study effect was included as a random variable in the global regression model. (A) Ruminal N outflow (g of N per day) versus dietary N intake (g of N per day): Y= 20.14 + 0.86 X (R^2_m = 0.56 and R^2_c =0.91); (B) Ruminal microbial N outflow (g of N per day) versus dietary N intake (g of N per day): Y= 15.76 + 0.51 X (R^2_m = 0.67 and R^2_c =0.84); (C) Ruminal NANM outflow (g of N per day) versus dietary N intake (g of N per day):Y= 2.35 + 0.46 X (R^2_m = 0.44 and R^2_c =0.85). R^2_m is marginal R^2, which represents a proportion of variance that can be explained by the fixed effect, and R^2_c is conditional R^2, which indicates a proportion of variance that can be explained by the fixed effect plus the random effect.

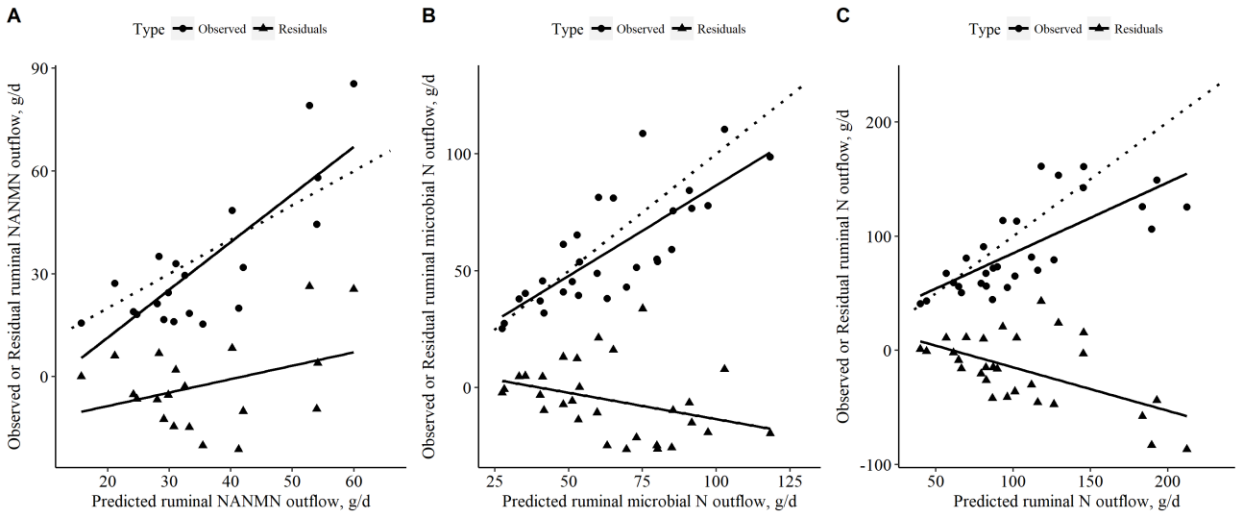

Figure 3-4. A) Observed or residual ruminal non-ammonia, non-microbial N outflows (g/d) versus predicted flows using the modified model. B) Observed or residual ruminal microbial N outflow (g/d) versus predicted values using the modified model. C) Observed or residual ruminal total N outflow (g/d) versus predicted values using the modified model. The dotted lines represent the line of unity.

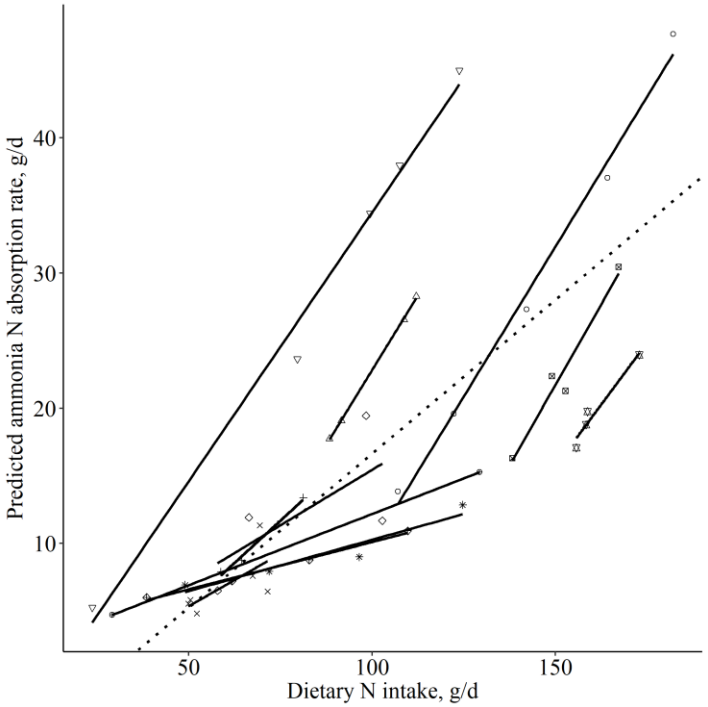

Figure 3-5. Relationships between observed dietary N intake and predicted ammonia N absorption rate by the modified Molly model. The solid lines represent the results of linear regression for individual studies. The dotted line indicates the regression result for the full data set. Study effect was included as a random variable in the regression model. The slopes for individual studies ranged from 0.1 to 0.4. The regression model for the whole dataset is Y= -6.17 + 0.23 X (R^2_m = 0.59 and R^2_c =0.87). R^2_m is marginal R^2, which represents a proportion of variance that can be explained by the fixed effect, and R^2_c is conditional R^2, which indicates a proportion of variance that can be explained by the fixed effect plus the random effect.

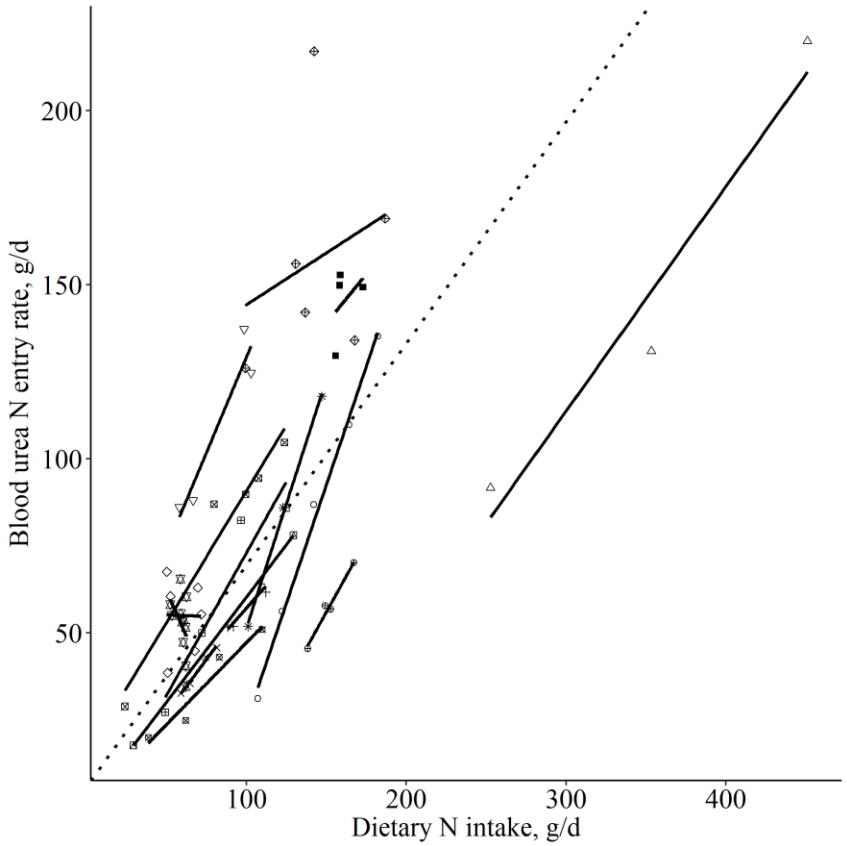

Figure 3-6. Relationship between observed dietary N intake (g of N per day) and observed urea N entry rate (g of N per day). Solid lines represent the results of linear regression for individual studies. The dotted line indicates the global regression for the full data set. Study effect was included as a random variable in the global regression model. The regression model for the whole dataset is Y= 5.95 + 0.64 X (R^2_m = 0.55 and R^2_c =0.94. R^2_m is marginal R^2, which represents a proportion of variance that can be explained by the fixed effect, and R^2_c is conditional R^2, which indicates a proportion of variance that can be explained by the fixed effect plus the random effect.

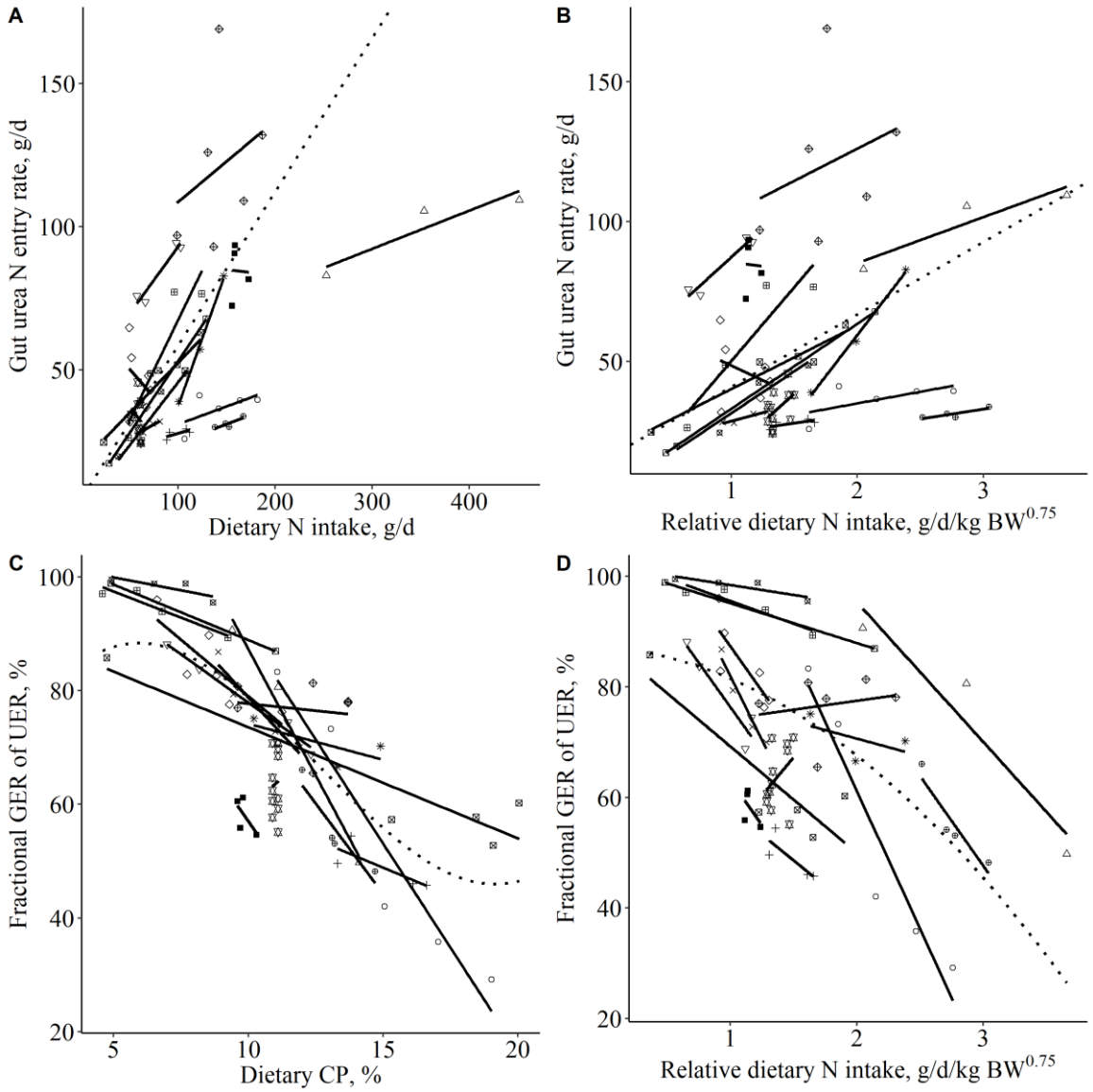

Figure 3-7. Relationships between observed dietary protein and observed gut urea entry. The solid lines represent the results of linear regression for individual studies. The dotted line indicates the global regression for the full data set. Study effects were included as a random variable in the global regression model. (A) Gut urea N entry rate (g of N per day) versus dietary N intake (g of N per day): Y= 19.62 + 0.31 X (R^2_m = 0.35 and R^2_c =0.88); (B) Gut urea N entry rate (g of N per day) versus dietary N intake relative to metabolic BW (g/d/kg $BW^{0.75}$): Y= 15.05 + 25.90 X (R^2_m = 0.20 and R^2_c =0.91); (C) Fractional gut urea entry rate (GER) of blood urea entry rate (UER) (%) versus dietary CP (%): Y= 55.2 + 0.037 X^3 – 1.38 X^2 + 12.49 X (R^2_m = 0.55 and R^2_c =0.87); (D) Fractional gut urea entry rate (GER) of blood urea entry rate (UER) (%) versus dietary N intake relative to metabolic BW (g/d/kg $BW^{0.75}$): Y= 87.3 – 4.09 X^2 -1.67 X (R^2_m = 0.29 and R^2_c =0.89). R^2_m is marginal R^2, which represents a proportion of variance that can be explained by the fixed effect, and R^2_c is conditional R^2, which indicates a proportion of variance that can be explained by the fixed effect plus the random effect.

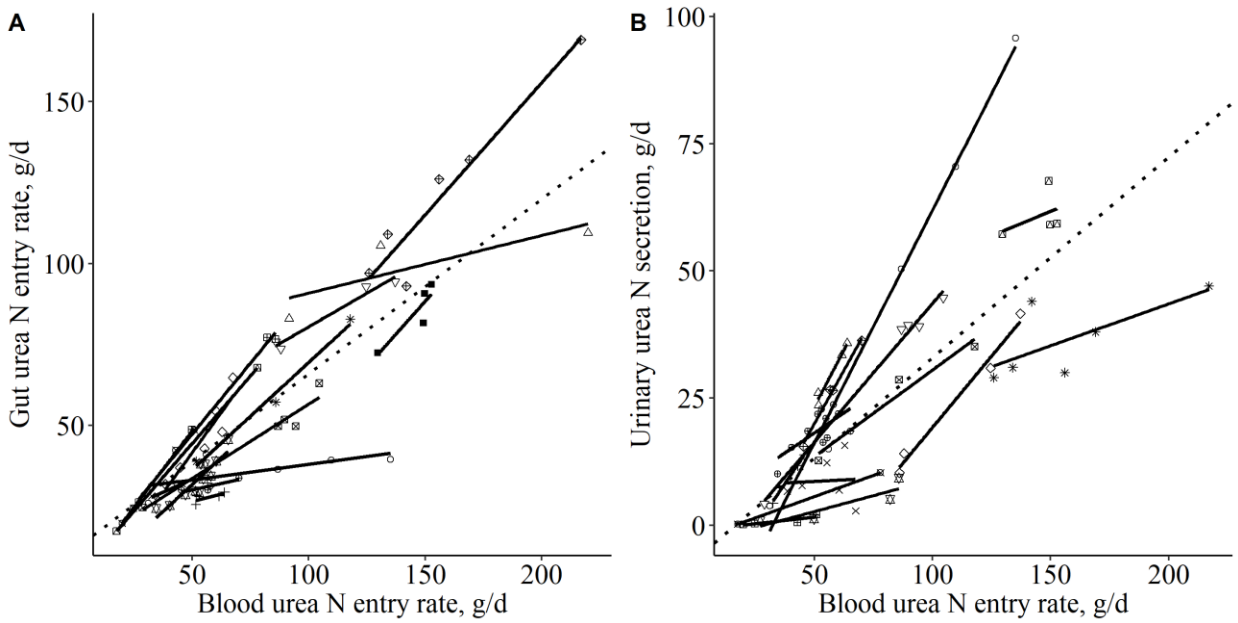

Figure 3-8. Relationships between observed blood urea entry rate (g of N per day) and observed gut urea entry rate or urinary urea N secretion (g of N per day). The solid lines represent the results of linear regression for individual studies. The dotted line indicates the global regression for the full data set. A) Gut urea entry rate versus blood urea entry: Y = 12.09 + 0.54 X (R^2_m = 0.75 and R^2_c = 0.91); B) Urinary urea N secretion versus blood urea entry rate: Y = -6.52 + 0.39 X (R^2_m = 0.62 and R^2_c = 0.88). The study effect was considered as a random variable. R^2_m is marginal R^2, which represents a proportion of variance that can be explained by the fixed effect, and R^2_c is conditional R^2, which indicates a proportion of variance that can be explained by the fixed effect plus the random effect.

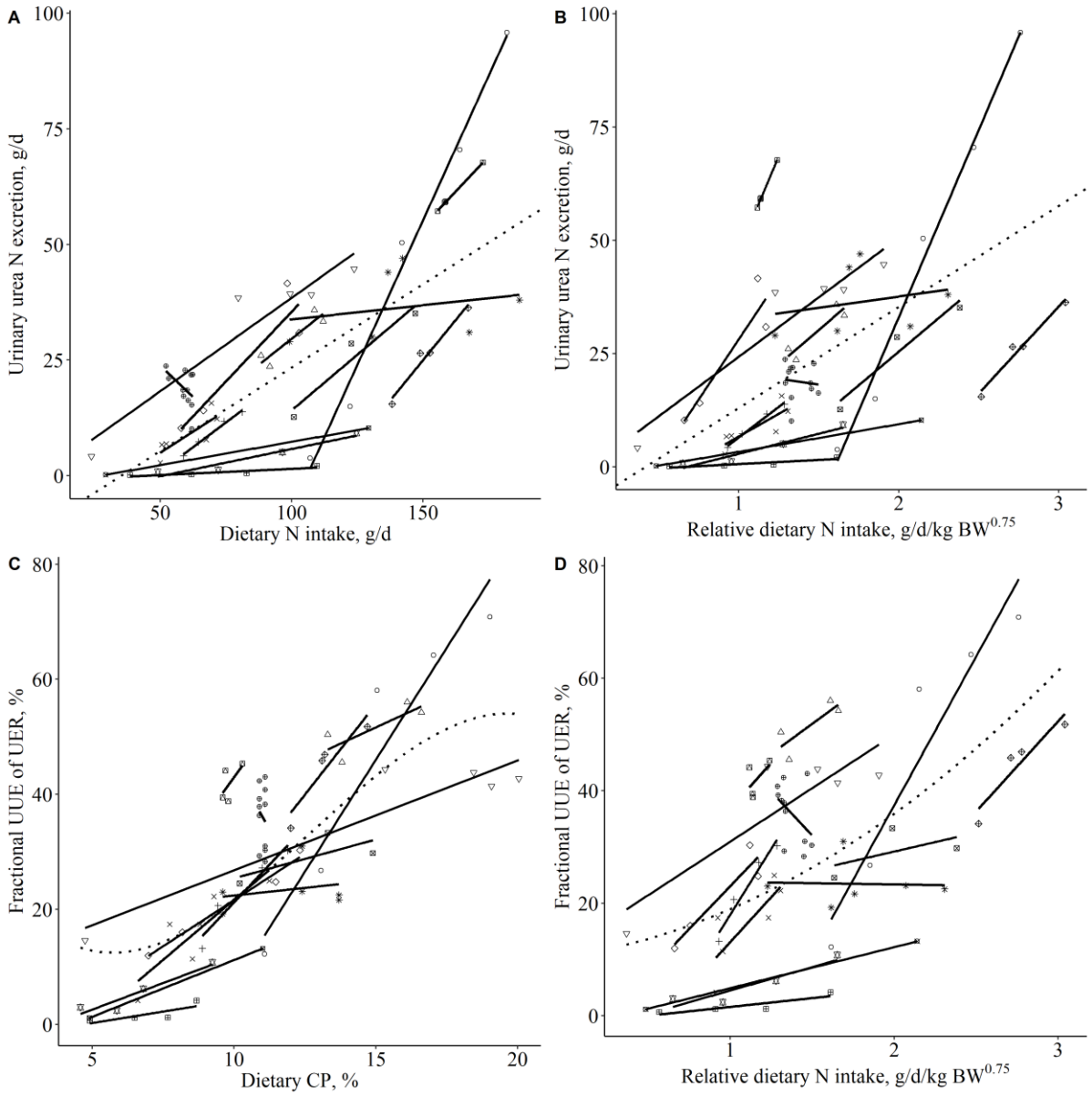

Figure 3-9. Relationships between dietary protein and urinary urea excretion. The solid lines represent the results of linear regression for individual studies. The dotted line indicates the global regression for the full data set. Study effect was included as a random variable in the global regression model. (A) Urinary urea N secretion (g of N per day) versus dietary N intake (g of N per day): $Y= -7.42 + 0.31 X$ ($R^2_m = 0.47$ and $R^2_c =0.76$); (B) Urinary urea N secretion (g of N per day) versus dietary N intake relative to metabolic BW (g/d/kg $BW^{0.75}$): $Y= -3.47 + 18.33 X$ ($R^2_m = 0.23$ and $R^2_c =0.81$); (C) Fractional urinary urea secretion (UUE) of blood urea entry rate (UER) (%) versus dietary CP (%): $Y= 38.76 – 0.029 X^3 + 1.13 X^2 -10.06 X$ ($R^2_m = 0.51$ and $R^2_c =0.88$); (D) Fractional urinary urea secretion (UUE) of blood urea entry rate (UER) (%) versus dietary N intake relative to metabolic BW (g/d/kg $BW^{0.75}$): $Y= 15.6 + 5.65 X^2 -1.76 X$ ($R^2_m = 0.28$ and $R^2_c =0.87$). R^2_m is marginal R^2, which represents a proportion of variance that can be explained by the fixed effect, and R^2_c is conditional R^2, which indicates a proportion of variance that can be explained by the fixed effect plus the random effect.

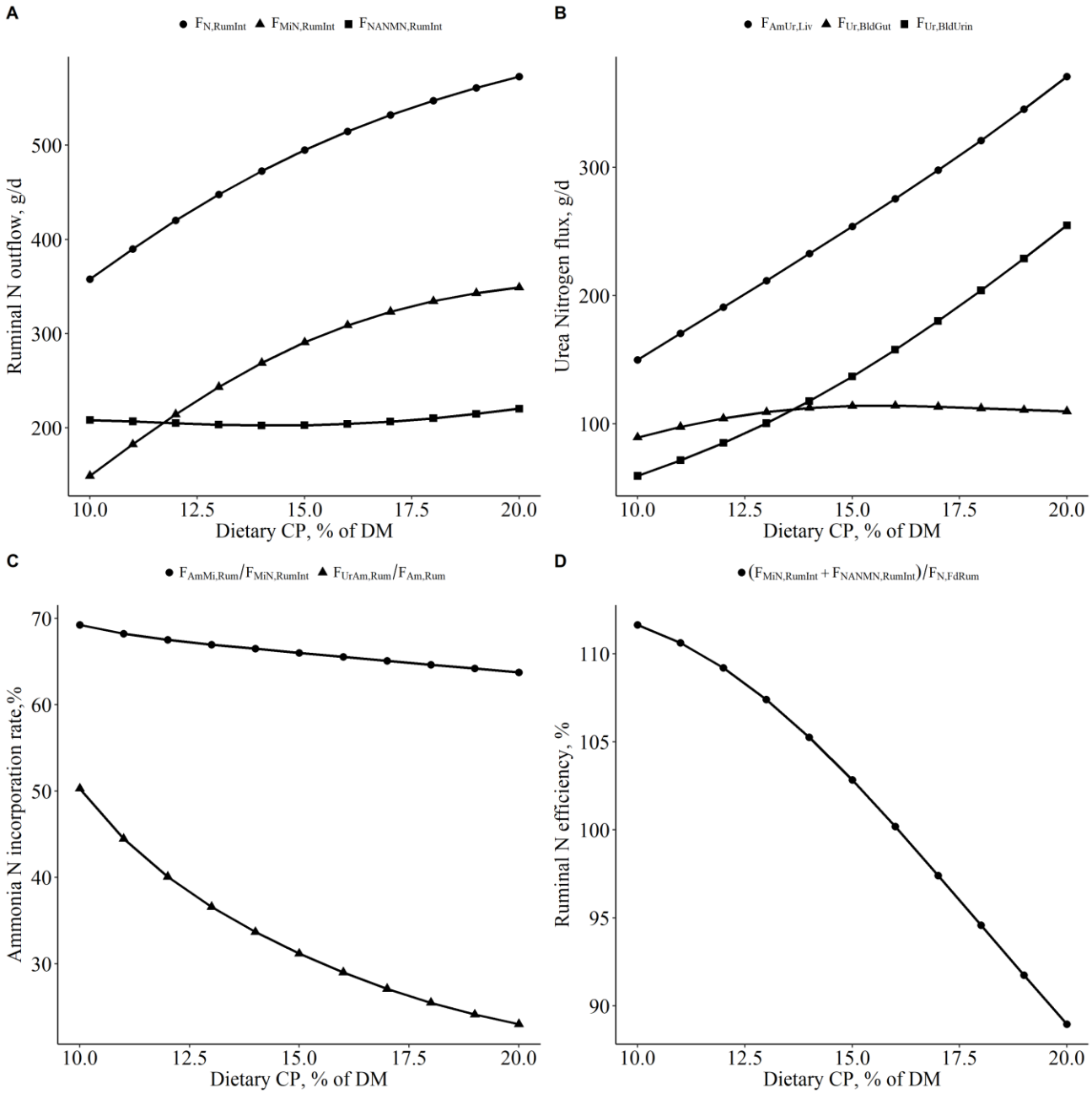

Figure 3-10. Effects of varying dietary CP concentrations on model behavior given a constant RUP proportion (6% of DM). DMI was constant among diets. $F_{N,RumInt}$ represents ruminal total N outflow; $F_{MiN,RumInt}$ represents ruminal microbial N outflow; $F_{NANMN,RumInt}$ is ruminal non-ammonia, non-microbial N outflow; $F_{AmUr,Liv}$ represents blood urea entry rate; $F_{Ur,BldGut}$ is gut urea entry rate; $F_{Ur,BldUrin}$ represents urinary urea secretion; $F_{AmMi,Rum}$ is a flux of ammonia N converted to microbial protein; $F_{UrAm,Rum}$ is flux of ammonia generated from recycled urea in the rumen; $F_{Am,Rum}$ is total ammonia production rate; $F_{N,FdRum}$ is total dietary N intake.

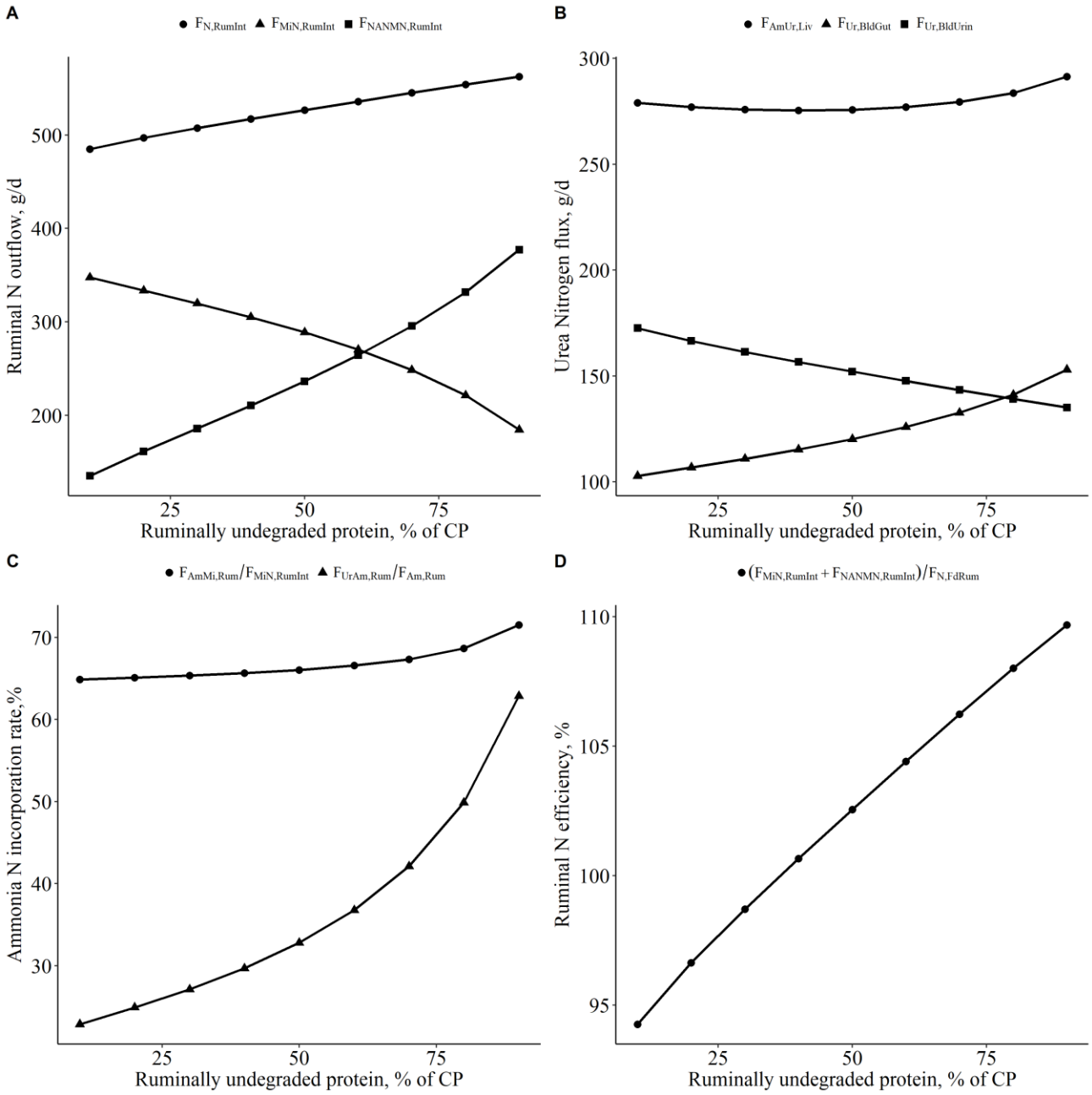

Figure 3-11. Effects of varying dietary RUP proportions on model behavior given a constant CP concentration (16% of DM). DMI was constant among diets. $F_{N,RumInt}$ represents ruminal total N outflow; $F_{MiN,RumInt}$ represents ruminal microbial N outflow; $F_{NANMN,RumInt}$ is ruminal non-ammonia, non-microbial N outflow; $F_{AmUr,Liv}$ represents blood urea entry rate; $F_{Ur,BldGut}$ is gut urea entry rate; $F_{Ur,BldUrin}$ represents urinary urea secretion$F_{AmMi,Rum}$ is a flux of ammonia N converted to microbial protein; $F_{UrAm,Rum}$ is flux of ammonia generated from recycled urea in the rumen; $F_{Am,Rum}$ is total ammonia production rate; ; $F_{N,FdRum}$ is total dietary N intake.

Table 3-1. A summary of observed nutrient intake, ruminal metabolism, ruminal N outflow, and urea transfers from the meta data.

Items	N	Mean	SD	Min	Max
Body weight, kg	69	297.1	145.1	139.0	723.0
Intake, kg/d					
DM	69	6.1	3.4	2.9	20.0
OM	49	5.2	2.2	2.7	10.0
ADF	9	1.6	0.6	0.9	2.2
NDF	4	4.4	0.1	4.3	4.6
Starch	13	3.9	0.8	2.9	5.6
Nitrogen	31	135.3	88.7	52.2	451.2
Rumen fermentation					
pH	35	6.3	0.4	5.6	6.9
Ammonia, mM	44	4.6	4.4	0.1	15.9
Total VFA, mM	39	88.5	21.9	52.2	139.0
Acetate, % of VFA	39	67.3	8.8	41.2	77.1
Propionate, % of VFA	37	18.8	5.7	12.0	43.0
Butyrate, % of VFA	39	8.8	2.5	5.3	14.9
Ruminal N outflow, g/d					
Total N	32	95.5	42.7	40.8	181.0
Microbial N	32	61.2	24.0	25.3	110.6
Non-ammonia non-microbial N	23	37.9	24.4	15.3	97.0
N metabolism					
Blood urea N, mg/dl	62	7.7	5.9	0.7	27.0
Blood urea N entry, g/d	69	79.4	45.5	17.6	219.9
Gut urea N entry, g/d	69	54.3	31.7	17.4	169.0
Urea N returned to the ornithine cycle, g/d	57	26.3	19.9	2.8	84.0
Urea N utilized for anabolism, g/d	53	27.0	15.5	8.8	79.0
Urinary urea N, g/d	66	24.0	19.8	0.1	95.8
Urinary N, g/d	69	42.6	25.5	13.4	139.4
Fecal N, g/d,	69	37.3	24.6	14.7	142.0
Fecal urea N, g/d	53	2.9	2.0	0.3	6.9
Retained N, g/d	69	28.9	19.1	-8.3	87.6

Table 3-2. Residual error analyses for predictions of urea N recycling and ruminal N outflows in Molly

Items	N	Observed mean	Predicted mean		RMSE, % mean		Mean bias, % MSE		Slope bias, % MSE		CCC	
			Initial	Modified	Initial	Modified	Initial	Modified	Initial	Modified	Initial	Modified
Ruminal outflow, g/d												
Total N	29	88.5	112.0	105.3	55.0	39.5	23.4	22.4	45.7	22.3	0.56	0.67
Microbial N	29	58.5	75.1	63.8	56.6	27.8	25.1	10.6	55.0	10.4	0.57	0.76
Non-ammonia, non-microbial N	20	32.9	31.9	35.4	38.6	35.9	0.57	3.9	29.8	12.8	0.68	0.70
N metabolism												
Ruminal ammonia, mmol/L	32	5.0	2.2	4.8	75.9	48.3	55.1	0.5	5.8	0.4	0.66	0.87
Blood urea N, mg/dl	44	8.4	2.6	8.3	100.4	48.9	45.6	0.1	11.9	2.1	0.12	0.75
Blood urea N entry, g/d	46	71.0	77.09	74.1	46.9	26.3	2.2	2.8	6.6	3.2	0.59	0.84
Gut urea N entry, g/d	46	47.4	22.0	43.6	81.2	36.3	58.4	4.9	0.5	1.2	0.17	0.62
Urinary urea N, g/d	46	23.6	55.1	30.5	132.6	55.6	83.0	27.5	2.3	9.2	0.45	0.79
Urinary N, g/d	46	42.3	55.1	38.2	41.1	29.3	43.0	10.9	1.2	9.2	0.76	0.85
Fecal N, g/d	46	36.0	41.1	33.8	48.9	30.2	20.6	4.2	60.7	11.3	0.42	0.61
Fecal N from urea, g/d	33	3.0	NA	3.1	NA	66.2	NA	0.3	NA	13.4	NA	0.48
Retained N, g/d	46	21.5	-14.8	16.0	172.4	58.6	85.6	19.4	1.7	50.2	0.15	0.73

Table 3-3 Model parameters estimates when the model was fitted to the observed data

Model parameter	Description	Previous values[1]	Final estimate	SE
$K_{RUP,Rum}$	Intercept scalar to adjust in situ determined ruminal protein degradation rates ($mole^{-1}$)	2.17	1.81	0.08
$K_{slpRUP,Rum}$	Slope scalar to adjust in situ determined ruminal protein degradation rates ($mole^{-1}$)	0.03	0.16	0.003
$K_{Am,RumBld}$	Rate constant for ammonia absorption (d^{-1})	10.44	5.01	0.09
$K_{YATP,Rum}$	Efficiency constant defining the yield of microbial DM per mole of ATP (g/mole)	0.03	0.055	0.001
$K_{AmMi,Rum}$	Rate constant for the effect of ammonia on microbial growth (L/mole)	2.0×10^{-4}	0.007	1.6×10^{-4}
X_{EAm}	Exponential factor to adjust the effect of ammonia on microbial growth (mole/mole)	NA	8.85	0.58
J_{Am}	Rate constant for the inhibititory effect of ammonia on blood urea conversion to ruminal ammonia (L/mole)	0.003	0.0026	8.46×10^{-5}
$Vm_{UrAm,Rum}$	Maximal rate of the blood urea conversion to ruminal ammonia (mole/d)	0.0567	0.069	1.6×10^{-3}
$K_{SlpUr,IntFec}$	Slope scalar to predict fecal urea excretion ($mole^{-1}$)	NA	1×10^{-7}	6.5×10^{-9}
$K_{Ur,IntFec}$	Intercept scalar to predict fecal urea excretion ($mole^{-1}$)	NA	0.113	0.003
$Vm_{AaOth,Vis}$	Maximal rate of the AA conversion to lean body tissue (mole/d)	223.2	539.2	16.6
$K_{Ur,BldUrin}$	Rate constant for urea excretion by the kidney ($mole^{-1}$)	2134[2]	2.46	0.049
$K_{Protein,IntFec}$	Intestinal digestion coefficient for protein (g/g)	0.68	0.79	0.018

[1] K_{RUP}, K_{SlpRUP}, $K_{Am,RumBld}$, and $K_{YATP,Rum}$ were refitted to a dataset reported by Hanigan et al. (2013) after revising water kinetics. $K_{AmMi,Rum}$ and $K_{Protein,IntFec}$ were from Hanigan et al. (2013). $K_{Ur,BldUrin}$ was from Hanigan et al. (2009b). J_{Am}, $Vm_{UrAm,Rum}$ and $Vm_{AaOth,Vis}$ were from the original model as described by Baldwin (1995).

[2]The unit for $K_{Ur,BldUrin}$ in the initial model was (L/mole).

Chapter 4: Simulation of nutritional strategies to improve energy and nitrogen efficiency in the bovine: a modeling approach

Abstract

Balancing rations to optimize energy and protein supplies is critical for optimizing feed efficiency. The objectives of this study were to further improve the representation of pH and to refit parameters related to ruminal metabolism and nutrient digestion in the Molly cow model, and to use the improved model to estimate nitrogen and energy fluxes with varying RUP (40 vs. 60%) and ruminally undegraded starch (RUStarch; 25 vs. 50%). A dataset assembled from the literature containing 284 peer reviewed studies with 1223 treatment means was used to derive parameter estimates for ruminal metabolism and nutrient digestions. Refitting the parameters significantly improved the accuracy and precision of the model predictions for ruminal nutrient outflow (ADF, NDF, total N, microbial N, non-ammonia N, and non-ammonia, non-microbial N), ammonia concentrations, and fecal nutrient outflow (protein, ADF, and NDF). Adding ammonia concentration as a driver to the pH equation increased the precision of predicted ruminal pH, and thereby, the precision of predicted VFA concentrations due to an improved representation of pH regulation of VFA production rates. Although minor mean and slope bias were observed for ruminal pH and VFA concentrations, the small values for concordance correlations indicated much of the observed variation in these variables remains unexplained. Overall, the biological functions of nutrient degradation and digestion appear to be well properly represented in the model. The simulation results indicated increasing RUP proportions and decreasing RUStarch proportions in a moderately low protein diet can be employed to improve feed efficiency.

Key words: mathematic model, simulation, nitrogen, energy

Introduction

On most dairy operations, feed is the single largest cost representing approximately 70% of total operating costs (Short, 2004). As a result, improving the efficiency with which feed is converted into salable milk is a primary goal of many operations. Within a diet, protein and energy are the most expensive nutrients (St-Pierre and Glamocic, 2000), suggesting that careful ration balancing to optimize energy and protein supplies is a critical step toward optimizing feed efficiency.

Models such as the NRC (2001) and Cornell Net Carbohydrate and Protein System (Fox et al., 1992; Russell et al., 1992; Sniffen et al., 1992; O'Connor et al., 1993) are examples of nutrient requirement systems that are used for ration balancing. Based on these models, a least cost formulation programs based on these models have been developed and this approach has been extensively used to optimize the combination of feed ingredients to meet the required nutrient needs at least cost (St-Pierre and Thraen, 1999). However, considering the mostly linearity nature of these requirement response models, it did not match empirical relationships between nutrient inputs and level of productivity are not well matched (Huhtanen and Hristov, 2009; Vyas and Erdman, 2009; Hollmann et al., 2011; Leduc et al., 2017).

The level of aggregation of such empirical models does not capture critical components of some metabolic reactions, and thus they do not completely reflect the potential range of nutritional efficiency. It is also difficult to simulate management strategies that are time dependent, given the static nature of these models. Molly is a dynamic and mechanistic model that integrates biological knowledge at the pathway level. Therefore it allows assessment of energy and nitrogen efficiency by comparing various biological measurements (Hanigan et al., 2006). A series of work has been conducted to evaluate and improve predictions of ruminal metabolism, nutrient digestion, and animal metabolism by the model which have yielded

significant improvements in accuracy and precision (Hanigan et al., 2006; Hanigan et al., 2009b; Hanigan et al., 2013; Gregorini et al., 2015). A series of efforts has been conducted to evaluate and improve the predictions of the model of ruminal metabolism, and nutrient digestion, and animal metabolism which have yielded significant improvements in the accuracy and precision (Hanigan et al., 2009b; Hanigan et al., 2013; Gregorini et al., 2015). Most recently, the representation of nitrogen cycling between blood and the gut was improved which yielded unbiased predictions of ammonia concentration when evaluated with a small data set (Li et al., under review). Li et al. (2018a), hypothesized, based on residual errors, that consideration of the effects of ammonia concentrations in the ruminal pH equation would improve the representation and thereby improve predictions of VFA production. Ammonia was found to be an important driver of pH in the original equation by Briggs et al. (1957). As ammonia and pH are regulators of microbial growth, which in turn regulates nutrient degradation and fermentation, any changes in these representations necessitates reparameterization work to re-center predictions of ruminal metabolism and nutrient digestion in the observed data.

The objectives of this study were to 1) further improve the representation of pH; 2) refit parameters related to ruminal metabolism and nutrient digestion in the Molly cow model; 3) use the improved model to estimate nitrogen and energy fluxes with varying RUP and ruminally undegraded starch. We hypothesized that the model could properly reflect the underlying biological functions of ruminal metabolism and nutrient digestion after reparameterizations, and the improved model can be used to compare nitrogen and energy efficiency by estimating different nutritional strategies.

Materials and Methods

Data collection

The dataset used to derive parameters and evaluate the model predictions was assembled from studies used by Li et al. (2018a) and Fleming et al. (under review). The selection criteria for inclusion of studies in the database were: the work was conducted in beef or dairy cattle; DMI and the ingredient composition of the diets were reported; and either ruminal fermentation variables (pH, ammonia, and VFA concentrations) or nutrient digestion variables (ADF, NDF, starch, protein, or fat digestibility, ruminal outflow, or fecal outflow) were reported or could be calculated. In total, 284 studies with 1223 treatment means were included in the dataset. A descriptive summary of the dataset is presented in Table 4-1.

Model description

The model used was that of Baldwin et al. (1987a; 1987b; 1987c) with modifications described by Baldwin (1995), Hanigan et al.(2006; 2007; 2009b; 2013), Gregorini et al. (2015), and Li et al. (under review). It is important to note that the work of Li et al. included significant changes to the representation of urea entry into the rumen, ammonia absorption from the rumen, and ammonia effects on urea entry and microbial growth. Thus, the behavior of the model after this update would be expected to deviate from the behavior before those changes were implemented. Required model input variables included DMI, BW, chemical composition of the diet (CP, starch, NDF, ADF, and fat), ruminal solubility and degradability of protein and starch, ruminal degradability of ADF, forage NDF, and diet particle size distribution. These variables were prepared following the same procedure as descripted by Li et al. (2018a).

Ammonia concentrations were added to the existing ruminal pH equation to improve representations of acid-base balance in the rumen.

$$pH = (K_{VFApH,Rum} \times C_{VFA,rum} + 1.5 \times C_{La,Rum} - K_{AmpH,Rum} \times C_{Am,Rum}) \times K_{SlppH,Rum} + K_{pH,Rum} \quad (25)$$

where $C_{VFA,Rum}$, $C_{La,Rum}$, and $C_{Am,Rum}$ represented total VFA, lactate, and ammonia concentrations; $K_{VFApH,Rum}$ and $K_{AmpH,Rum}$ were VFA and ammonia coefficients for ruminal pH; $K_{SlppH,Rum}$ and $K_{pH,Rum}$ were the slope and intercept scalars to adjust predicted pH for better fitness.

The model was compiled in ACSLX (version 3.1.4.2, Aegis Technologies Group Inc., Huntsville, AL) and solved using a 4th order, variable step Runge-Kutta integration algorithm with a maximum step size of 0.005 d. The parameters listed in Table 4-3 were estimated simultaneously using the Direction Set algorithm to maximize the log-likelihood function (Press et al., 2007). The model was set to simulate 14 d before comparison to observed values to ensure that model had reached steady state. Model values from the last day were aligned with observed values to determine residual errors. The accuracy and precision of model predictions before and after reparameterizations were assessed, respectively, using root mean squared errors (RMSE), mean bias, and slope bias as described by Bibby and Toutenburg (1977); and concordance correlation coefficients (CCC) as described by Lawrence and Lin (1989).

Efficiency Simulations

Four isonitrogenous and isocaloric diets were designed to examine the effect of nutritional changes on nitrogen and energy efficiency. The four diets were a combination of RUP (40% vs. 60%) and ruminally undegraded starch (RUStarch; 25% vs. 50%). All diets contained the same concentrations of 6% fat, 30% starch, 16% protein, 30% NDF, 20% ADF, and 6% ash. The animal was assumed to be a Holstein dairy cow weighing 600 kg and 70 d in milk. All simulations were performed at an intake of 20 kg of DMI/d. Model values from d 14 of the simulation were used to represent steady state values. Given that the model has been fit to a large number of observations from the literature, it is assumed that the model represents an average

cow from the research herd population. There was no replication for the experimental unit, so no statistical analyses were conducted for the simulation results. All the evaluations of nitrogen and energy metabolism were assessed based on the numeric differences.

Results and Discussion

Residual error analyses for the model predictions before and after reparameterizations are presented in Table 4-2. With the exception of ruminal pH, ruminal ammonia concentration, total VFA concentrations, and fecal protein output predictions for the initial model, both the initial and modified models had only minor slope bias, suggesting the model was an appropriate representation of ruminal metabolism and nutrient digestion of those predictions. Refitting the model parameters listed in Table 4-3 to the data after updating the ruminal pH prediction equation significantly increased the accuracy and precision of model predictions for ruminal nutrient outflow (ADF, NDF, total N, microbial N, non-ammonia N, and non-ammonia, non-microbial N), ammonia concentrations, and fecal nutrient outflow (protein, ADF, and NDF), primarily due to decreased mean bias. Improvements on ruminal outflow and fecal outflow of DM, starch, and fat were negligible. Minor mean and slope bias remained for predicted ruminal pH and VFA concentrations in the modified model. However, the small CCC values suggest the predictions fail to capture a large proportion of the observed variation. In some cases, such for ruminal pH and VFA concentrations, this may reflect variation in sample time with respect to a meal and sample location, neither of which were captured in the data. Therefore, it is unclear how much of the total variation is truly random and not definable by such a model.

Nutrient outflow from the rumen

Roughly 40.0 % of ADF and 44.1% of NDF were degraded by rumen microbes. In the model, an estimate of undegraded ADF (% of ADF) is used as a model input. The intent of this input is to allow use of in situ data to set the intrinsic degradation characteristics of each feed as

is done for RUP. However, the available data for feed ingredients is not as extensive as for protein degradability, and thus in practice, this input is often set using observed ruminal digestibility values. Thus the predictions of ruminal outflow are not completely independent of the data. The rate constant for hemicellulose degradation was calculated as a proportion ($K_{HcCs1,Rum}$) of the cellulose rate constant (Baldwin, 1995). Because in situ determined degradation rates might be biased compared with measurements of duodenal or omasal fiber flows, intercept ($K_{RUADF,Rum}$) and slope scalars ($K_{slpRUADF,Rum}$) were introduced to adjust in situ determined ruminal cellulose degradation rate constants to better reflect the observed data (Hanigan et al., 2013; Gregorini et al., 2015). After refitting $K_{RUADF,Rum}$, $K_{slpRUADF,Rum}$, and $K_{HcCs1,Rum}$ to the literature data, root mean squared errors for ruminal outflow of ADF and NDF were decreased from 26.6to 20.1% and 33.8 to 24.4%, with mean bias decreased from 37.7 to 1.1% and 42.5 to 1.1%. These reductions in error were mirrored by CCC increases from 0.75 to 0.82 for ruminal ADF outflow and 0.61 to 0.72 for NDF outflow. Thus both accuracy and precision were improved by the model changes and reparameterization.

Ruminal starch outflow exhibited a RMSE of 56.0% and a CCC of 0.55 in the modified model, suggesting starch degradation was still poorly estimated. However, 98% of the error segregated as random implying that most of the error was random. The lack of mean and slope bias suggests the predictions were unbiased. Similar results were also reported in previous studies (Hanigan et al., 2013; Gregorini et al., 2015; Li et al., 2018a). Although variable by diet type, approximately 66.5 ± 18.8% of starch is degraded in the rumen. Although there is an official AOAC method for determining starch content, the inter laboratory variation in starch analysis was very high (Mills et al., 1999; Firkins et al., 2001). Because the proportion of starch within the various particle sizes were different (Galyean et al., 1981), large variations could be

introduced when collecting digesta samples from duodenal or omasal cannula due to sampling bias. Additionally, factors that affect starch degradability, such as grain type (Firkins et al., 2001), processing methods (Svihus et al., 2005), and animal genetic variation (Channon et al., 2004), were not represented in the model. Therefore, refitting the intercept ($K_{RUSt,Rum}$) and slope scalars ($K_{slpRUSt,Rum}$), while improving accuracy, did not improve the precision of model predictions for ruminal starch degradation.

Approximately 59.2 ± 18.2% of dietary protein was degraded in the rumen. Similar to ruminally undegraded ADF and starch, RUP determined from in situ evaluations was a model input which was used to calculate the model rate parameter for protein degradation with adjustment using intercept ($K_{RUP,Rum}$) and slope scalars ($K_{slpRUP,Rum}$). Refitting the latter 2 parameters led to a decrease in mean bias from 17.3 to 8.8% and a reduction in slope bias from 6.8 to 5.9% for ruminal NANMN outflow. Overall error in ruminal NANMN outflow was reduced from 39.5 to 37.5%. As for starch flows, it is difficult to assess the proportion of this error that is due to random animal, sampling, and analytical error, but the lack of mean and slope bias in the predictions suggests the predictions are an unbiased representation of the mechanism.

Microbial protein accounts for more than 50% of metabolizable protein. As originally described by Baldwin (1995), microbial growth is driven by ruminally available substrate (AA, peptides, and ammonia) and energy, and inhibited by supplemental dietary fat. Refitting the rate constants for the effect of ammonia on microbial growth ($K_{AmMi,Rum}$), the yield of microbial DM per mole of ATP ($K_{YATP,Rum}$), and the inhibitory effect of fat on microbial growth ($K_{\mathrm{FatMi},Rum}$) significantly decreased mean bias (from 65.9 to 16.0%) and slope bias (from 6.1 to 1.2%) for ruminal microbial N outflow predictions, resulting in a reduction of RMSE from 50.5 to 30.3%.

Ruminal fermentation parameters

Mean observed daily ruminal pH values ranged from 5.44 to 6.96. After the modification and refitting to the observations, ruminal pH was predicted with a RMSE of 4.78 with essentially no mean bias and minor slope bias. The CCC increased from -0.09 to 0.11, suggesting that some improvement was realized. However, the small CCC value suggests considerable unexplained variation remains. As for microbial predictions, the pH equation is highly empirical, and assuming much of the residual error is explainable, a more mechanistic representation of pH may be required to significantly improve precision. Although there was a negative correlation between ruminal VFA concentrations and ruminal pH, the relationship appears to be weak (Allen, 1997). Ruminal pH fluctuations are responsive to meals and chewing behavior, suggesting that ruminal pH varied significantly within a day. Although factors such as particle sizes, chewing behavior, and time after a meal have been considered in the model, such observations are rarely reported in the literature with pH measurements.

Volatile fatty acids are produced by the carbohydrate fermentation of ruminal microbes, and most of them were absorbed through rumen wall. Therefore, VFA concentrations are influenced by VFA production and absorption rates. RMSE and its portioning were not significantly improved by the model changes. Between 11 and 16% of the errors are due to mean bias. Because such errors are easily resolvable through adjustment of the rate constants for absorption, its presence suggests there may be other factors that are driven by VFA concentrations that prevented removal of that bias during parameter estimation. As described by Argyle and Baldwin (1988), VFA production rates are regulated by ruminal pH. Our previous work found significant correlations between observed pH and residuals for VFA concentrations suggesting that the effects of pH on VFA production were not properly represented (Li et al., 2018a). In the current study, correlations between VFA residuals and ruminal pH were not

significant, implying that the improvements in pH precision contributed to improved predictions of VFA production as originally described by Argyle and Baldwin (1988). Additionally, the newly derived rate constants for acetate, propionate, and butyrate absorption ($K_{Ac,RumBld}$, $K_{Pr,RumBld}$, and $K_{Bu,RumBld}$) could also result in improved accuracy of VFA concentrations through changing absorption rates.

Ruminal ammonia concentrations are affected by protein degradation rate, recycled urea from blood or saliva, and ammonia absorption rate. Parameter estimates for the rate constant for ammonia absorption ($K_{Am,RumBld}$, d^{-1}) substantially increased from 5.01 to 9.32, suggesting the ammonia absorption rate increased 86%. In the prior work, most diets contained moderate to high forage content which has slower protein degradation rate (Li et. al under review), therefore, leading to a lower ammonia absorption rate. However, in the current study, more low forage diets were included in the dataset, which might have contributed to greater ammonia production rates. Consequently, the rate constant for ammonia absorption was increased. Nolan (1975) indicated that the ammonia pool can completely turnover in 2 h, which was consistent with our current results. After refitting to the observed values, the RMSE for predicted ammonia concentrations significantly decreased from 129 to 37.2% primarily due to decreased mean bias (81.9 to 0.5%). The CCC increased from 0.1 to 0.45, suggesting both the accuracy and precision were improved.

Nutrient digestion

The RMSE for fecal outflow of protein, ADF, and NDF were substantially decreased from 48.85 to 23.3%, 23.69 to 18.18%, and 36.03 to 22.90%, respectively. While the reductions for fecal outflow of DM, fat, and starch were less than 5%. Although a small mean bias and slope bias were observed for fecal starch outflow, the relatively high prediction errors suggest it is difficult to predict fecal starch outflow since over 90% of starch has been digested in the

digestive tract. Considering a mass action function is used to represent the relationship between ruminal nutrient outflow and fecal nutrient outflow, the improved representations of ruminal nutrient outflow and reparametrized nutrient digestion coefficients for protein, starch, ADF, and fat ($K_{Protein,IntFec}$, $K_{Starch,IntFec}$, $K_{Fiber,IntFec}$, and $K_{Lipid,IntFec}$) have contributed to the decreased prediction errors of fecal nutrient outflow.

Model simulations

Protein fluxes. The results from simulations of high and low RUP and high and low RUStarch are presented in Table 4-4. As anticipated, the diets with 40% RUP had greater protein degradation and ammonia production rates than the diets with 60% RUP, which led to reductions in NANMN outflow, increases in ammonia and AA outflow, and increases in ammonia absorption rate. Because of the positive effect of fermentable energy supply on microbial growth and activity, the diets containing 25% RUStarch had increased protein degradation rates and ammonia production rates compared to the diets with 50% RUStarch. There was an interaction between RUP and RUStarch on microbial protein synthesis. Low RUP diets provided more substrate for microbial protein synthesis, but because microbial protein synthesis is an energy dependent process, lower RUStarch diets produced more ATP which facilitated microbial growth. Consequently, the greatest capture of AA and ammonia by rumen microbes occurred for theh 40% RUP and 25% RUStarch diet which had 28% more synthesized microbial protein than the 60% RUP and 50% RUStarch diet.

Consistent with the ruminal N outflow, diets with lower RUStarch had more digested microbial protein while diets with lower RUP had less digested protein. Although the diets with 50% RUStrach increased microbial N captured from recycled urea, the diets with 25% RUStarch had greater AA absorption rates. Overall, the diets with 60% RUP had greater AA absorption than diets with 40% RUP. Within RUP diets, lower RUStarch diets had grater AA absorption

rates. Compared to the diet with 40% RUP and 50% RUStarch, the diet with 60% RUP and 25% RUStarch had 5% greater absorbed AA. The differences in AA absorption among the diets was less than one may have hypothesized due to the effects of microbial action on feed protein degradation and the ability of microbes to recapture some N from ammonia.

Blood urea entry accounts for approximately 60% of N intake, which is consistent with previous studies (Lapierre and Lobley, 2001; Reynolds and Kristensen, 2008; Bailey et al., 2012b). Diets with 40% RUP had increased blood urea entry, primarily due to increased ammonia absorption. The diets with 25% RUStarch had slightly increased ruminal urea entry, while the diets with 50% RUStarch largely increased intestinal blood urea entry, suggesting that gut urea entry is positively correlated with fermentable energy availability in the gut lumen. In summary, diets with high RUP had greater blood urea entry rate than low RUP diets, and high RUStarch diets tended to increase gut urea entry. The opposite was observed for urinary urea excretion. Because urea is the major nitrogenous component in urine, similar results were observed for urinary N excretion.

Considering both ruminal N degradation and post rumen N digestion, diets with 60% RUP had greater fecal N outflow. There was an interaction of RUP and RUStarch on milk N secretion. The diet with 40% RUP and 25% RUStarch had greatest milk N (83.72 g N/d), while the diet with 60% RUP and 25% RUStarch had the lowest milk N output (59.78 g N/d). Compared to the latter diet, the former diet increased 23.94 g N/d representing 4.7% of N efficiency.

Energy fluxes. The results from simulations of varying RUP and RUStarch diets on energy metabolism are presented in Table 4-5. Although the diets with 60% RUP tended to increase fecal energy compared to the diets with 40% RUP, and low RUStarch diets exhibited

greater urinary energy and CH_4 energy than high RUStarch diets, and thus metabolizable energy was very similar among the four diets. Although total absorbed energy was similar, the energy profile was different. The diets with 25% RUStarch had greater absorbed energy from AA and glucose than the diets with 50% RUStarch, and the high RUP diets had increased absorbed energy from AA and glucose compared to the low RUP diets. Absorbed VFA energy accounted for approximately 61% of total absorbed energy. The low RUStarch diets had greater absorbed energy from acetate, propionate and butyrate than the high RUStarch diets. The absorbed VFA profiles were very similar between the rumen and the post-rumen as the model uses the ruminal profile to set the post-ruminal profile which is a potential limitation of the model. The model simulation results indicated acetate absorbed from the post-rumen accounts for approximately 68% of acetate absorbed from the rumen, while propionate and butyrate account for 47% of them absorbed from the rumen. Overall, diets with 25% RUStarch and the diets with 60% RUP had greater milk energy output than their corresponding diets, indicating that milk energy is strongly correlated with the post-absorptive energy metabolism. The diet with 60% RUP and 25% RUStarch exhibited the highest milk energy which was 17.55 Mcal/d, while the diet with 40% RUP and 50% RUStarch had the lowest milk energy which was 15.21 Mcal/d. The milk energy difference between these two diets was 2.34 Mcal/d which equals to 2.6% of energy efficiency.

Conclusions

After reparameterizations, 19.7 to 37.5% of RMSE with essentially no slope bias and minor mean bias were exhibited for ruminal outflow of ADF, NDF, fat, total N, NANMNA, and microbial N, suggesting the model is even more robust in representing ruminal nutrient degradation compared to the initial model. Consequently, improved representations of ruminal nutrient degradation have contributed to the increased accuracy and precision fecal excretion of protein, ADF, NDF, and fat.

Adding ammonia concentration as a driver to the pH equation increased the precision of predicted ruminal pH, and, thereby, the precision of predicted VFA concentrations due to an improved representation of pH regulation of VFA production rates. Although minor mean bias for pH and moderately mean bias and slope bias for VFA concentrations were observed in the modified model, the small CCC values suggest considerable unexplained variation remains.

The results from simulations of diets with varying RUP and RUStarch displayed the model is capable to estimate detailed metabolic reactions for nitrogen and energy metabolism. In a moderately low protein diet, decreasing RUP and RUStarch proportions could improve N efficiency, while increasing RUP and decreasing RUStarch proportions could increase energy efficiency.

References

Allen, M. S. 1997. Relationship between fermentation acid production in the rumen and the requirement for physically effective fiber. J Dairy Sci 80(7):1447-1462.

Argyle, J. and R. Baldwin. 1988. Modeling of rumen water kinetics and effects of rumen pH changes. J Dairy Sci 71(5):1178-1188.

Bailey, E., E. Titgemeyer, K. Olson, D. Brake, M. Jones, and D. Anderson. 2012. Effects of supplemental energy and protein on forage digestion and urea kinetics in growing beef cattle. Journal of animal science 90(10):3492-3504.

Baldwin, R. 1995. Modeling ruminant digestion and metabolism. Springer Science & Business Media.

Baldwin, R. L., J. France, D. E. Beever, M. Gill, and J. H. Thornley. 1987a. Metabolism of the lactating cow: III. Properties of mechanistic models suitable for evaluation of energetic relationships and factors involved in the partition of nutrients. Journal of Dairy Research 54(01):133-145.

Baldwin, R. L., J. France, and M. Gill. 1987b. Metabolism of the lactating cow: I. Animal elements of a mechanistic model. Journal of Dairy Research 54(01):77-105.

Baldwin, R. L., J. H. Thornley, and D. E. Beever. 1987c. Metabolism of the lactating cow: II. Digestive elements of a mechanistic model. Journal of Dairy Research 54(01):107-131.

Bibby, J. and H. Toutenburg. 1977. Prediction and improved estimation in linear models. Wiley.

Briggs, P., J. Hogan, and R. Reid. 1957. Effect of volatile fatty acids, lactic acid and ammonia on rumen pH in sheep. Crop and Pasture Science 8(6):674-690.

Channon, A., J. Rowe, and R. Herd. 2004. Genetic variation in starch digestion in feedlot cattle and its association with residual feed intake. Australian Journal of Experimental Agriculture 44(5):469-474.

Firkins, J., M. Eastridge, N. St-Pierre, and S. Noftsger. 2001. Effects of grain variability and processing on starch utilization by lactating dairy cattle. Journal of animal science 79(suppl_E):E218-E238.

Fox, D., C. Sniffen, J. O'connor, J. Russell, and P. Van Soest. 1992. A net carbohydrate and protein system for evaluating cattle diets: III. Cattle requirements and diet adequacy. Journal of animal science 70(11):3578-3596.

Galyean, M., D. Wagner, and F. Owens. 1981. Dry matter and starch disappearance of corn and sorghum as influenced by particle size and processing. J Dairy Sci 64(9):1804-1812.

Gregorini, P., P. Beukes, G. Waghorn, D. Pacheco, and M. Hanigan. 2015. Development of an improved representation of rumen digesta outflow in a mechanistic and dynamic model of a dairy cow, Molly. Ecological Modelling 313:293-306.

Hanigan, M., H. Bateman, J. Fadel, and J. McNamara. 2006. Metabolic models of ruminant metabolism: recent improvements and current status. J Dairy Sci 89:E52-E64.

Hanigan, M. D., J. A. Appuhamy, and P. Gregorini. 2013. Revised digestive parameter estimates for the Molly cow model. J Dairy Sci 96(6):3867-3885.

Hanigan, M. D., C. C. Palliser, and P. Gregorini. 2009. Altering the representation of hormones and adding consideration of gestational metabolism in a metabolic cow model reduced prediction errors. J Dairy Sci 92(10):5043-5056.

Hanigan, M. D., A. G. Rius, E. S. Kolver, and C. C. Palliser. 2007. A redefinition of the representation of mammary cells and enzyme activities in a lactating dairy cow model. J Dairy Sci 90(8):3816-3830.

Hollmann, M., M. Allen, and D. Beede. 2011. Dietary protein quality and quantity affect lactational responses to corn distillers grains: A meta-analysis. J Dairy Sci 94(4):2022-2030.

Huhtanen, P. and A. Hristov. 2009. A meta-analysis of the effects of dietary protein concentration and degradability on milk protein yield and milk N efficiency in dairy cows. J Dairy Sci 92(7):3222-3232.

Lapierre, H. and G. Lobley. 2001. Nitrogen recycling in the ruminant: A review. J Dairy Sci 84:E223-E236.

Lawrence, I. and K. Lin. 1989. A concordance correlation coefficient to evaluate reproducibility. Biometrics:255-268.

Leduc, M., M.-P. Létourneau-Montminy, R. Gervais, and P. Chouinard. 2017. Effect of dietary flax seed and oil on milk yield, gross composition, and fatty acid profile in dairy cows: A meta-analysis and meta-regression. J Dairy Sci 100(11):8906-8927.

Li, M. M., R. R. White, and M. D. Hanigan. 2018. An evaluation of Molly cow model predictions of ruminal metabolism and nutrient digestion for dairy and beef diets. J Dairy Sci 101(11):9747-9767.

Mills, J., J. France, and J. Dijkstra. 1999. A review of starch digestion in the lactating dairy cow and proposals for a mechanistic model: 1. Dietary starch characterisation and ruminal starch digestion. J. Anim. Feed Sci 8(3):219-340.

Nolan, J. 1975. Quantitative models of nitrogen metabolism in sheep. Digenstion and Metabolism in the Ruminant.

NRC. 2001. Nutrient requirements of dairy cattle. 7th ed. National Academy Press, Washington, D.C. National Research Council.

O'Connor, J., C. Sniffen, D. Fox, and W. Chalupa. 1993. A net carbohydrate and protein system for evaluating cattle diets: IV. Predicting amino acid adequacy. Journal of animal science 71(5):1298-1311.

Press, W. H., S. A. Teukolsky, W. T. Vetterling, and B. P. Flannery. 2007. Numerical recipes 3rd edition: The art of scientific computing. Cambridge university press.

Reynolds, C. and N. B. Kristensen. 2008. Nitrogen recycling through the gut and the nitrogen economy of ruminants: an asynchronous symbiosis. Journal of animal science 86(14_suppl):E293-E305.

Russell, J. B., J. O'connor, D. Fox, P. Van Soest, and C. Sniffen. 1992. A net carbohydrate and protein system for evaluating cattle diets: I. Ruminal fermentation. Journal of animal science 70(11):3551-3561.

Short, S. D. 2004. Characteristics and production costs of US dairy operations.

Sniffen, C., J. O'connor, P. Van Soest, D. Fox, and J. Russell. 1992. A net carbohydrate and protein system for evaluating cattle diets: II. Carbohydrate and protein availability. Journal of animal science 70(11):3562-3577.

St-Pierre, N. and D. Glamocic. 2000. Estimating unit costs of nutrients from market prices of feedstuffs. J Dairy Sci 83(6):1402-1411.

St-Pierre, N. and C. Thraen. 1999. Animal grouping strategies, sources of variation, and economic factors affecting nutrient balance on dairy farms. Journal of animal science 77(suppl_2):72-83.

Svihus, B., A. K. Uhlen, and O. M. Harstad. 2005. Effect of starch granule structure, associated components and processing on nutritive value of cereal starch: A review. Animal Feed Science and Technology 122(3-4):303-320.

Vyas, D. and R. Erdman. 2009. Meta-analysis of milk protein yield responses to lysine and methionine supplementation. J Dairy Sci 92(10):5011-5018.

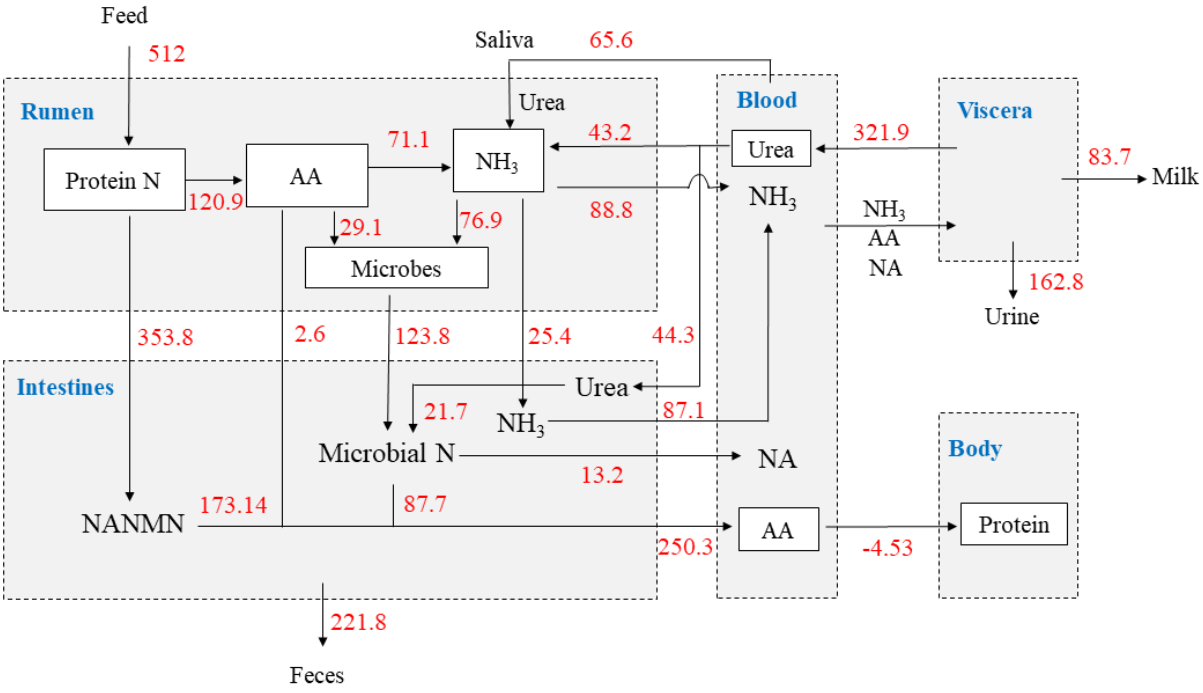

Figure 4-1. Nitrogen flux diagram derived from the model simulation. Solid boxes represent pools, and open boxes represent compartments. Numbers indicate nitrogen fluxes. The unit is g N/d. A diet contained fat, starch, protein, NDF, ADF, and ash concentrations of 6, 30, 16, 30, 20, and 6 % of DM was designed to feed a Holstein dairy cow weighing 600 kg at 70 day of lactation. There was 40 % RUP and 25% of rumen undegraded starch in the diet. 20 kg DMI was consumed by the animal.

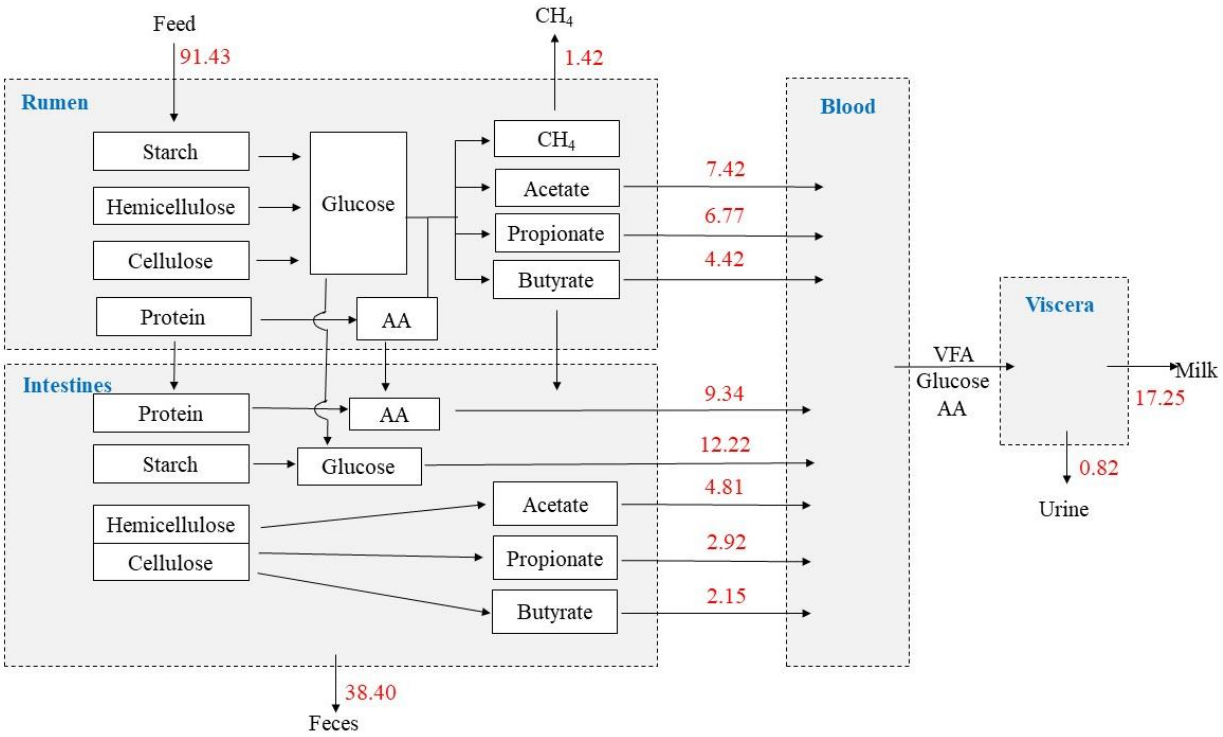

Figure 4-2. Energy metabolism diagram derived from the model simulation. Solid boxes represent pools, and open boxes represent compartments. Numbers indicate energy fluxes. The unit is Mcal/d. A diet contained fat, starch, protein, NDF, ADF, and ash concentrations of 6, 30, 16, 30, 20, and 6 % of DM was designed to feed a Holstein dairy cow weighing 600 kg at 70 day of lactation. There was 40 % RUP and 25% of rumen undegraded starch in the diet. 20 kg DMI was consumed by the animal.

Table 4-1. A descriptive summary of observed nutrient intake, ruminal digestibility, ruminal outflow and fermentation, and total tract digestibility

Items	n	Mean	SD	Minimum	Maximum
BW, kg	1013	573.64	95.14	248.00	807.00
Intake, kg/d					
DM	1223	17.61	5.83	3.99	31.80
OM	681	16.30	5.02	3.77	29.50
ADF	396	3.72	1.28	0.30	6.90
NDF	549	6.10	2.07	1.01	11.29
Starch	347	5.23	1.99	0.07	11.00
Protein	1014	3.01	1.18	0.62	6.01
Ruminal digestibility, %					
OM	476	57.76	10.51	29.10	84.20
Protein	380	59.18	14.49	5.73	103.32
ADF	305	39.95	12.18	6.20	77.10
NDF	454	44.08	12.26	11.40	83.00
Starch	297	66.54	18.83	9.70	96.70
Ruminal outflow, kg/d					
DM	183	13.54	4.27	3.50	25.70
OM	444	10.54	3.92	1.83	21.00
ADF	237	2.25	0.81	0.23	4.76
NDF	344	3.60	1.32	0.74	7.35
Starch	226	2.25	1.64	0.09	7.12
Fat	39	0.96	0.37	0.40	2.00
Total N	524	0.48	0.16	0.11	1.00
Microbial N	667	0.26	0.10	0.05	0.60
Non-ammonia N	624	0.47	0.15	0.07	0.93
Non-ammonia, non-microbial N	614	0.20	0.09	0.003	0.46
Ruminal fermentation					
pH	632	6.13	0.28	5.44	6.92
Ammonia, mM	558	7.37	2.90	0.71	16.76
Total VFA, mM	612	111.55	22.47	11.00	183.08
Acetate, mM	605	68.46	21.56	6.51	101.52
Propionate, mM	605	26.31	11.13	2.43	78.00
Butyrate, mM	605	13.42	4.87	1.51	33.73
Total tract digestibility, %					
DM	402	0.69	0.06	0.50	0.86
OM	626	0.71	0.06	0.54	0.87
Protein	587	0.68	0.06	0.44	0.87
ADF	333	0.45	0.11	0.12	0.76
NDF	529	0.51	0.11	0.20	0.84
Starch	303	0.94	0.05	0.76	1.00
Fat	161	0.72	0.11	0.37	0.94

Table 4-2. Residual error analyses for Molly predictions before and after reparameterizations

Items	N	Observed mean	Predicted mean		RMSE, % mean		Mean bias, % MSE		Slope bias, % MSE		CCC	
			Initial	Modified	Initial	Modified	Initial	Modified	Initial	Modified	Initial	Modified
Ruminal outflow, kg/d												
DM	183	13.54	12.87	12.66	20.32	20.47	5.94	10.02	2.15	2.93	0.72	0.72
ADF	237	2.25	2.62	2.30	26.59	20.10	37.71	1.10	3.71	0.13	0.75	0.82
NDF	344	3.60	4.39	3.70	33.77	24.42	42.52	1.13	3.20	0.03	0.61	0.72
Starch	226	2.25	2.31	2.13	54.70	56.03	0.23	0.99	0.33	0.89	0.59	0.55
Fat	39	0.96	0.94	0.99	20.10	20.10	1.11	2.33	1.00	0.76	0.85	0.85
Total N	524	0.48	0.39	0.45	27.28	19.69	48.57	8.65	2.16	0.10	0.65	0.80
Microbial N	667	0.26	0.16	0.23	50.48	30.28	65.88	15.99	6.10	1.19	0.26	0.59
Non-ammonia N	624	0.47	0.39	0.46	26.06	19.84	39.25	0.88	2.43	0.21	0.62	0.76
NANMN	614	0.20	0.24	0.23	39.45	37.52	17.25	8.83	6.78	5.85	0.52	0.53
Ruminal fermentation												
pH	632	6.13	6.16	6.10	4.85	4.78	0.58	1.04	15.96	13.91	-0.09	0.11
Ammonia, mM	558	7.37	15.95	7.18	128.89	37.18	81.87	0.46	10.45	10.84	0.10	0.45
Total VFA, mM	612	111.55	92.69	93.81	27.53	26.95	37.74	34.84	10.12	10.28	0.09	0.16
Acetate, mM	605	68.46	60.05	60.42	33.91	33.51	13.14	12.29	3.71	2.75	0.11	0.09
Propionate, mM	605	26.31	22.24	22.12	47.00	47.15	10.87	11.44	8.24	8.24	0.00	0.07
Butyrate, mM	605	13.42	10.40	11.27	43.40	40.52	26.89	15.71	4.09	5.00	0.05	0.07
Fecal outflow, kg/d												
DM	404	5.75	5.27	5.26	19.04	18.68	19.64	20.98	6.26	9.34	0.86	0.87
Protein	538	0.97	0.59	1.06	48.85	23.23	63.86	17.34	19.51	5.33	0.34	0.82
ADF	278	2.05	2.37	2.11	23.69	18.18	43.18	2.46	0.69	2.13	0.85	0.90
NDF	446	3.00	3.83	3.28	36.03	22.90	58.91	16.91	5.64	0.67	0.71	0.84
Fat	137	0.30	0.29	0.32	33.47	32.98	1.32	3.72	7.96	3.03	0.79	0.81
Starch	278	0.35	0.41	0.38	87.91	85.82	3.75	0.81	3.06	1.74	0.35	0.34

NANMN is Non-ammonia, non-microbial N.

Table 4-3. Model parameters estimates when the model was fitted to the observed data summarized in Table 1

Model parameter	Description	Previous values	Final estimate	SE
Ruminal				
$K_{RUSt,Rum}$	Intercept scalar to adjust in situ determined ruminal starch degradation rates ($mole^{-1}$)	0.153	0.152	0.006
$K_{slpRUSt,Rum}$	Slope scalar to adjust in situ determined ruminal starch degradation rates ($mole^{-1}$)	0.179	0.177	0.011
$K_{RUADF,Rum}$	Intercept scalar to adjust in situ determined ruminal cellulose degradation rates ($mole^{-1}$)	2.70	3.77	0.002
$K_{slpRUADF,Rum}$	Slope scalar to adjust in situ determined ruminal cellulose degradation rates ($mole^{-1}$)	0.48	0.028	0.002
$K_{HcCs1,Rum}$	Scalar to calculate the hemicellulose degradation rate constant from the cellulose rate constant($mole^{-1}$)	0.69	0.82	0.003
$K_{RUP,Rum}$	Intercept scalar to adjust in situ determined ruminal protein degradation rates ($mole^{-1}$)	1.81	1.33	0.019
$K_{slpRUP,Rum}$	Slope scalar to adjust in situ determined ruminal protein degradation rates ($mole^{-1}$)	0.16	0.064	0.003
$K_{AmMi,Rum}$	Rate constant for the effect of ammonia on microbial growth (L/mole)	0.0071	0.0074	0.0002
$K_{\mathrm{FatMi},Rum}$	Constant to calculate the effect of fat on microbial growth (mole of DM/mole of dietary fat)	0.07	0.02	0.001
$K_{YATP,Rum}$	Efficiency constant defining the yield of microbial DM per mole of ATP (g/mole)	0.01	0.04	0.002
$K_{AmpH,Rum}$	Slope for ammonia effect on pH (mol^{-1})	0	50.1	71.14
$K_{\mathrm{pH},Rum}$	Intercept for pH prediction	-0.68	-1.42	0.003
$K_{VFA\mathrm{pH},Rum}$	Slope for total VFA effect on pH (mol^{-1})	3.94	13.9	0.001
$K_{Am,RumBld}$	Rate constant for ammonia absorption (d^{-1})	5.01	9.32	0.168
$K_{Ac,RumBld}$	Rate constant for acetate absorption (d^{-1})	4.20	4.49	0.025
$K_{Pr,RumBld}$	Rate constant for propionate absorption (d^{-1})	6.45	6.86	0.004
$K_{Bu,RumBld}$	Rate constant for butyrate absorption (d^{-1})	6.45	6.10	0.037
Post-ruminal				
$K_{Protein,IntFec}$	Intestinal digestion coefficient for protein (g/g)	0.79	0.53	0.003
$K_{Starch,IntFec}$	Intestinal digestion coefficient for starch (g/g)	0.81	0.79	0.003
$K_{Fiber,IntFec}$	Intestinal digestion coefficient for fiber (g/g)	0.12	0.11	0.001
$K_{Lipid,IntFec}$	Intestinal digestion coefficient for lipid (g/g)	0.71	0.69	0.001

Table 4-4. Using Molly to simulate the effects of RUP and rumen undegraded starch (RUStarch) on nitrogen fluxes in a dairy cow[1]

Item	40% RUP		60% RUP	
	25% RUStarch	50% RUStarch	25% RUStarch	50% RUStarch
N balance, g N/d				
N intake	512	512	512	512
Fecal N	221.77	229.13	234.41	242.02
Urinary N	162.81	149.73	142.64	128.64
Retained N	43.70	62.70	62.72	81.56
Milk N	83.72	70.44	72.23	59.78
Ruminal N Fluxes, g N/d				
Degraded protein	102.79	93.85	75.14	66.66
Deaminated AA	71.12	66.33	48.13	43.39
AA captured in microbes	29.09	24.45	25.10	21.10
AA outflow	2.58	3.07	1.90	2.17
Ammonia produced	191.07	182.43	166.28	157.07
Ammonia captured in microbes	76.90	64.99	72.33	61.09
Ammonia outflow	25.39	26.12	20.89	21.34
Non-ammonia, non-microbial N outflow	353.78	363.90	382.63	392.00
Microbial N outflow	123.83	106.18	113.07	96.78
Total N outflow	503.0	496.20	516.59	510.12
Absorbed ammonia N	88.78	91.32	73.06	74.64
Post-Rumen, g N/d				
Digested microbial protein	74.54	63.91	68.06	58.25
Digested microbial non-protein	13.23	11.34	12.08	10.34
Digested RUP	173.14	177.88	187.73	192.21
Absorbed AA	250.26	244.86	257.69	252.63
Recycled urea captured in microbes	21.72	28.95	23.06	30.44
Urea recycling, g N/d				
Blood urea entry	321.90	319.50	314.82	313.11
Urea entry through rumen wall	43.24	42.25	43.72	42.65
Urea entry via saliva	65.61	60.98	62.53	57.34

Intestinal urea entry	44.30	57.73	48.37	64.72
Urinary urea excretion	168.75	158.54	160.21	148.41

[1]Isonitrogenous and isocaloric diets contained fat, starch, protein, NDF, ADF, and ash concentrations of 6, 30, 16, 30, 20, and 6 % of DM was designed to feed a Holstein dairy cow weighing 600 kg at 70 day of lactation. 20 kg DMI was consumed by the animal.

Table 4-5. Using Molly to simulate the effects of RUP and rumen undegraded starch (RUStarch) on energy metabolism in a diary cow[1]

Item	40% RUP		60% RUP	
	25% RUStarch	50% RUStarch	25% RUStarch	50% RUStarch
Gross energy, Mcal	91.43	91.43	91.43	91.43
Metabolizable energy, Mcal	50.78	50.64	50.55	50.40
Fecal energy, Mcal	38.40	38.75	38.77	39.13
Milk energy, Mcal	17.25	15.21	17.55	15.76
Urinary energy, Mcal	2.24	2.04	2.11	1.90
CH_4 energy, Mcal	1.42	1.28	1.39	1.25
Absorbed energy, Mcal	55.94	55.79	54.04	53.83
Energy from absorbed AA, Mcal	9.34	9.16	9.22	9.07
Energy from absorbed glucose, Mcal	10.24	13.98	10.41	14.24
Energy from absorbed acetate, Mcal	12.22	10.71	11.48	9.90
Acetate from rumen, Mcal	7.42	6.46	6.89	5.88
Acetate from post-rumen, Mcal	4.81	4.25	4.59	4.01
Energy from absorbed propionate, Mcal	9.69	8.36	8.97	7.58
Propionate from rumen, Mcal	6.77	5.81	6.24	5.24
Propionate from post-rumen, Mcal	2.92	2.55	2.73	2.34
Energy from absorbed butyrate, Mcal	6.57	5.68	6.09	5.17
Butyrate from rumen, Mcal	4.42	3.80	4.08	3.43
Butyrate from post-rumen, Mcal	2.15	1.88	2.02	1.74

[1]Isonitrogenous and isocaloric diets contained fat, starch, protein, NDF, ADF, and ash concentrations of 6, 30, 16, 30, 20, and 6 % of DM was designed to feed a Holstein dairy cow weighing 600 kg at 70 day of lactation. 20 kg DMI was consumed by the animal.

Chapter 5: Metatranscriptomic and Compositional Analyses Reveal Low pH Changes the Microbial Community and Metabolic Pathways for Fiber Fermentation in the Rumen

Abstract

Understanding the role of the microbial community in response to a challenge of ruminal pH reductions would help develop more effective strategies to improve feeding efficiency. The objective of this study was to investigate how ruminal pH affects the microbial community, expression of carbohydrate-active enzyme transcripts (CAZymes), fiber degradation, and short chain fatty acid (SCFA) concentrations. Six cannulated Holstein heifers with an initial BW of 362 ± 22 kg (mean ± SD) were subjected to each of 2 treatments in a cross-over design. The treatments were 10 days of intraruminal infusions of 1) distilled water (Control), and 2) a dilute blend of hydrochloric and phosphoric acids to achieve a pH reduction of 0.5 units (LpH). Ruminal liquid and solid fractions were collected on day 9 of each period. Microbial RNA was extracted from ruminal liquid and solid samples respectively and used for 150 bp paired-end sequencing using Illumina HiSeq sequencing technology. Degradability of dietary hemicellulose, cellulose, and lignin, and ruminal SCFA concentrations were negatively affected by a prolonged period of low pH. Metatranscriptomic analyses identified 19 bacterial phyla with 121 genera, 3 archaeal genera, 26 protozoal genera, 3 fungal genera, and 97 CAZymes in the rumen. Within the community, 4 bacterial phyla (*Proteobacteria*, *Firmicutes*, *Bacteroidetes*, and *Spirochaetes*), 2 archaeal genera (*Candidatus_Methanomethylophilus* and *Methanobrevibacter*), 2 fungal genera (*Densospora* and *Acidomyces*), and 5 protozoal genera (*Entodinium*, *Polyplastron*, *Isotricha*, *Eudiplodinium*, and *Eremoplastron*) were observed as the core active microbes. Cellulase, endo-1,4-beta- xylanase, amylase, and alpha-N-arabinofuranosidase were the most abundant CAZymes in the rumen. Statistical analyses indicated 19 bacterial genera and 4 protozoal genera were affected by low ruminal pH, and 30 bacterial genera, 1 archaeal genus,

and 7 protozoal genera exhibited different proportions between ruminal liquid and solid fractions**.** Consequently, 8 enzymes were affected by ruminal pH, and 2 enzymes had different distributions in the liquid and solid fractions. We observed significant correlations between 54 microbes (43 bacterial and 11 protozoal genera) and 25 enzymes, of which 8 key enzymes participated in reactions leading to SCFA production, suggesting that the ruminal microbial community alters fiber catalysis and fermentation in response to altered pH through a shift in CAZymes expression.

Introduction

In the modern cattle industry, high-concentrate diets (50-90% grain) are often fed to maintain high milk or meat production, which is associated with altered microbial ecology and metabolic disorders such as subclinical rumen acidosis (Russell and Rychlik, 2001; McCann et al., 2016; Wetzels et al., 2016; Zhang et al., 2017). Studies have indicated that the activity or numbers of cellulolytic microbes are inhibited if ruminal pH is less than 6.0, primarily due to the regulation of intracellular pH, resulting in inhibition of cellobiose transport activity (Russell, 1987; Russell and Wilson, 1996). However, because ruminal pH declines occur at the same time as the amount of concentrate fed increases, the results are often confounded between feeding high concentrate diets and ruminal pH declines.

Short-chain fatty acids (SCFA), including acetate, propionate, and butyrate, are the major end products of microbial fermentation of dietary carbohydrate. Intraruminal SCFA production accounts for up to 75% of total metabolizable energy in ruminants (Siciliano-Jones and Murphy, 1989; France and Dijkstra, 2005). The production of SCFA share glycolysis as a common pathway with pyruvate as the central branching point, and conversion of pyruvate to the individual SCFA at least partially driven by thermodynamic conditions (Ungerfeld and Kohn, 2006). Various in vitro studies indicated pH significantly affects the profile and production of

SCFA (Marounek et al., 1985; Russell, 1998; Calsamiglia et al., 2008). Changes in production appear to occur through a shift in the biochemical pathways expressed by the overall microbial population in the rumen. Because different diets can result in altered ruminal pH, understanding microbial responses to pH in vivo will allow for improved predictions of SCFA production in response to different diets and feeding strategies.

High-throughput sequencing techniques such as metatranscriptomics can analyze RNA transcripts expressed by a microbial community at a specific point in time, which allows a simultaneous investigation of the gene expression and abundance of active microbiomes in an ecosystem (Tveit et al., 2014). Because high-throughput sequencing generates compositional data (transcript proportions of total reads rather than absolute values) (Gloor et al., 2017), they do not map to Euclidean space, which can be problematic for statistical analyses (Aitchison, 1982; Fernandes et al., 2014; Gloor and Reid, 2016; Gloor et al., 2017). Therefore, compositional data need to be transformed before statistical analyses to avoid invalid conclusions (Li, 2015; Lovell et al., 2015; Gloor et al., 2017). In this work, we used metatranscriptomic and compositional analyses to investigate how ruminal pH declines alter microbial community structure and transcript expressions of CAZymes as well as fiber degradation and SCFA concentrations through a continuous 10-day intraruminal infusion trial. We hypothesized that low pH would alter biochemical pathways to affect fiber degradation and SCFA production via a shift in expression of the CAZymes expressed by the microbes in the rumen.

Materials and Methods

Animals, Experimental Design, and Feeding management

This study was conducted in accordance with the Federation of Animal Science Societies' Guide for the Care and Use of Agricultural Animal in Research and Teaching and approved by the Virginia Tech Institutional Animal Care and Use Committee.

Six cannulated Holstein heifers with an initial BW of 362 ± 22 kg (mean ± SD) were subjected to each of 2 treatments in a two-period, cross-over design. The treatments were 10 days of continuous intraruminal infusions of 1) distilled water (Control), or 2) a dilute blend of hydrochloric and phosphoric acids to achieve 0.5 pH reduction (LpH), as depicted in

Figure 5-1. There was a 5 day recovery period between the infusion periods.

The animals were housed in individual tie stalls with rubber mattresses bedded with wood shavings. They had continuous access to water, and were fed a common total mixed ration (TMR) formulated according to National Research Council (2001) recommendations. Ingredient composition and nutrient content of the diet are listed in Table 5-1. The ration was fed every 4 hours with approximately 17% of the total daily feed allocated at each feeding to maintain stable rumen fermentation rates. Feed offered and refused was recorded at each feeding time and used to calculate daily feed intake.

The acid solution consisted of 73 g H_3PO_4, 185 g HCl and 800 g distilled water. Infusates were delivered into the rumen using indwelling infusion apparatus and clinical infusion pumps (LifeCare 5000, Abbott Laboratories, North Chicago, IL). The infusion apparatus consisted of an infusion line with an 8 mm diameter and a 500 ml plastic bottle with around 30 small holes bored in the top part of the bottle. The infusion line entered the rumen via a small hole bored in the cannula plug. The plastic bottle was connected at the end of the infusion line and filled with iron metal vector screw nuts. In that way, the bottle can indwell in the rumen and stand upright to disperse the infusates and prevent the acid solutions touching the rumen wall. Ruminal pH was monitored every 4 hours, and the acid infusion rate was varied by animal to achieve a ruminal pH between 6.0 and 6.1. When the ruminal pH dropped below 6.0, the infusion rate was decreased by 10 ml/h, and the ruminal pH was rechecked in 30 to 60 minutes. The infusion rate

was adjusted upwards if ruminal pH was above 6.1. Water was infused at a constant rate of 25 ml/h in the control animals.

Sample collection

Rumen sampling was conducted by placing 2 small tubes with an 8 mm diameter via the cannula into the rumen contents in different locations within the rumen (cranial and caudal areas of the rumen) to collect rumen fluid prior to each feeding. Multiple layers of nylon net were tied around the end of the tubes to filter out the solid fractions. A total of 10 ml of rumen fluid was drawn from the tubes at each sampling event. Ruminal pH was immediately measured using a portable pH meter (Starter 300, Ohaus, Parsippany, NJ), and ruminal liquid samples were stored at -20 °C for SCFA analyses.

Prior to the morning feeding on day 9 of each period, rumen contents were collected via the ruminal cannula for RNA extraction. Ruminal liquid samples were drawn from the tubes. Rumen solid samples were collected from multiple rumen locations (dorsal, ventral, cranial, and caudal areas of the rumen) and squeezed by hand when taking samples out of the rumen. The collected liquid and solid samples were immediately flash-frozen in liquid nitrogen, crushed into small pellets and stored in cryovials in liquid nitrogen, transported to the laboratory, and RNA extraction was completed within 12 hours to avoid RNA degradation.

The mixed ration was sampled daily and dried at 55°C in a forced-air oven for DM determination. Subsamples were ground to pass a 2-mm screen in a Wiley Mill (A.H. Thomas, Philadelphia, PA), and composited by period. A subsample of the 2 mm material was used for further in-situ tests, and additional subsample was ground through a 1mm screen (Cyclone lab sample mill, UDY Corporation, Fort Collins, CO) and used for chemical analyses.

In-situ degradability

In situ degradation of dietary hemicellulose, cellulose, and lignin were determined by the nylon bag technique of Ørskov and McDonald (1979) on the last 3 days of each period. Briefly, approximately 5 g of dried, ground (2 mm) sample was weighed into duplicate 5 × 10 cm polyester bags (50 μm pore size, Ankom Technology, Macedon, NY) and suspended in the rumen in a large (36 × 42 cm) nylon mesh bag secured to the ruminal cannula via a nylon cord. The sample were inserted into the rumen of each heifer before the morning meal and removed after 2, 8, 12, 24, 36, and 48 hours of incubation. Upon removal, the bags were rinsed multiple times in cold water until the water became clear, dried at 55°C in a forced-air oven, and weighed to determine DM content. After weighing, the duplicate bags from each time point within an animal were pooled and ground through a 1mm screen. The ground material was subjected to chemical analyses.

Degradation rates were estimated as described by (Ørskov and McDonald, 1979) using using a non-linear least squares regression procedure (NLI) in R (version 3.51; R development Core Team, 2015). The equations fitted to the data were:

$$Degradibility(\%) = a + b\ (1 - e^{-K_d t}) \tag{26}$$

$$Effective\ \text{degradability}(\%) = \text{a} + \frac{bc}{c + K_p} \tag{27}$$

where a represented the soluble fraction (%), b represented the potentially degradable fraction (%), K_d represented the degradation rate constant for the b fraction (%/h), t represented incubation time in the rumen (h), and K_p was the outflow rate, which was assumed to be 4%/h according to Mertens (1993).

Chemical analyses

Dry matter content was determined in the nutrition lab at Virginia Tech according to the National Forage Testing Association method 2.1.4 (NFTA, 2006). Neutral detergent fiber (NDF) was determined as described by Van Soest et al. (1991b) using heat-stable α-amylase (FAA, Ankom Technology, Macedon, NY) and sodium sulfite. Acid detergent fiber (ADF) and lignin concentrations were determined according to AOAC method 973.18 (1997). Ash content was determined according to AOAC method 942.05 (AOAC, 1997). Hemicellulose was calculated as the difference between NDF and ADF. Cellulose was calculated by subtracting ash and lignin from ADF.

For measurement of ruminal SCFA concentrations, rumen fluid samples were thawed and composited by day, animal, and period. The fluid samples were centrifuged for 30 min at 2,500 × *g* at room temperature, derivatized as described by Kristensen (2000), and analyzed for isotopic ratio using a Thermo Electron Polaris Q mass spectrometer (MS) (Thermo Electron Corporation, Austin, TX) in tandem with a Thermo Electron Focus gas chromatography (GC) (Thermo Electron Corporation, Austin, TX) using XCalibur software (version 1.4, Thermo Fisher Scientific, Waltham, MA). The column used was a Varian Factor Four capillary column VF-170ms (30 m, 0.25 mm, 0.25 um). 1uL of the sample was loaded with inlet temp set to 225°C on a split ratio of 80 running a constant flow of helium carrier gas set to 1.2mL/min. The initial column temperature was 75°C with ramping at 5°C /min to 135°C followed by 40°C /min to 225°C. The MS was programmed to run in positive selected ion monitoring mode to determine ions with m/z pairs (43/46 for acetate; 57/62 for propionate; 41/46 for butyrate and isobutyrate; and 43/46 for valerate and isovalerate) based on their elution order. Ion ratios were determined from the integrated peak areas for each ion.

RNA extraction and sequencing

RNA from ruminal liquid and solid samples were extracted using an RNA Clean & Concentrator kit from Zymo Research (Irvine, CA, USA), which included a bead-beating step to mechanically break bacterial cell walls. DNA was removed by a treatment with Baseline-ZERO™ DNase (Epicentre Biotechnologies, Madison, WI) following the manufacturer's instructions. The quality of total RNA was checked using a 2100 Bioanalyzer (Agilent Technologies, Palo Alto, California). Concentration of total RNA were determined using the Qubit® RNA Assay Kit (Thermo Fisher Scientific, Waltham, MA). DNA free, RNA samples were used for library preparation using the TruSeq™ RNA LT Sample Preparation Kit (Illumina). Following library preparation, the final concentration of DNA in each library was measured using the Qubit® dsDNA HS Assay Kit (Thermo Fisher Scientific, Waltham, MA), and the average library size was determined using the Agilent 2100 Bioanalyzer (Agilent Technologies, Palo Alto, California). The libraries were then pooled in equimolar ratios of 2nM, and 4pM of the library pool was clustered using the Illumina's cBot (Illumina, San Diego, USA). The 150 bp, paired-end sequencing reaction was performed on a HiSeq 2500 platform (Illumina, San Diego, USA) at Molecular Research LP (MRDNA, Shallowater, Texas).

Transcriptome mapping

The quality of raw paired-end reads was evaluated using the FastQC program (http://www.bioinformatics.babraham.ac.uk/projects/fastqc/). Residual adaptor sequences, low quality bases with quality scores below 20, and reads shorter than 50 bp were removed using the Trimmomatic program (version 0.36; Bolger et al., 2014). The total rRNA reads were subsequently extracted from the filtered RNA dataset for taxonomic profiling using the SortMeRNA program (version 2.1; Kopylova et al., 2012) through alignment with the rRNA reference databases SILVA_SSU, SILVA_LSU (Quast et al., 2012), and the non-coding RNA

reference database Rfam 11.0 (Burge et al., 2012). The remaining reads of the filtered reads were aligned to the UMD3.1 *Bos Taurus* reference genome (Elsik et al., 2009; Zimin et al., 2009) with TopHat2 using the default setting to remove host reads (version 2.1.1; Kim et al., 2013). The filtered reads that were not match with the host genome were considered putative microbial mRNA, which were used for further functional analyses.

Taxonomic Profiling of the Rumen Microbial Community

The pipeline DADA2 (version 1.6) was used to infer amplicon sequence variants (ASVs) from the aligned total rRNA using R (version 3.4.3; R development Core Team, 2015) as described by Callahan et al. (2016). Specifically, forward and reverse reads were trimmed with a maximum number of expected errors of 1 based on their quality scores. After that, errors rates were learned using 1 million training sequences each for forward and reverse reads, and the resulting specific error rates for each possible transition (such as A to C, A to G) were used to infer ASVs for each sample from the trimmed reads. Then the forward and reverse sequences were merged, chimeras were removed, and bacterial, archaeal, and protozoal taxonomic assignments were implemented by comparison to the SILVA database (version 132; Quast et al., 2012), and fungal taxonomic assignments were conducted by comparison to the UNITE ITS database (version 1.3.3; UNITE Community, 2017) using the naïve Bayesian classifier algorithm (Wang et al., 2007). The richness of taxa was presented as relative abundance using the phyloseq package (version 1.24.2; McMurdie and Holmes, 2013).

Identification of Transcripts Encoding CAZymes

The putative microbial mRNA sequences were assembled and aligned with the CAZymes database (Lombard et al., 2013; URL: http://www.cazy.org/) to annotate glycoside hydrolases (GH) (Henrissat, 1991; Henrissat and Bairoch, 1993; Davies and Henrissat, 1995; Henrissat and Bairoch, 1996; Henrissat and Davies, 1997), glycosyltransferases (GT) (Campbell et al., 1997;

Coutinho et al., 2003), carbohydrate binding modules (CBM) (Boraston et al., 2004), polysaccharide lyases (PL), and carbohydrate esterases (CE) (Lombard et al., 2010). Only the best alignments with expectation values lower than 1×10^{-4} were considered for functional gene annotation using the UBLAST algorithm implemented in USEARCH (version 9.2.64; Edgar, 2010). To remove biases associated with the length of the transcript and the sequencing depth of a sample, transcripts per million (TPM) were used to normalize read count values.

Statistical analysis

All statistical analyses were conducted using R software (version 3.5.1; R development Core Team, 2015). Dry matter intake (DMI), ruminal pH, and SCFA concentration data were summarized by day. Ruminal fiber (hemicellulose, cellulose, and lignin) degradability data were summarized by hour within a sampling period. Analysis of variance was conducted in a mixed model with treatment and period as fixed effects and animal as a random effect. Day within animal was included as a repeated measure for DMI, ruminal pH, and SCFA concentrations, and hour within animal was included as a repeated measure for ruminal fiber degradability. The interaction between treatment and day or hour was included as a fixed effect in the mixed model. Autoregressive covariance and heterogeneous variance were used in the repeated measures using the nlme package (version 3.1-137; Pinheiro et al., 2018). The kinetic parameters associated with fiber degradation were analyzed using the lmer function in the lme4 package (version 1.1-17; Bates et al., 2014).

The relative abundance and gene expression data were transformed to a centered log ratio:

$$\begin{bmatrix} x_1 & x_2 & \dots & x_n \end{bmatrix} \Rightarrow \begin{bmatrix} \log(\frac{x_1}{(x_1\times x_2\dots x_n)^{\frac{1}{n}}}+e-1) & \log(\frac{x_2}{(x_1\times x_2\dots x_n)^{\frac{1}{n}}}+e-1) & \dots & \log(\frac{x_n}{(x_1\times x_2\dots x_n)^{\frac{1}{n}}}+e-1) \end{bmatrix} \quad (28)$$

where $(x_1 \times x_2 \ldots x_n)^{1/n}$ represents the geometric mean of the vector. Zero value components should be excluded when dealing with log ratio transformation. However, the sequencing read counts contained an excessive number of zeros, which presents an obstacle for log ratio transformation (Gloor et al., 2017), results in non-normality (Li, 2015), can cause spurious correlations (Lovell et al., 2015), and may contribute to high false positive issues (Hawinkel et al., 2017). This was resolved by replacement of zero count values prior to transformation based on posterior distribution using a Markov Chain Monte Carlo iterative algorithm in the zCompositions package (version 1.1.1; Palarea-Albaladejo and Martín-Fernández, 2015). We added a small constant of e-1 to all ratios prior to transformation to avoid negative values. The e is Euler's number. In this case, if the gene or transcript counts equals the geometric mean, the log transformed value equals 1, so the log transformed value above 1 means read counts greater than the geometric mean, less than 1 means read counts lower than the geometric mean. Thus, the relationships among the features in the taxa and gene expression data were captured in the log ratio abundances, which have the mathematical property of real random variables and can be analyzed using standard statistical methods (Gloor et al., 2017).

Pairwise correlations between microbes and CAZymes were conducted using R. In the correlation matrix, correlation coefficient -0.5 and 0.5 were used as cutoff values. To decrease the correlation matrix size, at least one correlation coefficient should above 0.5 or lower than -0.5 within each row and column. Correlations among CAZymes transcripts, effective degradability of fibers (hemicellulose, cellulose, and lignin), the rate constants for fiber degradation, and SCFA concentrations were explored. The same selection standard as above was used for identification of important CAZymes correlations.

Multiple regression of SCFA concentrations on hemicellulose, cellulose, and lignin degradation rate and effective degradability and all identified CAZymes were conducted to identify key factors associated with SCFA production rates. It was assumed that concentrations were proportional to production rates for this effort (Sutton et al., 2003). Because there were a large number of independent variables and a small number of observations, least absolute shrinkage and selection operator (LASSO) regression was conducted first to select the top 8 variables by setting shrinkage parameter lambda. After that, a backward elimination approach with a significance level of 0.1 was used to build the linear regression model. Multicollinearity was assessed by calculation of variance inflation factors. Only variables with variance inflation factors less than 5 were included in the final linear model (Craney and Surles, 2002).

Sequencing Data Accession Number

All raw sequence data have been deposited in the NCBI Sequence Read Archive under accession number PRJNA497850.

Results

Intake, Fiber degradation, and SCFA concentrations

As designed, the mean ruminal pH achieved for the control and LpH treatments were 6.44 and 6.09, respectively. Compared to the control, DMI was inhibited by decreasing ruminal pH ($P = 0.04$).

In situ degradation of dietary DM, hemicellulose, cellulose, and lignin with respect to the rumen incubation time are shown in Figure 5-2. Although the individual parameters a, b, and k_d were not affected by lower ruminal pH, effective degradabilities of dietary DM, hemicellulose, cellulose, and lignin were decreased ($P = 0.06$, 0.02, 0.02, and 0.002). Decreased DMI and ruminal fiber degradability were associated with decrease of SCFA concentrations and presumably production rates. As a result, concentrations of ruminal total SCFA, acetate,

propionate, butyrate, isobutyrate, valerate, and isovalerate were decreased in response to lower ruminal pH (P= 0.001, 0.001, 0.001, 0.001, 0.001, 0.04, and 0.003).

Overall Variance Structure of Bacterial Phyla

Multivariate analyses were conducted to compare overall composition of bacterial phyla among all samples (Figure 5-3). Principle component analyses indicated the first component accounted for 40.4 % of the total variation, and the second component accounted for 19.4% of the total variation. Principle components are linear combinations of the original variables with their original location at the center of the multi-dimensional data.

Loading factors for the first two components (the arrows in Figure 5-3A) reveal the contribution rate of each variable on the first two components. The arrow direction represents the quality of representation on the factor map, and the arrow length indicates the contributions to the principal components. The first component was negatively correlated with *Bacteroidetes* and *Kiritimatiellaeota*, and positively correlated with *Chloroflexi* and *Actinobacteria*; While the second component was negatively correlated with *Firmicutes* and *Proteobacteria*, and positively correlated with *Epsilonbacteraeota*, and *Synergistetes*. The locations of individual observations were distributed in Figure 5-3B based on their projections. Following their underlying information, all observations were grouped by different treatments and rumen sample fractions. Although there was an overlap between the Control and LpH group, the second component can separate different ruminal pH treatments (Figure 5-3C), and the first component can clearly separate ruminal liquid and solid fractions (Figure 5-3D).

Changes of Community Diversity in the Rumen

In total, 417.5 million sequences deriving from 24 samples with an average read length of 155 bp were obtained, with a mean of 17.4 million reads per sample. After removing low quality sequences, 93.7 % of reads remained for further processing. After aligning with the rRNA

reference databases, 32.6% of sequences were classified as 16S rRNA, the rest were considered as putative mRNA.

Approximately 63 and 102 bacterial genera were identified in the ruminal liquid and solid fractions, respectively, suggesting greater bacterial genera existed in the solid than the liquid fraction (Table 5-5). A lower pH environment tended to increase numbers of bacterial genera compared to normal pH. When considering the total number of individuals, Menhinick's and Margalef's indices indicated low pH increased bacterial richness in the liquid fraction while it did not affect the richness in the solid fraction. Menhinick's index suggested the liquid fraction had a greater richness than the solid fraction, however, Margalef's index indicated the opposite, primarily due to different weights within the calculation. Pilou and Hill's ratio indicated the liquid fraction was more homogenous than the solid fraction. The Pilou index also suggested that low pH increased the evenness in the ruminal liquid fraction. Alpha diversity combined richness and evenness calculations, suggested that low pH increased bacterial community diversity in the liquid fraction, but had no effect on the solid fraction.

About 15 and 21 protozoal genera were observed in the liquid and solid fractions, respectively. The solid fraction had greater richness, evenness, and diversity than the liquid fraction, and this was not affected by pH.

Changes of Taxonomic Distribution in the Rumen

Ruminal bacterial communities at the phylum level are displayed in Figure 5-4. Overall, there were 19 bacterial phyla with a relative abundance greater than 0.05% identified in the rumen samples (Table 5-4). The most abundant phyla were *Firmicutes, Proteobacteria, Bacteroidetes,* and *Spirochaetes* (Figure 5-4). However, their proportions were dependent on treatments and rumen sample fractions. Approximately 25.46% *Firmicutes*, 34.51% *Proteobacteria*, 17.07% *Bacteroidetes*, and 9.28 % *Spirochaetes* were distributed in the control

group, while there were 25.98 % *Firmicutes*, 25.64 % *Proteobacteria*, 15.95 % *Bacteroidetes*, and 11.14% *Spirochaetes* in the LpH group (Table 5-4). The population contained 18.24% *Firmicutes*, 32.59% *Proteobacteria*, 21.29% *Bacteroidetes*, and 6.35% *Spirochaetes* in the ruminal liquid fraction, as compared to 33.2% *Firmicutes*, 27.56 % *Proteobacteria*, 11.73 % *Bacteroidetes*, and 14.07% *Spirochaetes* in the solid fraction (Table 5-4).

Analysis of variance results are displayed in Figure 5-5 and summarized in Table 5-6. *Bacteroidetes*, *Chloroflexi*, *Proteobacteria*, and *Patescibacteria* were influenced by lower ruminal pH (P = 0.0003, 0.05, and 0.03), and *Bacteroidetes*, *Firmicutes*, *Kirtimatiellaeota*, *Lentisphaerae*, *Patescibacteria*, and *Spirochaetes* had different distributions in ruminal sample fractions (P = 0.01, 0.03, 0.003, 0.02, 0.001, and < 0.0001). *Bacteroidetes*, *Proteobacteria*, and *Patescibacteria* were also affected by the interaction between ruminal pH and sample fractions (P=0.04, 0.01, and 0.01). Compared to normal ruminal pH, the low pH treatment increased the proportion of *Chloroflexi* in both liquid and solid fractions, while the proportions of *Bacteroidetes* and *Proteobacteria* in the liquid fraction were decreased (Figure 5-6). With decreased ruminal pH, *Patescibacteria* was decreased in the liquid fraction and increased in the solid fraction. The ruminal liquid fraction had greater proportions of *Bacteroidetes*, *Kirtimatiellaeota*, and *Lentisphaerae*, and lesser proportions of *Firmicutes* and *Spirochaetes* than the ruminal solid fraction (Figure 5-6).

Analyses at the bacterial genus level were performed to gain further insights into changes in the taxonomic distributions. In total, 121 bacterial genera were identified in the samples, with 20 of them having relative abundances greater than 0.5% (Table 5-7). *Succinivibrionaceae_UCG-002*, *Treponema_2*, *Fibrobacter*, *Ruminobacter*, *Christensenellaceae_R-7_group*, *Erysipelotrichaceae_UCG-004*, *Ruminococcus_2*,

Prevotella_1, *Succinivibrionaceae_UCG-001*, and *CAG-352* were the10 most abundant genera, accounting for 17.48, 8.93, 4.41, 4.05, 3.55, 3.05, 3.04, 3.87, 2.75, and 3% of total bacteria in the rumen, respectively (Figure *5-7*). In total, 19 bacterial genera were affected by low ruminal pH, and 30 bacterial genera had different proportions between the ruminal liquid and solid samples (Figure *5-8*). Of these, 11 genera were only affected by ruminal pH; 25 genera were only affected by sample location; 5 bacterial genera were influenced by both ruminal pH and sample location; and 6 were affected by the interaction between ruminal pH and sample location. In addition, there were 3 bacterial genera only affected by the interaction.

In terms of ruminal pH effects on bacterial genera (Figure 5-9), low ruminal pH decreased *Lachnospiraceae_UCG-007*(*P* = 0.02), *Succinimonas* (*P* = 0.003), *Anaerosporobacter* (*P* = 0.002), *Pseudomonas* (*P* = 0.003), *M2PT2-76_termite_group* (*P* = 0.02), *Clostridium_sensu_stricto_1* (*P* = 0.004), and *Prevotella_1* (*P* = 0.04) compared to normal ruminal pH, and increased *Victivallis* (*P* = 0.02), *Ruminococcaceae_UCG-010* (*P* = 0.01), *Sediminispirochaeta* (*P* = 0.03), *Pyramidobacter* (*P* = 0.01), *Papillibacter* (*P* = 0.01), *Treponema* (*P* = 0.03), and *Ruminococcaceae_UCG-005* (*P* = 0.03).

Compared to normal ruminal pH, lower pH decreased the proportion of *Succinivibrionaceae_UCG-002* (*P* = 0.02) in the liquid fraction but did not change the proportion in the solid fraction. The proportion of *Lachnoclostridium_1* (*P* = 0.01) was decreased by low pH in the solid fraction, and it was not affected in the liquid fraction. Under a low ruminal pH conditions, the proportions of *Pantoea* (*P* = 0.04), *Prevotella_9* (*P* = 0.001), and *Pseudomonas* (*P* = 0.005) were increased in the solid fraction but decreased in the liquid fraction. The opposite occurred for *Synergistes* (*P* = 0.04), *Mogibacterium* (*P* = 0.01), *Flexilinea* (*P* = 0.01), and

Christensenellaceae_R-7_group (*P* = 0.03) where decreased ruminal pH resulted in decreased proportions in the solid fraction and increased proportions in the liquid fraction.

The ruminal liquid fraction had greater proportions of *CPla-4_termite_group* (*P* = 0.04), *Horsej-a03* (*P* = 0.01), *Pirellula* (*P* = 0.01), *Sediminispirochaeta* (*P* = 0.04), *Ruminococcaceae_UCG-010* (*P* = 0.01), *Elusimicrobium* (*P* = 0.002), *Erysipelotrichaceae_UCG-004* (*P* = 0.01), *Sporobacter* (*P* = 0.001), and *Anaeromusa* (*P* = 0.02) as compared to the solid fraction, and reduced proportions of *Lachnospiraceae_ND3007_group* (*P* = 0.04), *Lachnospiraceae_AC2044_group* (*P* = 0.003), *Desulfovibrio* (*P* = 0.03), *Butyrivibrio_2* (*P* = 0.01), *Family_XIII_AD3011_group* (*P* = 0.01), *Moryella* (*P* = 0.001), *U29-B03* (*P* = 0.04), *Family_XIII_UCG-001* (*P* = 0.001), *Lachnospiraceae_NK3A20_group* (*P* = 0.04), *Olsenella* (*P* = 0.004), *Ruminococcaceae_UCG-004* (*P* = 0.05), *Saccharofermentans* (*P* = 0.004), *Ruminococcus_1* (*P* = 0.0004), *Selenomonas_1* (*P* = 0.02), *Lachnospiraceae_NK4A136_group* (*P* = 0.001), *Prevotellaceae_UCG-001*(*P* = 0.03), *Pseudobutyrivibrio* (*P* = 0.002), *Candidatus_Saccharimonas* (*P* = 0.01).

The relative abundances of ruminal archaeal genera are shown in Figure 5-10. *Candidatus_Methanomethylophilus* and *Methanobrevibacter* were the most abundant genera, accounting for approximately 54.34 and 25.08% of total ruminal archaea (Table 5-9). Low ruminal pH did not change archaeal composition. However, compared to the liquid sample, a greater proportion of *Methanobrevibacter* was observed in the ruminal solid fraction (*P* = 0.02, Table 5-10).

The relative abundances of ruminal fungal phyla and genera are shown in Figure 5-11. *Mucoromycota*, *Ascomycota*, and *Basidiomycota* were the predominant fungal phyla in the rumen, accounting for 22.3, 19.2, and 18.2% of total ruminal fungal sequences. Within them,

Densospora and *Acidomyces* were the most abundant fungal genera, representing 22.2 and 6.7% of total ruminal fungi. No significant treatment effect or sample effect were found for either the fugal phyla or genera.

Twenty six protozoan genera were identified through analysis of microbial composition, and 10 of them had relative abundances greater than 0.08% of the total population (Table 5-11). *Entodinium, Polyplastron, Isotricha, Eudiplodinium,* and *Eremoplastron* were highly abundant representing 35.66, 5.6, 5.08, 1.3, and 1.4% of the population (Figure 5-12). *Cyllamyces*, *Isotricha*, *Mortierella*, and *Ophryoscolex* were affected by ruminal pH (P = 0.001, 0.01, 0.04, and 0.02). *Brachypodium*, *Diploplastron*, *Entodinium*, *Ophryoscolex*, *Panax*, *Trichomitus*, and *Triticum* (P = 0.001, 0.04, 0.001, 0.02, 0.03, 0.04, and 0.01) had different distributions between the solid and liquid fraction. Within them, *Cyllamyces* and *Ophryoscolex* were also affected by the interaction (P = 0.03 and 0.02).

As displayed in Figure 5-14, low pH decreased the proportion of *Isotricha*, while it increased *Mortierella* in both the liquid and solid samples. Decreasing ruminal pH increased the proportion of *Cyllamyces* and *Ophryoscolex* in the liquid fraction but did not change in the solid fraction. The ruminal liquid fraction had greater proportions of *Diploplastron, Entodinium*, and *Trichomitus* than the solid fraction, and lesser proportions of *Brachypodium*, *Panax*, and *Triticum* (Table 5-12).

Changes of CAZymes Expressed by Rumen Microbiota

In total, 97 CAZymes were identified, and 22 of them had a relative abundance above 1% (Table 5-13). As displayed in Figure 5-15, cellulase, endo-1,4-beta- xylanase, amylase, and alpha-N-arabinofuranosidase were the most abundant enzymes, accounting for 12.83, 11.87, 7.72, and 2.75 % of the total enzyme transcripts. In Figure 5-16, 8 enzymes were significantly affected by ruminal pH, within them 2 enzymes were also affected by sample fractions, and 3

were affected by their interaction. Seven enzymes were expressed differently between ruminal solid and liquid samples, and 1 enzyme was only affected by the interaction between ruminal pH and sample location.

Figure 5-17 shows that the expression of rhamnogalacturonan acetylesterase, glucan phosphorylase, and pectate lyase/amb allergen were upregulated by lower ruminal pH (P =0.05, 0.05, and 0.0001), while glycosyl hydrolase family 16 were downregulated (P =0.02). Low pH resulted in downregulations of glycosyl hydrolase family 43 and UDP-3-0-acyl N-acetylglucosamine deacetylase in the solid fraction, and upregulations in the liquid fraction (P = 0.03 and 0.02). The low pH treatment was associated with increased expression of putative glycosyl transferase in the solid fraction and decreased that expression in the liquid fraction (P = 0.03). In addition, decreasing pH caused a decrease in the proportional abundance of sucrose alpha-glucosidase in the liquid fraction, but did not change its expression in the solid fraction (P = 0.005). The ruminal liquid fraction contained a greater proportion of sequences for beta-galactosidase, putative 1,4-alpha-glucan branching enzyme, glucosidase cel1C, cellulase celA, putative carbohydrate-active enzyme, amylase, and putative 4-alpha-glucanotransferase than the solid fraction (P = 0.01, 0.02, 0.03, 0.01, 0.002, 0.01, and 0.01), while it had lesser expression of glycoside hydrolase family 43 (P = 0.02).

Correlations Among Ruminal Microbes and CAZymes

Pairwise correlations among microbes and CAZymes are displayed in Figure 5-18. There were 54 microbes (43 bacterial genera and 11 protozoal genera) and 25 enzymes that had at least one correlation coefficient above 0.5 which was the criteria for inclusion in the matrix. There were no significant correlations identified among archaeal genera and CAZymes.

Within bacteria genera group, *Acetanaerobacterium* was positively correlated with glucan 1,4-alpha-maltotetraohydrolase, and glycosyltransferase 36. *Acetitomaculum* was

positively correlated with glycosyltransferase 36 and isoamylase domain/esterase family protein, and negatively correlated with glycosyl hydrolase family 57 and sucrose alpha-glucosidase. There was a positive correlation between *Anaeromusa* and glycosyl hydrolase family 43, putative carbohydrate-active enzyme, glycosyl hydrolase family 31, sucrose alpha-glucosidase, glucan phosphorylase, pectate lyase/amb allergen, isoamylase domain/esterase family protein, UDP-3-0-acyl N-acetylglucosamine deacetylase, and glycoside hydrolase family 2 TIM barrel, and a negative correlation between putative alpha-N-arabinofuranosidase and glycoside hydrolase family 43. *Anaerostipes* was positively correlated with glucan phosphorylase. Both *Anaeroplasma* and *Asteroleplasma* were negatively correlated with glycoside hydrolase family 43 and putative alpha-N-arabinofuranosidase. A positive correlation existed between *Bifidobacterium* and cellulase celA and putative alpha-xylosidase. *Butyrivibrio_2* was positively correlated with glycosyltransferase group 1 family, amylase, pectate lyase/amb allergen, and glycosyl hydrolase family 43, and negatively correlated with galacturan 1,4-alpha-galacturonidase, cellulase celA, putative 4-alpha-glucanotransferase, and UDP-3-0-acyl N-acetylglucosamine deacetylase. There was a negative correlation between *Candidatus_Endomicrobium* and acetylglucosaminyltransferase were positively correlated with cellulase celA. There was a negative correlation between *Candidatus_Saccharimonas* and glycosyl hydrolase family 43, glycosyltransferase group 1 family, and putative alpha-N-arabinofuranosidase. *Clostridium_sensu_stricto_1* exhibited a positive relationship with glycosyltransferase 36, glycosyl hydrolase family 57, alpha-glucosidase, putative carbohydrate-active enzyme, glucuronan lyase, putative alpha-N-arabinofuranosidase, and glycoside hydrolase family 43, and a negative relationship with glycosyl hydrolase family 43. *CPla-4_termite_group* was positively correlated with glucuronan lyase, acetylglucosaminyltransferase, amylase,

glycosyltransferase 36, glycosyl hydrolase family 57, galacturan 1,4-alpha-galacturonidase, and putative alpha-N-arabinofuranosidase, and negatively correlated with isoamylase domain/esterase family protein. A positive correlation was found between *Desulfovibrio* and glucan 1,4-alpha-maltotetraohydrolase, putative alpha-xylosidase, and glucan phosphorylase, and a negative correlation with cellodextrin-phosphorylase, glucuronan lyase, alpha-glucosidase, and glycosyl hydrolase family 57. There was a positive correlation between Erysipelothrix and cellulase celA, glycosyltransferase 36, isoamylase domain/esterase family protein, and glycosyltransferase group 1 family, and a negative correlation with glycoside hydrolase family 43. *Family_XIII_AD3011_group* exhibited a positive relationship with glycoside hydrolase family 2 TIM barrel, putative carbohydrate-active enzyme, galacturan 1,4-alpha-galacturonidase, pectate lyase/Amb allergen, and putative alpha-xylosidase, and negatively correlated with isoamylase domain/esterase family protein. *Family_XIII_UCG-001* was positively correlated with glucuronan lyase, amylase, putative alpha-N-arabinofuranosidase, glycosyl hydrolase family 57, and UDP-3-0-acyl N-acetylglucosamine deacetylase. There was a positive correlation between *Flexilinea* and amylase, glycosyl hydrolase family 57, sucrose alpha-glucosidase, and putative carbohydrate-active enzyme, and a negative correlation with pectate lyase/amb allergen, glucan 1,4-alpha-maltotetraohydrolase, and glucan phosphorylase. *Herbinix* was negatively correlated with galacturan 1,4-alpha-galacturonidase and UDP-3-0-acyl N-acetylglucosamine deacetylase. A positive correlation was found between *Lachnospiraceae_NK3A20_group* and glycosyltransferase 36 and isoamylase domain/esterase family protein, while a negative correlation was observed between Lachnospiraceae_NK3A20_group and Glycosyl hydrolase family 57, sucrose alpha-glucosidase, putative carbohydrate-active enzyme, amylase, and cellulase celA. *Lachnospiraceae_UCG-007* was positively correlated with galacturan 1,4-alpha-

galacturonidase. *Lachnospiraceae_XPB1014_group* exhibited a positive correlation with glycosyl hydrolase family 57, glycoside hydrolase family 43, putative alpha-xylosidase, and sucrose alpha-glucosidase, and a negative correlation with isoamylase domain/esterase family protein. There was a positive correlation between *Mogibacterium* and glucuronan lyase, amylase, glycosyltransferase group 1 family and putative 4-alpha-glucanotransferase, and a negative correlation with putative alpha-N-arabinofuranosidase, cellodextrin-phosphorylase, and glycosyl hydrolase family 43. *Moryella* was positively correlated with sucrose alpha-glucosidase, alpha-glucosidase, beta-galactosidase, glucan phosphorylase, and glycoside hydrolase family 2 TIM barrel, and negatively correlated with acetylglucosaminyltransferase. There was a positive correlation between *Olsenella* and alpha-glucosidase, sucrose alpha-glucosidase, putative alpha-xylosidase, and beta-galactosidase, and a negative correlation with acetylglucosaminyltransferase. Oribacterium was positively correlated with sucrose alpha-glucosidase and alpha-glucosidase, and negatively correlated with acetylglucosaminyltransferase. A positive correlation was observed between *Papillibacter* and cellodextrin-phosphorylase, pectate lyase/amb allergen, glycosyl hydrolase family 43, and putative alpha-N-arabinofuranosidase, and a negative correlation was identified between *Prevotella_1* and glycosyl hydrolase family 31, pectate lyase/amb allergen, and putative carbohydrate-active enzyme. *Prevotellaceae_NK3B31_group* was positively correlated with beta-galactosidase, glycosyl hydrolase family 31 and pectate lyase/amb allergen, and *Prevotellaceae_YAB2003_group* was negatively correlated with glycosyltransferase 36, glycoside hydrolase family 43, glucan 1,4-alpha-maltotetraohydrolase. There was a positive correlation between *Pyramidobacter* and alpha-glucosidase and glycosyl hydrolase family 31, and a negative correlation with cellodextrin-phosphorylase, acetylglucosaminyltransferase, and

isoamylase domain/esterase family protein. *Ruminococcaceae_UCG-004* was positively correlated with sucrose alpha-glucosidase, cellulase celA, glycoside hydrolase family 2 TIM barrel, and alpha-glucosidase, and negatively correlated with acetylglucosaminyltransferase. *Ruminococcus_1* was positively correlated with glycosyl hydrolase family 31, beta-galactosidase, putative carbohydrate-active enzyme, and glycosyl hydrolase family 57, and negatively correlated with isoamylase domain/esterase family protein, glucan phosphorylase, putative alpha-xylosidase, UDP-3-0-acyl N-acetylglucosamine deacetylase, and glucuronan lyase. In contrast, *Ruminococcus_2* was positively correlated with UDP-3-0-acyl N-acetylglucosamine deacetylase and acetylglucosaminyltransferase, and negatively correlated with glycosyl hydrolase family 31, sucrose alpha-glucosidase, cellulase celA, putative carbohydrate-active enzyme, putative alpha-xylosidase, amylase, and alpha-glucosidase. There was a positive correlation between *Saccharofermentans* and glycosyl hydrolase family 31 and pectate lyase/amb allergen, and a negative correlation with isoamylase domain/esterase family protein and UDP-3-0-acyl N-acetylglucosamine deacetylase. *Selenomonas_1* was negatively correlated with acetylglucosaminyltransferase, amylase, and glycosyl hydrolase family 43. There was a positive correlation between *Sphaerochaeta* and isoamylase domain/esterase family protein, glucan 1,4-alpha-maltotetraohydrolase, and glycosyltransferase group 1 family, and a negative correlation with pectate lyase/amb allergen. *Sporobacter* was positively correlated with isoamylase domain/esterase family protein, UDP-3-0-acyl N-acetylglucosamine deacetylase, putative alpha-xylosidase, glucan phosphorylase, glucuronan lyase, acetylglucosaminyltransferase, glycosyltransferase 36, and glycoside hydrolase family 2 TIM barrel, and negatively correlated with pectate lyase/amb allergen, glycosyl hydrolase family 31, putative alpha-N-arabinofuranosidase, and beta-galactosidase. There was a negative correlation

between *Succinivibrio* and glycosyltransferase 36, glycoside hydrolase family 43, glucan 1,4-alpha-maltotetraohydrolase. *Treponema_2* was positively correlated with pectate lyase/amb allergen and putative alpha-N-arabinofuranosidase, and negatively correlated with UDP-3-0-acyl N-acetylglucosamine deacetylase, glycosyltransferase 36, putative alpha-xylosidase, glycoside hydrolase family 2 TIM barrel, glucuronan lyase, isoamylase domain/esterase family protein, and glucan phosphorylase. There was a positive correlation between *Tyzzerella_3* and UDP-3-0-acyl N-acetylglucosamine deacetylase, glucan phosphorylase, glucuronan lyase, putative alpha-xylosidase, isoamylase domain/esterase family protein, glycoside hydrolase family 2 TIM barrel, acetylglucosaminyltransferase, and glycosyltransferase 36, and a negative correlation with putative alpha-N-arabinofuranosidase, pectate lyase/amb allergen, beta-galactosidase, and glycosyl hydrolase family 31. *U29-B03* was positively correlated with sucrose alpha-glucosidase, alpha-glucosidase, glycoside hydrolase family 2 TIM barrel, beta-galactosidase, and putative alpha-xylosidase.

In terms of protozoal genera, *Glycine* was negatively correlated with amylase, putative carbohydrate-active enzyme, and cellulase celA. *Brachypodium* was negatively correlated with glucan phosphorylase. There was a positive correlation between *Cycloposthium* and glycosyl hydrolase family 57, and a negative correlation with sucrose alpha-glucosidase. *Dasytricha* was positively correlated with cellodextrin-phosphorylase, glycosyl hydrolase family 57, glycosyltransferase group 1 family, glycosyl hydrolase family 43, amylase, putative 4-alpha-glucanotransferase, putative carbohydrate-active enzyme, acetylglucosaminyltransferase, isoamylase domain/esterase family protein, and pectate lyase/amb allergen, and negatively correlated with glucan phosphorylase and putative alpha-xylosidase. *Diploplastron* exhibited a positive correlation with glycosyl hydrolase family 57, glycosyltransferase group 1 family,

glycosyl hydrolase family 43, and cellodextrin-phosphorylase, and a negative correlation with alpha-glucosidase. There was a positive correlation between *Eremoplastron* and glycosyl hydrolase family 57, glycosyltransferase group 1 family, and glycosyl hydrolase family 43. *Eudiplodinium* was positively correlated with putative carbohydrate-active enzyme. *Foaina* was positively correlated with putative alpha-N-arabinofuranosidase, galacturan 1,4-alpha-galacturonidase, and cellodextrin-phosphorylase. There was a positive correlation between *Tritrichomonas* and putative alpha-N-arabinofuranosidase, cellodextrin-phosphorylase, and galacturan 1,4-alpha-galacturonidase.

Correlations among CAZymes and Fiber Degradation and Ruminal SCFA Concentrations

Pairwise correlations between CAZymes and fiber degradation and SCFA concentrations are displayed in Figure 5-19. No strong correlations were identified between hemicellulose degradation rate and CAZymes. However, effective degradability of hemicellulose was positively correlated with fucosylgalactoside 3-alpha-galactosyltransferase and mannosyl-oligosaccharide 1,3-1,6-alpha-mannosidase, and negatively correlated with pectate lyase/amb allergen. There was a negative correlation between cellulose degradation rate and alpha-glucosidase family protein. The effective degradability of cellulose was negatively correlated with pectate lyase/amb allergen. Lignin degradation rate was positively correlated with cellulase celA, alpha-glucosidase, and putative carbohydrate-active enzyme, and negatively correlated with cellodextrin-phosphorylase. Only pectate lyase/amb allergen was observed to be negatively correlated with effective degradability of lignin.

Acetate concentrations were positively correlated with glycosyl hydrolase family 31, while no significant correlations were identified for propionate concentrations. There was a positive correlation between butyrate concentrations and putative 4-alpha-glucanotransferase,

glycosyl hydrolase family 31, sucrose alpha-glucosidase, and endo-1,4-xylanase/ferulic acid esterase. Similar correlations were also observed for isobutyrate, valerate, and isovalerate except there was a negative correlation between isobutyrate and pectate lyase/amb allergen. Meanwhile, isovalerate was positively correlated with putative alpha-xylosidase, putative carbohydrate-active enzyme, and amylase.

Using CAZymes and Fiber Degradation Dynamics to Predict Ruminal SCFA Concentrations

Multiple regression of ruminal SCFA concentrations on CAZymes and fiber degradation is summarized in Table 5-15. Ruminal acetate concentrations were positively correlated with hemicellulose degradation rate, effective degradability of lignin, glycosyl hydrolase family 31, and negatively correlated with galacturan 1,4-alpha-galacturonidase, and maltopentaose-forming amylase. Approximately 74% of the acetate variance was explained by the regression model.

There was a positive correlation between propionate concentrations and hemicellulose degradation rate, glycosyl hydrolase family 16, and glycosyltransferase group 1 family, and a negative correlation with glycogen synthase-like protein and maltopentaose-forming amylase. The regression model captured aproximately 87% of the observed variance in propionate concentrations.

Butyrate concentrations were positively correlated with cellulose degradation rate, effective degradability of cellulose, endo-1,4-xylanase / ferulic acid esterase, and glycosyl hydrolase family 31, and 74% of the variance of butyrate was explained by these variables.

Effective degradability of cellulose and lignin, glycosyl hydrolase family 16, and glycosyl hydrolase family 31 were positively correlated with isobutyrate concentrations, and maltopentaose-forming amylase was negatively correlated with isobutyrate. Around 81% of the variance of isobutyrate was explained.

Valerate concentrations were positively correlated with cellulose degradation rate, effective degradability of cellulose, glycosyl hydrolase family 31, and negatively correlated with galacturan 1,4-alpha-galacturonidase and maltopentaose-forming amylase. Approximately 85% variance of valerate was explained by the regression model.

There was a positive correlation between isovalerate concentrations and effective degradability of cellulose, endo-1,4-xylanase / ferulic acid esterase, glucuronan lyase, glycosyl hydrolase family 16 and glycosyl hydrolase family 31. Roughly 89% of the variance of isovalerate concentrations can be explained by the model.

Discussions

The Distribution of Active Microbes in the Rumen

While metagenomics can reflect the comprehensive diversity of all the active and inactive microorganisms, metatranscriptomics is a more reliable tool to obtain insights into the most active microorganisms. In the present study, *Proteobacteria*, *Firmicutes*, *Bacteroidetes,* and *Spirochaetes* were the most predominant bacterial phyla in the rumen, accounting for 30.08, 25.72, 16.51, and 10.21% of the total bacterial sequences. These results were consistent with bacterial phylum profiles in beef cattle (Li, 2017). Within *Proteobacteria*, *Succinivibrionaceae_UCG-002*, *Ruminobacter*, and *Succinivibrionaceae_UCG-001* were the most predominant genera. *Christensenellaceae_R-7_group*, *Erysipelotrichaceae_UCG-004*, and *Ruminococcus_2* were highly abundant within *Firmicutes*. *Prevotella_1* was the most predominant genus in *Bacteroidetes*. Although same phyla were identified as dominant bacteria in metagenomic studies, their community structure is quite different with approximately 50.5, 29.8, and 10.6% of *Firmicutes*, *Bacteroidetes,* and *Proteobacteria* (Jami and Mizrahi, 2012; Petri et al., 2013; Henderson et al., 2015; De Mulder et al., 2017), implying there was a difference of bacterial community structure at genomic and transcriptional levels. Kang et al. (2013) indicated

the abundance of *Proteobacteria* was greater in RNA derived rumen bacterial materials than the DNA derived materials through a high throughput analysis, and this difference was validated using denaturing gradient gel electrophoresis (DGGE) and qRT-PCR techniques.

Candidatus_Methanomethylophilus and *Methanobrevibacter* were the most abundant active archaeal genera, representing 54.34 and 25.08% of total archaeal sequences. Similar results in the rumen of black goats were reported by Wang et al. (2017).

Entodinium, *Polyplastron*, *Isotricha*, *Eudiplodinium*, and *Eremoplastron* with 35.66, 5.6, 5.08, 1.3, and 1.4% of relative abundance were the core protozoal genera. It was previously observed that dairy heifers had protozoal populations with 72.3 *Entodinium* and 15.0 % *Ostracodinium* (Zhang et al., 2017). *Entodinium* and *Diplodiniinae* were the dominate protozoal genera in buffalo (Franzolin and Wright, 2016). *Entodinium* (80%), *Diploplastron* (5%), *Dasytricha* (8.3%), and *Isotricha* (3.3%) were characterized in the rumen of cattle (Abrar et al., 2016). In all the studies, *Entodinium* was the predominate protozoa genus in the rumen, however, the rest of the protozoal genera were highly varied. Henderson et al. (2015) demonstrated the variability of protozoa between and within cohorts of co-located animals was much greater than bacteria and archaea. Considering most of the previous studies were conducted using metagenomics, further investigations into profiles of active rumen protozoa remain to be conducted.

Ruminal microbes are distributed into 3 domains: a solid-adherent fraction, the liquid fraction and those associated with the rumen epithelium. More microbial species were observed in the solid fraction, suggesting a more diverse bacterial community existed in the ruminal solid sample. As expected, no unique taxonomic groups were identified for the solid and liquid environment, since they are prone to continuous interaction and mutual influences (De Mulder et

al., 2017). Substantial differences in the abundance of species were observed. The difference in microbial composition has previously been observed to be associated with substrate availability (Leng, 2011; Huo et al., 2014; Deusch et al., 2017), rumen kinetics with respect to particle size (Gregorini et al., 2015), and physical and chemical properties (Legay-Carmier and Bauchart, 1989). We found that free-floating bacteria that readily degrade metabolizable carbohydrate such as *Bacteroidetes* and *Lentisphaerae*, were more prevalent in the liquid fraction, while the cellulolytic bacteria, such as *Firmicutes* and *Spirochaetes*, are prominent members in the solid fraction. These results were consistent with previous studies (Myer et al., 2015; De Mulder et al., 2017; Deusch et al., 2017). Within the *Firmicutes* phylum, 12 genera (*Lachnospiraceae_ND3007_group*, *Lachnospiraceae_AC2044_group*, *Butyrivibrio_2*, *Moryella*, *Family_XIII_AD3011_group*, *Family_XIII_UCG-001*, *Lachnospiraceae_NK3A20_group*, *Ruminococcaceae_UCG-004*, *Ruminococcus_1*, *Saccharofermentans*, *Selenomonas_1*, *Lachnospiraceae_NK4A136_group*, and *Pseudobutyrivibrio*) were more abundant in the solid fraction, while 3 genera (*Erysipelotrichaceae_UCG-004*, *Sporobacter*, and *Anaeromusa*) were more abundant in the liquid fraction.

A greater proportion of the bacterial phylum *Kirtimatiellaeota* was found in the liquid phase than in the solid phase (5.44% vs 1.67% of total bacterial sequences). *Kirtimatiellaeota* is a newly recognized phylum, which is an obligate anaerobe and saccharolytic bacterium that can grow in suboxic transition zones of a hypersaline environment (Spring et al., 2016). However, the role of *Kirtimatiellaeota* in rumen microbial ecosystem needs further investigation.

A greater proportion of archaeal genus *Methanobrevibacter* was observed in the ruminal solid fraction compared with the liquid fraction. Similar results were reported by Henderson et al. (2013) and De Mulder et al. (2017). *Methanobrevibacter* is a methanogen related to the

bioconversion of cellulose fiber to methane by a symbiotic relationship with a rumen anaerobic fungus (Joblin et al., 1990). Mountfort et al. (1982) demonstrated *Methanobrevibacter* can convert lactate and ethanol to methane by removing hydrogen and formate to shift electron flow away from the formation of electron sink.

Ruminal liquid and solid fractions had distinct protozoal communities with a greater proportion of *Diploplastron, Entodinium*, and *Trichomitus* in the liquid fraction whereas *Brachypodium, Panax*, and *Triticum* were observed in the solid. However, De Menezes et al. (2011) observed that protozoan communities were very similar between ruminal liquid and solid fractions. The protozoal community was affected by rumen sample fractions which might be caused by the factors related to ruminal dynamics and protozoa growth. Inversely related to the rumen retention time, liquid associated protozoa have a greater ruminal outflow rate than solid associated protozoa. To counteract washout and maintain populations, they have to actively metabolize to generate energy for growth. The ruminal liquid fraction contains a greater proportion of soluble carbohydrate and starch than the solid fraction, which might generate more energy for microbial growth resulting in a greater proportion of amylolytic protozoa. *Entodinium* as the predominant protozoal genus in the rumen and has been characterized as a starch feeder. Maltase and amylase activity was prevalent in the cell free extracts made from the *Entodinium* suspensions (Akkada and Howard, 1960). Michałowski et al. (1986) indicated *Diploplastron* could digest and ferment starch to generate SCFA in the ruminal liquid.

Trichomitus, Brachypodium, *Panax*, and *Triticum* represented less than 0.3% of the protozoal population. Unfortunately, little information related to their charactristics and function has been published. We observed that *Brachypodium* was negatively correlated with glucan phosphorylase. Coleman (1969) indicated that protozoa could not effectively use glucose and

maltose to maintain growth because of the absence of glucan phosphorylase. Consequently, glucose and the glucose of maltose could not be phosphorylated to glucose-6-phophate in protozoa. Obviously, this is not applicable to all protozoa, because a positive correlation between glucan phosphorylase and a protozoal genus *Cyllamyces* was identified in the study.

Ruminal pH Alters Rumen Microbial Ecology

Various studies have been conducted to elucidate microbial community changes associated with dietary changes (De Menezes et al., 2011; Deusch et al., 2017; Zhang et al., 2017) and subclinical ruminal acidosis (Petri et al., 2013; Huo et al., 2014; McCann et al., 2016; Wetzels et al., 2016). However, because ruminal pH declines occur at the same time as the amount of concentrate fed increases, the results are often confounded between concentrate amount and ruminal pH. In the current study, we fed the same diet to all animals and manipulated ruminal pH by intraruminal infusion. In this scenario, all the microbial changes should be due to the pH reduction although the associated decline in DMI may have contributed. Although some feedback of fermentation end products on ruminal pH may be expected, such potential effects were masked by our attempts to maintain pH in a certain range by varying the rate of acid infusion. Thus any such feedback should have had negligible impact on the results.

A reduction of 0.5 ruminal pH decreased the proportions of *Bacteroidetes* and *Proteobacteria* in the liquid fraction but did not affect their proportions in the solid fraction, suggesting that *Bacteroidetes* and *Proteobacteria* were less sensitive to low ruminal pH in the solid fraction than the liquid fraction. Schulze et al. (2017) demonstrated that there was a decreased SCFA concentrations and increased pH gradient from the medial to the ventral part of the rumen, due to that microbial fermentation takes place in the medial part of the rumen, while SCFA absorption occurs in the ventral part of the rumen through rumen epithelium. Therefore,

the original pH gradient in the rumen might have contributed to different responses to pH challenges.

A reduction of ruminal pH decreased the proportion of the bacterial genera *Lachnospiraceae_UCG-007, Succinimonas, Anaerosporobacter, Pseudomonas, M2PT2-76_termite_group, Clostridium_sensu_stricto_1*, and *Prevotella_1* compared to normal ruminal pH, and increased *Victivallis, Ruminococcaceae_UCG-010, Sediminispirochaeta, Pyramidobacter, Papillibacter, Treponema,* and *Ruminococcaceae_UCG-005*. The diffident responses to low pH among bacterial genera might reflect their specific acid resistance. Petri et al. (2013) reported that the relative abundance of *Prevotella, Acetitomaculum, Pseudobutyrivibrio, Selenomonas, Succinivibrio, Treponema,* and *vadinHA42* genera in the rumen fluid increased following a high grain diet challenge. Plaizier et al. (2017) found the abundance of *Succinivibrio*in the rumen fluid was increased by the high grain diet challenge. Surprisingly, none of these genera was significantly affected in our study, implying different mechanisms of changing the bacterial community between high grain diet and pH declines. An increase of grain intake might have contributed to increased nonstructural carbohydrate as substrates to generate energy for maintenance and growth of microbes. However, low ruminal pH tended to inhibit microbial growth through intracellular regulation. Ruminal bacteria attempt to maintain a constant intracellular pH when extracellular pH is low. As a consequence, transmembrane pH gradient and electrical potential were increased, resulting in an inhibited transport activity (Russell and Wilson, 1996; Russell, 1998).

We observed that *Succinivibrionaceae_UCG-002* was the most abundant active bacterial genus in the rumen, and low ruminal pH decreased its abundance in the liquid fraction, but had no effect on the solid fraction. In contrast, Henderson et al. (2015) observed that

Succinivibrionaceae was more abundant in concentrate fed animals implying that substrate availability is a stronger driver of growth than ruminal pH. *Succinivibrionaceae_UCG-002* belongs to the phylum *Proteobacteria*, and was observed to convert whey lactose to succinate and acetate (Samuelov et al., 1999).

Franzolin and Dehority (1996) reported that feeding a high concentrate diet increased the proportions of the protozoal genera *Isotricha* and *Epidinium*. *Hook et al. (2011) found that a* high concentrate diet increased the number of *Entodinium*, *Ophryoscolex*, *Isotricha*, and *Dasytricha*. *In the current study, we observed that* low ruminal pH was associated with decreased proportions of *Isotricha*, but increased proportions of *Ophryoscolex* in the liquid fraction. The combined results suggest the growth of *Isotricha* is more responsive to starch availability whereas *Ophryoscolex* was more sensitive to ruminal pH.

The Distribution of CAZymes in the Rumen

Structural and nonstructural carbohydrate are efficiently degraded in the rumen via numerous enzymes produced by resident microorganisms. Studies have been conducted to gain insights into CAZymes gene expressions in response to various diets through metagenomic (Wang et al., 2013; Deusch et al., 2017) or metatranscripomic approaches (Dai et al., 2015; Güllert et al., 2016; Shinkai et al., 2016; Comtet-Marre et al., 2017). These studies reported enzymes at the family level. For example, glycoside hydrolases are classified into 153 families according to their substrate specificity, structural features, or sequence similarities. Similar individual enzymes can also be classified into different families. Therefore, transcript expression of specific enzymes should more precisely reflect the mechanistic functions of rumen microbes. However, to our knowledge, such an effort has not been previously undertaken. Relationships among enzymes and microbes have generally been quantified based on the encoded gene

sequence of the microbes and the amino acid sequence of enzymes. These associations need to be verified in vivo through statistical analyses.

We observed that cellulase, endo-1,4-beta- xylanase, amylase, and alpha-N-arabinofuranosidase were the dominate enzyme transcripts in the rumen. Cellulase has been assigned to multiple carbohydrate binding module families (CBM), such as CBM1 to 6, 9, 10, 17, 22, 28, 32, 37, and glycoside hydrolase families (GH), including GH1, 3, 5 to 9, 45, and 48. Carbohydrate binding modules are non-catalytic proteins that have affinity for carbohydrates. Deusch et al. (2017) found that CBM were more abundant in the solids fraction of the rumen. Wang et al. (2013) indicated GH5 and GH9 were the most frequent cellulases found in the metagenomic study. Similar results were also reported in metatranscriptomic studies (Dai et al., 2015; Güllert et al., 2016).

The main function of cellulase is to hydrolyze 1,4-beta-D-glycosidic linkages to release monomers. Based on its structure and functionality, cellulases can be categorized as endocellulases, exocellulases, and cellobiases. Endocellulases cleave internal bounds at amorphous sites, and exocellulases are capable of cleaving two to four units from the non-reducing ends of the cellulose polymer. Cellobiase can hydrolyze the exocellulase products into individual monosaccharides (Lynd and Zhang, 2002). In the current study, we did not find a significant pH or rumen sample fraction effect on cellulase expression, implying cellulose transcription was stable in response to pH shifts, and equally distributed in the liquid and solid fractions.

Endo-1,4-beta- xylanase catalyzes the hydrolysis of glycosidic linkages in the xylan backbone (Shallom and Shoham, 2003). It is categorized into CBM1 to 6, 9, 22, 31, 37, 59, 60, and 64; CE1, and 4; and GH 5, 8, 10, 11, and 38. GH10 and GH11 represent the two major

families of endo-1,4-beta- xylanase (Dai et al., 2015). Similar to cellulases, no treatment or sample effects were observed on the expression of endo-1,4-beta- xylanase transcripts.

Amylases are a group of enzymes that hydrolyze glycosidic bonds present in starch. They have been grouped into multiple CBM families and GH13, 14, 15, 31, and 57. Deusch et al. (2017) observed that GH 57 was the most abundant family across all samples. Comtet-Marre et al. (2017) reported amylases represent 20% of total GH. The greater proportion of amylase in the liquid fraction than in the solid fraction suggests that more starch may be degraded in the rumen liquid fraction.

Arabinose units are attached to xylan via alpha-1,2, 1,3, or 1,5 bonds, or linked to the C2 or C3 position on arabinoxylan, and thus segregate into the hemicellulose fraction. Alpha-N-arabinofuranosidase cleaves arabinose from the xylose backbone, thus contributing to the degradation of hemicellulose. Alpha-N-arabinofuranosidases belong to 8 CBM families and 15 GH families. Ruminal pH shifts did not change arabinofuranosidase expression implying that the enzyme activity was not affected by low pH. Zhou et al. (2012) tested the biochemical and kinetic characterization of arabinofuranosidase in GH43 and GH30, and reported that the maximum arabinofuranosidase activity was observed at pH 5.5, with 60% of maximal enzyme activity occuring when the pH ranged from 4.5 to 7.0. Given such broad tolerance to pH, it is perhaps not surprising to find that transcription was not regulated by ruminal pH.

Carbohydrate-active enzymes are generally secreted by microbes into the ruminal fluid. Based on this, one may hypothesize that the distribution of CAZymes expression would be associated with the locations of the microbial community. For example, we observed cellulase celA, putative carbohydrate-active enzyme, amylase, and putative 4-alpha-glucanotransferase were more highly expressed in the liquid fraction than in the solid. Conversely, glycoside

hydrolase family 43 was more prevalent in the solid fraction. Correlation analyses indicated that these enzymes were all positively correlated with *Diploplastron*, *CPla-4_termite_group*, *Sporobacter*, and negatively correlated with *Desulfovibrio*, *Candidatus_Saccharimonas*, *Ruminococcus_1*, and *Lachnospiraceae_NK3A20_group*. There was a positive correlation between glycoside hydrolase family 43 and *Desulfovibrio, Family_XIII_AD3011_group* , *Moryella*, *U29-B03, Family_XIII_UCG-001*, *Olsenella*, *Ruminococcaceae_UCG-004*, *Butyrivibrio_2*, *Saccharofermentans*, and a negative correlation with *Sporobacter*, *Anaeromusa*, and *Diploplastron.* The composition of all of these microbes differed between the liquid and solid fractions in the rumen which coincided with the enzyme expression patterns. Thus our hypothesis of colocalization of microbes possessing genes for specific enzymes and the expression of such enzyme transcripts was supported.

Ruminal pH Effect on Expressions of CAZymes in the Rumen

Ruminal pH could affect CAZymes expression via a shift in microbial abundance or a shift in transcripts expressed by the same microbes. In this study, the expression of rhamnogalacturonan acetylesterase, glucan phosphorylase, and pectate lyase/amb allergen were upregulated in association with decreased ruminal pH.

Rhamnogalacturonan acetylesterase is responsible for a deacetylation of rhamnogalacturoan (Mølgaard et al., 2000). It has been cloned and expressed in the fungus *Aspergillus oryzae* and found to have an optimum pH of 6.0 (Kauppinen et al., 1995). Glucan phosphorylase was positively correlated with *Cyllamyces*, *Desulfovibrio*, *Tritrichomonas*, *Flexilinea*, *Foaina*, *Olsenella*, *Treponema_2*, *Papillibacter*, *Family_XIII_UCG-001*, and *U29-B03*. Potentially, all these microbes might have contributed to the increased glucan phosphorylase. Proportions of *Cyllamyces* and *Papillibacter* increased with decreased ruminal pH, but the remainder were not significantly affected by pH. Thus these 2 microbes may be the

main contributors to upregulation of glucan phosphorylase transcription in response to decreased pH.

Pectate lyase/amb allergen is classified as a polysaccharide lyase, and is responsible for the eliminative cleavage of pectate. Pectin is a compound in grass cell walls, containing linear alpha-1,4-linked D galacturonic acid residues plus other sugars (Somerville et al., 2004), which is fermented at a faster rate and greater extent compared to hemicellulose and cellulose (Chesson and Monro, 1982). Pectate lyase/amb allergen was positively correlated with *Bifidobacterium*, *Papillibacter*, *Pyrami dobacter*, and *Flexilinea*. There was a positive correlation between pectate lyase/amb allergen and *Papillibacter*, suggesting the increased *Papillibacter* might be responsible for the upregulated pectate lyase/amb allergen. *Papillibacter cinnamivorans* was isolated from an anaerobic digester fed with shea cake rich in tannins and aromatic compounds, which can transform cinnamate by degrading the aliphatic side chain to produce acetate (Defnoun et al., 2000), implying *Papillibacter* was correlated with lignin degradation and acetate production.

Nutritional Consequence of Low pH Regulation

Low ruminal pH for prolonged periods negatively affected DMI, fiber degradation, and SCFA concentrations, which agreed with previous studies (Russell and Rychlik, 2001; Sung et al., 2007; Calsamiglia et al., 2008; Hook et al., 2011; Dijkstra et al., 2012). Sung et al. (2007) found that ruminal pH modulated fiber digestion through an effect on bacteria attachment to fiber substrates. Russell and Wilson (1996) indicated low intracellular pH inhibited the cellular metabolism of substrates. In this study, we investigated the direct effects of CAZymes on fiber degradation and SCFA concentrations. Surprisingly, the expression of pectate lyase/amb allergen was negatively correlated with the in situ degradation rate of hemicellulose, cellulose, and lignin, and ruminal SCFA concentrations.

We observed there was a positive correlation between lignin degradation rate and cellulase celA, alpha-glucosidase, and putative carbohydrate-active enzyme, suggesting these enzymes might have contributed to release of lignin from the fiber matrix in the rumen. Zverlov et al. (1998) indicated cellulase celA exhibited significant activity towards microcrystalline cellulose, and it was most active towards soluble substrates such as CM-cellulose and beta-glucan.

Ruminococcus flavefaciens and the fugus *Neocallimastix patriciarum* have been reported to express cellulase celA (Whitehead and Flint, 1995; Ekinci et al., 2002). The abundance of the protozoal genera *Eremoplastron, Dasytricha, Diploplastron,* and bacterial genera *Anaeromusa, Clostridium_sensu_stricto_1, Sporobacter, Tyzzerella_3, Candidatus_Endomicrobium,* and *CPla-4_termite_group* were positively correlated with transcript expression of cellulase celA, alpha-glucosidase, and putative carbohydrate-active enzyme, implying these microbes were potentially responsible for lignin solubilization in the rumen.

Dietary carbohydrates including hemicellulose, cellulose, and starch, are the primary fermentation substrates in the rumen. They are degraded to hexoses and pentoses, and fermented to SCFA via pyruvate. Ruminal SCFA concentrations reflect the balance between the rate of production and rate of absorption. Previous studies indicated SCFA concentrations are reliable indexes for the relative production rates (Sutton et al., 2003; Nolan et al., 2014), although the manipulation of pH independent of SCFA production in the current study may have partially delinked production and concentrations due to potential stimulation of transport activity.

France and Dijkstra (2005) hypothesized that fermentation patterns are determined by the composition of the microbial population which is driven by substrate composition. This implies that microbes have little adaptability within a family. Regardless of whether fermentation shifts

due to a change in microbial structure or due to a change in the expression patterns of a constant structure, characterization of the transcriptome should provide insight into the pathways being used and the microbes expressing those genes.

We observed a positive correlation between hemicellulose degradation rate and acetate and propionate concentrations, and a positive correlation between cellulose degradation rate and butyrate and valerate concentrations. These results support the concept of substrate availability defining fermentation patterns leading to variable SCFA profiles. These SCFA profiles was consistent with the stoichiometric yield pattern estimated by analysis of a large number of in vivo observations (Murphy et al., 1982).

Regression results indicated endo-1,4-xylanase / ferulic acid esterase, galacturan 1,4-alpha-galacturonidase, glucuronan lyase, glycogen synthase-like protein, glycosyl hydrolase family 16, glycosyl hydrolase family 31, glycosyltransferase group 1 family, and maltopentaose-forming amylase were the key enzymes regulating SCFA production rates in the rumen. Considering these enzymes in the regression model explained 70 to 90% of the variance for SCFA concentrations, which was significantly better than an empirical model lacking representations of enzyme activity (Li et al., 2018b). Endo-1,4-xylanase / ferulic acid esterase, glucuronan lyase, glycosyl hydrolase family 16, and glycosyl hydrolase family 31 are enzymes responsible for hydrolyzing xylan, hemicellulose, cellulose, lignin, and pectin as reported by previous studies (Shallom and Shoham, 2003; Brulc et al., 2009). Therefore, the positive correlation between these enzymes and individual SCFA concentrations could be explained by the enzyme activities.

Galacturan 1,4-alpha-galacturonidase, glycogen synthase-like protein, and maltopentaose-forming amylase were negatively correlated with SCFA concentrations.

Galacturan 1,4-alpha-galacturonidase catalyzes 1,4-alpha-D-falacturonide to generate glucuronate and participates in pentose and glucuronate interconversions (Hasegawa and Nagel, 1968). Beaud et al. (2005) indicated that beta-glucuronidase was responsible for the generation of toxic and carcinogenic metabolites in the large intestines by the hydrolysis of the glucuronides. The presence of galacturan 1,4-alpha-galacturonidase might inhibit SCFA production leading to a negative correlation with acetate and valerate concentrations.

Glycogen synthase-like protein participates in glycogenesis and the conversion of glucose into glycogen (Buschiazzo et al., 2004), while propionate is the main substrate for gluconeogenesis. The negative correlation between glycogen synthase-like protein and propionate concentrations was consistent with their biological functions.

Maltopentaose-forming amylase leads to the production of maltotetraose instead of glucose hydrolysis (Li et al., 2015), which was in line with the negative correlation between maltopentaose-forming amylase and acetate, propionate, isobutyrate, and valerate concentrations.

Conclusions

In the study, we investigated the distribution and functional characteristics of the active microbial community in the rumen through metatranscriptomic and compositional data analyses. In total, 19 bacterial phyla with 121 genera, 3 archaeal genera, 26 protozoal genera, and 97 CAZymes were identified in the rumen. Within these, 4 bacteria phyla (*Proteobacteria*, *Firmicutes*, *Bacteroidetes*, and *Spirochaetes*), 2 archaeal genera (*Candidatus_Methanomethylophilus* and *Methanobrevibacter*), and 5 protozoal genera (*Entodinium*, *Polyplastron*, *Isotricha*, *Eudiplodinium*, and *Eremoplastron*) were considered as the core active microbes, and cellulase, endo-1,4-beta- xylanase, amylase, and alpha-N-arabinofuranosidase were the most abundant CAZymes distributed in the rumen.

Both ruminal pH and There were significant differences in the microbial ecosystem between the liquid and solid fractions of the ruminal contents, and ruminal pH affected the ecosystem. 19 bacterial genera and 4 protozoal genera were affected by low ruminal pH, and 30 bacterial genera, 1 archaeal genus, and 7 protozoal genera exhibited different proportions between ruminal liquid and solid fractions**.** Their interactions indicated microbes exhibited different acid resistance in the liquid and solid fraction, due to the existing pH gradient. Low ruminal pH altered different bacterial taxa compared to feeding high grain diets in the previous studies, implying different mechanism or contributions to changing microbial activity.

The ruminal microbiome changed the expression of transcripts for biochemical pathways in response to reduced pH, and at least a portion of the shifts in enzyme transcripts was associated with altered microbial structure. The prevalence of 54 microbes, including 43 bacterial and 11 protozoal genera was correlated with expression levels of 25 CAZymes, which could help interpret microbial functionality in future studies. Regression analyses results indicated endo-1,4-xylanase / ferulic acid esterase, galacturan 1,4-alpha-galacturonidase, glucuronan lyase, glycogen synthase-like protein, glycosyl hydrolase family 16, glycosyl hydrolase family 31, glycosyltransferase group 1 family, and maltopentaose-forming amylase were the key enzymes to regulate SCFA production rates in the rumen. Considering enzyme functions in the linear model largely increased the accuracy to predict SCFA concentrations.

Acknowledgements

This work was supported by the Virginia Agricultural Council: the USDA National Institute of Food and Agriculture, Hatch project NC-2040; and the College of Agriculture and Life Sciences Pratt Endowment at Virginia Tech.

Compliance with ethical standards

The authors declare that they have no conflict of interest.

References

Abrar, A., H. Watanabe, T. Kitamura, M. Kondo, T. Ban‐Tokuda, and H. Matsui. 2016. Diversity and fluctuation in ciliate protozoan population in the rumen of cattle. Animal Science Journal 87(9):1188-1192.

Aitchison, J. 1982. The statistical analysis of compositional data. Journal of the Royal Statistical Society. Series B (Methodological):139-177.

Akkada, A. A. and B. Howard. 1960. The biochemistry of rumen protozoa. 3. The carbohydrate metabolism of Entodinium. Biochemical Journal 76(3):445.

Allen, M. S. 1997. Relationship between fermentation acid production in the rumen and the requirement for physically effective fiber. J Dairy Sci 80(7):1447-1462.

AOAC. 1997. Official Methods of Analysis, 16th edition. Association of Official Analytical Chemists, Gaithersburg, MD.

Apelo, S. A., J. Knapp, and M. Hanigan. 2014. Invited review: Current representation and future trends of predicting amino acid utilization in the lactating dairy cow. J Dairy Sci 97(7):4000-4017.

Archibeque, S., J. Burns, and G. Huntington. 2001. Urea flux in beef steers: effects of forage species and nitrogen fertilization. Journal of animal science 79(7):1937-1943.

Archibeque, S., J. Burns, and G. Huntington. 2002. Nitrogen metabolism of beef steers fed endophyte-free tall fescue hay: effects of ruminally protected methionine supplementation. Journal of animal science 80(5):1344-1351.

Argyle, J. and R. Baldwin. 1988. Modeling of rumen water kinetics and effects of rumen pH changes. J Dairy Sci 71(5):1178-1188.

Arndt, C., J. Powell, M. Aguerre, P. Crump, and M. Wattiaux. 2015. Feed conversion efficiency in dairy cows: Repeatability, variation in digestion and metabolism of energy and nitrogen, and ruminal methanogens. J Dairy Sci 98(6):3938-3950.

Bach, A., S. Calsamiglia, and M. Stern. 2005. Nitrogen metabolism in the rumen. J Dairy Sci 88:E9-E21.

Bailey, E., E. Titgemeyer, K. Olson, D. Brake, M. Jones, and D. Anderson. 2012a. Effects of ruminal casein and glucose on forage digestion and urea kinetics in beef cattle. Journal of animal science 90(10):3505-3514.

Bailey, E., E. Titgemeyer, K. Olson, D. Brake, M. Jones, and D. Anderson. 2012b. Effects of supplemental energy and protein on forage digestion and urea kinetics in growing beef cattle. Journal of animal science 90(10):3492-3504.

Baldwin, R. 1995. Modeling ruminant digestion and metabolism. Springer Science & Business Media.

Baldwin, R. L., J. France, D. E. Beever, M. Gill, and J. H. Thornley. 1987a. Metabolism of the lactating cow: III. Properties of mechanistic models suitable for evaluation of energetic relationships and factors involved in the partition of nutrients. Journal of Dairy Research 54(01):133-145.

Baldwin, R. L., J. France, and M. Gill. 1987b. Metabolism of the lactating cow: I. Animal elements of a mechanistic model. Journal of Dairy Research 54(01):77-105.

Baldwin, R. L., J. H. Thornley, and D. E. Beever. 1987c. Metabolism of the lactating cow: II. Digestive elements of a mechanistic model. Journal of Dairy Research 54(01):107-131.

Bates, D., M. Mächler, B. Bolker, and S. Walker. 2014. Fitting linear mixed-effects models using lme4. arXiv preprint arXiv:1406.5823.

Batista, E., E. Detmann, E. C. Titgemeyer, S. Valadares Filho, R. Valadares, L. Prates, L. Rennó, and M. Paulino. 2016. Effects of varying ruminally undegradable protein supplementation on forage digestion, nitrogen metabolism, and urea kinetics in Nellore cattle fed low-quality tropical forage. Journal of animal science 94(1):201-216.

Beaud, D., P. Tailliez, and J. Anba-Mondoloni. 2005. Genetic characterization of the β-glucuronidase enzyme from a human intestinal bacterium, Ruminococcus gnavus. Microbiology 151(7):2323-2330.

Bibby, J. and H. Toutenburg. 1977. Prediction and improved estimation in linear models. Wiley.

Bjork, R. A. 1973. Why mathematical models? American Psychologist 28(5):426.

Boardman, T. J. 1979. Prediction and improved estimation in linear models. Taylor & Francis.

Bolger, A. M., M. Lohse, and B. Usadel. 2014. Trimmomatic: a flexible trimmer for Illumina sequence data. Bioinformatics 30(15):2114-2120.

Boraston, A. B., D. N. Bolam, H. J. Gilbert, and G. J. Davies. 2004. Carbohydrate-binding modules: fine-tuning polysaccharide recognition. Biochemical Journal 382(3):769-781.

Brake, D., E. Titgemeyer, and M. Jones. 2011. Effect of nitrogen supplementation and zilpaterol–HCl on urea kinetics in steers consuming corn‐based diets. Journal of animal physiology and animal nutrition 95(4):409-416.

Brake, D., E. Titgemeyer, M. Jones, and D. Anderson. 2010. Effect of nitrogen supplementation on urea kinetics and microbial use of recycled urea in steers consuming corn-based diets1. Journal of animal science 88(8):2729-2740.

Briggs, P., J. Hogan, and R. Reid. 1957. Effect of volatile fatty acids, lactic acid and ammonia on rumen pH in sheep. Crop and Pasture Science 8(6):674-690.

Brulc, J. M., D. A. Antonopoulos, M. E. B. Miller, M. K. Wilson, A. C. Yannarell, E. A. Dinsdale, R. E. Edwards, E. D. Frank, J. B. Emerson, and P. Wacklin. 2009. Gene-centric metagenomics of the fiber-adherent bovine rumen microbiome reveals forage specific glycoside hydrolases. Proceedings of the National Academy of Sciences:pnas. 0806191105.

Burge, S. W., J. Daub, R. Eberhardt, J. Tate, L. Barquist, E. P. Nawrocki, S. R. Eddy, P. P. Gardner, and A. Bateman. 2012. Rfam 11.0: 10 years of RNA families. Nucleic acids research 41(D1):D226-D232.

Buschiazzo, A., J. E. Ugalde, M. E. Guerin, W. Shepard, R. A. Ugalde, and P. M. Alzari. 2004. Crystal structure of glycogen synthase: homologous enzymes catalyze glycogen synthesis and degradation. The EMBO journal 23(16):3196-3205.

Callahan, B. J., P. J. McMurdie, M. J. Rosen, A. W. Han, A. J. A. Johnson, and S. P. Holmes. 2016. DADA2: high-resolution sample inference from Illumina amplicon data. Nature methods 13(7):581.

Calsamiglia, S., P. Cardozo, A. Ferret, and A. Bach. 2008. Changes in rumen microbial fermentation are due to a combined effect of type of diet and pH. Journal of animal science 86(3):702-711.

Cameron, M., T. Klusmeyer, G. Lynch, J. Clark, and D. Nelson. 1991. Effects of urea and starch on rumen fermentation, nutrient passage to the duodenum, and performance of cows1. J Dairy Sci 74(4):1321-1336.

Campbell, J. A., G. J. Davies, V. Bulone, and B. Henrissat. 1997. A classification of nucleotide-diphospho-sugar glycosyltransferases based on amino acid sequence similarities. Biochemical Journal 326(Pt 3):929.

Cecava, M., N. Merchen, L. Berger, R. Mackie, and G. Fahey. 1991. Effects of dietary energy level and protein source on nutrient digestion and ruminal nitrogen metabolism in steers. Journal of animal science 69(5):2230-2243.

Chan, S., J. Huber, C. Theurer, Z. Wu, K. Chen, and J. Simas. 1997. Effects of supplemental fat and protein source on ruminal fermentation and nutrient flow to the duodenum in dairy cows. J Dairy Sci 80(1):152-159.

Channon, A., J. Rowe, and R. Herd. 2004. Genetic variation in starch digestion in feedlot cattle and its association with residual feed intake. Australian Journal of Experimental Agriculture 44(5):469-474.

Chesson, A. and J. A. Monro. 1982. Legume pectic substances and their degradation in the ovine rumen. Journal of the Science of Food and Agriculture 33(9):852-859.

Clauss, M., A. Schwarm, S. Ortmann, W. J. Streich, and J. Hummel. 2007. A case of non-scaling in mammalian physiology? Body size, digestive capacity, food intake, and ingesta passage in mammalian herbivores. Comparative Biochemistry and Physiology Part A: Molecular & Integrative Physiology 148(2):249-265.

Coleman, G. 1969. The metabolism of starch, maltose, glucose and some other sugars by the rumen ciliate Entodinium caudatum. Microbiology 57(3):303-332.

Comtet-Marre, S., N. Parisot, P. Lepercq, F. Chaucheyras-Durand, P. Mosoni, E. Peyretaillade, A. R. Bayat, K. J. Shingfield, P. Peyret, and E. Forano. 2017. Metatranscriptomics reveals the active bacterial and eukaryotic fibrolytic communities in the rumen of dairy cow fed a mixed diet. Frontiers in microbiology 8:67.

Coutinho, P. M., E. Deleury, G. J. Davies, and B. Henrissat. 2003. An evolving hierarchical family classification for glycosyltransferases. Journal of molecular biology 328(2):307-317.

Craney, T. A. and J. G. Surles. 2002. Model-dependent variance inflation factor cutoff values. Quality Engineering 14(3):391-403.

Dai, X., Y. Tian, J. Li, X. Su, X. Wang, S. Zhao, L. Liu, Y. Luo, D. Liu, and H. Zheng. 2015. Metatranscriptomic analyses of plant cell wall polysaccharide degradation by microorganisms in the cow rumen. Appl. Environ. Microbiol. 81(4):1375-1386.

Davies, G. and B. Henrissat. 1995. Structures and mechanisms of glycosyl hydrolases. Structure 3(9):853-859.

Davies, K., J. McKinnon, and T. Mutsvangwa. 2013. Effects of dietary ruminally degradable starch and ruminally degradable protein levels on urea recycling, microbial protein production, nitrogen balance, and duodenal nutrient flow in beef heifers fed low crude protein diets. Canadian journal of animal science 93(1):123-136.

De Menezes, A. B., E. Lewis, M. O'Donovan, B. F. O'Neill, N. Clipson, and E. M. Doyle. 2011. Microbiome analysis of dairy cows fed pasture or total mixed ration diets. FEMS Microbiology Ecology 78(2):256-265.

De Mulder, T., K. Goossens, N. Peiren, L. Vandaele, A. Haegeman, C. De Tender, T. Ruttink, T. V. de Wiele, and S. De Campeneere. 2017. Exploring the methanogen and bacterial communities of rumen environments: solid adherent, fluid and epimural. FEMS Microbiology Ecology 93(3).

Defnoun, S., M. Labat, M. Ambrosio, J.-L. Garcia, and B. Patel. 2000. Papillibacter cinnamivorans gen. nov., sp. nov., a cinnamate-transforming bacterium from a shea cake digester. International journal of systematic and evolutionary microbiology 50(3):1221-1228.

Deusch, S., A. Camarinha-Silva, J. Conrad, U. Beifuss, M. Rodehutscord, and J. Seifert. 2017. A structural and functional elucidation of the rumen microbiome influenced by various diets and microenvironments. Frontiers in microbiology 8:1605.

Dijkstra, J. 1993. Mathematical modelling and integration of rumen fermentation processes. Dijkstra.

Dijkstra, J., H. Boer, J. Van Bruchem, M. Bruining, and S. Tamminga. 1993. Absorption of volatile fatty acids from the rumen of lactating dairy cows as influenced by volatile fatty acid concentration, pH and rumen liquid volume. British Journal of Nutrition 69(2):385-396.

Dijkstra, J., J. Ellis, E. Kebreab, A. Strathe, S. López, J. France, and A. Bannink. 2012. Ruminal pH regulation and nutritional consequences of low pH. Animal Feed Science and Technology 172(1-2):22-33.

Donkoh, A. and P. Moughan. 1994. The effect of dietary crude protein content on apparent and true ileal nitrogen and amino acid digestibilities. British Journal of Nutrition 72(1):59-68.

Dumas, A., J. Dijkstra, and J. France. 2008. Mathematical modelling in animal nutrition: a centenary review. The Journal of Agricultural Science 146(2):123-142.

Edgar, R. C. 2010. Search and clustering orders of magnitude faster than BLAST. Bioinformatics 26(19):2460-2461.

Ekinci, M. S., J. C. Martin, and H. J. Flint. 2002. Expression of a cellulase gene, celA, from the rumen fungus Neocallimastix patriciarum in Streptococcus bovis by means of promoter fusions. Biotechnology letters 24(9):735-741.

Ellis, J., J. Dijkstra, A. Bannink, E. Kebreab, S. Archibeque, C. Benchaar, K. Beauchemin, J. Nkrumah, and J. France. 2014. Improving the prediction of methane production and representation of rumen fermentation for finishing beef cattle within a mechanistic model. Canadian journal of animal science 94(3):509-524.

Ellis, J., E. Kebreab, N. Odongo, B. McBride, E. Okine, and J. France. 2007. Prediction of methane production from dairy and beef cattle. J Dairy Sci 90(7):3456-3466.

Elsik, C. G., R. L. Tellam, and K. C. Worley. 2009. The genome sequence of taurine cattle: a window to ruminant biology and evolution. Science 324(5926):522-528.

Endres, M. and M. Stern. 1993. Effects of pH and diets containing various levels of lignosulfonate-treated soybean meal on microbial fermentation in continuous culture. J. Dairy Sci 76(Suppl 1):177.

Eriksson, L. and M. Valtonen. 1982. Renal urea handling in goats fed high and low protein diets. J Dairy Sci 65(3):385-389.

Fernandes, A. D., J. N. Reid, J. M. Macklaim, T. A. McMurrough, D. R. Edgell, and G. B. Gloor. 2014. Unifying the analysis of high-throughput sequencing datasets: characterizing RNA-seq, 16S rRNA gene sequencing and selective growth experiments by compositional data analysis. Microbiome 2(1):15.

Firkins, J., M. Eastridge, N. St-Pierre, and S. Noftsger. 2001. Effects of grain variability and processing on starch utilization by lactating dairy cattle. Journal of animal science 79(suppl_E):E218-E238.

Firkins, J. and C. Reynolds. 2005. Whole animal nitrogen balance in cattle. Nitrogen and phosphorus nutrition of cattle: reducing the environmental impact of cattle operations'.(Eds E Pfeffer, A Hristov) pp:167-186.

Fox, D., C. Sniffen, J. O'connor, J. Russell, and P. Van Soest. 1992. A net carbohydrate and protein system for evaluating cattle diets: III. Cattle requirements and diet adequacy. Journal of animal science 70(11):3578-3596.

France, J. and J. Dijkstra. 2005. Volatile fatty acid production. Quantitative aspects of ruminant digestion and metabolism 2:157-175.

Franzolin, R. and B. Dehority. 1996. Effect of prolonged high-concentrate feeding on ruminal protozoa concentrations. Journal of animal science 74(11):2803-2809.

Franzolin, R. and A.-D. G. Wright. 2016. Microorganisms in the rumen and reticulum of buffalo (Bubalus bubalis) fed two different feeding systems. BMC research notes 9(1):243.

Furuya, S. and Y. Kaji. 1989. Estimation of the true ileal digestibility of amino acids and nitrogen from their apparent values for growing pigs. Animal Feed Science and Technology 26(3-4):271-285.

Gabriel, I., M. Lessire, H. Juin, J. Burstin, G. Duc, L. Quillien, J. Thibault, M. Leconte, J. Hallouis, and P. Ganier. 2008. Variation in seed protein digestion of different pea (Pisum sativum L.) genotypes by cecectomized broiler chickens: 1. Endogenous amino acid losses, true digestibility and in vitro hydrolysis of proteins. Livestock Science 113(2-3):251-261.

Galyean, M., D. Wagner, and F. Owens. 1981. Dry matter and starch disappearance of corn and sorghum as influenced by particle size and processing. J Dairy Sci 64(9):1804-1812.

Ghimire, S., P. Gregorini, and M. D. Hanigan. 2014. Evaluation of predictions of volatile fatty acid production rates by the Molly cow model. J Dairy Sci 97(1):354-362.

Gloor, G. B., J. M. Macklaim, V. Pawlowsky-Glahn, and J. J. Egozcue. 2017. Microbiome datasets are compositional: and this is not optional. Frontiers in microbiology 8:2224.

Gloor, G. B. and G. Reid. 2016. Compositional analysis: a valid approach to analyze microbiome high-throughput sequencing data. Canadian journal of microbiology 62(8):692-703.

Godwin, I. and V. Williams. 1984. Renal control of plasma urea level in sheep: The diuretic effect of urea, potassium and sodium chloride. Experimental Physiology 69(1):49-59.

Gonda, H. L. and J. E. Lindberg. 1994. Evaluation of dietary nitrogen utilization in dairy cows based on urea concentrations in blood, urine and milk, and on urinary concentration of purine derivatives. Acta Agriculturae Scandinavica A-Animal Sciences 44(4):236-245.

Gregorini, P., P. Beukes, G. Waghorn, D. Pacheco, and M. Hanigan. 2015. Development of an improved representation of rumen digesta outflow in a mechanistic and dynamic model of a dairy cow, Molly. Ecological Modelling 313:293-306.

Griswold, K., G. Apgar, J. Bouton, and J. Firkins. 2003. Effects of urea infusion and ruminal degradable protein concentration on microbial growth, digestibility, and fermentation in continuous culture 1. Journal of animal science 81(1):329-336.

Güllert, S., M. A. Fischer, D. Turaev, B. Noebauer, N. Ilmberger, B. Wemheuer, M. Alawi, T. Rattei, R. Daniel, and R. A. Schmitz. 2016. Deep metagenome and metatranscriptome analyses of microbial communities affiliated with an industrial biogas fermenter, a cow rumen, and elephant feces reveal major differences in carbohydrate hydrolysis strategies. Biotechnology for biofuels 9(1):121.

Hanigan, M. 2005. Quantitative aspects of ruminant predicting animal performance. Animal Science 80(01):23-32.

Hanigan, M., H. Bateman, J. Fadel, and J. McNamara. 2006. Metabolic models of ruminant metabolism: recent improvements and current status. J Dairy Sci 89:E52-E64.

Hanigan, M., L. Crompton, C. Reynolds, D. Wray-Cahen, M. Lomax, and J. France. 2004. An integrative model of amino acid metabolism in the liver of the lactating dairy cow. Journal of theoretical biology 228(2):271-289.

Hanigan, M. D., J. A. Appuhamy, and P. Gregorini. 2013. Revised digestive parameter estimates for the Molly cow model. J Dairy Sci 96(6):3867-3885.

Hanigan, M. D., C. C. Palliser, and P. Gregorini. 2009a. Altering the representation of hormones and adding consideration of gestational metabolism in a metabolic cow model reduced prediction errors. Journal of Dairy Science 92(10):5043-5056.

Hanigan, M. D., C. C. Palliser, and P. Gregorini. 2009b. Altering the representation of hormones and adding consideration of gestational metabolism in a metabolic cow model reduced prediction errors. J Dairy Sci 92(10):5043-5056.

Hanigan, M. D., A. G. Rius, E. S. Kolver, and C. C. Palliser. 2007. A redefinition of the representation of mammary cells and enzyme activities in a lactating dairy cow model. J Dairy Sci 90(8):3816-3830.

Hasegawa, S. and C. Nagel. 1968. Isolation of an oligogalacturonate hydrolase from a Bacillus specie. Archives of biochemistry and biophysics 124:513-520.

Hawinkel, S., F. Mattiello, L. Bijnens, and O. Thas. 2017. A broken promise: microbiome differential abundance methods do not control the false discovery rate. Briefings in bioinformatics.

Henderson, G., F. Cox, S. Ganesh, A. Jonker, W. Young, G. R. C. Collaborators, L. Abecia, E. Angarita, P. Aravena, and G. N. Arenas. 2015. Rumen microbial community composition varies with diet and host, but a core microbiome is found across a wide geographical range. Scientific reports 5:14567.

Henderson, G., F. Cox, S. Kittelmann, V. H. Miri, M. Zethof, S. J. Noel, G. C. Waghorn, and P. H. Janssen. 2013. Effect of DNA extraction methods and sampling techniques on the apparent structure of cow and sheep rumen microbial communities. PloS one 8(9):e74787.

Henrissat, B. 1991. A classification of glycosyl hydrolases based on amino acid sequence similarities. Biochemical Journal 280(2):309-316.

Henrissat, B. and A. Bairoch. 1993. New families in the classification of glycosyl hydrolases based on amino acid sequence similarities. Biochemical Journal 293(3):781-788.

Henrissat, B. and A. Bairoch. 1996. Updating the sequence-based classification of glycosyl hydrolases. Biochemical Journal 316(Pt 2):695.

Henrissat, B. and G. Davies. 1997. Structural and sequence-based classification of glycoside hydrolases. Current opinion in structural biology 7(5):637-644.

Hess, V., P. Ganier, J.-N. Thibault, and B. Seve. 2000. Comparison of the isotope dilution method for determination of the ileal endogenous amino acid losses with labelled diet and labelled pigs. British Journal of Nutrition 83(2):123-130.

Holder, V., J. Tricarico, D. Kim, N. Kristensen, and D. Harmon. 2015. The effects of degradable nitrogen level and slow release urea on nitrogen balance and urea kinetics in Holstein steers. Animal Feed Science and Technology 200:57-65.

Hollmann, M., M. Allen, and D. Beede. 2011. Dietary protein quality and quantity affect lactational responses to corn distillers grains: A meta-analysis. J Dairy Sci 94(4):2022-2030.

Hook, S. E., M. A. Steele, K. S. Northwood, A.-D. G. Wright, and B. W. McBride. 2011. Impact of high-concentrate feeding and low ruminal pH on methanogens and protozoa in the rumen of dairy cows. Microbial ecology 62(1):94-105.

Huang, K., V. Ravindran, X. Li, and W. Bryden. 2005. Influence of age on the apparent ileal amino acid digestibility of feed ingredients for broiler chickens. British poultry science 46(2):236-245.

Huhtanen, P., S. Ahvenjärvi, G. Broderick, S. Reynal, and K. Shingfield. 2010. Quantifying ruminal digestion of organic matter and neutral detergent fiber using the omasal sampling technique in cattle—A meta-analysis1. J Dairy Sci 93(7):3203-3215.

Huhtanen, P. and A. Hristov. 2009. A meta-analysis of the effects of dietary protein concentration and degradability on milk protein yield and milk N efficiency in dairy cows. J Dairy Sci 92(7):3222-3232.

Huntington, G. and S. Archibeque. 2000. Practical aspects of urea and ammonia metabolism in ruminants. Journal of animal science 77(E-Suppl):1-11.

Huo, W., W. Zhu, and S. Mao. 2014. Impact of subacute ruminal acidosis on the diversity of liquid and solid-associated bacteria in the rumen of goats. World Journal of Microbiology and Biotechnology 30(2):669-680.

Jami, E. and I. Mizrahi. 2012. Composition and similarity of bovine rumen microbiota across individual animals. PloS one 7(3):e33306.

Joblin, K., G. Naylor, and A. Williams. 1990. Effect of Methanobrevibacter smithii on xylanolytic activity of anaerobic ruminal fungi. Applied and environmental microbiology 56(8):2287-2295.

Johnson, H. A. and R. L. Baldwin. 2008. Evaluating model predictions of partitioning nitrogen excretion using the dairy cow model, Molly. Animal Feed Science and Technology 143(1-4):104-126.

Kang, S., P. Evans, M. Morrison, and C. McSweeney. 2013. Identification of metabolically active proteobacterial and archaeal communities in the rumen by DNA-and RNA-derived 16 S rRNA gene. Journal of applied microbiology 115(3):644-653.

Kauppinen, S., S. Christgau, L. V. Kofod, T. Halkier, K. Dörreich, and H. Dalbøge. 1995. Molecular Cloning and Characterization of a Rhamnogalacturonan Acetylesterase from Aspergillus aculeatus SYNERGISM BETWEEN RHAMNOGALACTURONAN DEGRADING ENZYMES. Journal of Biological Chemistry 270(45):27172-27178.

Kim, D., G. Pertea, C. Trapnell, H. Pimentel, R. Kelley, and S. L. Salzberg. 2013. TopHat2: accurate alignment of transcriptomes in the presence of insertions, deletions and gene fusions. Genome biology 14(4):R36.

Kohn, R. and M. Allen. 1995. In vitro protein degradation of feeds using concentrated enzymes extracted from rumen contents. Animal Feed Science and Technology 52(1-2):15-28.

Kononoff, P. and A. Heinrichs. 2003. The effect of corn silage particle size and cottonseed hulls on cows in early lactation. J Dairy Sci 86(7):2438-2451.

Kononoff, P., A. Heinrichs, and H. Lehman. 2003. The effect of corn silage particle size on eating behavior, chewing activities, and rumen fermentation in lactating dairy cows. J Dairy Sci 86(10):3343-3353.

Kopylova, E., L. Noé, and H. Touzet. 2012. SortMeRNA: fast and accurate filtering of ribosomal RNAs in metatranscriptomic data. Bioinformatics 28(24):3211-3217.

Kristensen, N. B. 2000. Quantification of whole blood short-chain fatty acids by gas chromatographic determination of plasma 2-chloroethyl derivatives and correction for dilution space in erythrocytes. Acta Agriculturae Scandinavica, Section A-Animal Science 50(4):231-236.

Lane, G., C. Noller, V. Colenbrander, K. Cummings, and R. Harrington. 1968. Apparatus for Obtaining Ruminoreticular Samples and the Effect of Sampling Location on pH and Volatile Fatty Acids1. J Dairy Sci 51(1):114-116.

Lapierre, H., R. Berthiaume, G. Raggio, M. Thivierge, L. Doepel, D. Pacheco, P. Dubreuil, and G. Lobley. 2005. The route of absorbed nitrogen into milk protein. Animal Science 80(1):11-22.

Lapierre, H. and G. Lobley. 2001. Nitrogen recycling in the ruminant: A review. J Dairy Sci 84:E223-E236.

Lawrence, I. and K. Lin. 1989. A concordance correlation coefficient to evaluate reproducibility. Biometrics:255-268.

Leduc, M., M.-P. Létourneau-Montminy, R. Gervais, and P. Chouinard. 2017. Effect of dietary flax seed and oil on milk yield, gross composition, and fatty acid profile in dairy cows: A meta-analysis and meta-regression. J Dairy Sci 100(11):8906-8927.

Legay-Carmier, F. and D. Bauchart. 1989. Distribution of bacteria in the rumen contents of dairy cows given a diet supplemented with soya-bean oil. British Journal of Nutrition 61(3):725-740.

Leng, R. 2011. The rumen–a fermentation vat or a series of organized structured microbial consortia: implications for the mitigation of enteric methane production by feed additives. Livestock Research for Rural Development 23:Article# 258.

Li, F. 2017. Metatranscriptomic profiling reveals linkages between the active rumen microbiome and feed efficiency in beef cattle. Applied and environmental microbiology:AEM. 00061-00017.

Li, H. 2015. Microbiome, metagenomics, and high-dimensional compositional data analysis. Annual Review of Statistics and Its Application 2:73-94.

Li, M. M., R. R. White, and M. D. Hanigan. 2018a. An evaluation of Molly cow model predictions of ruminal metabolism and nutrient digestion for dairy and beef diets. J Dairy Sci 101(11):9747-9767.

Li, M. M., R. R. White, and M. D. Hanigan. 2018b. An evaluation of Molly cow model predictions of ruminal metabolism and nutrient digestion for dairy and beef diets. J Dairy Sci.

Li, Z., J. Wu, B. Zhang, F. Wang, X. Ye, Y. Huang, Q. Huang, and Z. Cui. 2015. Characterization of a novel maltohexaose-forming α-amylase AmyM from Corallococcus sp. strain EGB. Applied and environmental microbiology:AEM. 03934-03914.

Lobley, G., D. Bremner, and G. Zuur. 2000. Effects of diet quality on urea fates in sheep as assessed by refined, non-invasive [15N15N] urea kinetics. British Journal of Nutrition 84(4):459-468.

Lobley, G. and H. Lapierre. 2003. Post-absorptive metabolism of amino acids. PUBLICATION-EUROPEAN ASSOCIATION FOR ANIMAL PRODUCTION 109:737-756.

Lofgreen, G., J. Hull, and K. K. Otagaki. 1962. Estimation of empty body weight of beef cattle. Journal of animal science 21(1):20-24.

Lombard, V., T. Bernard, C. Rancurel, H. Brumer, P. M. Coutinho, and B. Henrissat. 2010. A hierarchical classification of polysaccharide lyases for glycogenomics. Biochemical Journal 432(3):437-444.

Lombard, V., H. Golaconda Ramulu, E. Drula, P. M. Coutinho, and B. Henrissat. 2013. The carbohydrate-active enzymes database (CAZy) in 2013. Nucleic acids research 42(D1):D490-D495.

Lovell, D., V. Pawlowsky-Glahn, J. J. Egozcue, S. Marguerat, and J. Bähler. 2015. Proportionality: a valid alternative to correlation for relative data. PLoS computational biology 11(3):e1004075.

Lynd, L. R. and Y. Zhang. 2002. Quantitative determination of cellulase concentration as distinct from cell concentration in studies of microbial cellulose utilization: analytical framework and methodological approach. Biotechnology and bioengineering 77(4):467-475.

Marini, J. and M. Van Amburgh. 2003. Nitrogen metabolism and recycling in Holstein heifers. Journal of animal science 81(2):545-552.

Marounek, M., S. Bartos, and P. Brezina. 1985. Factors influencing the production of volatile fatty acids from hemicellulose, pectin and starch by mixed culture of rumen microorganisms. Zeitschrift für Tierphysiologie Tierernährung und Futtermittelkunde 53(1-5):50-58.

Maulfair, D., M. Fustini, and A. Heinrichs. 2011. Effect of varying total mixed ration particle size on rumen digesta and fecal particle size and digestibility in lactating dairy cows. J Dairy Sci 94(7):3527-3536.

Maulfair, D. and A. Heinrichs. 2013. Effects of varying forage particle size and fermentable carbohydrates on feed sorting, ruminal fermentation, and milk and component yields of dairy cows. J Dairy Sci 96(5):3085-3097.

McCann, J. C., S. Luan, F. C. Cardoso, H. Derakhshani, E. Khafipour, and J. J. Loor. 2016. Induction of subacute ruminal acidosis affects the ruminal microbiome and epithelium. Frontiers in microbiology 7:701.

McMurdie, P. J. and S. Holmes. 2013. phyloseq: an R package for reproducible interactive analysis and graphics of microbiome census data. PloS one 8(4):e61217.

Mertens, D. 1993. Kinetics of cell wall digestion and passage in ruminants. Forage cell wall structure and digestibility (foragecellwalls):535-570.

Michałowski, T., P. Szczepkowski, and P. Muszyński. 1986. The nutritive factors affecting the growth of the rumen ciliate Diploplastron affine in vitro. Acta Protozool 25:419-426.

Miller-Webster, T. and W. Hoover. 1998. Nutrient analysis of feedstuffs including carbohydrates. Anim. Sci. Report (1).

Mills, J., J. France, and J. Dijkstra. 1999. A review of starch digestion in the lactating dairy cow and proposals for a mechanistic model: 1. Dietary starch characterisation and ruminal starch digestion. J. Anim. Feed Sci 8(3):219-340.

Mills, J., J. France, J. Ellis, L. Crompton, A. Bannink, M. Hanigan, and J. Dijkstra. 2017. A mechanistic model of small intestinal starch digestion and glucose uptake in the cow. J Dairy Sci.

Mølgaard, A., S. Kauppinen, and S. Larsen. 2000. Rhamnogalacturonan acetylesterase elucidates the structure and function of a new family of hydrolases. Structure 8(4):373-383.

Mountfort, D. O., R. A. Asher, and T. Bauchop. 1982. Fermentation of cellulose to methane and carbon dioxide by a rumen anaerobic fungus in a triculture with Methanobrevibacter sp. strain RA1 and Methanosarcina barkeri. Applied and environmental microbiology 44(1):128-134.

Murphy, M., R. Baldwin, and L. Koong. 1982. Estimation of stoichiometric parameters for rumen fermentation of roughage and concentrate diets. Journal of animal science 55(2):411-421.

Myer, P. R., T. P. Smith, J. E. Wells, L. A. Kuehn, and H. C. Freetly. 2015. Rumen microbiome from steers differing in feed efficiency. PloS one 10(6):e0129174.

NFTA. 2006. National forage testing association reference method: dry matter by oven drying for 3 hours at 105 C. NFTA Reference Methods. National Forage Testing Association, Omaha, NB.

Nolan, J. 1975. Quantitative models of nitrogen metabolism in sheep. Digenstion and Metabolism in the Ruminant.

Nolan, J. and R. Leng. 1972. Dynamic aspects of ammonia and urea metabolism in sheep. British Journal of Nutrition 27(1):177-194.

Nolan, J., R. Leng, R. Dobos, and R. Boston. 2014. The production of acetate, propionate and butyrate in the rumen of sheep: fitting models to 14C-or 13C-labelled tracer data to determine synthesis rates and interconversions. Animal Production Science 54(12):2082-2088.

NRC. 2001. Nutrient requirements of dairy cattle. 7th ed. National Academy Press, Washington, D.C. National Research Council.

O'Connor, J., C. Sniffen, D. Fox, and W. Chalupa. 1993. A net carbohydrate and protein system for evaluating cattle diets: IV. Predicting amino acid adequacy. Journal of animal science 71(5):1298-1311.

Ørskov, E. and I. McDonald. 1979. The estimation of protein degradability in the rumen from incubation measurements weighted according to rate of passage. The Journal of Agricultural Science 92(2):499-503.

Palarea-Albaladejo, J. and J. A. Martín-Fernández. 2015. zCompositions—R package for multivariate imputation of left-censored data under a compositional approach. Chemometrics and Intelligent Laboratory Systems 143:85-96.

Parker, D., M. Lomax, C. Seal, and J. Wilton. 1995. Metabolic implications of ammonia production in the ruminant. Proceedings of the Nutrition Society 54(2):549-563.

Petri, R. M., T. Schwaiger, G. B. Penner, K. A. Beauchemin, R. J. Forster, J. J. McKinnon, and T. A. McAllister. 2013. Characterization of the core rumen microbiome in cattle during transition from forage to concentrate as well as during and after an acidotic challenge. PloS one 8(12):e83424.

Pilgrim, A., F. Gray, R. Weller, and C. Belling. 1970. Synthesis of microbial protein from ammonia in the sheep's rumen and the proportion of dietary nitrogen converted into microbial nitrogen. British Journal of Nutrition 24(2):589-598.

Pinheiro, J., D. Bates, S. DebRoy, D. Sarkar, and R. C. Team. 2018. nlme: Linear and nonlinear mixed effects models. R package version version 3.1-137.

Plaizier, J. C., S. Li, A. M. Danscher, H. Derakshani, P. H. Andersen, and E. Khafipour. 2017. Changes in microbiota in rumen digesta and feces due to a grain-based subacute ruminal acidosis (SARA) challenge. Microbial ecology 74(2):485-495.

Press, W. H. 2007. Numerical recipes : the art of scientific computing. 3rd ed. Cambridge University Press, Cambridge, UK ; New York.

Press, W. H., S. A. Teukolsky, W. T. Vetterling, and B. P. Flannery. 2007. Numerical recipes 3rd edition: The art of scientific computing. Cambridge university press.

Quast, C., E. Pruesse, P. Yilmaz, J. Gerken, T. Schweer, P. Yarza, J. Peplies, and F. O. Glöckner. 2012. The SILVA ribosomal RNA gene database project: improved data processing and web-based tools. Nucleic acids research 41(D1):D590-D596.

R development Core Team. 2015. R: A language and environment for statistical computing. http://www.R-project.org.

Rabinowitz, L., R. A. Gunther, E. S. Shoji, R. A. Freedland, and E. H. Avery. 1973. Effects of high and low protein diets on sheep renal function and metabolism. Kidney international 4(3):188-207.

Ramirez, H. R., K. Harvatine, and P. Kononoff. 2016. Forage particle size and fat intake affect rumen passage, the fatty acid profile of milk, and milk fat production in dairy cows consuming dried distillers grains with solubles. J Dairy Sci 99(1):392-398.

Reynal, S. and G. Broderick. 2005. Effect of dietary level of rumen-degraded protein on production and nitrogen metabolism in lactating dairy cows. J Dairy Sci 88(11):4045-4064.

Reynolds, C. and N. B. Kristensen. 2008. Nitrogen recycling through the gut and the nitrogen economy of ruminants: an asynchronous symbiosis. Journal of animal science 86(14_suppl):E293-E305.

Ruiz, R., L. Tedeschi, J. Marini, D. Fox, A. Pell, G. Jarvis, and J. Russell. 2002. The effect of a ruminal nitrogen (N) deficiency in dairy cows: evaluation of the Cornell net carbohydrate and protein system ruminal N deficiency adjustment. J Dairy Sci 85(11):2986-2999.

Russell, J. 1998. The importance of pH in the regulation of ruminal acetate to propionate ratio and methane production in vitro. J Dairy Sci 81(12):3222-3230.

Russell, J. B. 1987. Effect of extracellular pH on growth and proton motive force of Bacteroides succinogenes, a cellulolytic ruminal bacterium. Applied and environmental microbiology 53(10):2379-2383.

Russell, J. B., J. O'connor, D. Fox, P. Van Soest, and C. Sniffen. 1992. A net carbohydrate and protein system for evaluating cattle diets: I. Ruminal fermentation. Journal of animal science 70(11):3551-3561.

Russell, J. B. and J. L. Rychlik. 2001. Factors that alter rumen microbial ecology. Science 292(5519):1119-1122.

Russell, J. B. and D. B. Wilson. 1996. Why are ruminal cellulolytic bacteria unable to digest cellulose at low pH? J Dairy Sci 79(8):1503-1509.

Rustomo, B., O. AlZahal, N. Odongo, T. Duffield, and B. McBride. 2006. Effects of rumen acid load from feed and forage particle size on ruminal pH and dry matter intake in the lactating dairy cow. J Dairy Sci 89(12):4758-4768.

Samuelov, N. S., R. Datta, M. K. Jain, and J. G. Zeikus. 1999. Whey fermentation by Anaerobiospirillum succiniciproducens for production of a succinate-based animal feed additive. Applied and environmental microbiology 65(5):2260-2263.

Satter, L. D. and L. L. Slyter. 1974. Effect of ammonia concentration of rumen microbial protein production in vitro. British Journal of Nutrition 32(2):199-208.

Schulze, A., A. C. Storm, M. R. Weisbjerg, and P. Nørgaard. 2017. Effects of forage neutral detergent fibre and time after feeding on medial and ventral rumen pH and volatile fatty acids concentration in heifers fed highly digestible grass/clover silages. Animal Production Science 57(1):129-132.

Shallom, D. and Y. Shoham. 2003. Microbial hemicellulases. Current opinion in microbiology 6(3):219-228.

Shinkai, T., M. Mitsumori, A. Sofyan, H. Kanamori, H. Sasaki, Y. Katayose, and A. Takenaka. 2016. Comprehensive detection of bacterial carbohydrate-active enzyme coding genes expressed in cow rumen. Animal Science Journal 87(11):1363-1370.

Short, S. D. 2004. Characteristics and production costs of US dairy operations.

Siciliano-Jones, J. and M. Murphy. 1989. Production of Volatile Fatty Acids in the Rumen and Cecum-Colon of Steers as Affected by Forage: Concentrate and Forage Physical Form1. J Dairy Sci 72(2):485-492.

Smith, R. 1969. Section G. General. Nitrogen metabolism and the rumen. Journal of Dairy Research 36(2):313-331.

Sniffen, C., J. O'connor, P. Van Soest, D. Fox, and J. Russell. 1992. A net carbohydrate and protein system for evaluating cattle diets: II. Carbohydrate and protein availability. Journal of animal science 70(11):3562-3577.

Somerville, C., S. Bauer, G. Brininstool, M. Facette, T. Hamann, J. Milne, E. Osborne, A. Paredez, S. Persson, and T. Raab. 2004. Toward a systems approach to understanding plant cell walls. Science 306(5705):2206-2211.

Spek, J., A. Bannink, G. Gort, W. Hendriks, and J. Dijkstra. 2012. Effect of sodium chloride intake on urine volume, urinary urea excretion, and milk urea concentration in lactating dairy cattle. J Dairy Sci 95(12):7288-7298.

Spek, J., A. Bannink, G. Gort, W. Hendriks, and J. Dijkstra. 2013. Interaction between dietary content of protein and sodium chloride on milk urea concentration, urinary urea excretion, renal recycling of urea, and urea transfer to the gastrointestinal tract in dairy cows. J Dairy Sci 96(9):5734-5745.

Spring, S., B. Bunk, C. Spröer, P. Schumann, M. Rohde, B. J. Tindall, and H.-P. Klenk. 2016. Characterization of the first cultured representative of Verrucomicrobia subdivision 5 indicates the proposal of a novel phylum. The ISME journal 10(12):2801.

St-Pierre, N. and D. Glamocic. 2000. Estimating unit costs of nutrients from market prices of feedstuffs. J Dairy Sci 83(6):1402-1411.

St-Pierre, N. and C. Thraen. 1999. Animal grouping strategies, sources of variation, and economic factors affecting nutrient balance on dairy farms. Journal of animal science 77(suppl_2):72-83.

Storm, A. C., M. D. Hanigan, and N. B. Kristensen. 2011. Effects of ruminal ammonia and butyrate concentrations on reticuloruminal epithelial blood flow and volatile fatty acid absorption kinetics under washed reticulorumen conditions in lactating dairy cows. Journal of Dairy Science 94(8):3980-3994.

Storm, A. C., N. B. Kristensen, and M. D. Hanigan. 2012. A model of ruminal volatile fatty acid absorption kinetics and rumen epithelial blood flow in lactating Holstein cows. Journal of Dairy Science 95(6):2919-2934.

Sung, H. G., Y. Kobayashi, J. Chang, A. Ha, I. H. Hwang, and J. Ha. 2007. Low ruminal pH reduces dietary fiber digestion via reduced microbial attachment. Asian Australasian Journal of Animal Sciences 20(2):200.

Sutton, J., M. Dhanoa, S. Morant, J. France, D. Napper, and E. Schuller. 2003. Rates of production of acetate, propionate, and butyrate in the rumen of lactating dairy cows given normal and low-roughage diets. J Dairy Sci 86(11):3620-3633.

Svihus, B., A. K. Uhlen, and O. M. Harstad. 2005. Effect of starch granule structure, associated components and processing on nutritive value of cereal starch: A review. Animal Feed Science and Technology 122(3-4):303-320.

Tamminga, S., A. Van Vuuren, C. Van der Koelen, R. Ketelaar, and P. van der Togt. 1990. Ruminal behaviour of structural carbohydrates, non-structural carbohydrates and crude protein from concentrate ingredients in dairy cows. Netherlands Journal of Agricultural Science 38(3B):513-526.

Tedeschi, L. O., D. G. Fox, R. D. Sainz, L. G. Barioni, S. R. d. Medeiros, and C. Boin. 2005. Mathematical models in ruminant nutrition. Scientia Agricola 62(1):76-91.

Thoetkiattikul, H., W. Mhuantong, T. Laothanachareon, S. Tangphatsornruang, V. Pattarajinda, L. Eurwilaichitr, and V. Champreda. 2013. Comparative analysis of microbial profiles in cow rumen fed with different dietary fiber by tagged 16S rRNA gene pyrosequencing. Current microbiology 67(2):130-137.

Titgemeyer, E., K. Spivey, S. Parr, D. Brake, and M. Jones. 2012. Relationship of whole body nitrogen utilization to urea kinetics in growing steers. Journal of animal science 90(10):3515-3526.

Tran, H., A. Caprez, P. Kononoff, P. Miller, and W. Weiss. 2016. Automation of statistical procedures to screen raw data and construct feed composition databases. Journal of animal science 94(suppl_5):681-682.

Turgeon, O., D. Brink, and R. Britton. 1983. Corn particle size mixtures, roughage level and starch utilization in finishing steers diets. Journal of animal science 57(3):739-749.

Tveit, A., T. Urich, and M. M. Svenning. 2014. Metatranscriptomic analysis of arctic peat soil microbiota. Applied and environmental microbiology:AEM. 01030-01014.

Ungerfeld, E. and R. Kohn. 2006. The role of thermodynamics in the control of ruminal fermentation. Ruminant physiology: Digestion, metabolism and impact of nutrition on gene expression, immunology and stress:55-85.

UNITE Community (2017): Full UNITE+INSD dataset. Version 01.12.2017. https://doi.org/10.15156/BIO/587474

Van Soest, P., J. Robertson, and B. Lewis. 1991a. Symposium: carbohydrate methodology, metabolism, and nutritional implications in dairy cattle. J Dairy Sci 74(10):3583-3597.

Van Soest, P. v., J. Robertson, and B. Lewis. 1991b. Methods for dietary fiber, neutral detergent fiber, and nonstarch polysaccharides in relation to animal nutrition. J Dairy Sci 74(10):3583-3597.

Vyas, D. and R. Erdman. 2009. Meta-analysis of milk protein yield responses to lysine and methionine supplementation. J Dairy Sci 92(10):5011-5018.

Wang, L., A. Hatem, U. V. Catalyurek, M. Morrison, and Z. Yu. 2013. Metagenomic insights into the carbohydrate-active enzymes carried by the microorganisms adhering to solid digesta in the rumen of cows. PloS one 8(11):e78507.

Wang, Q., G. M. Garrity, J. M. Tiedje, and J. R. Cole. 2007. Naive Bayesian classifier for rapid assignment of rRNA sequences into the new bacterial taxonomy. Applied and environmental microbiology 73(16):5261-5267.

Wang, Z., C. O. Elekwachi, J. Jiao, M. Wang, S. Tang, C. Zhou, Z. Tan, and R. J. Forster. 2017. Investigation and manipulation of metabolically active methanogen community composition during rumen development in black goats. Scientific reports 7(1):422.

Wetzels, S. U., E. Mann, B. U. Metzler-Zebeli, P. Pourazad, M. Qumar, F. Klevenhusen, B. Pinior, M. Wagner, Q. Zebeli, and S. Schmitz-Esser. 2016. Epimural indicator phylotypes of transiently-induced subacute ruminal acidosis in dairy cattle. Frontiers in microbiology 7:274.

White, R., Y. Roman-Garcia, J. Firkins, P. Kononoff, M. VandeHaar, H. Tran, T. McGill, R. Garnett, and M. Hanigan. 2017a. Evaluation of the National Research Council (2001) dairy model and derivation of new prediction equations. 2. Rumen degradable and undegradable protein. J Dairy Sci 100(5):3611-3627.

White, R., Y. Roman-Garcia, J. Firkins, M. VandeHaar, L. Armentano, W. Weiss, T. McGill, R. Garnett, and M. Hanigan. 2017b. Evaluation of the National Research Council (2001) dairy model and derivation of new prediction equations. 1. Digestibility of fiber, fat, protein, and nonfiber carbohydrate. J Dairy Sci.

Whitehead, T. R. and H. J. Flint. 1995. Heterologous expression of an endoglucanase gene (endA) from the ruminai anaerobe Ruminococcus flavefaciens 17 in Streptococcus bovis and Streptococcus sanguis. FEMS microbiology letters 126(2):165-169.

Wickersham, T., E. Titgemeyer, and R. Cochran. 2009. Methodology for concurrent determination of urea kinetics and the capture of recycled urea nitrogen by ruminal microbes in cattle. Animal 3(3):372-379.

Wickersham, T., E. Titgemeyer, R. Cochran, E. Wickersham, and D. Gnad. 2008a. Effect of rumen-degradable intake protein supplementation on urea kinetics and microbial use of recycled urea in steers consuming low-quality forage. Journal of animal science 86(11):3079-3088.

Wickersham, T., E. Titgemeyer, R. Cochran, E. Wickersham, and E. Moore. 2008b. Effect of frequency and amount of rumen-degradable intake protein supplementation on urea kinetics and microbial use of recycled urea in steers consuming low-quality forage. Journal of animal science 86(11):3089-3099.

Wickersham, T. A., E. C. Titgemeyer, R. C. Cochran, and E. E. Wickersham. 2008c. Effect of undegradable intake protein supplementation on urea kinetics and microbial use of recycled urea in steers consuming low-quality forage. British Journal of Nutrition 101(2):225-232.

Wilkinson, J. 2011. Re-defining efficiency of feed use by livestock. Animal 5(7):1014-1022.

Wirsenius, S., C. Azar, and G. Berndes. 2010. How much land is needed for global food production under scenarios of dietary changes and livestock productivity increases in 2030? Agricultural Systems 103(9):621-638.

Wohlt, J., J. Clark, and F. Blaisdell. 1976. Effect of Sampling Location, Time, and Method of Concentration of Ammonia Nitrogen in Rumen Fluid1. J Dairy Sci 59(3):459-464.

Yang, W., K. Beauchemin, and L. Rode. 2001. Effects of grain processing, forage to concentrate ratio, and forage particle size on rumen ph and digestion by dairy cows1. J Dairy Sci 84(10):2203-2216.

Zhang, J., H. Shi, Y. Wang, S. Li, Z. Cao, S. Ji, Y. He, and H. Zhang. 2017. Effect of dietary forage to concentrate ratios on dynamic profile changes and interactions of ruminal microbiota and metabolites in Holstein heifers. Frontiers in microbiology 8:2206.

Zhou, J., L. Bao, L. Chang, Y. Zhou, and H. Lu. 2012. Biochemical and kinetic characterization of GH43 β-D-xylosidase/α-L-arabinofuranosidase and GH30 α-L-arabinofuranosidase/β-D-xylosidase from rumen metagenome. Journal of industrial microbiology & biotechnology 39(1):143-152.

Zhu, J., S. Stokes, and M. Murphy. 1997. Substitution of neutral detergent fiber from forage with neutral detergent fiber from by-products in the diets of lactating cows. J Dairy Sci 80(11):2901-2906.

Zimin, A. V., A. L. Delcher, L. Florea, D. R. Kelley, M. C. Schatz, D. Puiu, F. Hanrahan, G. Pertea, C. P. Van Tassell, and T. S. Sonstegard. 2009. A whole-genome assembly of the domestic cow, Bos taurus. Genome biology 10(4):R42.

Zverlov, V., S. Mahr, K. Riedel, and K. Bronnenmeier. 1998. Properties and gene structure of a bifunctional cellulolytic enzyme (CelA) from the extreme thermophile 'Anaerocellum thermophilum'with separate glycosyl hydrolase family 9 and 48 catalytic domains. Microbiology 144(2):457-465.

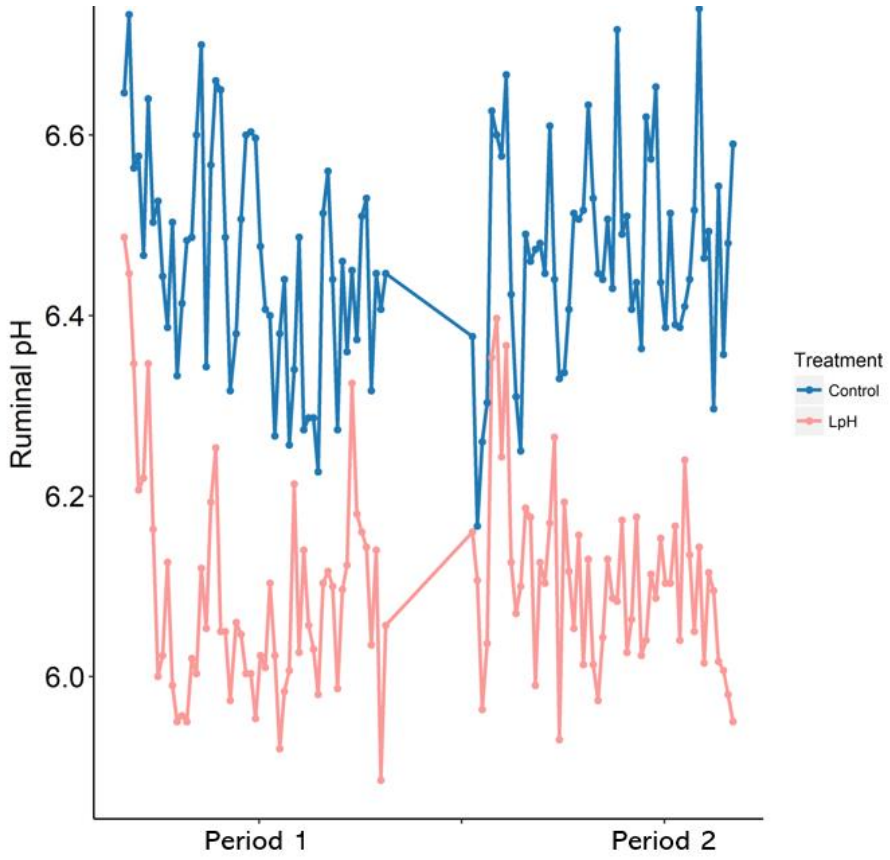

Figure 5-1. Ruminal pH achieved during each of 10-day period.

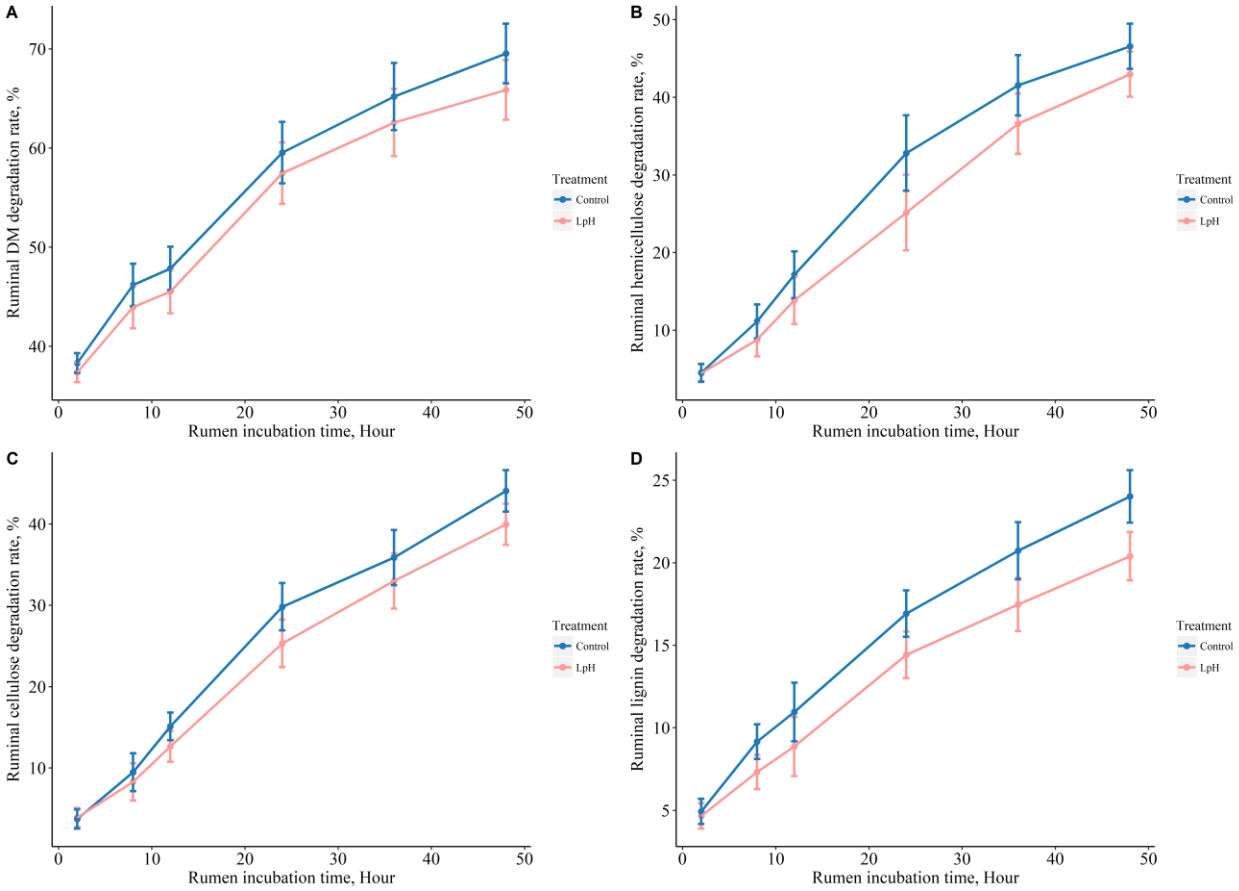

Figure 5-2. In situ degradation of dietary DM, hemicellulose, cellulose, and lignin with respect to the rumen incubation time.

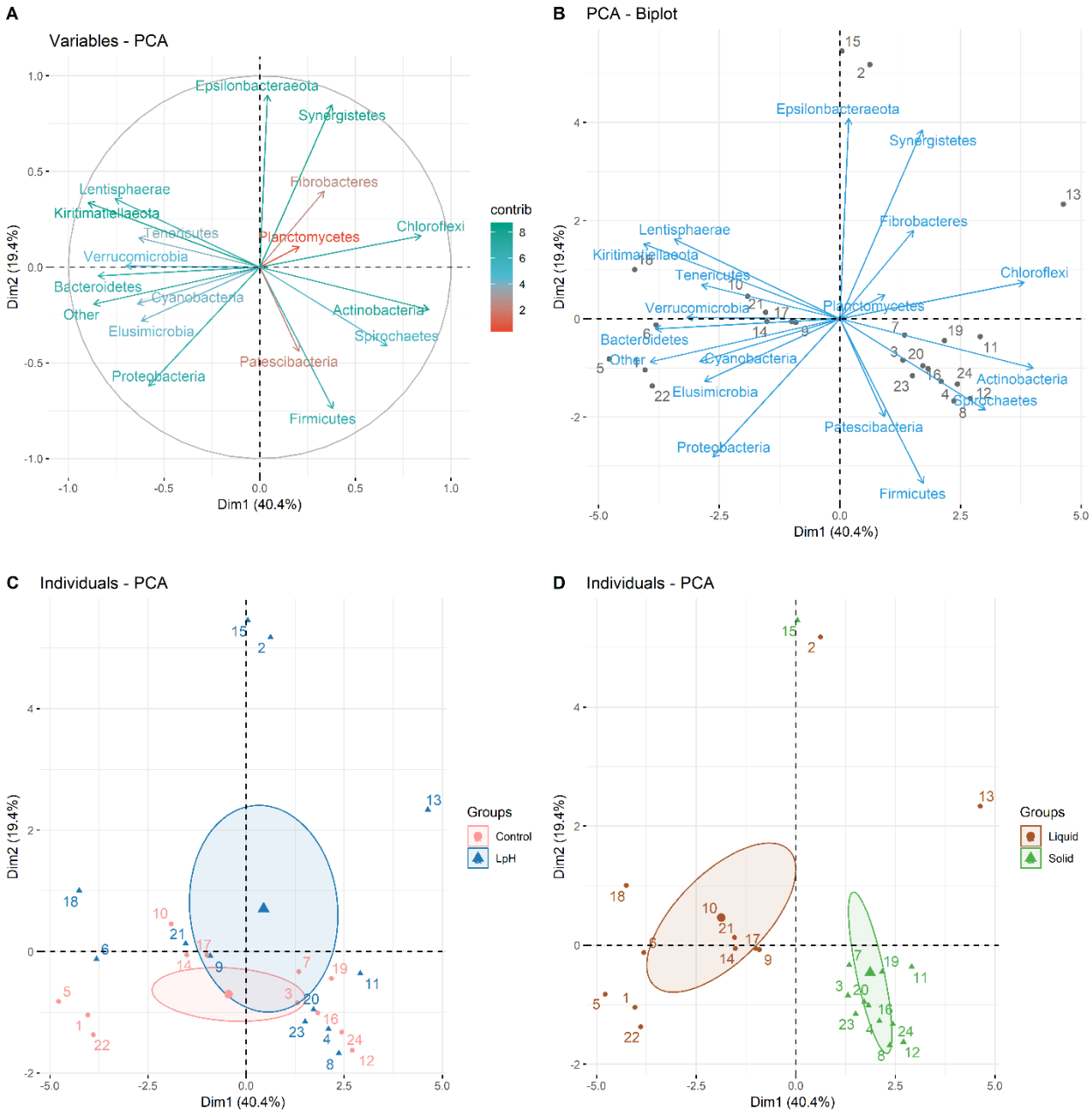

Figure 5-3. Principal component analyses (PCA) of overall bacterial composition among all samples at the phylum level. These analyses were performed based on centered log ratios of sequence counts. Variable contributions to the first two components are labelled with different colors (A), where the arrow direction represents the quality of representation on the factor map, and the arrow length indicates the contributions to the principal components. All variables were represented by arrows and individuals were represented by points with numbers (B). Points were colored by treatment group (C) or ruminal sample fraction group (D).

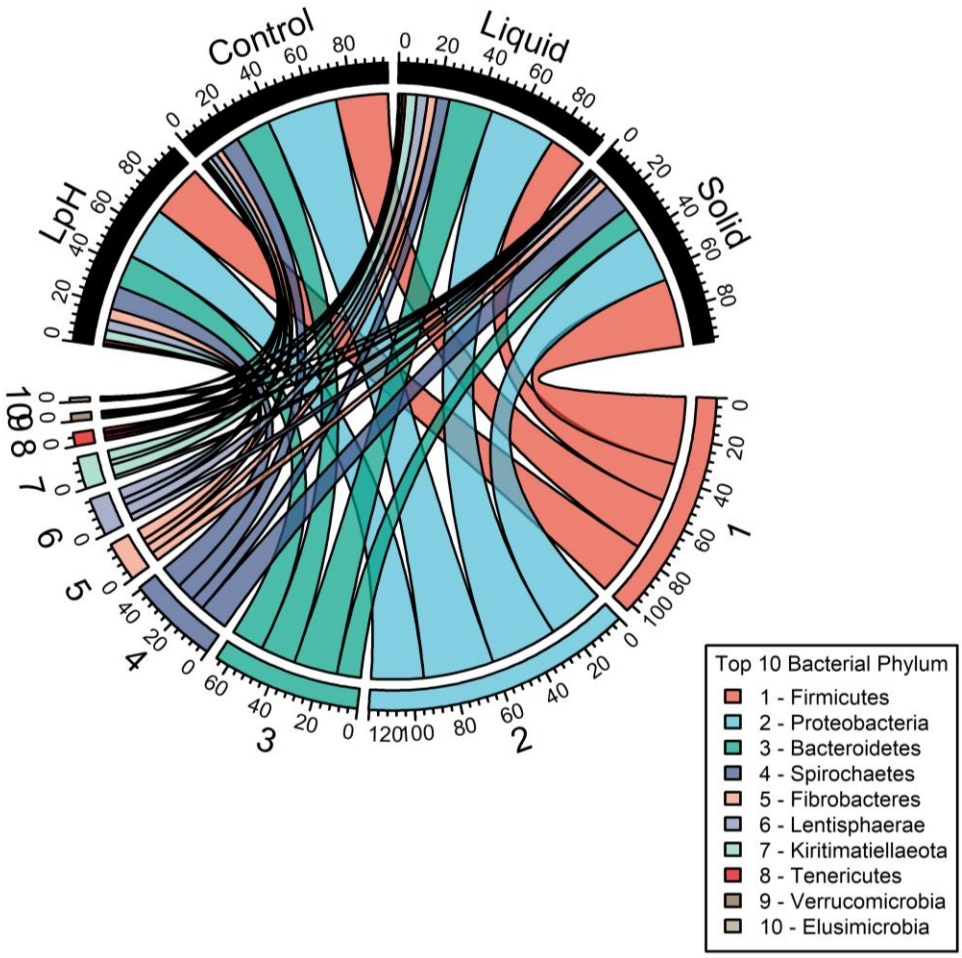

Figure 5-4. Taxonomic composition of the ruminal microbiome in the liquid and solid fractions in response to high and low pH. The top 10 bacterial phyla were selected. Sequences were expressed as relative abundance.

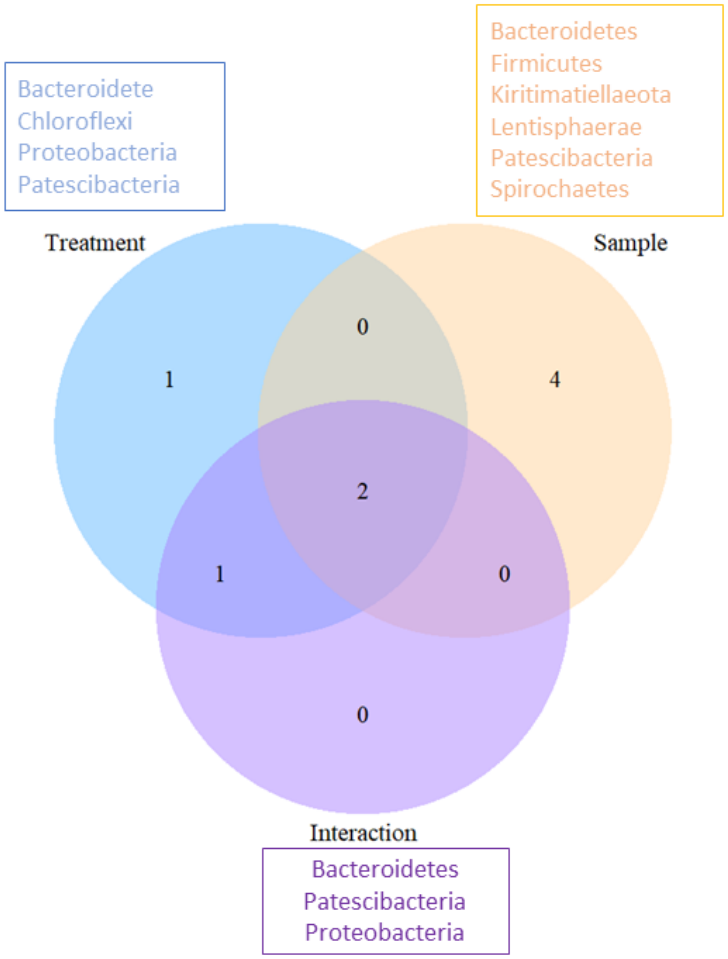

Figure 5-5. Bacterial phyla that significantly affected by treatments, rumen sample (solid versus liquid), and their interactions at phylum level. Sequences of the phyla were transformed to centered log ratio to avoid compositional data problem.

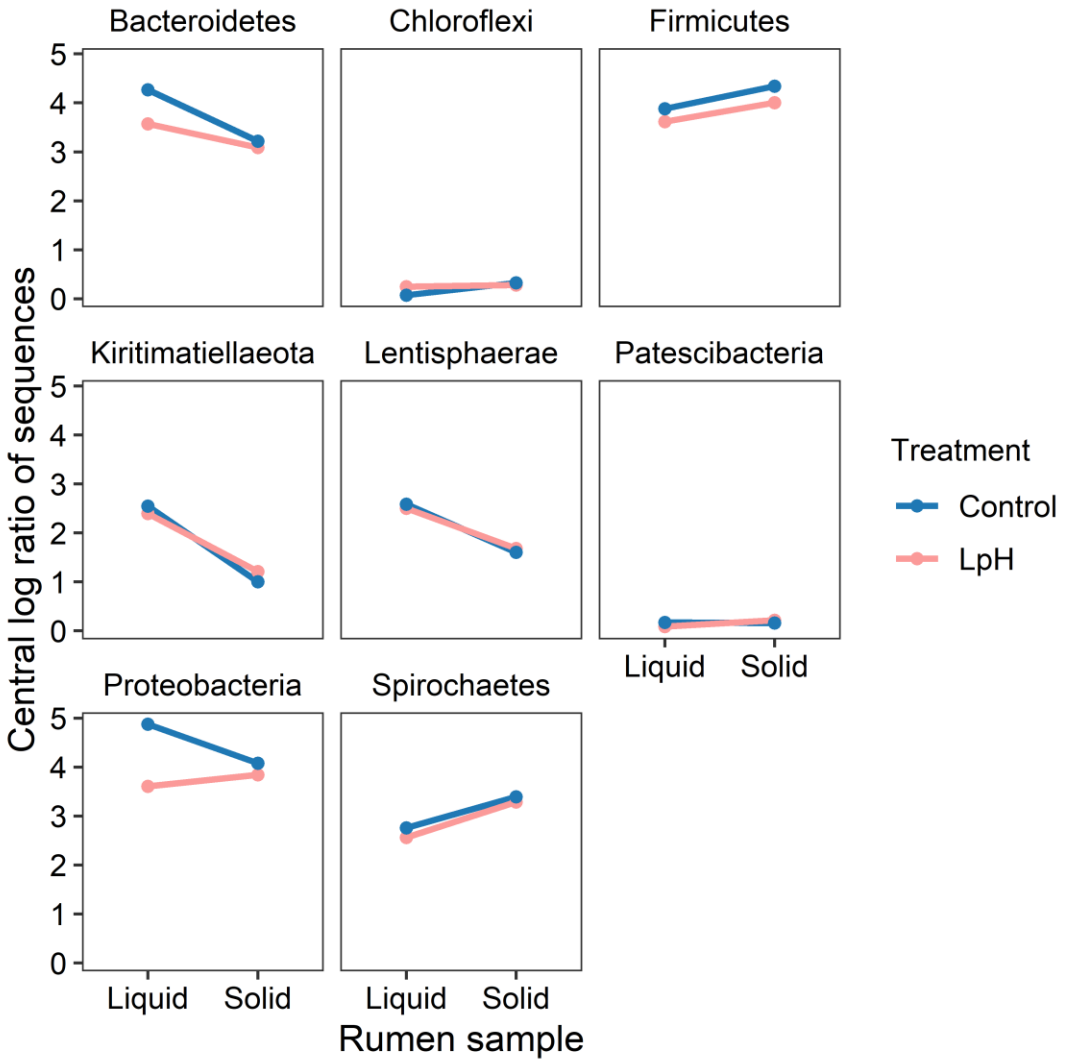

Figure 5-6. Bacteria phyla that were significantly affected by treatments, ruminal sample fractions (solid versus liquid). Sequences of the phyla were transformed to centered log ratio.

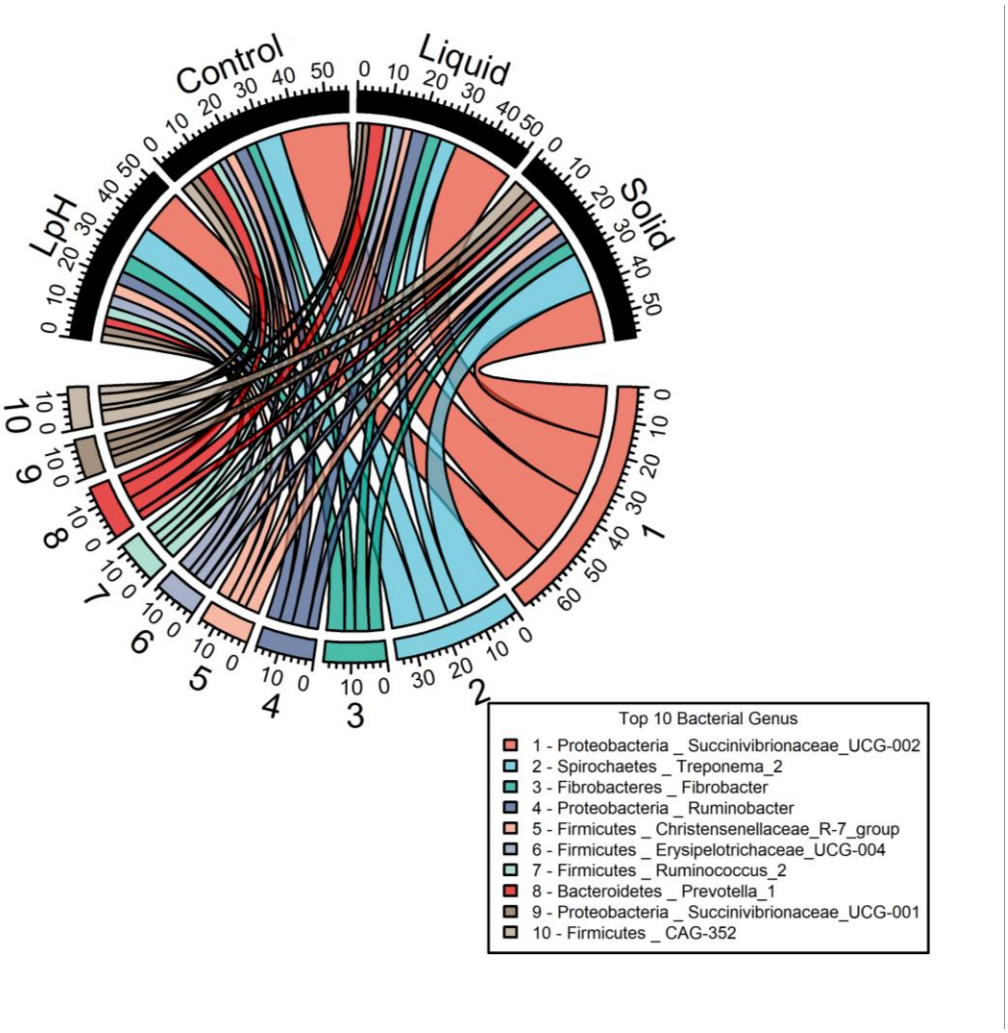

Figure 5-7. Taxonomic composition of the ruminal bacteria. The top 10 bacterial genera were selected. Sequences were expressed as relative abundance.

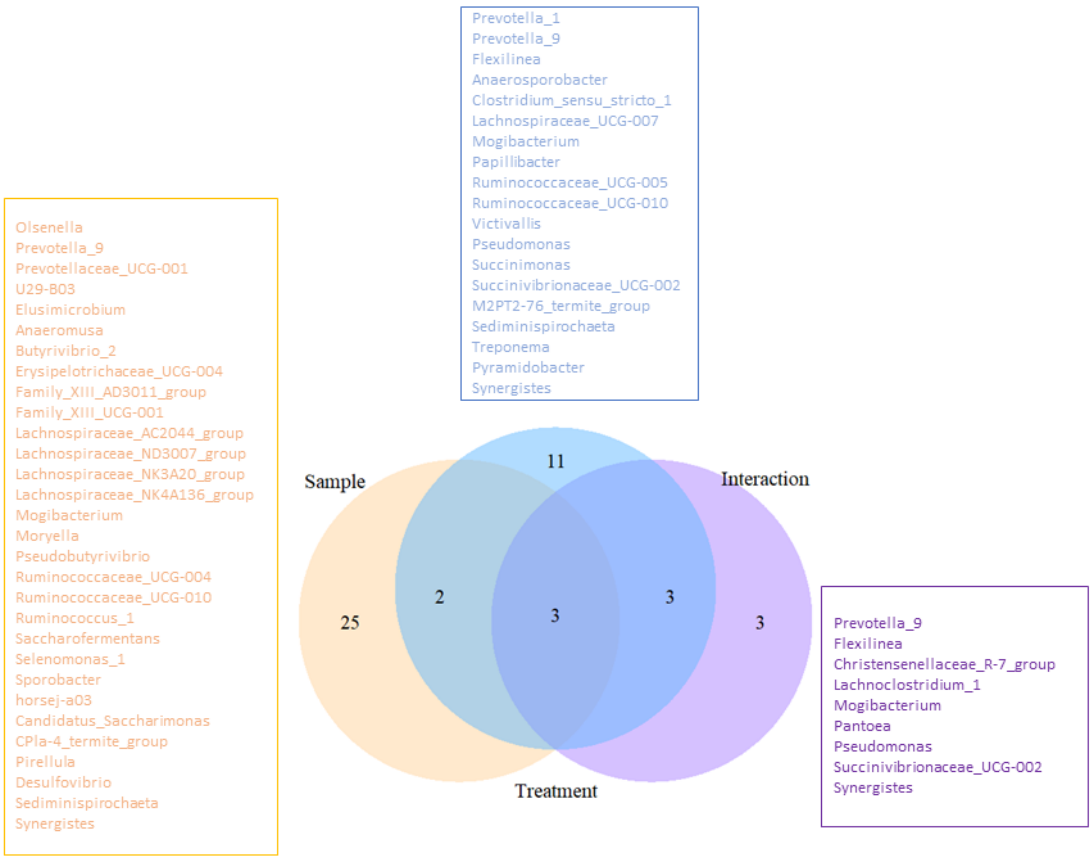

Figure 5-8. Bacterial genera that were significantly affected by treatments, rumen sample (solid versus liquid), and their interactions. Sequences of the genera were transformed to centered log ratio to avoid compositional data problem.

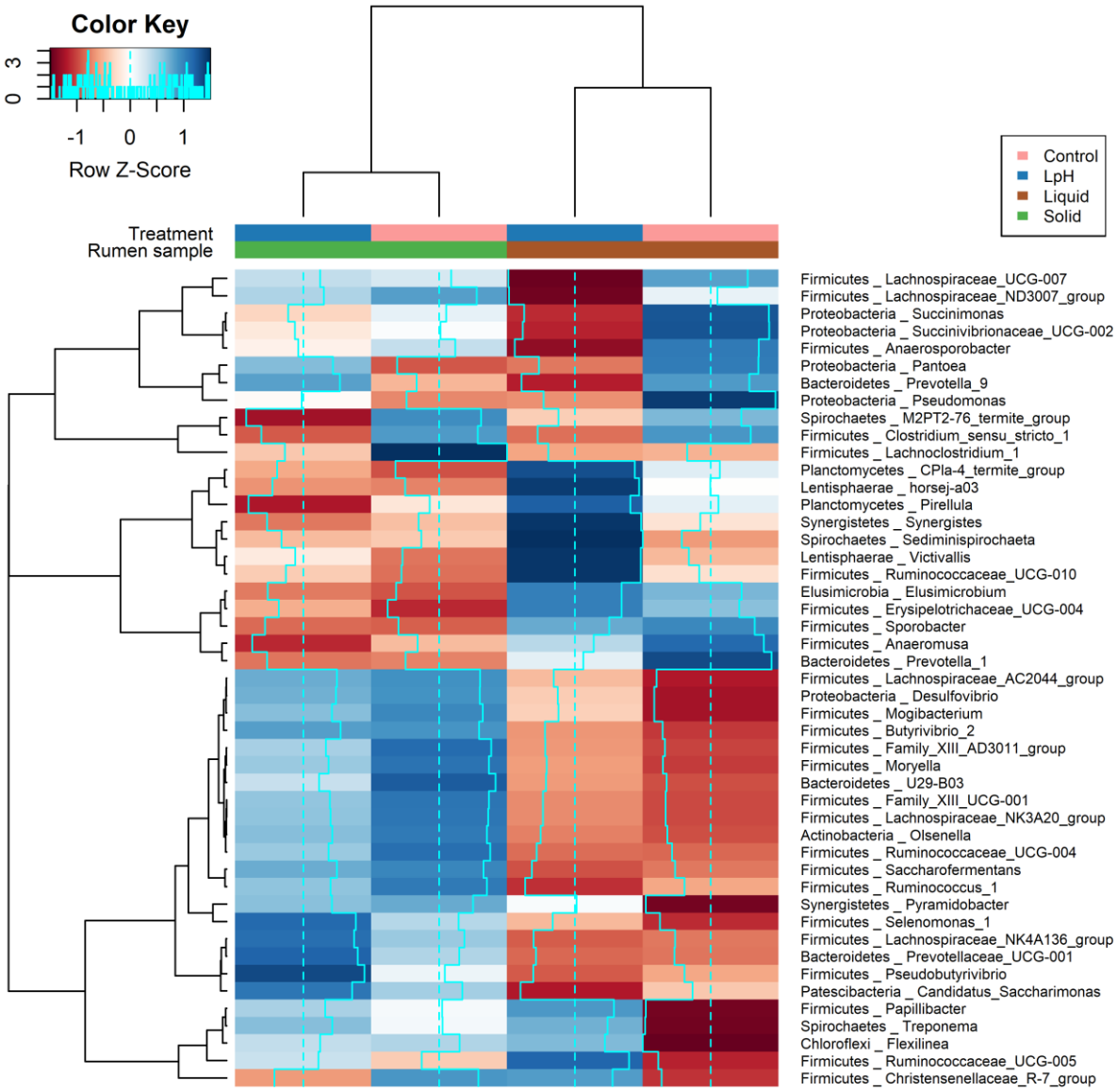

Figure 5-9. Heatmap indicating genera that were significantly affected by treatment, rumen sample location, and their interaction. At least one of the treatment effect, rumen sample effect, or their interaction was significant. Rows are color coded according to *Z*-score. A *Z*-score change of +1 is equal to one standard deviation above the row mean. Blue represents upregulation, and red represents downregulation.

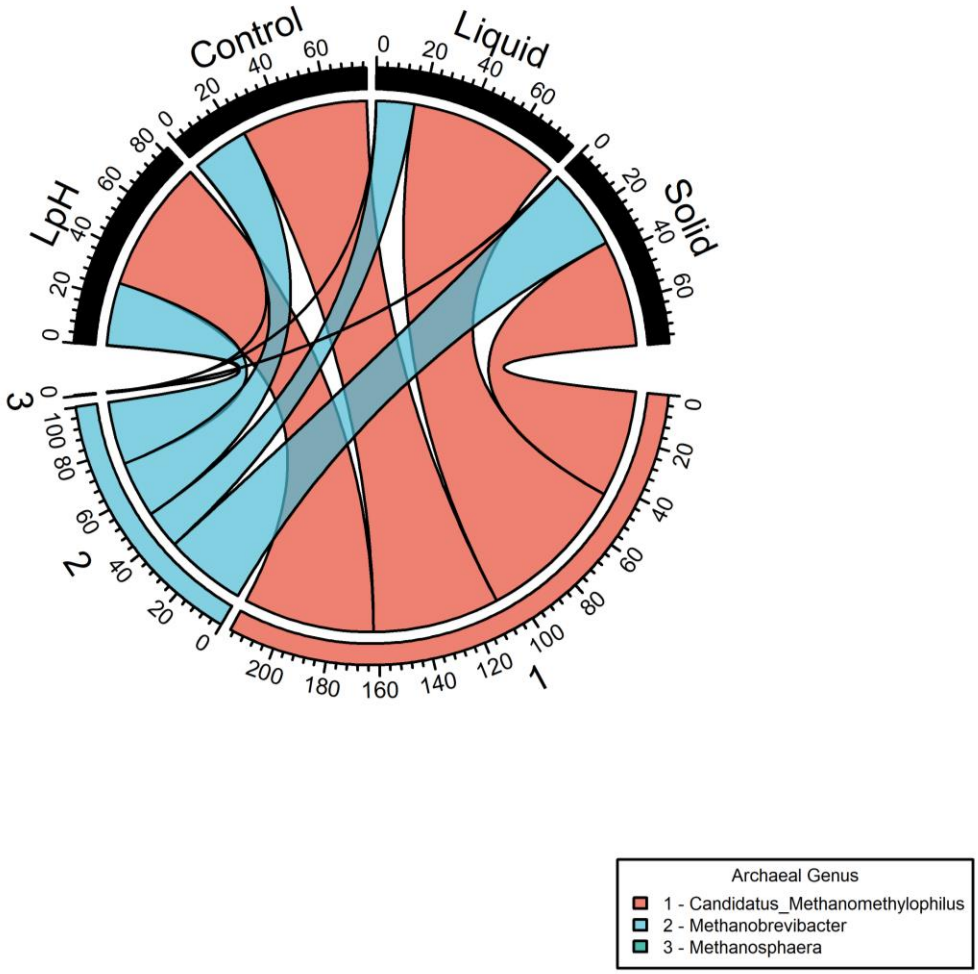

Figure 5-10. Taxonomic composition of the ruminal archaea. Sequences were expressed as relative abundance.

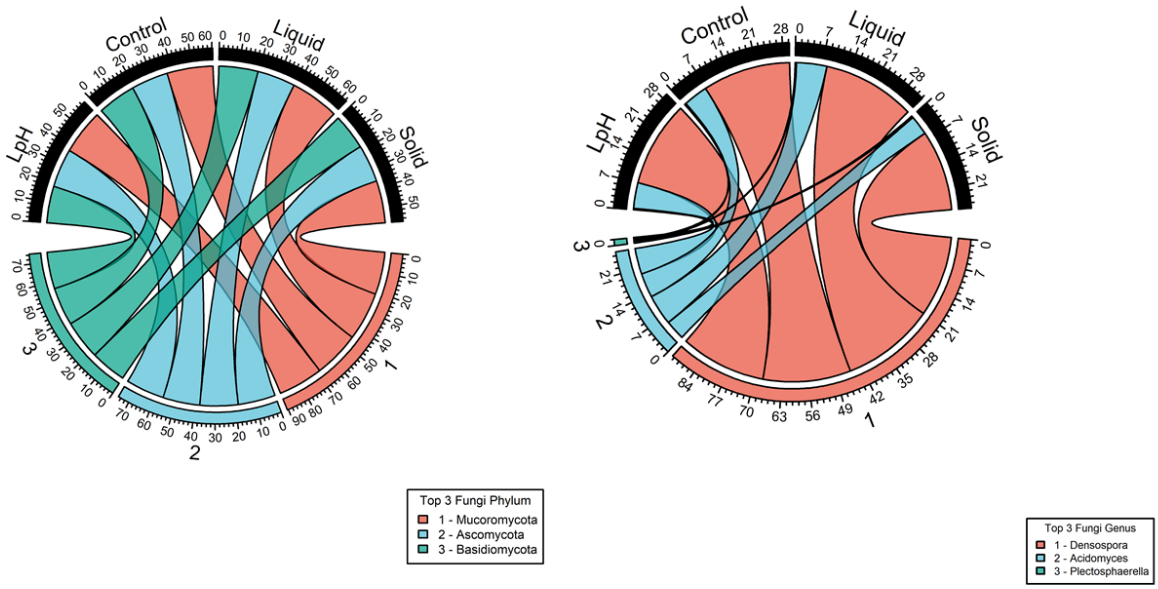

Figure 5-11 Taxonomic composition of the ruminal Fungi. The top 3 fungal phyla and genera were selected. Sequences were expressed as relative abundance.

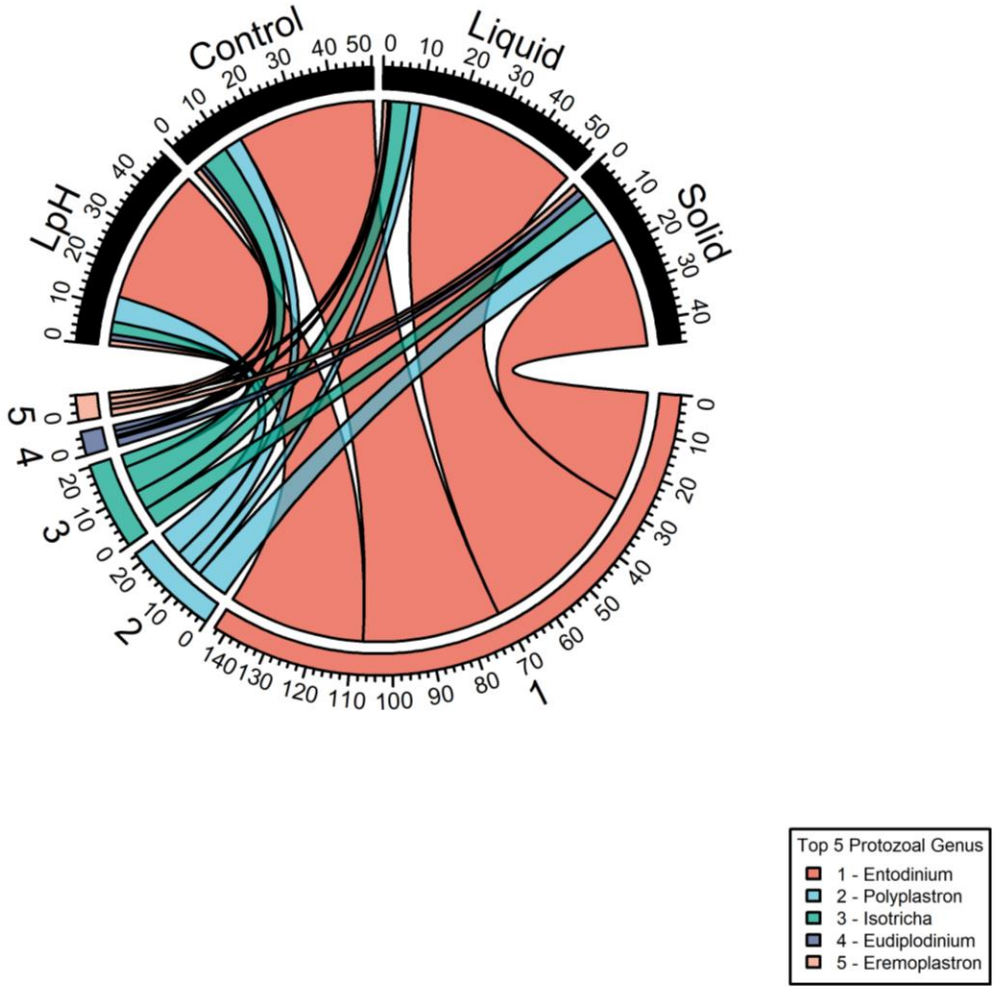

Figure 5-12. Taxonomic composition of the ruminal Protozoa. The top 5 protozoan genera were selected. Sequences were expressed as relative abundance.

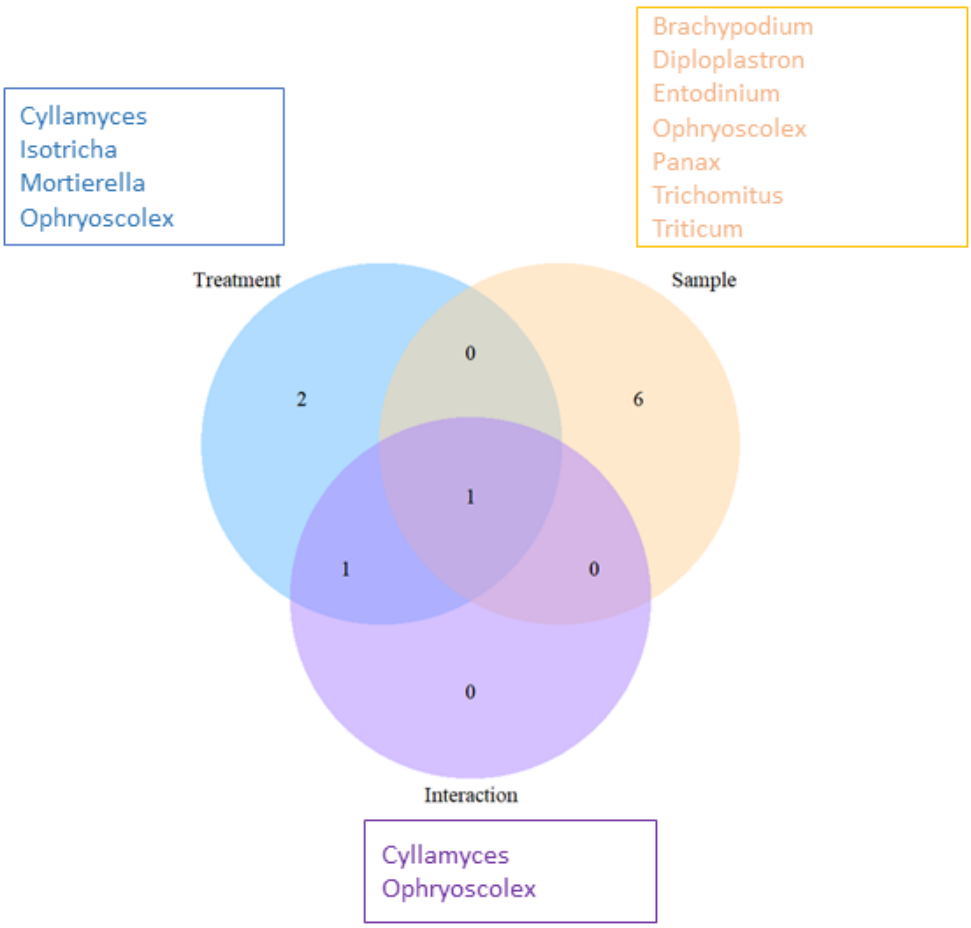

Figure 5-13. Protozoan genera that significantly changed among treatments, rumen sample (solid versus liquid), and their interactions. Sequences of the genera were transformed to centered log ratio.

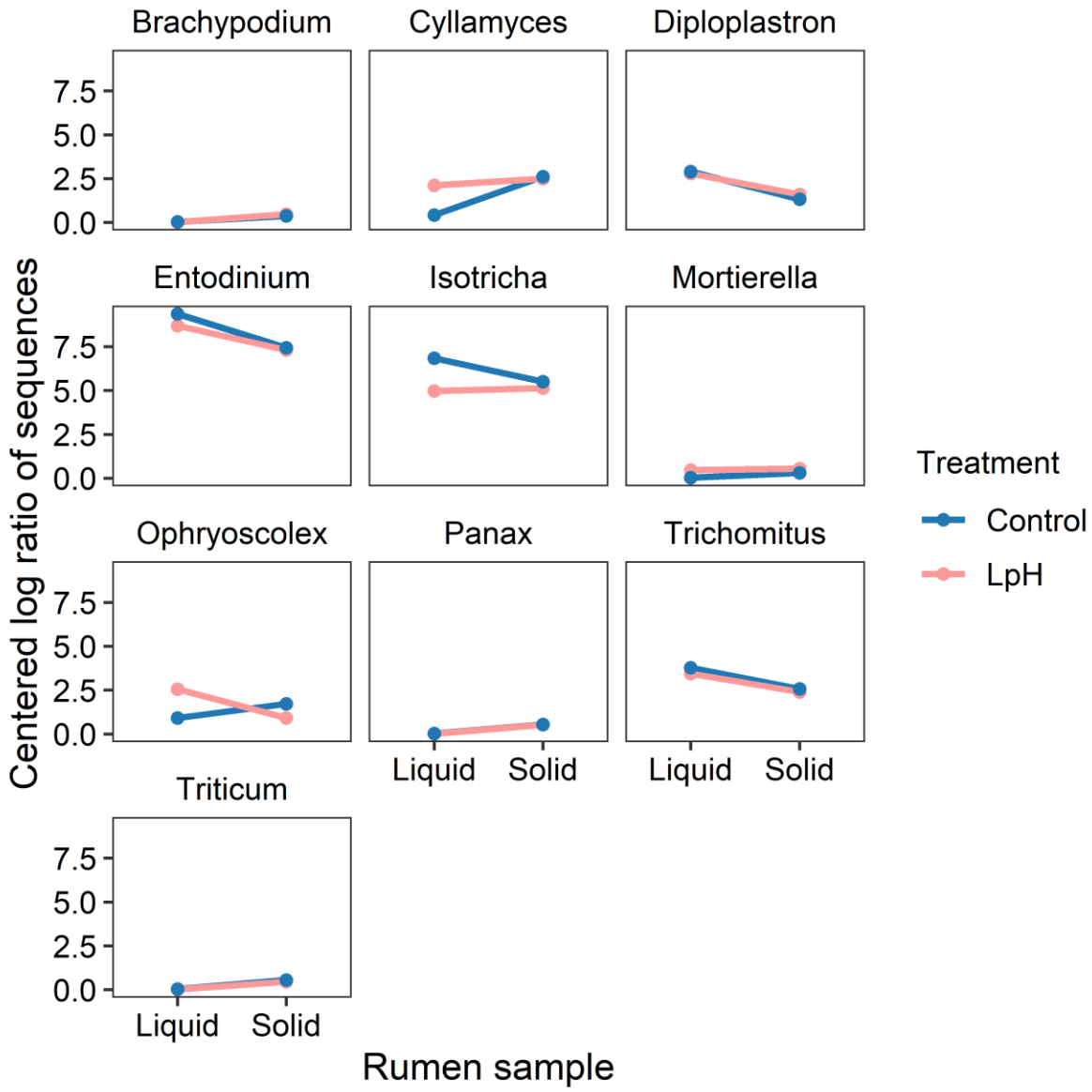

Figure 5-14. Protozoan genera that were significantly affected by treatments, ruminal fractions (solid versus liquid) or their interaction. Sequences of the phyla were transformed to centered log ratio.

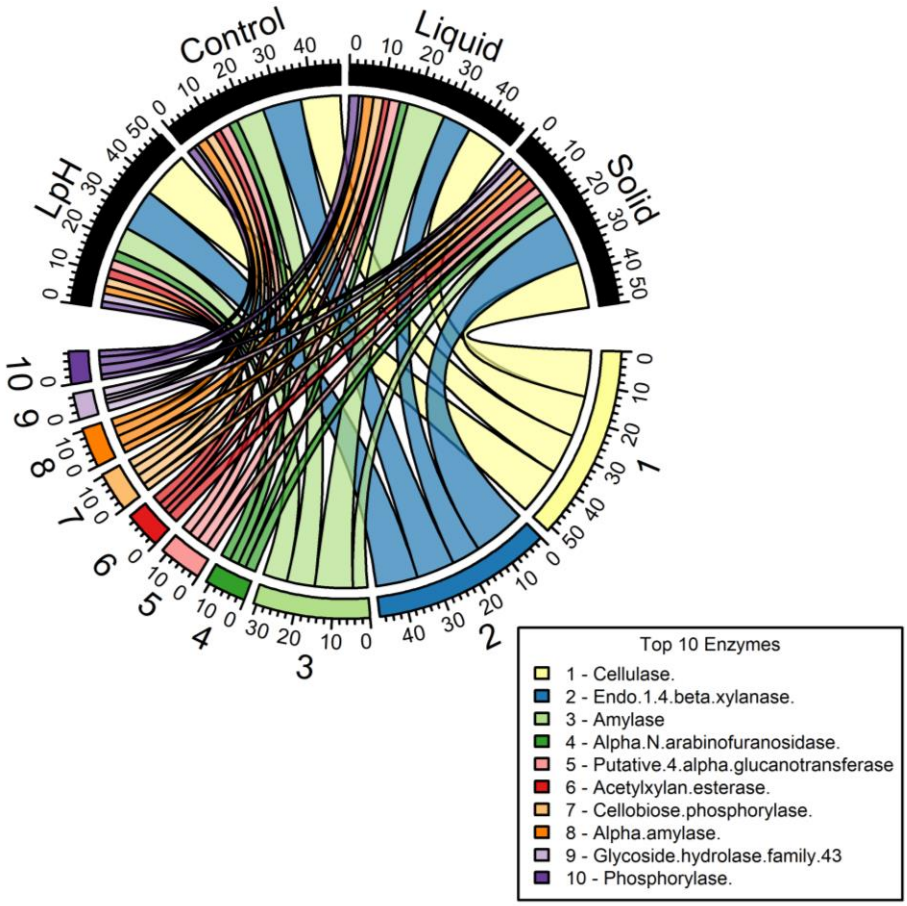

Figure 5-15. mRNA expressions of the carbohydrate-active degrading enzymes. The top 10 enzymes were selected. Sequence counts were expressed as relative abundance (%).

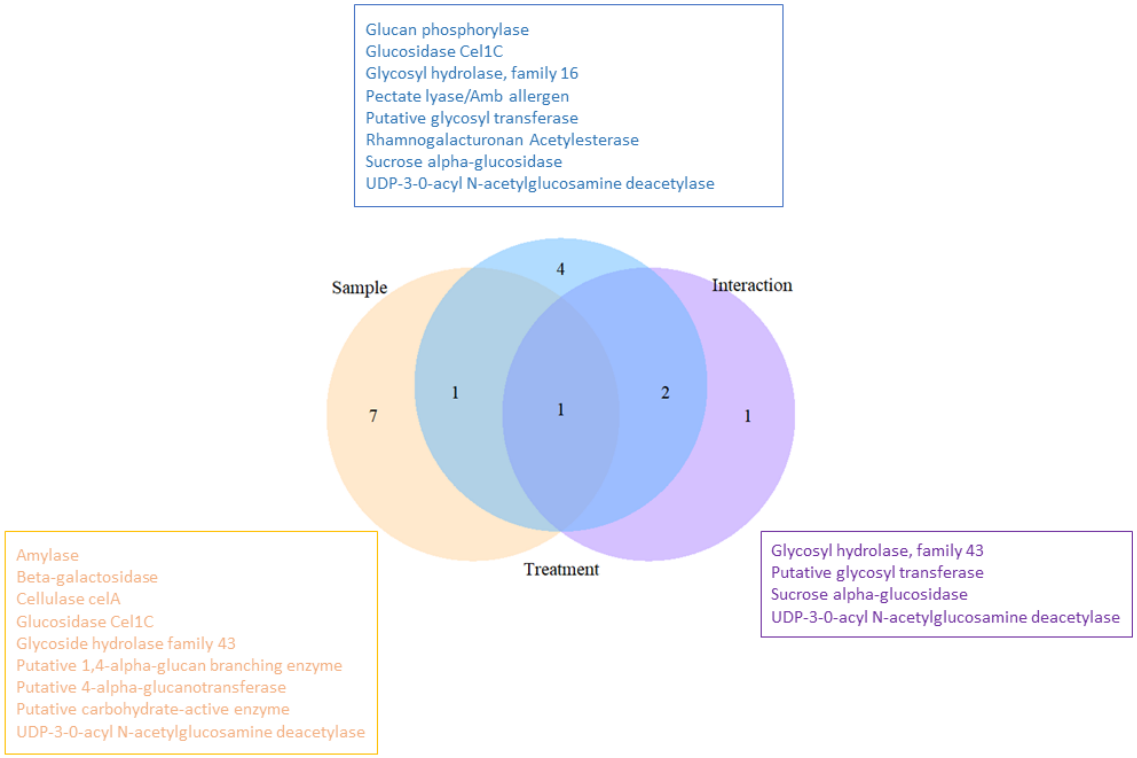

Figure 5-16. Carbohydrate-active degrading enzymes that significantly changed among treatments, rumen sample (solid versus liquid), and their interactions. Read counts were transformed to centered log ratio to avoid compositional data problem.

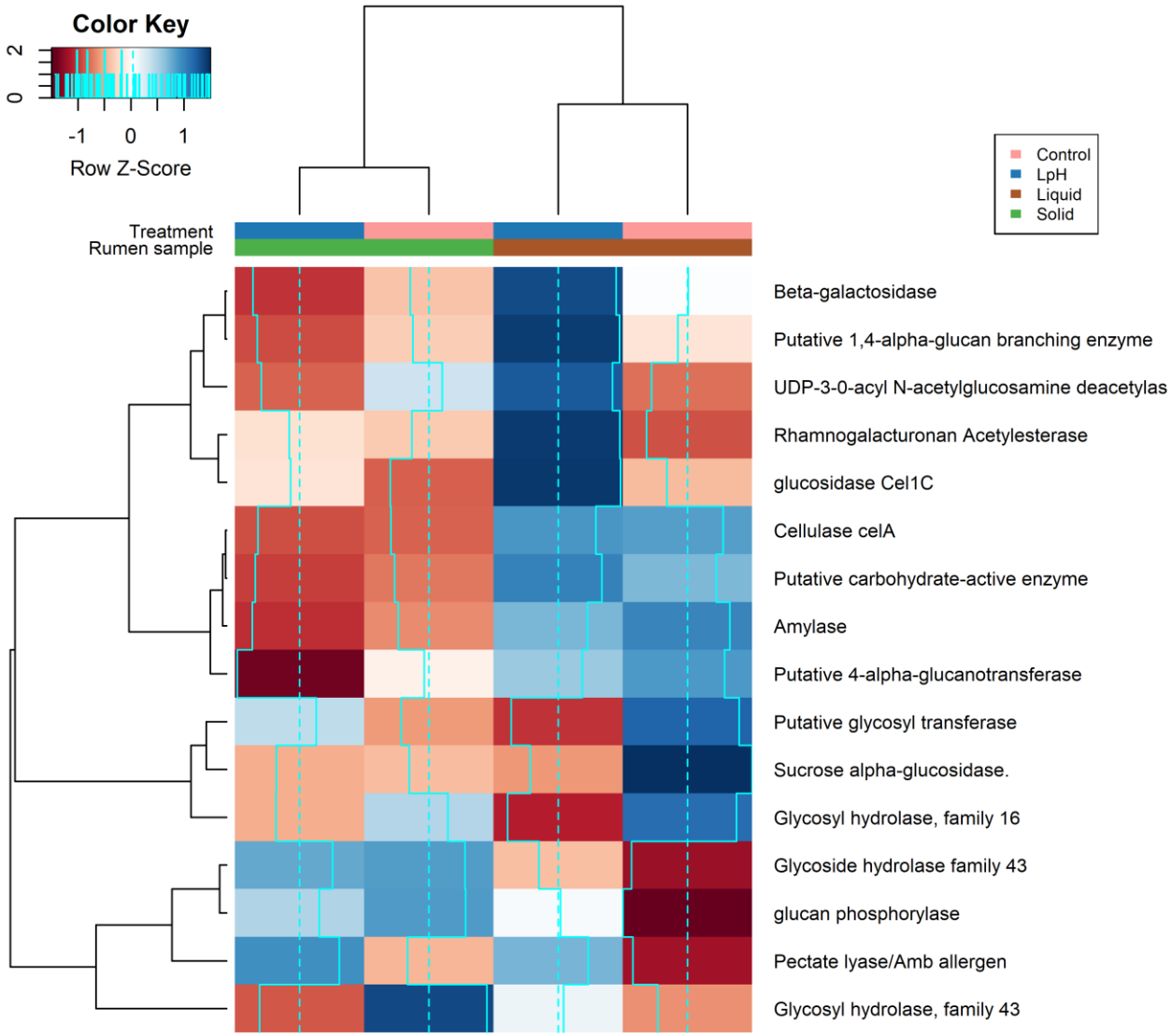

Figure 5-17. Heatmap indicating significantly affected enzymes in the assembled metatranscriptome data sets. At least one of the pH treatments, rumen samples, or their interaction was significant. Rows are color coded according to *Z*-score. A *Z*-score change of +1 is equal to one standard deviation above the row mean. Blue represents upregulation, and red represents downregulation.

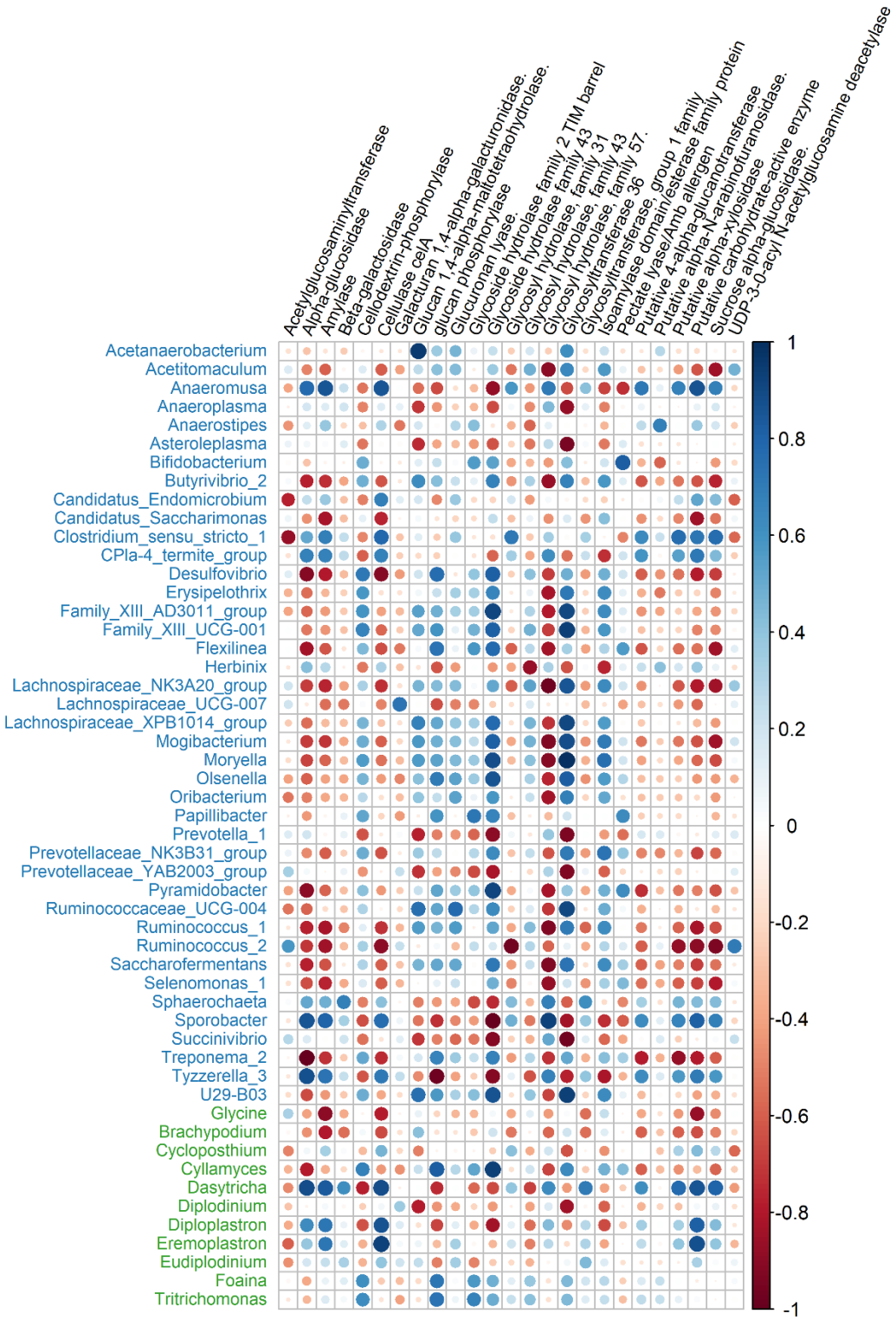

Figure 5-18. Pairwise correlations between microbial genera and carbohydrate-active degrading enzymes. Only the enzyme expressions that were significantly correlated with bacterial genera were shown (*P* value < 0.05, |r| > 0.5). The bacterial genera were colored by blue, and protozoan genera were colored by green.

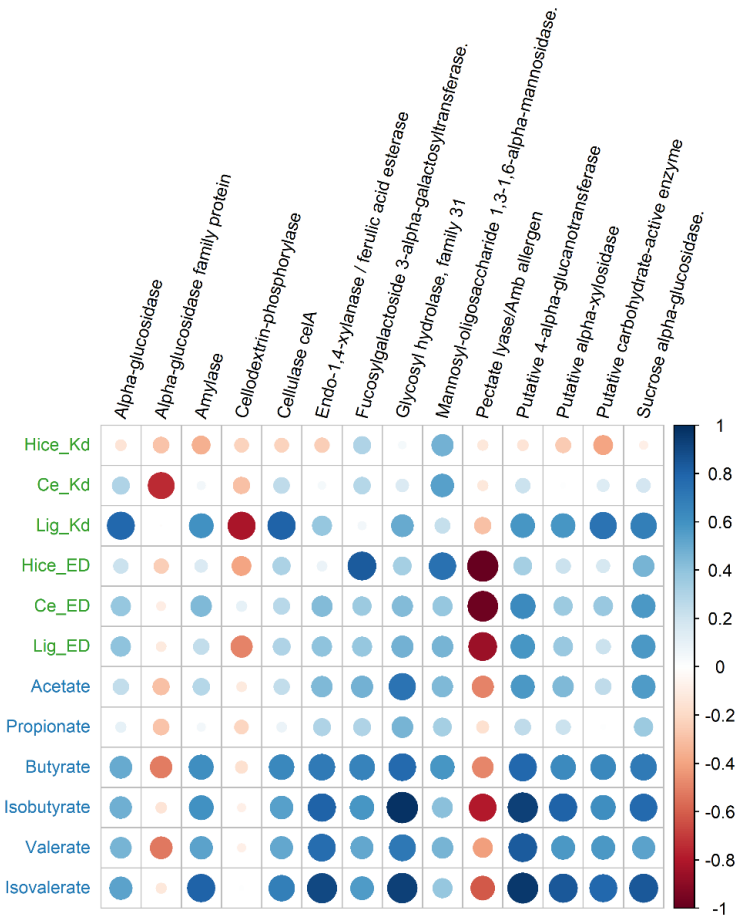

Figure 5-19. Pairwise correlations between carbohydrate-active degrading enzymes and fiber degradation dynamics and SCFA concentrations. Only the enzyme expressions that were significantly correlated with at least one of row variables were shown (*P* value < 0.05, |r| > 0.5). The fiber degradation dynamics were colored by green, and SCFA concentrations were colored by blue.

Table 5-1. Ingredient composition and nutrient content of the ration[1].

Ingredient	% of DM
Corn silage	33.54
Chopped hay	48.52
Wheat middlings	5.27
Corn meal	2.53
Corn distillers dried grains	1.01
Gluten feed	3.53
Soybean meal	3.33
Soybean hulls	1.67
Limestone	0.28
Salt	0.22
Vitamin-mineral mix[2]	0.11
Nutrient content	% of DM
DM (59.8% as fed)	100
CP	12.6
NDF	46.2
ADF	23.6
Hemicellulose	22.6
Cellulose	21.0
Lignin	2.6
Starch	15.4

[1]Ingredients other than the corn silage and chopped hay were provided as a pelleted mix.

[2]Provided (per kg of pellet concentrate): vitamin A (9600 IU), vitamin D (3200 IU), vitamin E (41.2 mg), copper (26.9 mg), manganese (126 mg), zinc (200 mg), selenium (1.2 mg), monensin (27.2 mg), cobalt (0.1 mg), and iodine (2.1 mg).

Table 5-2. Effects of ruminal pH on DMI and ruminal short chain fatty acid concentrations.

Variable	Treatment		SEM	P value
	Control	LpH		
pH	6.44	6.09	0.04	<0.0001
DMI, kg/d	9.75	7.82	0.66	0.04
Total SCFA, mM	82.84	62.31	3.80	0.001
Acetate, mM	54.71	42.12	2.38	0.001
Propionate, mM	20.05	14.61	1.24	0.001
Butyrate, mM	5.94	3.96	0.50	0.001
Isobutyrate, Mm	0.79	0.58	0.05	0.001
Valerate, mM	0.68	0.51	0.06	0.04
Isovalerate, Mm	0.43	0.31	0.03	0.003

Table 5-3. Effects of ruminal pH change on in situ fiber degradation kinetics[1].

Variable	Treatment		SEM	*P* value
	Control	LpH		
DM				
a	35.15	34.14	0.94	0.31
b	47.19	45.84	6.11	0.81
K_d	0.033	0.036	0.012	0.78
ED	50.62	48.76	0.64	0.06
Hemicellulose				
a	-0.79	-0.03	0.78	0.43
b	65.97	79.19	7.8	0.13
K_d	0.033	0.020	0.005	0.09
ED	20.53	17.3	0.74	0.02
Cellulose				
a	-0.08	0.50	0.94	0.33
b	69.78	72.81	5.61	0.61
K_d	0.023	0.018	0.002	0.15
ED	18.15	16.24	0.63	0.02
Lignin				
a	3.49	3.19	0.34	0.49
b	33.03	35.77	8.39	0.75
K_d	0.027	0.022	0.005	0.50
ED	12.12	10.29	0.31	0.002

[1]a represents proportion of rapidly degradable fraction (%); b represents proportion of potentially degradable fraction (%); K_d represents the degradation rate constant of b (%/h); ED is effective degradability (%).

Table 5-4. The effects ruminal pH and sampling location on the taxonomic composition of bacterial phyla in the rumen[1].

Phylum[2]	LpH	Control	Liquid	Solid
Firmicutes	25.98 ± 9.33	25.46 ± 12.11	18.24 ± 7.98	33.2 ± 6.93
Proteobacteria	25.64 ± 11.37	34.51 ± 10.76	32.59 ± 14.43	27.56 ± 8.12
Bacteroidetes	15.95 ± 6.97	17.07 ± 8.49	21.29 ± 7.88	11.73 ± 3.06
Spirochaetes	11.14 ± 5.6	9.28 ± 4.98	6.35 ± 4.23	14.07 ± 2.77
Fibrobacteres	5.53 ± 3.98	3.29 ± 1.14	4.36 ± 4.3	4.46 ± 1.19
Lentisphaerae	5.18 ± 4.06	3.22 ± 2.17	5.35 ± 2.37	3.05 ± 3.85
Kiritimatiellaeota	4.8 ± 5.79	2.32 ± 1.81	5.44 ± 4.88	1.67 ± 2.94
Tenericutes	1.75 ± 0.83	1.27 ± 0.52	1.55 ± 0.55	1.46 ± 0.88
Verrucomicrobia	0.78 ± 0.87	0.97 ± 1.6	1.35 ± 1.64	0.4 ± 0.39
Elusimicrobia	0.43 ± 0.31	0.52 ± 0.45	0.59 ± 0.48	0.36 ± 0.21
Actinobacteria	0.33 ± 0.41	0.2 ± 0.18	0.15 ± 0.38	0.38 ± 0.19
Chloroflexi	0.21 ± 0.22	0.11 ± 0.09	0.12 ± 0.23	0.19 ± 0.09
Synergistetes	0.21 ± 0.33	0.06 ± 0.05	0.13 ± 0.28	0.14 ± 0.22
Cyanobacteria	0.17 ± 0.23	0.21 ± 0.23	0.3 ± 0.28	0.07 ± 0.06
Patescibacteria	0.1 ± 0.07	0.07 ± 0.06	0.06 ± 0.05	0.11 ± 0.07
Epsilonbacteraeota	0.07 ± 0.12	0.01 ± 0.02	0.05 ± 0.1	0.03 ± 0.09
WPS-2	0.06 ± 0.12	0.02 ± 0.03	0.01 ± 0.04	0.07 ± 0.11
Planctomycetes	0.05 ± 0.04	0.05 ± 0.07	0.04 ± 0.06	0.06 ± 0.06

[1]Sequence counts were calculated as relative abundance (%). Data were expressed as mean ± standard deviation.
[2]Bacteria phyla that had a mean relative abundance greater than 0.5% were listed.

Table 5-5. Effects of sampling site and ruminal pH on index of richness, alpha diversity, and evenness among treatments at bacterial and protozoal genera level.

Variable	Control		LpH		SEM	*P* value		
	Liquid	Solid	Liquid	Solid		Treatment	Sample	Treatment×Sample
Bacterial genera								
Observed Species	56.33	102.83	70.83	101.67	6.82	0.07	0.0001	0.17
Richness Index								
Menhinick's	0.19	0.19	0.25	0.19	0.02	0.01	0.004	0.06
Margalef's	4.82	8.05	6.11	7.98	0.46	0.02	0.0005	0.07
Evenness Index								
Pilou	0.19	0.19	0.21	0.19	0.004	0.02	0.01	0.08
Hill's ratio	0.04	0.02	0.04	0.02	0.003	0.19	0.001	0.33
Alpha diversity								
Shannon-Wiener	2.25	2.87	2.68	2.87	0.09	0.000002	0.04	0.001
Simpson's	0.78	0.9	0.87	0.89	0.02	0.00002	0.26	0.001
Protozoal genera								
Observed Species	15.00	20.83	16.33	21.33	1.37	0.33	0.001	0.67
Richness Index								
Menhinick's	2.04	3.01	2.28	3.14	0.23	0.30	0.001	0.73
Margalef's	3.51	5.13	3.89	5.31	0.38	0.31	0.001	0.70
Evenness Index								
Pilou	0.12	0.18	0.11	0.18	0.03	0.79	0.05	0.90
Hill's ratio	0.10	0.08	0.09	0.08	0.01	0.27	0.66	0.50
Alpha diversity								
Shannon-Wiener	0.69	1.16	0.74	1.13	0.13	0.75	0.02	0.75
Simpson's	0.33	0.54	0.32	0.53	0.07	0.87	0.02	0.98

Table 5-6. The effect of sampling site and treatment on bacterial phyla[1].

Variable	Control		LpH		SEM	*P* value[2]		
	Liquid	Solid	Liquid	Solid		Treatment	Sample	Treatment×Sample
Bacteroidetes	4.27	3.22	3.57	3.09	0.17	0.0003	0.01	0.04
Chloroflexi	0.07	0.33	0.25	0.28	0.07	0.05	0.71	0.08
Firmicutes	3.88	4.34	3.62	4.00	0.13	0.15	0.03	0.77
Kiritimatiellaeota	2.55	1.00	2.40	1.21	0.29	0.71	0.004	0.54
Lentisphaerae	2.58	1.60	2.50	1.68	0.33	0.81	0.02	0.75
Patescibacteria	0.17	0.16	0.09	0.21	0.06	0.03	0.001	0.01
Proteobacteria	4.88	4.08	3.60	3.84	0.27	0.000004	0.38	0.01
Spirochaetes	2.76	3.39	2.56	3.28	0.13	0.28	0.0001	0.73

[1] Centered log ratios of sequence counts of the bacterial phyla.

[2]Test of the effect of treatment, sample location, or their interaction.

Table 5-7. Summary statistics of taxonomic compositions of bacteria genera in different treatments and ruminal liquid and solid fractions[1].

Genus[2]	LpH	Control	Liquid	Solid
Proteobacteria _ Succinivibrionaceae_UCG-002	13.58 ± 10.91	21.39 ± 10.07	18.87 ± 13.69	16.1 ± 7.88
Spirochaetes _ Treponema_2	9.84 ± 5.5	8.02 ± 4.66	5.12 ± 3.93	12.75 ± 2.56
Fibrobacteres _ Fibrobacter	5.53 ± 3.98	3.29 ± 1.14	4.36 ± 4.3	4.46 ± 1.19
Proteobacteria _ Ruminobacter	4.03 ± 4.53	4.08 ± 2.3	4.93 ± 4.74	3.18 ± 1.29
Firmicutes _ Christensenellaceae_R-7_group	3.8 ± 2.7	3.29 ± 2.13	2.66 ± 2.72	4.44 ± 1.7
Firmicutes _ Erysipelotrichaceae_UCG-004	3.78 ± 1.97	2.31 ± 0.96	3.6 ± 1.3	2.49 ± 1.9
Firmicutes _ Ruminococcus_2	3.26 ± 1.68	2.83 ± 1.73	2.21 ± 1.61	3.87 ± 1.34
Bacteroidetes _ Prevotella_1	2.81 ± 1.04	4.94 ± 5.21	5.03 ± 5.11	2.72 ± 1.28
Proteobacteria _ Succinivibrionaceae_UCG-001	2.66 ± 4.55	2.84 ± 5.93	2.01 ± 4.2	3.49 ± 6.09
Firmicutes _ CAG-352	2.46 ± 2.16	3.53 ± 2.6	1.66 ± 1.26	4.33 ± 2.56
Proteobacteria _ Succinimonas	1.86 ± 1.43	3.57 ± 2.08	2.69 ± 2.24	2.73 ± 1.7
Firmicutes _ Ruminococcus_1	1.8 ± 1.62	2.06 ± 1.66	0.57 ± 0.46	3.3 ± 1.07
Firmicutes _ Ruminococcaceae_NK4A214_group	1.5 ± 0.77	1.53 ± 0.86	1.06 ± 0.58	1.97 ± 0.74
Tenericutes _ Anaeroplasma	1.47 ± 0.78	1.06 ± 0.51	1.32 ± 0.47	1.22 ± 0.86
Firmicutes _ Lachnospiraceae_NK3A20_group	1.16 ± 1.09	1.19 ± 1.3	0.27 ± 0.38	2.08 ± 0.96
Bacteroidetes _ Rikenellaceae_RC9_gut_group	0.68 ± 0.53	0.43 ± 0.19	0.54 ± 0.49	0.57 ± 0.32
Firmicutes _ Saccharofermentans	0.56 ± 0.43	0.55 ± 0.42	0.23 ± 0.25	0.88 ± 0.26
Proteobacteria _ Succinivibrio	0.54 ± 0.32	0.49 ± 0.48	0.68 ± 0.48	0.34 ± 0.2
Lentisphaerae _ horsej-a03	0.53 ± 0.48	0.25 ± 0.19	0.45 ± 0.43	0.33 ± 0.34
Firmicutes _ Anaerosporobacter	0.5 ± 0.61	0.79 ± 0.57	0.58 ± 0.62	0.71 ± 0.59

[1]Sequence counts were calculated as relative abundance (%). Genera that had a mean relative abundance greater than 0.5% were listed. Data were expressed as mean ± standard deviation.
[2]Genus name was represented as Phylum name_Genus name.

Table 5-8. Bacterial genera that significantly changed among treatments[1].

Variable	Control		LpH		SEM	*P* value[2]		
	Liquid	Solid	Liquid	Solid		Treatment	Sample	Treatment×Sample
Actinobacteria								
Olsenella	0.97	2.53	1.13	2.21	0.44	0.67	0.004	0.36
Bacteroidetes								
Prevotella_1	6.37	4.90	5.55	4.85	0.30	0.04	0.09	0.18
Prevotella_9	2.35	1.36	0.85	2.32	0.57	0.003	0.003	0.001
Prevotellaceae_UCG-001	1.81	2.48	1.78	2.88	0.33	0.92	0.001	0.36
U29-B03	0.24	1.36	0.41	0.91	0.17	0.48	0.04	0.06
Chloroflexi								
Flexilinea	1.08	2.25	2.38	2.21	0.27	0.0004	0.63	0.01
Elusimicrobia								
Elusimicrobium	2.71	1.18	3.04	1.34	0.56	0.55	0.002	0.83
Firmicutes								
Anaeromusa	0.14	0.06	0.11	0.03	0.02	0.26	0.02	0.92
Anaerosporobacter	4.00	3.49	2.27	3.15	0.60	0.002	0.11	0.07
Butyrivibrio_2	1.18	2.88	1.53	2.83	0.39	0.49	0.01	0.58
Christensenellaceae_R-7_group	5.19	5.50	5.50	5.26	0.13	0.08	0.18	0.03
Clostridium_sensu_stricto_1	1.42	1.40	0.10	0.02	0.81	0.004	0.86	0.92
Erysipelotrichaceae_UCG-004	5.69	4.51	5.95	4.90	0.27	0.48	0.01	0.81
Family_XIII_AD3011_group	0.24	1.79	0.50	1.32	0.21	0.39	0.01	0.09
Family_XIII_UCG-001	0.26	1.17	0.39	0.95	0.19	0.63	0.03	0.35
Lachnoclostridium_1	0.15	0.97	0.13	0.20	0.12	0.87	0.66	0.002
Lachnospiraceae_AC2044_group	0.15	1.63	0.66	1.52	0.37	0.08	0.003	0.13
Lachnospiraceae_ND3007_group	1.41	1.81	0.46	1.59	0.39	0.09	0.04	0.35
Lachnospiraceae_NK3A20_group	2.02	4.69	2.39	4.07	0.57	0.65	0.04	0.39
Lachnospiraceae_NK4A136_group	0.15	0.44	0.12	0.56	0.11	0.84	0.001	0.41
Lachnospiraceae_UCG-007	0.94	0.73	0.09	0.77	0.62	0.02	0.07	0.09
Lachnospiraceae_XPB1014_group	0.13	1.49	0.33	0.80	0.22	0.52	0.13	0.05
Mogibacterium	0.48	3.10	1.53	2.71	0.27	0.01	0.002	0.01

Moryella	0.32	3.08	0.87	2.38	0.32	0.22	0.001	0.05
Papillibacter	0.61	1.58	2.09	1.85	0.67	0.01	0.67	0.13
Pseudobutyrivibrio	1.02	1.43	0.82	2.15	0.31	0.64	0.002	0.13
Ruminococcaceae_UCG-004	0.23	1.23	0.23	0.94	0.30	0.98	0.05	0.56
Ruminococcaceae_UCG-005	0.58	0.90	1.55	1.20	0.39	0.03	0.42	0.28
Ruminococcaceae_UCG-010	2.15	1.68	3.58	2.05	0.40	0.01	0.01	0.19
Ruminococcus_1	3.95	5.20	3.56	4.86	0.26	0.28	0.0004	0.92
Saccharofermentans	2.86	3.86	2.77	3.73	0.24	0.78	0.004	0.93
Selenomonas_1	0.59	1.41	0.93	1.80	0.28	0.36	0.02	0.92
Sporobacter	0.13	0.02	0.12	0.02	0.02	0.66	0.001	0.70
Lentisphaerae								
Horsej-a03	2.99	2.50	3.94	2.54	0.44	0.07	0.01	0.22
Victivallis	0.14	0.02	0.86	0.25	0.22	0.02	0.05	0.27
Patescibacteria								
Candidatus_Saccharimonas	0.42	0.73	0.16	0.92	0.29	0.36	0.01	0.27
Planctomycetes								
CPla-4_termite_group	0.13	0.06	0.19	0.09	0.06	0.22	0.04	0.57
Pirellula	0.13	0.10	0.22	0.02	0.06	0.27	0.01	0.13
Proteobacteria								
Desulfovibrio	0.83	2.05	1.33	1.95	0.29	0.09	0.03	0.15
Pantoea	0.37	0.05	0.07	0.30	0.19	0.11	0.21	0.04
Pseudomonas	1.01	0.09	0.10	0.38	0.32	0.003	0.35	0.005
Succinimonas	5.85	4.98	3.98	4.60	0.54	0.003	0.33	0.10
Succinivibrionaceae_UCG-002	7.88	6.68	5.55	6.48	0.51	0.0004	0.16	0.02
Spirochaetes								
M2PT2-76_termite_group	1.28	1.44	0.61	0.04	0.66	0.02	0.05	0.08
Sediminispirochaeta	2.31	2.41	3.17	2.37	0.35	0.03	0.04	0.11
Treponema	2.35	2.92	3.16	3.13	0.31	0.03	0.94	0.27
Synergistetes								
Pyramidobacter	0.52	1.63	1.27	1.57	0.26	0.01	0.32	0.06
Synergistes	0.13	0.09	0.44	0.03	0.09	0.01	0.001	0.04

[1] Sequence counts of the bacterial genera were transformed to centered log ratio to avoid compositional data problem.

[2]At least one of the treatment effects (Treatment, Sample, or their interaction) was significantly different (P <0.05).

Table 5-9. Summary statistics of taxonomic compositions of the archaea genus in different treatments and ruminal liquid and solid fractions[1].

Genus	LpH	Control	Liquid	Solid
Candidatus_Methanomethylophilus	55.32 ± 21.88	53.36 ± 23.59	63.82 ± 22.11	44.86 ± 18.77
Methanobrevibacter	26.45 ± 12.32	23.7 ± 12.94	16.02 ± 9.08	34.13 ± 7.86
Methanosphaera	0.14 ± 0.28	0.1 ± 0.28	0.03 ± 0.1	0.22 ± 0.36

[1]Sequence counts were calculated as relative abundance (%). Data were expressed as mean ± standard deviation.

Table 5-10. Archaea genera that significantly changed among treatments[1]

Variable	Control		LpH		SEM	*P* value		
	Liquid	Solid	Liquid	Solid		Treatment	Sample	Treatment×Sample
Candidatus_Methanomethylophilus	2.72	2.28	2.69	2.25	0.22	0.91	0.16	0.99
Methanobrevibacter	1.39	2.13	1.56	2.02	0.19	0.38	0.02	0.31
Methanosphaera	0.03	0.02	0.02	0.03	0.01	0.71	0.83	0.72

[1] Sequence counts of the bacterial genera were transformed to centered log ratio to avoid compositional data problem.

Table 5-11. Summary statistics of taxonomic compositions of the protozoan genera in different treatments and ruminal liquid and solid fractions[1].

Genus	Acid	Control	Liquid	Solid
Entodinium	35.41 ± 10.71	35.91 ± 11.38	42.64 ± 7.69	28.68 ± 8.88
Polyplastron	6.56 ± 5.27	4.64 ± 4.04	2.85 ± 1.6	8.35 ± 5.19
Isotricha	3.27 ± 2.69	6.89 ± 5.44	4.93 ± 5.74	5.23 ± 3.32
Eudiplodinium	1.48 ± 1.21	1.27 ± 1.11	0.69 ± 0.43	2.07 ± 1.23
Eremoplastron	1.42 ± 0.85	1.58 ± 1.83	1.26 ± 0.84	1.74 ± 1.81
Cyllamyces	0.33 ± 0.56	0.12 ± 0.16	0.19 ± 0.57	0.26 ± 0.18
Trichomitus	0.28 ± 0.23	0.22 ± 0.14	0.23 ± 0.16	0.27 ± 0.22
Tetratrichomonas	0.12 ± 0.13	0.09 ± 0.1	0.09 ± 0.11	0.13 ± 0.12
Diploplastron	0.11 ± 0.08	0.09 ± 0.07	0.12 ± 0.08	0.08 ± 0.06
Ophryoscolex	0.09 ± 0.08	0.08 ± 0.1	0.08 ± 0.08	0.09 ± 0.1

[1]Sequence counts were calculated as relative abundance (%). Genera that had a mean relative abundance greater than 0.05% were listed. Data were expressed as mean ± standard deviation.

Table 5-12. Protozoan genera that significantly changed among treatments[1]

Variable	Control		LpH		SEM	*P* value[2]		
	Liquid	Solid	Liquid	Solid		Treatment	Sample	Treatment×Sample
Brachypodium	0.04	0.37	0.02	0.47	0.16	0.89	0.001	0.54
Cyllamyces	0.42	2.61	2.11	2.50	0.54	0.001	0.50	0.03
Diploplastron	2.91	1.32	2.79	1.59	0.54	0.84	0.04	0.63
Entodinium	9.37	7.44	8.69	7.30	0.35	0.09	0.001	0.34
Isotricha	6.84	5.51	4.97	5.14	0.62	0.01	0.82	0.15
Mortierella	0.04	0.31	0.46	0.55	0.24	0.04	0.69	0.51
Ophryoscolex	0.90	1.72	2.56	0.92	0.56	0.02	0.02	0.02
Panax	0.03	0.53	0.02	0.53	0.30	0.95	0.03	0.97
Trichomitus	3.78	2.56	3.43	2.40	0.36	0.50	0.04	0.80
Triticum	0.03	0.55	0.02	0.45	0.20	0.97	0.01	0.70

[1] Sequence counts of the bacterial genera were transformed to centered log ratio to avoid compositional data problem.

[2]At least one of the treatment effects (Treatment, Sample, or their interaction) was significantly different ($P < 0.05$).

Table 5-13. Summary statistics of carbohydrate-active degrading enzyme compositions in different treatments and ruminal liquid and solid fractions[1].

Carbohydrate-active degrading enzyme[2]	LpH	Control	Liquid	Solid
Cellulase	13.87 ± 4.03	11.8 ± 4.56	12.08 ± 5.25	13.58 ± 3.25
Endo-1,4-beta-xylanase	12.42 ± 4.18	11.32 ± 5.97	8.34 ± 4.14	15.39 ± 3.09
Amylase	7.14 ± 4.82	8.29 ± 7.38	11.2 ± 6.7	4.24 ± 2.66
Alpha-N-arabinofuranosidase	2.83 ± 1.44	2.67 ± 1.03	2.39 ± 1.55	3.12 ± 0.69
Putative 4-alpha-glucanotransferase	2.74 ± 1.63	2.97 ± 1.45	3.08 ± 1.82	2.63 ± 1.17
Acetylxylan esterase	2.7 ± 1.25	2.18 ± 0.88	1.88 ± 1.15	3 ± 0.69
Cellobiose phosphorylase	2.44 ± 0.73	2.76 ± 0.9	2.94 ± 0.87	2.26 ± 0.63
Alpha-amylase	2.33 ± 1.29	2.92 ± 1.79	3.13 ± 1.79	2.13 ± 1.15
Glycoside hydrolase family 43	2.29 ± 1.88	1.15 ± 1.1	1.12 ± 1.99	2.33 ± 0.83
Phosphorylase	1.88 ± 1.3	2.39 ± 1.7	2.83 ± 1.73	1.44 ± 0.81
Beta-glucosidase	1.55 ± 0.84	1.18 ± 0.66	1.58 ± 0.87	1.16 ± 0.61
Glycoside hydrolase family 2 TIM barrel	1.47 ± 1.13	0.89 ± 0.62	0.88 ± 1.05	1.49 ± 0.74
Pectinase family protein/glycosyl hydrolase family 88	1.42 ± 0.81	1.36 ± 0.89	1.58 ± 0.94	1.2 ± 0.69
Glycosyltransferase group 2 family	1.38 ± 0.64	1.17 ± 1.03	1.16 ± 1.04	1.39 ± 0.62
Glycosyl.hydrolase family 43	1.37 ± 0.93	2.25 ± 1.31	1.55 ± 1.33	2.08 ± 1.04
Putative 1,4-alpha-glucan branching enzyme	1.2 ± 0.81	1.12 ± 0.99	1.45 ± 1.1	0.87 ± 0.51
Alpha-glucosidase	1.13 ± 0.63	1.05 ± 0.58	1.33 ± 0.65	0.85 ± 0.44
Glycosyl hydrolase family 57	1.13 ± 0.46	1.34 ± 0.97	1.28 ± 0.98	1.19 ± 0.45
Endo-1,4-xylanase ferulic acid esterase	1.13 ± 0.59	0.99 ± 0.62	1.15 ± 0.68	0.97 ± 0.53
Putative carbohydrate active enzyme	1.09 ± 0.67	0.75 ± 0.47	1.19 ± 0.55	0.65 ± 0.53
1,4-alpha-glucan branching enzyme	1.04 ± 0.65	1.94 ± 1.04	1.54 ± 0.98	1.43 ± 0.98
Putative alpha-xylosidase	1.02 ± 0.44	0.96 ± 0.44	1.01 ± 0.47	0.97 ± 0.42

[1]Sequence counts were calculated as relative abundance (%). Data were expressed as mean ± standard deviation.
[2]Enzymes that had a mean relative abundance greater than 1% were listed.

Table 5-14. Carbohydrate-active degrading enzymes that significantly changed among treatments[1].

Variable	Control		LpH		SEM	*P* value[2]		
	Liquid	Solid	Liquid	Solid		Treatment	Sample	Treatment×Sample
Amylase	5.32	3.76	5.04	3.40	1.13	0.64	0.01	0.93
Beta-galactosidase	2.02	1.80	2.68	1.46	0.41	0.17	0.01	0.14
Cellulase celA	2.74	1.38	2.77	1.31	0.91	0.96	0.01	0.90
Glucan phosphorylase	0.83	2.15	1.70	1.92	0.42	0.05	0.62	0.08
Glucosidase Cel1C	0.92	0.63	2.22	1.10	0.42	0.01	0.03	0.26
Glycoside hydrolase family 43	0.30	3.19	1.45	3.08	0.54	0.11	0.02	0.22
Glycosyl hydrolase, family 16	1.16	0.85	0.13	0.41	0.35	0.02	0.52	0.34
Glycosyl hydrolase, family 43	2.00	3.52	2.60	1.82	0.59	0.42	0.29	0.03
Pectate lyase/Amb allergen	0.15	0.53	1.11	1.22	0.30	0.0001	0.65	0.42
Putative 1,4-alpha-glucan branching enzyme	2.35	2.29	3.05	2.02	0.31	0.11	0.02	0.12
Putative 4-alpha-glucanotransferase	3.97	3.53	3.82	2.92	0.40	0.67	0.01	0.33
Putative carbohydrate-active enzyme	3.00	1.91	3.25	1.72	0.82	0.61	0.002	0.53
Putative glycosyl transferase	2.17	1.03	0.75	1.66	0.45	0.03	0.16	0.02
Rhamnogalacturonan Acetylesterase	0.05	0.20	0.70	0.24	0.36	0.05	0.16	0.19
Sucrose alpha-glucosidase.	2.37	0.32	0.13	0.24	0.57	0.00004	0.84	0.005
UDP-3-0-acyl N-acetylglucosamine deacetylase	1.47	2.01	2.46	1.44	0.38	0.04	0.03	0.02

[1] Sequence counts of the enzyme expression were transformed to centered log ratio to avoid compositional data problem.

[2]At least one of the treatment effects (Treatment, Sample, or their interaction) was significantly different ($P < 0.05$).

Table 5-15. Multiple regressions of ruminal SCFA concentrations on carbohydrate active enzymes and ruminal effective degradability of hemicellulose, cellulose, and lignin[1].

Items	Acetate, mM	Propionate, mM	Butyrate, mM	Isobutyrate, mM	Valerate, mM	Isovalerate, mM
Intercept	15.61±10.05	10.13±1.53	-3.23±1.37	-0.38±0.18	-0.28±0.15	-0.26±0.07
Hemicellulose_Kd[2]	310.02±81.26	283.20±24.55				
Cellulose_Kd			126.22±31.39		17.34±2.52	
Hemicellulose_ED[3]			0.17±0.08			
Cellulose_ED				0.03±0.01	0.03±0.01	0.02±0.004
Lignin_ED	1.90±1.01			0.04±0.02		
Endo-1,4-xylanase / ferulic acid esterase			0.56±0.20			0.03±0.01
Galacturan 1,4-alpha-galacturonidase	-5.78±2.78				-0.19±0.04	
Glucuronan lyase						0.06±0.01
Glycogen synthase-like protein		-1.18±0.32				
Glycosyl hydrolase, family 16		1.36±0.42		0.04±0.02		0.03±0.01
Glycosyl hydrolase, family 31	2.57±1.00		0.39±0.18	0.07±0.02	0.04±0.01	0.03±0.01
Glycosyltransferase, group 1 family		1.35±0.41				
Maltopentaose-forming amylase	-3.70±1.48	-1.12±0.53		-0.04±0.02	-0.06±0.02	
Adjusted R^2	0.74	0.87	0.74	0.81	0.85	0.89

[1]Lasso regression was used to select top 8 variables, then multivariable regression was conducted based on back forward elimination approach. Every independent variable listed in the table had a *P* value less than 0.1 for regression coefficient. Collinearity was tested using variance inflation factor (VIF) which was less than 2.

[2]Kd represents degradation rate.

[3]ED is effective degradability.